SELECTED REACTIONS OF PHOTO-EXCITED CARBONYL COMPOUNDS IN THE LIQUID PHASE

A THESIS

by

JOHN D. HOLMES, B.A.

Submitted to the UNIVERSITY OF KEELE
in partial fulfilment of the
requirements for the degree of Doctor
of Philosophy.

University of Keele
October 1970

ACKNOWLEDGEMENTS

In presenting this thesis I should like to thank Dr. Peter Borrell for his supervision and constant encouragement.

I should also like to thank the following :

Professor H.D. Springall for the provision of laboratory facilities.

Dr. R.B. Cundall for his supervision in the absence of Dr. P. Borrell, December 1967 - June 1968.

The following members of the research group for numerous helpful discussions: Dr. A.E. Platt, Dr. A. Cervenka, Mr. G.E. Millward and, in particular, Dr. J. Sedlar for helpful advice on both theoretical and practical aspects of the work.

Mrs. G.C. Walker who typed this thesis.

The University of Keele for the provision of a Demonstratorship, without which this work would not have been possible.

All the work presented in this thesis was carried out by the author, under the supervision of Dr. Peter Borrell.

CONTENTS

		PAGE
1.	INTRODUCTION	
1.1	Preliminary Remarks	1
1.2	Molecular Excitation and Excited States	2
1.3	Absorption Spectra	7
1.4	Photochemical Reactions in Carbonyl Compounds	9
1.5	The Norrish Type II Elimination	15
1.6	Photochemical cis-trans Isomerisation	28
	References to Introduction	51
2.	EXPERIMENTAL	
2.1	Introductory work on Ethylidene Acetone	61
2.2	Materials	63
2.3	Light Sources	68
2.4	Optical Filters	71
2.5	Preparative Photolysis Apparatus	73
2.6	Low Temperature Photolysis	74
2.7	The Capillary Technique	75
2.8	The Semi-Micro Technique	86
2.9	Actinometry	90
2.10	Comparison of Capillary and Semi-Micro Techniques	93

PAGE

2.11 Spectra 95

2.12 Gas Chromatography 97

References to Chapter 2. 102

3. PHOTOISOMERISATION: RESULTS

3.1 Spectra 103

3.2 Preliminary Photolysis 105

3.3 The Nature of Product III 107

3.4 Thermal Isomerisation 110

3.5 Photolysis at 313 nm 111

3.6 Actinometry in Capillaries 112

3.7 Photolysis on Merry-go-Round; Temperature Variation 116

3.8 Photolysis on Merry-go-Round; Concentration Dependence 122

3.9 Semi-Micro Apparatus; Variation of Concentration 125

3.10 Effect of Solvent 128

3.11 Low Temperature Photolysis 129

3.12 Methyl Angelate to Methyl Tiglate Isomerisation 130

3.13 Photosensitisation - Preliminary Experiments 133

PAGE

3.14 Absorption Spectra in Ethyl Iodide 135

3.15 Benzophenone Photosensitisation 136

3.16 Other Sensitisers 137

3.17 Attempts at Quenching Photosensitisation 140

3.18 Effect of Benzophenone Concentration 141

3.19 Effect of Ester Concentration on Benzophenone Photosensitised Isomerisation 144

3.20 Addition Products with Benzophenone 148

3.21 Quenching Experiments 150

3.22 Summary of Results 155

References to Chapter 3. 157

4. QUENCHING OF PHOTOELIMINATION: RESULTS

4.1 U.V. Absorption Spectra 158

4.2 Photolysis of Pure Liquid Ketones 160

4.3 Effect of Solvent on Photoelimination from 2-Pentanone 162

4.4 Light Intensity of High Pressure Lamp 168

4.5 Quenching of Photoelimination in 2-Pentanone at 313 nm 169

4.6 Quenching of Photoelimination in 4-Methyl-2-Pentanone 178

PAGE

4.7 Quenching of Photoelimination in 2-Octanone 185

4.8 Variation of Quantum Yield of Elimination with Concentration in Cyclohexane 190

5. DISCUSSION

ISOMERISATION OF METHYL TIGLATE

5.1 The De-conjugation Reaction 193

5.2 Thermal Isomerisation 196

5.3 The Potential Energy Diagram of Methyl Tiglate/Angelate 198

5.4 Mechanism for Direct Isomerisation 202

5.5 Photosensitisation 207

QUENCHING OF THE NORRISH TYPE II REACTION

5.6 Background to Present Work 214

5.7 Quenching Experiments in Benzene 219

5.8 Effect of Solvent 225

5.9 Quantum Yield of Acetone Production in Different Ketons 230

5.10 Quenching in Cyclohexane 231

5.11 Summary and Suggestions for Further Work 233

References to Discussion 235

ABSTRACT

The work presented in this thesis falls into two parts; firstly, a study of the cis-trans isomerisation of methyl tiglate (trans 2-carbomethoxy-2-butene) and secondly, a study of the quenching of the Norrish Type II reaction by cyclohexene. Both sets of experiments were carried out by semi-micro photolytic techniques developed for the photolysis of small quantities of de-oxygenated liquids. A full description and comparison of the methods developed is presented.

In the first part of the work methyl tiglate was isomerised to its cis isomer, methyl angelate by the absorption of 254 nm light. The reaction was studied as a function of temperature, ester concentration and wavelength. The quantum yield of tiglate to angelate isomerisation was measured as 0.090 ± 0.003 and was found to be independent of initial ester concentration. Temperature was shown to have a small effect. The reaction was not affected by change of solvent and did not occur at 313 nm. The quantum yield of the reverse reaction was measured as 0.032 and was also independent of concentration. A minor side reaction to the β,γ-ester was investigated and had a quantum yield of 0.005. Methyl angelate was shown to be the precursor for this reaction and incorporation of deuterium in a suitable experiment showed the participation of an enol intermediate. A six-membered transition state is proposed. The isomerisation was found to be partially quenched by the addition

of oxygen and paramagnetic salts. Photosensitisation was investigated with a number of compounds using 313 and 366 nm exciting light. Acetone, acetophenone, benzophenone and anthraquinone were found to sensitise the reaction. Sensitisation was accompanied by oxetane formation in the case of the latter two compounds.

The results are discussed in relation to more detailed investigations of the isomerisation of ethylenic compounds and a potential energy versus angle of twist diagram is proposed for the lowest electronic states of the esters. There appears to be an efficient mechanism for internal conversion from the excited singlet state of both isomers as has been suggested for certain other n,π^* systems. A mechanism for photosensitised isomerisation is proposed involving a Schenck type of intermediate, based on studies of the effect of ester concentration on the benzophenone sensitised isomerisation.

The results presented in the second part of the work show how quenching of the photoelimination reaction in a ketone by an olefin of very similar triplet state energy can be used to obtain values of the quantum yields for the production of, and reaction from, singlet and triplet states of the ketone. It was shown, however, that quenching by compound formation observed in benzene is not the dominant reaction in cyclohexane. It is suggested that this is due to slight changes in the relative triplet state energies of donor and acceptor.

Quantum yields for acetone formation from a series of aliphatic ketones in the pure liquid phase were measured. Similar yields were also measured for acetone formation from 2-pentanone in a variety of solvents. The results of these studies suggested a number of solvent effects. The low quantum yields for acetone formation observed in benzene were explained by postulating reversible adduct formation as a route for internal conversion. This is in agreement with other recent work. Finally, it is shown that as pure ketone is replaced by cyclohexane as solvent for the reaction the quantum yield of acetone formation drops.

1. INTRODUCTION

1.1 Preliminary Remarks

Photochemistry can be defined as the study of chemical processes initiated by the absorption of light. From about 1850 to 1920, many photochemical reactions were discovered,[72] but useful application of these results was lacking. From 1920 to 1950, photochemistry was largely restricted to gas phase work by the physical chemist.[73] Since the 1950's modern techniques of analysis and spectroscopy allied to a greater understanding of the theory of electronically excited states have lead to a rapid expansion of the study of photochemistry. In the last few years the synthetic organic chemist has realised the usefulness of using photochemical reactions which can be highly selective.[74] At the same time many advances have been made in the understanding of the mechanisms and energy transfer processes operating in photoexcited systems. Of the groups of compounds studied, carbonyl compounds have received perhaps the most attention and it is in this area that this work was carried out.

The work in this thesis is divided between two topics : the quenching of type II photoelimination in alkanones and the cis-trans isomerisation of a conjugated ester. In this introduction the different types of photoprocesses found in carbonyl compounds are reviewed, after which a more detailed literature survey of the work in each of the two fields studied is set down. The objects of this are explained at the ends of Sections 1.5 and 1.6.

1.2 Molecular Excitation and Excited States

For a molecule to undergo a direct photochemical reaction it must absorb radiation in the visible or ultra-violet region of the spectrum. If it does possess such an absorption band, then a photon of the appropriate energy may cause an electronic transition to take place. For this to happen two criteria must be satisfied. Firstly, the frequency of the photon must equal $(E_2 - E_1)/h$, where E_1 is the energy of the stable ground state and E_2 that of the excited electronic state. Secondly, there must be a specific interaction of the electric vector of the photon with the molecule which induces the transition of the electron from its ground state orbital to its new orbital in the excited state. The transition usually involves promotion of an electron from a bonding or nonbonding molecular orbital to an antibonding molecular orbital. The molecule is thus raised to an excited electronic state which is usually vibrationally excited as well. From this state a number of photochemical and photophysical processes may take place.

The absorption of a monochromatic beam of light by a homogeneous absorbing system is described by the Beer-Lambert law. One form of this law which is commonly employed in photochemical studies is :

$$\frac{I}{Io} = 10^{-\varepsilon Cl}$$

where Io is the incident light intensity, I the transmitted light intensity, C the concentration of absorbing species,(mol litre^{-1})and

Fig. 1.1 Jablonski Diagram.

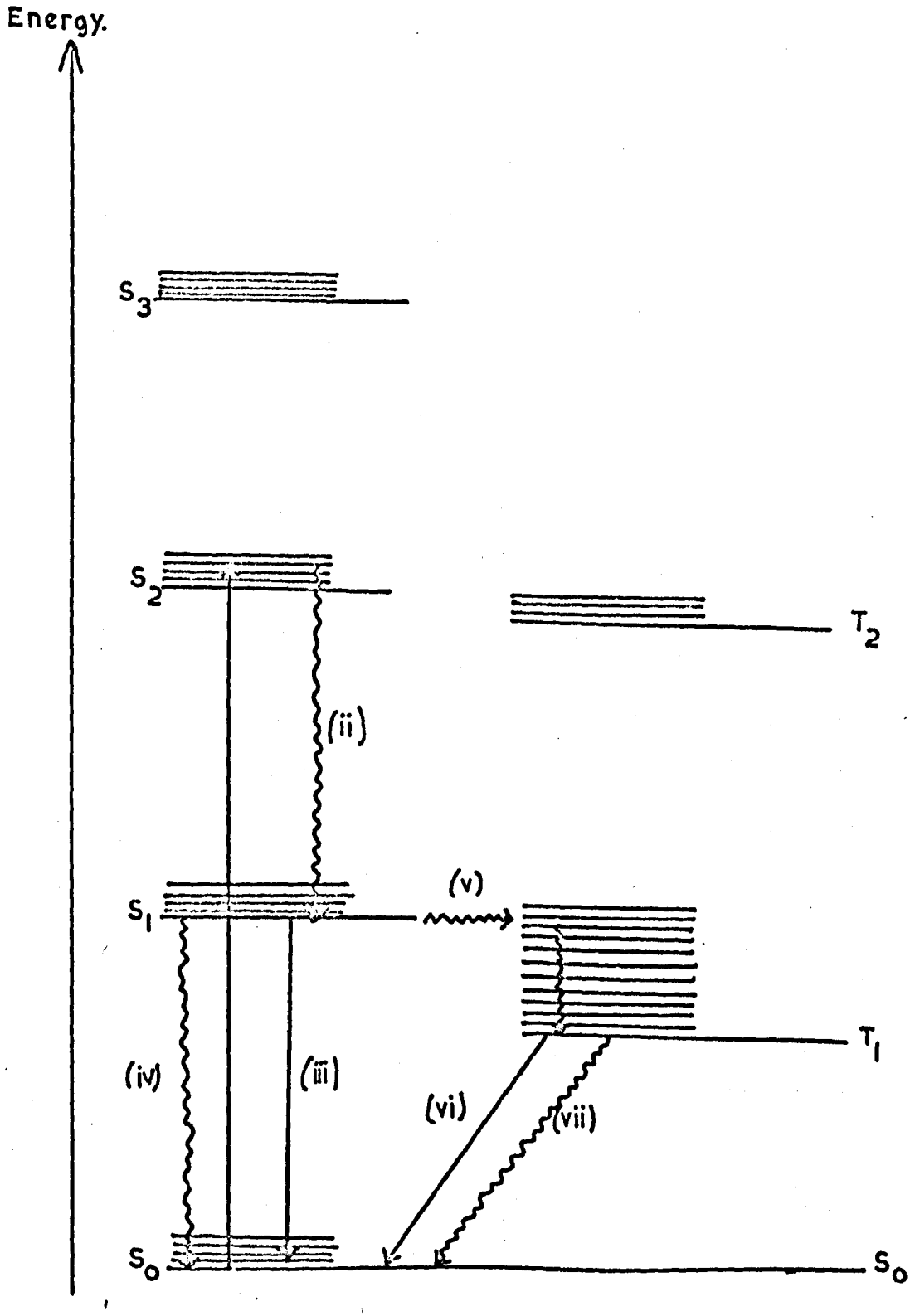

l. the path length of the light through the system,(cm). ε is then the molar extinction coefficient ($l.mol^{-1}cm^{-1}$) and is a measure of the probability that the photon-molecule interaction will lead to absorption of the photon. It is a constant for a given absorbing species at a given wavelength.

The ground state of most molecules has all electron spins paired, giving a multiplicity of 1 and is thus a singlet state, designated So. Since spin must be conserved in an electronic transition according to the Wigner spin rule,[66] the resulting excited states will also be singlets, S_1, S_2 etc. Direct excitation from a ground state singlet to an excited triplet is strongly forbidden, taking place only in the presence of strong perturbing influences such as oxygen at high pressure.[67] Once the molecule is in an excited state it is possible that spin inversion may take place (known as inter-system crossing) producing an excited state with a net spin of 1 and a multiplicity of 3: a triplet state. According to Hund's first rule, the triplet will be of lower energy than the corresponding singlet state.

Suppose that a molecule is excited to an upper vibrational level of the second excited singlet state, S_2, by absorbing light of suitable energy. The following physical processes can then occur from S_2 :

(i) Vibrational relaxation to the zero vibrational level of S_2. This will be very fast in solution, of the order of 10^{-13} s.

(ii) Non-radiative internal conversion to the lowest excited singlet state, S_1. This will take of the order of 10^{-11} s in solution.

From S_1 other deactivation processes are possible :

(iii) Return to So from S_1 by emission of a photon - fluorescence.

(iv) Non-radiative internal conversion to So.

(v) Inter-system crossing by spin inversion to T_1.

From T_1 the physical deactivation routes are :

(vi) Return to So from T_1 by emission of a photon - phosphorescence. This process is 'spin forbidden' and is usually only observed in solid matrices at very low temperatures.

(vii) Non-radiative inter-system crossing and internal conversion from T_1 to So.

These processes are shown diagrammatically in Fig.1.1, which is termed a Jablonski diagram. In this diagram, solid lines indicate processes accompanied by absorption or emission of light. Wavy lines indicate radiationless processes. Depending on the relative rates of processes (iii), (iv) and (v) the lifetime of S_1 in solution is typically 10^{-9}s. Since all processes from T_1 to So are 'spin forbidden', the lifetime of the triplet state in solution is much longer, around 10^{-3}s. For this reason, most photochemical processes take place from the triplet state.

In a typical organic molecule there are several possible electronic configurations in the excited state. Considering the molecular orbitals of the carbonyl chromophore of formaldehyde (Fig.1.2), in which the σ orbitals are ignored, the following types of electronic

Fig. 1.2

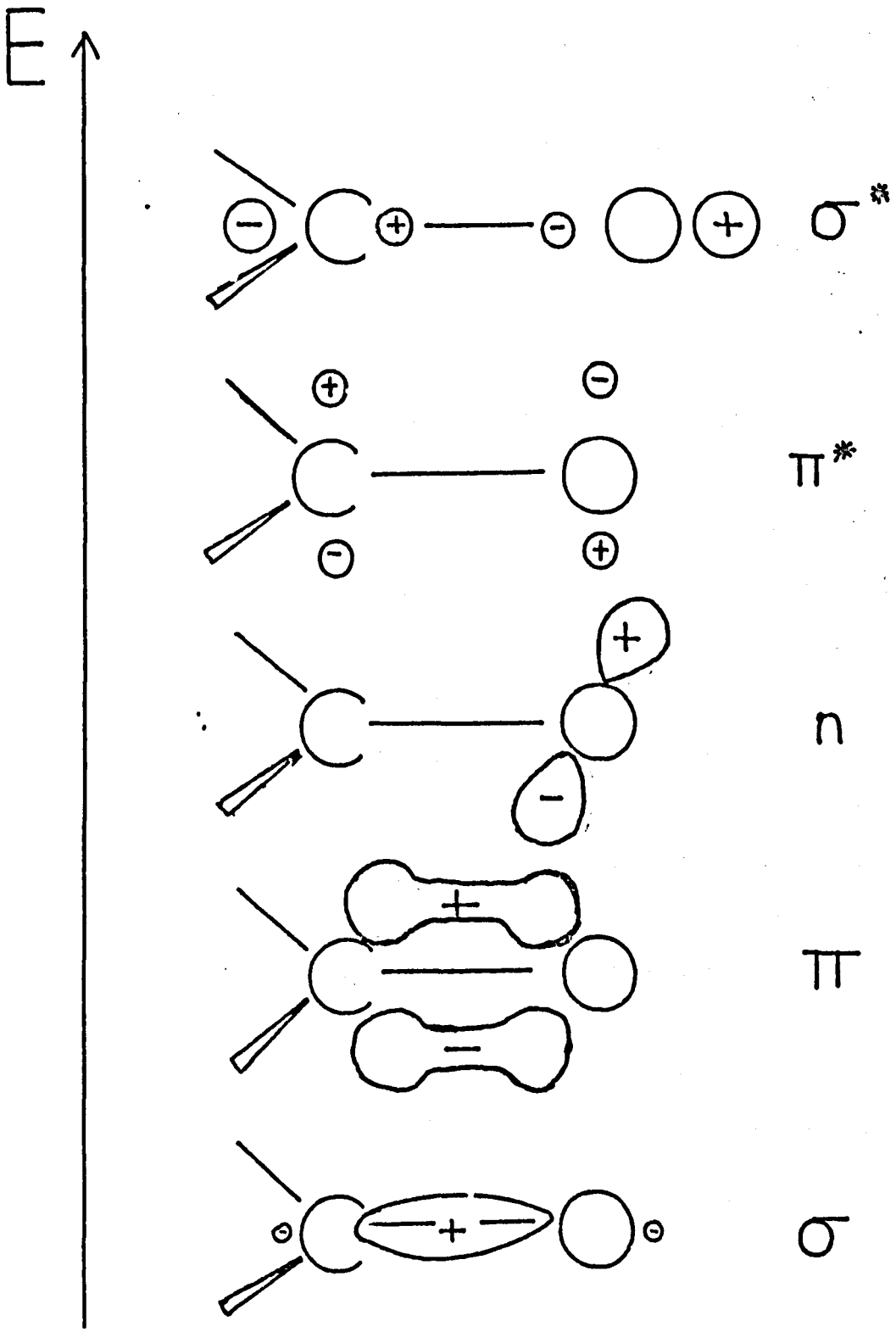

transition can occur : $\sigma - \sigma^*$, $\pi - \pi^*$, $n - \pi^*$ and $n - \sigma^*$ (using molecular orbital notation for the transitions). The first of these is a very high energy transition and would be expected to occur at exciting wavelengths shorter than 160 nm. The last three have all been observed. ($n - \pi^*$ at 290 nm, $n - \sigma^*$ at 190 nm and $\pi - \pi^*$ at 165 nm for formaldehyde). For a molecule like benzophenone, where the carbonyl group is in conjugation with the aromatic ring, the $\pi - \pi^*$ and $n - \pi^*$ transitions are shifted into the more accessible regions of the spectrum. ($n \rightarrow \pi^*$ at 345 nm and $\pi - \pi^*$ at 245 nm, leading to states S_1 and S_2 respectively).

In $\pi - \pi^*$ excitation there is no significant change in the carbonyl dipole. However, for $n - \pi^*$ excitation, an electron is promoted from an orbital associated with oxygen to an orbital shared by both atoms leaving, formally, a positive charge of $\frac{1}{2}$ on oxygen. In fact the C =O. dipole is not reversed, merely reduced, but this explains the electrophilic and free radical character of the n,π^* state. In benzophenone and similar molecules, the internal conversion from S_2 (π, π^*) to $S_1(n,\pi^*)$ is very rapid so that most chemical reactions are from the n,π^* state (usually the triplet).

Apart from chemical reaction and the various physical processes outlined above the excited state can lose its energy by energy transfer to another molecule. This is most important with triplet excited states, as they have a much longer lifetime in solution than singlet states. Photosensitisation and quenching by energy transfer are important processes in photochemistry. In general, most photosensitised reactions involve excitation energy transfer where the photosensitiser

is the donor and the reacting molecule is the acceptor :

$$D + h\nu \longrightarrow D^*$$
$$D^* + A \longrightarrow D + A^*$$
$$A^* \longrightarrow \text{Products (or } h\nu\text{, or thermal energy)}$$

In the gas phase, mercury photosensitisation from the ^3P states has been studied for over 30 years. The concept of triplet-triplet energy transfer between organic molecules in solution arose from the work of Ermolaev and Terenin in the 1950's, who found that benzophenone photosensitises the phosphorescence of naphthalene at 77K.[68] Since 1961, benzophenone and many other compounds with high inter-system crossing yields have been employed to sensitise a wide variety of chemical reactions (See Section 1.6). It has been shown that triplet energy transfer requires virtual collision but is effective upon nearly every encounter in condensed phases provided the triplet state energy of the donor is above that of the acceptor. Several recent reviews of electronic energy transfer have been published.[70, 3]

1.3 Absorption Spectra

The absorption spectra of simple ketones are similar to those of aldehydes and reflect the presence of the carbonyl group. They have a common absorption band, which is symmetrical and centred near 280 nm, related to the singlet-singlet $n - \pi^*$ transition involving the nonbonding electrons on the carbonyl oxygen. This transition is 'forbidden' on symmetry grounds as it involves a change in the position of the electronic charge (See Section 1.2). For this reason, the band shows a low absolute absorption intensity relative to a $\pi - \pi^*$ transition and the extinction coefficients for this band have a maximum value of around 20 $l.mol^{-1}cm^{-1}$. In aromatic ketones the singlet $n - \pi^*$ transition lies at longer wavelengths (around 350 nm). The width of the $n - \pi^*$ band in ketones means that both the mercury lines at 254 and 313 nm can be used to excite the transition $So \rightarrow S_1$. In aliphatic ketones the $\pi - \pi^*$ band lies at wavelengths below 200 nm and can only be studied in the far ultra-violet.

With simple acids and esters, such as acetic acid and ethyl acetate, the first absorption band is shifted to higher energies compared to the ketones. The first absorption maximum for acetic acid lies at 205 nm. This shift is attributed to the effect of electron releasing groups, -OH or -OR, attached to the carbonyl carbon atom and raising the energy of the π^* state. The intensity of this band (ε max around 50 $l.mol^{-1}cm^{-1}$) suggests that it is associated with the $n - \pi^*$ transition in the molecule.

When the ester group is conjugated with an olefinic bond, as in methyl tiglate, the $\pi - \pi^*$ transition shifts to longer wavelength. This transition is very much more intense than the $n - \pi^*$ and so the latter cannot be seen on the same scale. However, when the concentration was increased, no band or shoulder was seen which could be associated with the $n - \pi^*$ transition. It was assumed that the weak $n - \pi^*$ transition was masked under the more intense $\pi - \pi^*$ band. This agrees with the published spectra for crotonic acid and its derivatives which show no $n - \pi^*$ bands or only very faint shoulders.[71]

The spectra of the compounds studied are shown in Chapter 3. and Chapter 4.

1.4 Photochemical Reactions in Carbonyl Compounds

Carbonyl compounds undergo many interesting and often competing photochemical transformations, and consequently, have received much attention. These reactions can be classified into several types which are dealt with below.[1, 4]

1.4(a) Free Radical Decarbonylation - The Norrish Type I Split.[5, 6]

This process was first investigated by Norrish et al., who showed that the excited ketone can decompose into free radicals by rupture of the weakest bond, thus :

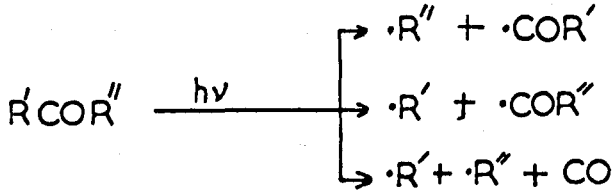

It is the dominant process in the gas phase decomposition of aldehydes and ketones. In solution at room temperature, however, the efficiency of this process is generally very low because of efficient recombination of the primary radicals in the solvent cage.[7] It is thought that the excited state involved in this process may be a singlet or a triplet.[8] With conjugated carbonyl compounds the efficiency of the type I process is reduced still further.

1.4(b) Photocycloelimination - The Norrish Type II Split.[9]

This is a general reaction of carbonyl compounds containing γ - hydrogen atoms. They are found to decompose by elimination of an olefin, thus

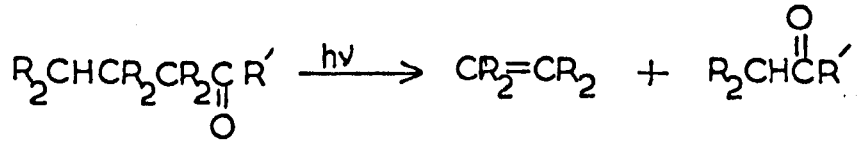

All aliphatic ketones containing γ - hydrogens participate in the type II process, and in solution, this is generally the dominant mode of decomposition. Again the reaction is less important for conjugated aliphatic carbonyl compounds.[10] A detailed discussion of this reaction is given below (Section 1.5).

1.4(c) The Type III process

It was found that in the photolysis of methyl isopropyl ketone at 254 nm acetaldehyde and propylene were the major products. It was suggested that they were formed by a "Norrish Type III" split involving transfer of a β - hydrogen atom.[11]

$$CH_3COCH(CH_3)_2 \xrightarrow{h\nu} CH_3CHO + C_3H_6$$

The detailed mechanism of this process is not fully established, though a cyclic intermediate has been postulated.[12] The reaction is very sensitive to wavelength and at 313 nm is negligible compared to the type I radical split.

1.4(d) Intramolecular Reduction of the Carbonyl Group

A primary intramolecular rearrangement involving reduction of the carbonyl group and the formation of the cyclic carbinol is common in simple aliphatic ketones with γ - hydrogens e.g.

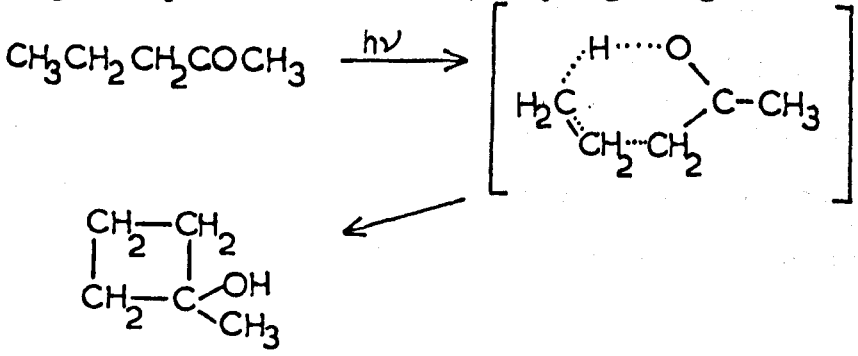

The cyclic alcohol formed in this reaction is often unstable and easily decomposes on gas chromatograph columns during analysis. Recent work has shown, however, that cyclic carbinols are produced from the same intermediate as the type II photoproducts.[13, 75]

1.4(e) Photocyclodimerisation

α, β - unsaturated carbonyl compounds have long been known to dimerise on photolysis in the condensed phase though the reaction is not known in the vapour phase.[14] Apparently either n, π* or π, π* states will undergo dimerization. Most of the ketones that have been reported to undergo such reactions are conjugated cyclic unsaturated ketones, and similar reactions have not been reported with α, β - unsaturated acyclic ketones. A much studied system in this respect is that of cyclopentenone.[15]

1.4(f) Carbonyl Photocycloaddition to Olefins

A comprehensive review of photochemical cycloaddition reactions has recently been published.[16] The cycloaddition of olefins to photoexcited carbonyl compounds to form oxetanes is a very general reaction and was first investigated by Büchi et.al.[17] If the olefin bears easily abstractable hydrogen atoms, the abstraction reaction will compete with oxetane formation. This competition can be expressed as a ratio of addition to abstraction products and this ratio is very delicately balanced. Seemingly small changes in the structure of either starting material can shift the predominant reaction. The excited state responsible for the cycloaddition seems to be the n,π* singlet or triplet excited state of the carbonyl compound.

1.4(g) Intramolecular Skeletal Rearrangement

Skeletal photorearrangements are particularly important in the photochemistry of α, β-unsaturated ketones and cyclic ketones. They can be divided into four main types :

(i) Rearrangement of the aliphatic chain

Apart from cis-trans isomerisation, a shift of the double bond and cyclisation of the carbon chain is illustrated in the liquid-phase photolysis of certain α, β-unsaturated aliphatic ketones. Yang et.al.[18] have shown that when the ketone has a quaternary carbon atom at the γ-position, irradiation in solution leads to cyclisation; whilst irradiation of α, β-unsaturated ketones having no γ-quaternary carbon gives either a facile isomerisation to the β, γ-isomer or no reaction at all, thus :

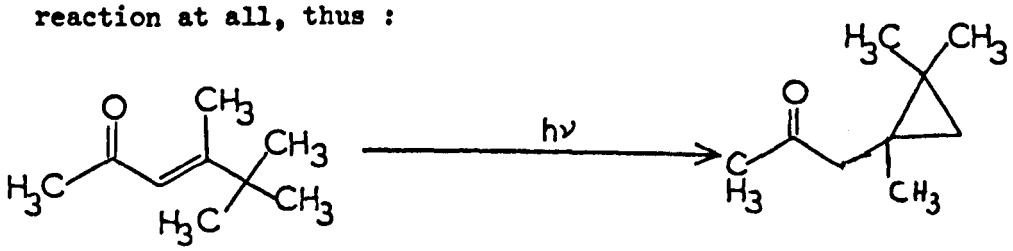

and

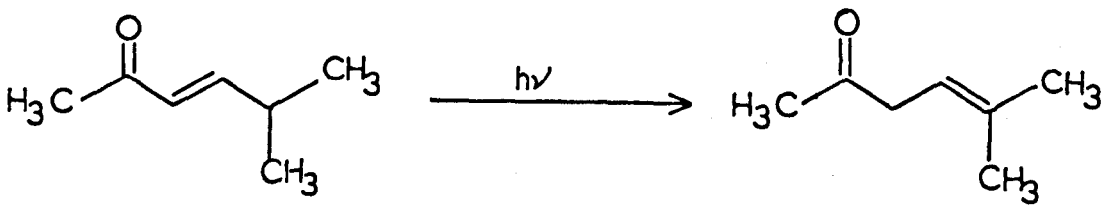

(ii) Rearrangement of cyclic to chain structure[19]

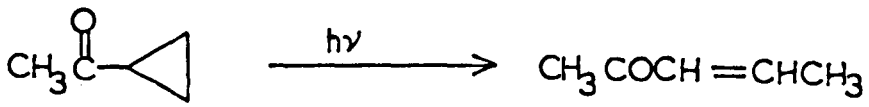

(iii) Ring contraction[20]

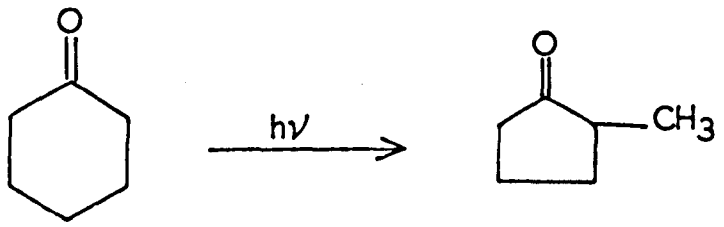

(iv) Mono-to bicyclic rearrangement[21]

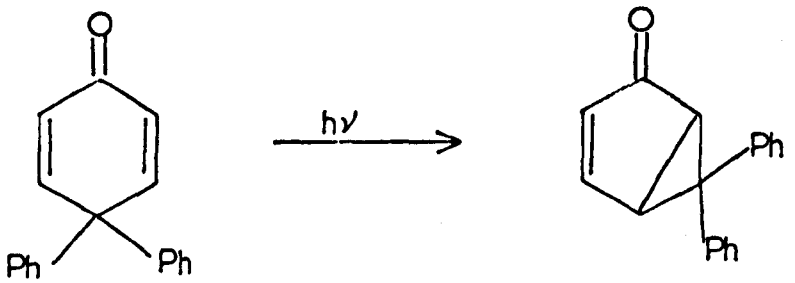

1.4(h) Cis-trans Photoisomerisation

This is a particular case of skeletal rearrangement, and will be dealt with in greater detail below (Section 1.6).

1.4(i) Intermolecular Hydrogen Abstraction

The reduction of benzophenone in 2-propanol was one of the earliest reported photochemical reactions.[22] Study of this reaction has sparked off much of the present interest in organic photochemistry. It has been found that the selectivity and absolute rates of reaction of benzophenone triplets towards hydrogen abstraction parallel those

of tertiary-butoxy radicals,[23] the ketone triplet being slightly more electrophilic than the radical.[24] These results are in agreement with the idea that the triplets have the n,π* configuration, in which an electron deficiency is created at the carbonyl oxygen by promotion of a nonbonding electron on oxygen to an antibonding π* orbital. There is some disagreement over the exact values of the rate constants for hydrogen abstraction by triplet benzophenone (e.g. abstraction from toluene[25, 26]).

Aliphatic ketones do undergo photoreduction.[32] Acetone is reduced in cyclohexane[27] and hexane.[28] Wagner showed that the excited singlet state of acetone is appreciably less reactive than the triplet towards hydrogen abstraction in experiments with tri-butyl stannane,[29] which is a very reactive hydrogen donor. Chien[30] has reported that the triplet states of diethyl ketone and benzophenone abstract hydrogen with comparable reactivity in work on the photo-oxidation of cumene. However, not very much work has been done on such reactions with aliphatic ketones, as other processes have always been thought to be dominant. It is worth noting here that Yang and Elliot[31] observed substantial intermolecular hydrogen abstraction from 2-pentanone in n-hexane solution. This was quenched by piperylene and was therefore assigned to the triplet excited state of the ketone.

1.5 The Norrish Type II Elimination

The type II reaction in alkyl ketones has been the subject of much research and is still controversial. Noyes and Davis[33] suggested that the reaction went through a six-membered cyclic intermediate to produce an enol ketone and an olefin. This was proved to be the case by Calvert et.al.,[34] who observed the enol acetone produced from the photolysis of 2-pentanone by infra-red techniques. They also showed that the keto form was partly monodeuterated when the reaction cell was treated with D_2O. Similar observations were made by Srinivasan[35] with 2-hexanone.

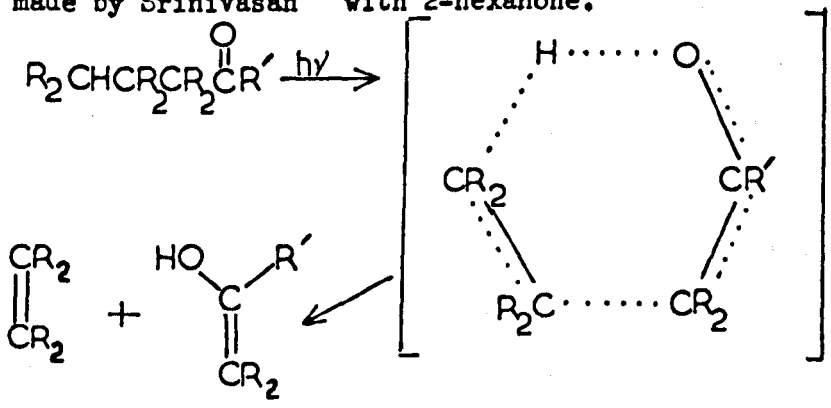

The nature of the excited states which participate in this primary process was the subject of much controversy. Noyes[36] found that high pressures of oxygen do not quench the photoelimination of 2-hexanone and Srinivasan found only slight quenching of methoxyacetone.[37] Consequently, they both concluded that the reaction proceeds from an excited singlet state. On the other hand, Ausloos[38] found that oxygen does quench photoelimination from 2-pentanone and inferred that the reaction proceeds from an excited triplet state. Michel and

Noyes[39] then found that biacetyl also quenches 2-pentanone and suggested that transfer of singlet energy was responsible. Ausloos and Rebbert[40] then showed that biacetyl quenches the elimination from 2-pentanone without disturbing the weak fluorescence of this compound; also that elimination from n-butyraldehyde can be sensitised by triplet energy transfer from oxygen.[41] This was convincing proof of a triplet intermediate.

The nature of the excited state involved is of interest in deciding between a biradical intermediate and a concerted process. Reaction from a triplet would probably produce a spin-unpaired biradical that has to undergo spin inversion to give products in their singlet ground states. Reaction from a singlet could lead to a completely concerted process with α, β-bond cleavage and hydrogen transfer taking place in one step. One piece of evidence in favour of a biradical is that cyclobutanol formation frequently accompanies elimination, especially in solution.[27] (See Section 1.4(d)).

Wagner and Hammond[42, 43, 44] have shown that the type II process takes place from <u>both</u> singlet and triplet states. They studied the quenching of various suitable ketones by piperylene, 1,3-pentadiene (up to 8M) and found that not all of the reaction was quenched even at very high concentrations of piperylene, which is a known triplet quencher.[45] They assumed that the amount of reaction in 8M piperylene is a measure of the singlet reaction and that the quenched part of the reaction is due to triplet excited ketone. In this way, they found that aromatic ketones undergo the reaction only from their triplet

state (inter-system crossing very fast) and then only if they possess an n,π* rather than a π, π* configuration. They plotted Stern-Volmer plots from the equation :

$$\frac{\phi_T^o}{\phi_T} = 1 + \frac{k_q[Q]}{k_r}$$

where ϕ_T is the triplet quantum yield, ϕ total - ϕ singlet and Q is the quencher. They obtained values of $^{kq}/kr$, where kq is the bimolecular quenching rate constant and k_r the unimolecular decomposition rate constant. Using diffusion controlled rate constants for quenching of 1×10^{10} l.mol^{-1}s^{-1} in n-hexane (the co-solvent used), they obtained values for k_r as 1×10^{9}s^{-1} for 2-hexanone, 2×10^{8}s^{-1} for 2-pentanone and 3×10^{6}s^{-1} for n-butyrophenone. (Diffusion controlled rate constants calculated from the Debye expression[46] $k = \frac{8RT}{3000\eta}$ l.mol^{-1}s^{-1} and modified by experience with flash photolysis.[43]) k_r can be taken as the rate constant for formation of the biradical intermediate if this is the route for formation of both acetone and cyclobutanols. They explained the findings of previous workers by the deduction that the triplet excited state is a more important source of type II reaction in 2-pentanone than in 2-hexanone. (ϕII(T)=0.22, ϕII(S)=0.04 for 2-pentanone and ϕII(T)=0.08, ϕII(S)=0.18 for 2-hexanone). Confirmation of the participation of both singlet and triplet states has come from several workers using quenching techniques to measure degrees of singlet and triplet reaction.[8, 47, 48, 49] The results show that the

excited singlets of 2-hexanone and methoxyacetone are sufficiently reactive to react extensively before they decay to triplets unlike 2-pentanone and butyraldehyde. At the same time, the fact that the excited triplets of 2-hexanone and methoxyacetone are also more reactive than those derived from 2-pentanone and butyraldehyde renders quenching of the former less efficient at comparable quencher concentrations.[44]

Reactivity in the elimination reaction is probably largely determined by the nature of the substituents attached to the γ-carbon atom. If the reaction goes through a biradical intermediate, it could be predicted that 2-hexanone or methoxyacetone would react faster than 2-pentanone, as the radical would be more stable in the first two cases. Such a conclusion is in line with the similarity shown by various ketone triplets in intermolecular reactions to the known selectivity of attack by t-butoxy radicals in inter-and intramolecular reactions.[23, 50] Nicol and Calvert[51] have studied the effects of structure on photodecomposition modes in the series of ketones, $n\text{-}C_3H_7COR$ in the gas phase and have established an empirical rule relating quantum yields to molecular structure.

Some interesting results were obtained when the cyclobutanol formation from (S)-(+)-5-methyl-2-heptanone was studied.[52, 31] Partial retention of configuration was observed. No racemisation was observed in the singlet state reaction of this compound (in 5M piperylene). This suggests that reaction from the singlet should be either concerted, or proceed via a spin-paired biradical, which would

cyclise extremely rapidly. The observed racemisation of the starting ketone suggests an explanation for the low quantum yield of these processes (~0.3). Wagner[53, 44] suggested that the likely process which could lower the quantum yield is the reverse of the initial biradical formation reaction; since the triplet reactions occur at rates much faster than any measured radiationless decay process :

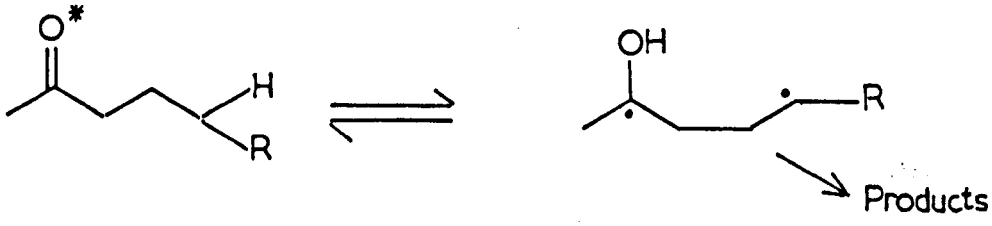

The racemisation would be explained if bond rotation is faster than spin inversion and decomposition to products in the triplet biradical.

Coulson and Yang[54] have produced other findings which point to such an interchange between the γ C-H bond and the carbonyl oxygen as being responsible for the low quantum yields. Quenching experiments indicate that the excited states of 2-hexanone-5,5-d_2 are less reactive than those of normal 2-hexanone, as might be expected. However, the γ-deuterated ketone undergoes type II elimination with approximately 25% greater quantum efficiency. Such behaviour would be explained by a biradical intermediate, as transfer of a deuterium atom would slow down reaction in both directions without effecting the rate of scission or coupling of the biradical.

Wagner and Kemppainen[55] came to a similar conclusion when they studied the quenching of a series of phenyl alkyl ketones with

γ-hydrogens. They pointed out that there is no reason to expect any correlation between triplet state reactivity and quantum yield if a biradical intermediate is assumed. They wrote a mechanism for the decay of the triplet state as :

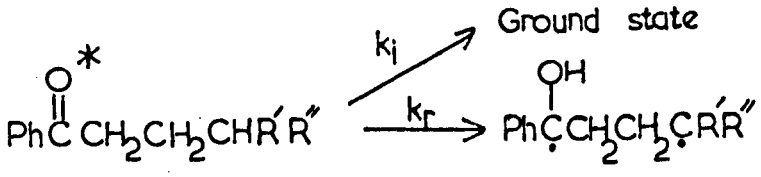

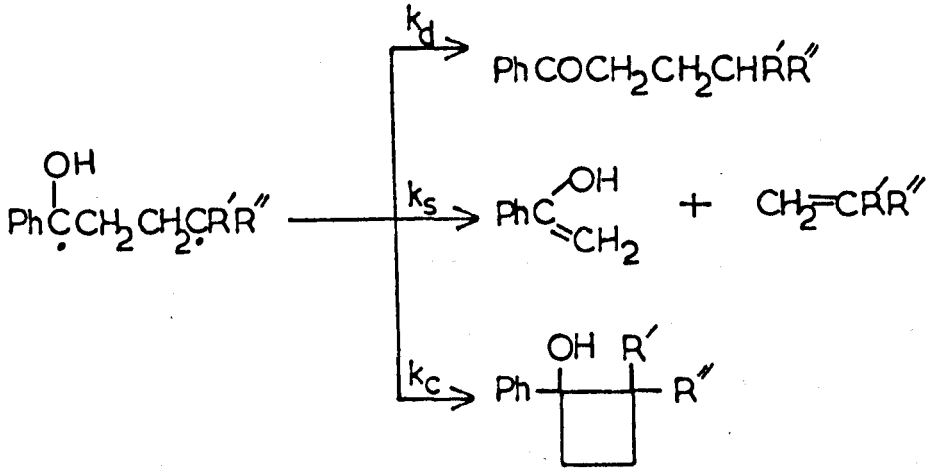

If ϕ BR = the probability that the triplet will form a biradical and ϕ_P = the probability that the biradical will give a type II reaction; then the total quantum yield, $\phi_{II} = \phi_{BR}\phi_P$

$$\text{i.e.} \quad \phi_{II} = \left[\frac{kr}{kr+ki}\right]\left[\frac{ks}{kd+ks+ki}\right]$$

They proposed that $\phi_{BR} = 1$ so that the total quantum yield depends upon the way in which the biradical decomposes, by three reactions with very similar rates. This will be governed by the structure of the

biradical.

Solvent effects have also been studied. It has been found that when irradiation is performed in polar solvents, such as alcohols, the overall quantum yield of the type II process increases to nearly unity in some cases.[56, 53] This effect is explained by invoking hydrogen bonding of the newly formed hydroxyl group in the biradical to a polar solvent molecule. Quenching studies indicate that the lifetime of the triplet state of the ketone does not vary by more than a factor of four among various solvents; so that the interaction of the solvent with the excited state is ruled out. Wagner[53] deduces that the lifetime of the biradical intermediate for valerophenone is somewhat longer than 10^{-10} s.

Barltrop and Coyle[48] carried out a similar series of experiments. They studied the solvent effects of four solvents (benzene, cyclohexane, methanol and t-butanol) on the intramolecular photochemistry of three ketones with primary, secondary and tertiary γ-hydrogens (2-pentanone, 2-octanone and 5-methyl-2-heptanone). They determined the quantum yields for the diminution of ketone and the formation of cyclobutanol, for each ketone in each solvent and also for each ketone in each solvent made 5M in piperylene. They assumed that in the latter cases they were observing singlet reaction only and that the mixed solvent was still efficient in solvating the biradical intermediate, if present. (Wagner[53] has shown that 25% alcohol in hydrocarbon solvents is efficient in solvating the biradical). Their results show that the triplet reaction is effected by solvent with the overall quantum yield tending towards unity in t-butanol, whilst

the singlet part of the reaction is unaffected by solvent. (This agrees with Yang[31]). They also measured rate constants for triplet intramolecular hydrogen abstraction by studying quenching in benzene. Their conclusions were that a triplet biradical is involved and that in the triplet excited states of aliphatic ketones intramolecular hydrogen abstraction is more favourable for a tertiary, than a secondary, than a primary γ-hydrogen atom. Also the ratio of singlet to triplet reaction increases as the rate constant for triplet abstraction increases, suggesting that the rate constant for singlet hydrogen abstraction also increases in the same order, if the rate of inter-system crossing is assumed equal for all three ketones.

Yang, Elliot and Kim[57, 31] have published similar findings to Barltrop and Coyle and interpret them to produce a complete picture of the reactions of alkanones with γ-hydrogens. They studied the three ketones: 2-pentanone, 2-hexanone and 5-methyl-2-hexanone, and in addition to observing the singlet and triplet reactions, as above, they also measured the inter-system crossing yield by following the triplet sensitised isomerisation of 1,3-pentadiene.[58] The lifetime of the singlet states were measured from slopes of Stern-Volmer plots ($K_q\tau_s$) using biacetyl as the energy acceptor in the presence of piperylene. From these data, they estimated values for the internal processes taking place in the three ketones. The results indicate that the rates of inter-system crossing for these compounds remain essentially the same ($3 \times 10^8 s^{-1}$) whilst the efficiency of inter-system crossing (Øst) decreases from primary to tertiary γ-hydrogens. The decrease in Øst is attributed to the increase in both the rate of

chemical reaction from the singlet state (k_s) and in the rate for non-radiative decay from the singlet state (k_{-s}). There is also a gradual decrease in the singlet state lifetime along the series. Clearly, both k_s and k_{-s} depend on the strength of the γ-H bond. As the bond energy decreases, these rates increase. Since k_{st} does not vary appreciably in this series, the results strongly imply that a chemical process may be involved in the rate of radiationless decay from the singlet excited state (k_{-s}). They propose that such a process is the abstraction of γ-hydrogen by the excited carbonyl group to form a singlet 1-4-biradical. This biradical can either give products or return to the starting ketone as in the case of the triplet biradical, but differs from the triplet case in that it may undergo chemical transformations without spin inversion.

They reinforce this conclusion by showing that 6-hepten-2-one (I) forms, amongst other products, 1-methyl-3-cyclohexenol (II) in the presence of piperylene (i.e. from the singlet state).

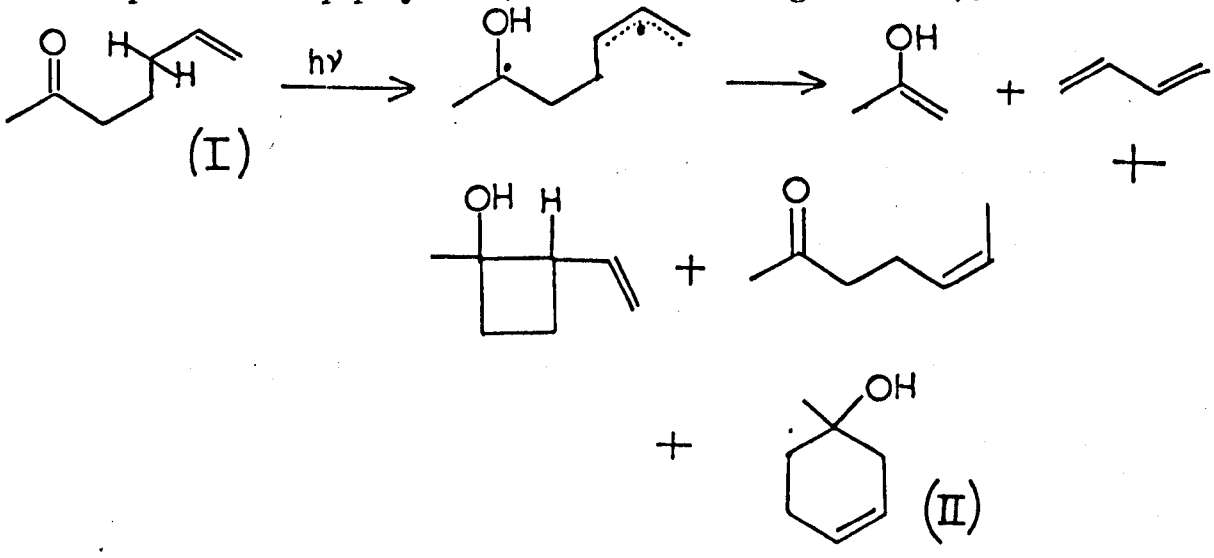

(I) (II)

This can be readily accounted for with a biradical intermediate. A concerted mechanism from the singlet state would require a highly strained transition state. The low efficiency of photolysis of certain ketones in solution, such as n-butyl, t-butyl ketone[59] is explained by an increase in k_{-s} which causes a decrease in intersystem crossing yield. This suggestion that chemical reaction may be involved in non-radiative decay is in agreement with theoretical work by Heller.[60]

A recent paper has cast some doubt on the findings of earlier workers on the quenching of ketone photoreactions by piperylene. Wettack et. al.[61] have shown that, contrary to earlier work in the gas phase,[62, 8] piperylene does quench the singlet excited states of acetone, 2-pentanone and other molecules. They observed quenching of the fluorescence of these compounds by the diene and obtained good Stern-Volmer plots to give values of the singlet quenching rate constant of about $10^7 l.mol^{-1}s^{-1}$. Since the lifetime of the singlet state of alkyl ketones is of the order of a few nanoseconds, it is clear that singlet interaction only becomes important at high diene concentration. However, as these conditions are used to determine the proportions of singlet and triplet excited state reaction in the type II reaction, earlier values are subject to correction. For 2-pentanone they calculate that the error in ϕs is a factor of 2, whilst for 2-hexanone it is a factor of 1.25. They quote a modified Stern-Volmer expression for the quenching of a reaction taking place from both singlet and triplet excited states by a quencher of both states.

They predict from this that when $k_{1q}\tau_s < k_{3q}\tau_t$, which is the case for quenching of the type II reaction at high concentration of quencher, the plot of ϕ^o/ϕ will approach a linear asymptote of slope $k_{1q}\tau_s(1+ \phi t/\phi_s)$. ($k_{1q}$ is the singlet quenching rate constant and k_{3q} is the triplet quenching rate constant. τ_s is the singlet state lifetime and ϕ_s is the quantum yield of reaction via the singlet state). This slope is 0.265 $l.mol^{-1}$ for 2-pentanone and hence about 70% of the type II reaction emanates from the triplet state, which agrees with the figure of 65% found in the gas phase.[8] (Wagner and Hammond's figure is around 90%). These results also mean that inter-system crossing yields calculated from the sensitised cis-trans isomerisation of diolefins are in doubt, e.g. the results of Yang.[57]

Borrell and Sedlar[63] have suggested a new way of determining the relative proportions of the internal process in type II photo-eliminations. They studied the quenching of the type II reaction in 2-pentanone using cyclohexene as a quencher. In earlier work on the photolysis of acetone-cyclohexene mixtures,[64] it was shown that quenching effects may be due to chemical reaction rather than energy transfer. With acetone, they observed hydrogen abstraction and oxetane formation with cyclohexene which is in agreement with other workers.[65, 16] In their recent work, they show that for cyclohexene, chemical reaction rather than energy transfer is responsible for the apparent inhibition of the photoreactions of 2-pentanone and that the efficiency of the reaction is equivalent to that of physical quenching. They showed that the extent of chemical reaction can be used to monitor that fraction of the molecules lost from the triplet state

by radiationless decay and so built up a complete picture of the breakdown and energy transfer occurring from the excited states.

The experiments were performed at 313 nm using the capillary technique (see the experimental section) and solutions of 2-pentanone (0.9M) in benzene. They followed the rate of production of acetone and the rate of diminution of ketone for various concentrations of added cyclohexene. The quantum yields were also measured. It was found that although the production of acetone was partly quenched, in the usual way, the rate of consumption of pentanone increased with increasing cyclohexene concentration. It was shown that this increase was due to chemical reaction between the cyclohexene and the triplet state of the ketone.

Summary

The best information available at the present time suggests that alkanones with γ hydrogens react almost exclusively via the type II process and cyclobutanol formation and that these products originate from the lowest excited singlet and triplet n,π^* states of the ketone. It seems that the process goes through a 1,4-biradical intermediate in each case but that this biradical exhibits different chemical behaviour when the radical spins are paired or unpaired. The inefficiency of the type II process is attributed to efficient radiationless decay of the excited electronic states via these

biradical intermediates.

The work described in Chapter 4. was carried out in an attempt to extend the method of Borrell and Sedlar for different ketones and solvents.

1.6 Photochemical Cis-Trans Isomerisation

Cis-trans isomerisation is one of the most widely studied of simple reactions. Its study has led to important information concerning the energy states of the double bond. As a reaction it has been extensively studied both from a preparative and a mechanistic point of view. Geometrical isomerisation can be brought about thermally, catalytically and photochemically. All three processes have been reviewed by Cundall.[76] The main concern of this review is the mechanistic study of photochemical cis-trans isomerisation, though thermal results are mentioned where relevant.

Most mechanistic studies have concentrated on simple molecules such as substituted ethylenes and butadienes. Many more complex molecules exhibit such isomerism and have been studied to a greater or lesser extent. Probably the most work has gone into the study of the isomerisation reaction in the stilbenes and their substituted analogues and this is reviewed below (Section 1.6(c)). The photo-isomerism of many compounds can be of considerable interest to the synthetic organic chemist as it represents a useful method of producing the thermodynamically less stable isomer in most cases. The reason for this is that usually the trans isomer absorbs light of longer wavelength more intensely than the cis. If such a wavelength is chosen to irradiate a trans isomer then a photostationary state will eventually be reached where the cis is predominant over the trans due to the pumping effect of the different extinction coefficients. (Assuming there is no other photochemical reaction taking place). The photostationary

state ratio of isomers is given by

$$\text{cis / trans} = K\varepsilon \text{ trans}/\varepsilon \text{ cis}$$

where K is a constant and ε the extinction coefficient at the wavelength used.

1.6(a) Simple Olefins

The simplest model for the understanding of photoisomerisation is ethylene, though unless it is labelled with deuterium the cis and trans isomers are indistinguishable. In 1930 Olsen[77] suggested that photochemical rearrangement reactions might be understood in terms of the properties of the potential energy curves for the excited electronic states of the molecule. 10 years later Lewis[78] and Eyring[79] and their co-workers applied this qualitative approach to a simple model describing hindered rotation about the double bond and thereby provided a new impetus for experimental work on this problem. Following on from this work, Mulliken and Roothan[80] used molecular orbital theory to calculate the potential energy curves of the lowest electronic states of ethylene as a function of the angle of twist about the double bond (Fig. 1.3). It is clear that the ground state for the perpendicular form is the triplet, T_1. Two paths are available for thermal isomerisation of an ethylene-like molecule. A low energy path requiring inter-system crossing at a and b may prevail or the molecule may remain in the singlet state for which the activation energy is considerably higher. Photochemical isomerisation starts from energies above S_o and T_1 and either excited singlet or triplet states may serve as intermediates for isomerisation. Conversion from either of these

Fig. 1.3 Ref.(2)

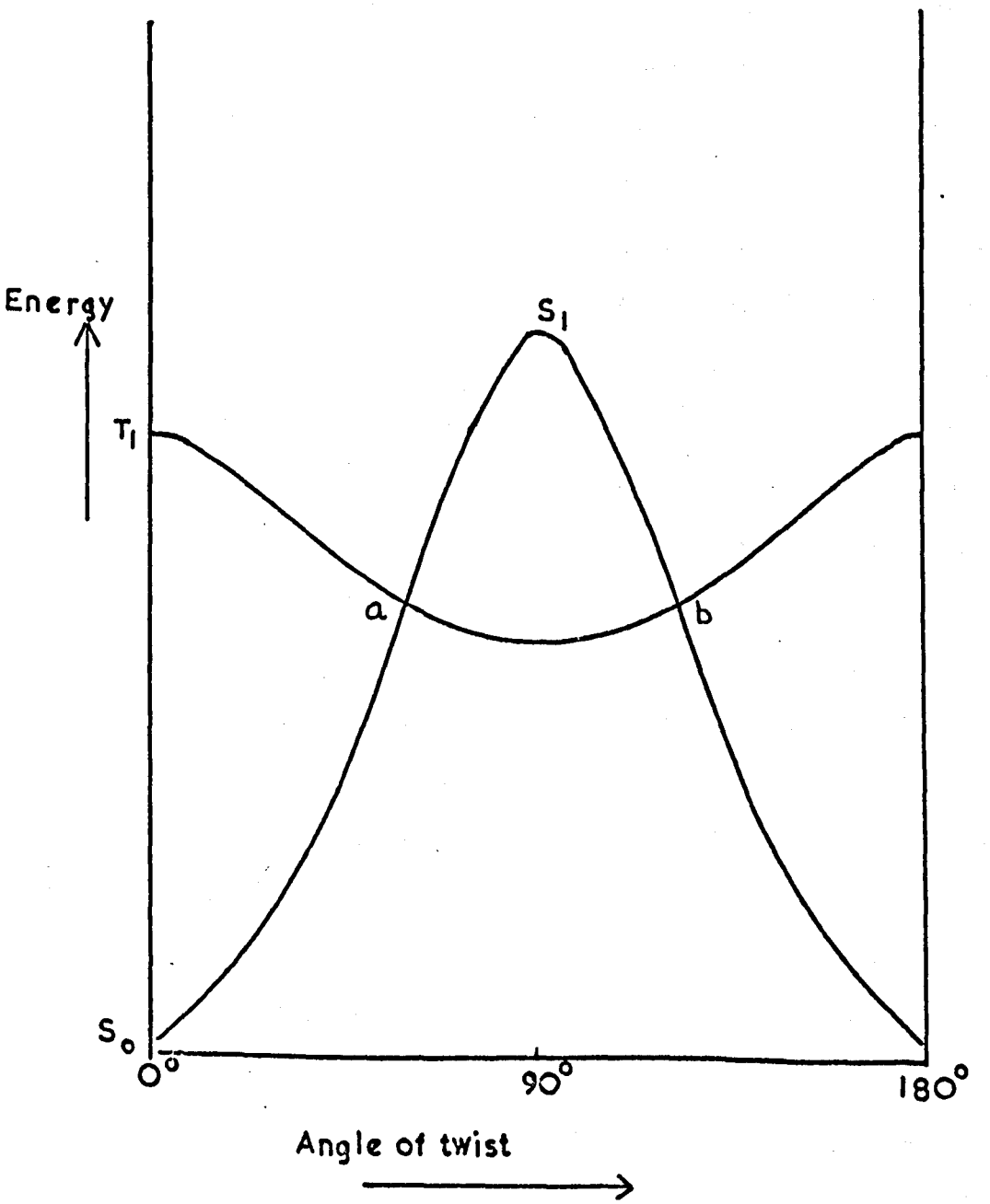

states may produce a vibrationally 'hot' ground state in which isomerisation is possible.[81] (Ultraviolet light of 200 nm wavelength is equivalent to 600 kJ mol^{-1} if absorbed).

The photoisomerisation of simple olefins is not easily studied by direct absorption of light as they do not absorb at wavelengths greater than 200 nm. Due to the high energy of the light absorbed dissociation becomes the predominant photoprocess although some isomerisation is observed, e.g. in cis-but-2-ene.[76] Okabe and McNesby[82] have studied the photolysis of $C_2H_2D_2$ at 185 nm but did not examine the cis-trans isomerisation. Grabowski and Bylina[83] studied the isomerisation of dichloroethylene directly excited to the triplet state by saturating with oxygen at 130 atmospheres. They suggested that a common intermediate triplet state is involved as they found that the sum of the forward and backward quantum yields are unity. The isomerisation of simple olefins has also been studied using photosensitisers to excite compounds that do not absorb in an accessible region of the spectrum. In the gas phase, mercury 6^3P_1 atoms have been used to photosensitise the isomerisation of dideuteroethylene[84] and but-2-ene.[85] All the features of the latter reaction can be explained by a vibrationally excited triplet state which can decompose or lose vibrational energy by collision. The benzene photosensitised isomerisation of but-2-ene has also been followed by the same workers.[85, 86] when again a common triplet state was implicated. Borkman and Kearns[87] have studied the cis-trans isomerisation of pent-2-ene in the liquid phase photosensitised by acetone. They found that energy

transfer from triplet acetone to pent-2-ene is virtually 100% efficient and measured rate constants for the reaction in various solvent systems.

1.6(b) Conjugated Compounds

Excitation is brought about by light of longer wavelength if the double bond is conjugated with a chromophore or another double bond. As the energy of the light absorbed drops, the probability of simple intramolecular reaction taking place rather than decomposition increases. Studies of trans-2-methyl-buta-1,3-diene at 254 nm indicate that cis-trans isomerisation is accompanied by the formation of 4-methyl cyclobutene and polymers.[88] If the diene function is conjugated with a phenyl group as in 1-phenyl-1,3-butadiene significant absorption above 300 nm is observed in ethanolic solution and cis-trans isomerisation takes place.[89] The same is observed with 1,4-diphenyl-1, 3-butadiene.[90] With some highly conjugated compounds isomerisation by daylight is observed. In indigo isomerisation may even proceed in the solid state.[91]

The mechanism of isomerisation of dienes in solution has recently been the subject of investigation. Saltiel et al.[92] propose that direct isomerisation of 2,4-hexadiene occurs from the singlet state via two cyclopropylmethylene radicals which then rearrange to the three geometrical isomers as shown overleaf.

S_1

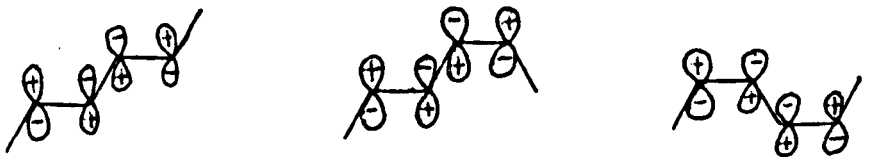

(tt) (ct) (cc)

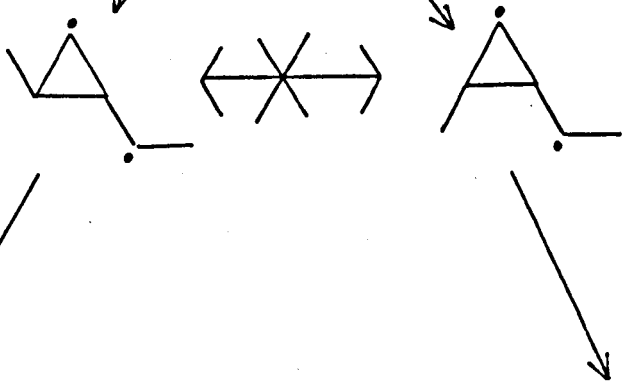

$\alpha(tt) + (1-\alpha)(ct)$ $\beta(cc) + (1-\beta)(ct)$

The benzophenone sensitised isomerisation of 2,4-hexadiene has been shown to proceed via common triplet state diene intermediates, transfer of triplet excitation to any of the three diene isomers leading to isomerisation of both double bonds.[93, 94] These results can be explained by assuming either a 1,4-biradical geometry for the common triplet state or the intermediacy of 2 rapidly equilibrating triplets of the allylmethylene type.[93]

In another recent paper[95] Boué and Srinivasan propose a similar pair of non-converting biradical intermediates for the direct isomerisation of cis and trans-1,3-pentadiene and to explain the observed formation of 1,3-dimethylcyclopropene at different rates from the two isomers.[96] They suggest that this different reactivity of the cis and trans forms is only explained if the lifetimes of the excited singlets is as small as the order of the time of rotation about the $C_3 - C_4$ bond in 1,3-pentadiene. The short radiative lifetime of the excited singlets of 1,3-dienes makes this a possibility.[97] The photosensitised isomerisation of the 1,3-pentadienes shows similar trends to the stilbene work discussed below.[98, 99] An interesting new result was observed by Hurley and Testa[100] who determined the quantum yield of isomerisation of cis-1,3-pentadiene photosensitised by benzophenone. They found that the apparent triplet yield of benzophenone rises linearly with pentadiene concentration exceeding unity at concentrations above 1 mol $l.^{-1}$ They suggested that a biradical mechanism was operative such as

$$P^3 + \text{cis-P} \longrightarrow \text{(biradical)} \longrightarrow \alpha\text{cis-P} + (2-\alpha)\text{trans-P}.$$

Fig. 1.4 Adapted from ref. 101 p. 256

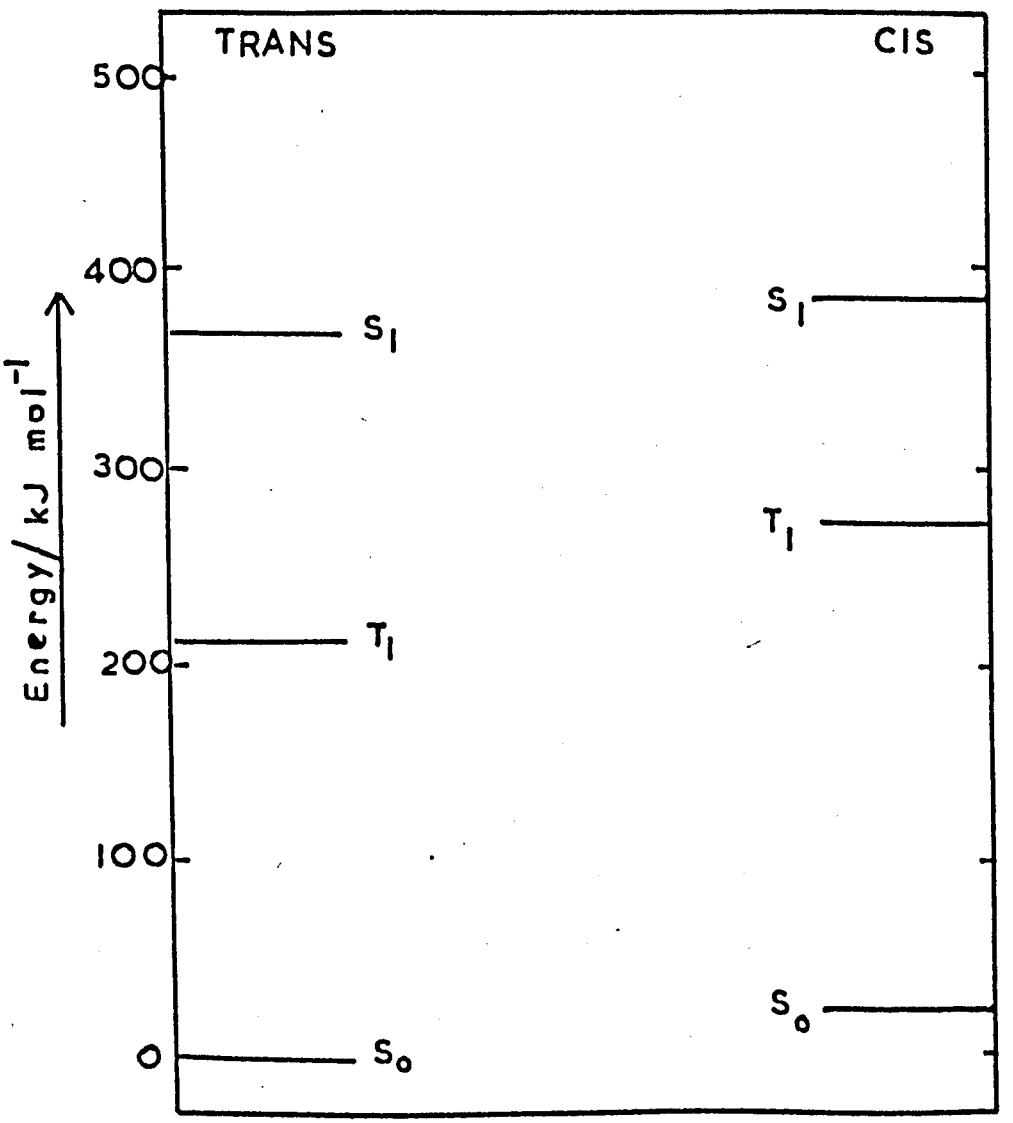

1.6(c) Stilbene

Stilbene (1,2-diphenyl ethylene) is a model compound for photoisomerisation studies. It was chosen for its highly conjugated nature so that it absorbs in the most convenient region of the spectrum for photochemical study. The cis and trans isomer of stilbene are well defined and easily purified. The relative energies for the ground state and lowest excited states of the stilbenes are shown in Fig. 1.4.[101] They were obtained from both spectroscopic and thermal measurements.[102] No phosphorescence has been observed from either of the stilbenes. Fluorescence is efficient from the trans isomer[103] but weak and unstructured from the cis.[104]

(i) Direct isomerisation

Independence of the cis to trans or trans to cis quantum yields on the wavelength of the exciting light eliminates the participation of singlet states higher than S_1. The remaining routes available could be via S_1, T_1 or a 'hot' ground state. Fischer et al.[105] have shown that as the temperature is lowered to below 100K ϕ_t (the quantum yield for *trans* to *cis*) drops whilst ϕ_c (quantum yield *cis* to *trans*) is unaffected. At the same time the fluorescence quantum yield increases above that at room temperature. This suggests that an activated process such as internal conversion or inter-system crossing competes with fluorescence from S_1 and that this process is an essential step in the mechanism of isomerisation. They suggested that this process is the formation of T_1. However, attempts to detect long-lived triplet state intermediates by means of phosphorescence or triplet absorption spectroscopy have failed. The same workers[106]

have shown that Øt is enhanced in a heavy atom solvent at low temperatures, maintaining its room temperature value at 170K. They also noticed internal enhancement of Øt in stilbenes with localised n, π* triplets such as 4-nitro-stilbene giving Øt independent of temperature. In high viscosity media it was found that fluorescence was uncoupled from trans to cis isomerisation.[106, 107] Thus for stilbene in glycerol at 193K, Øt = 0.001 whilst Øf (quantum yield for fluorescence) = 0.46. In a hydrocarbon solvent Øt = 0.22 and Øf = 0.35. This is ascribed to the fact that stilbene in the cis form occupies a larger volume in solution than the trans form. They suggested that in high viscosity media, isomerisation practically stops but inter-system crossing continues so that Øf is effectively unaltered.

As a result of these and other observations, they predicted the scheme of isomerisation shown in Fig. 1.5.[105] S_1 can decay by three processes: fluorescence, F, internal conversion S_1 to S_o, b, and inter-system crossing to triplet, d. They proposed that state X is a twisted triplet state and that isomerisation is constituted by steps f + g' and f' + g. Dependence on temperature is due to step d which is an activated process (approx. 5 kJ mol^{-1}) whilst viscosity dependence is due to steps f, g' or both. In high viscosity media the isomerisation step can be by-passed by one of the several processes returning to the ground state. (From the trans isomer: g, h or b). The major assumption that direct isomerisation proceeds via a triplet state is supported by experiments carried out in methyl iodide[108] when the singlet-triplet transition is seen in absorption at 436 nm. They

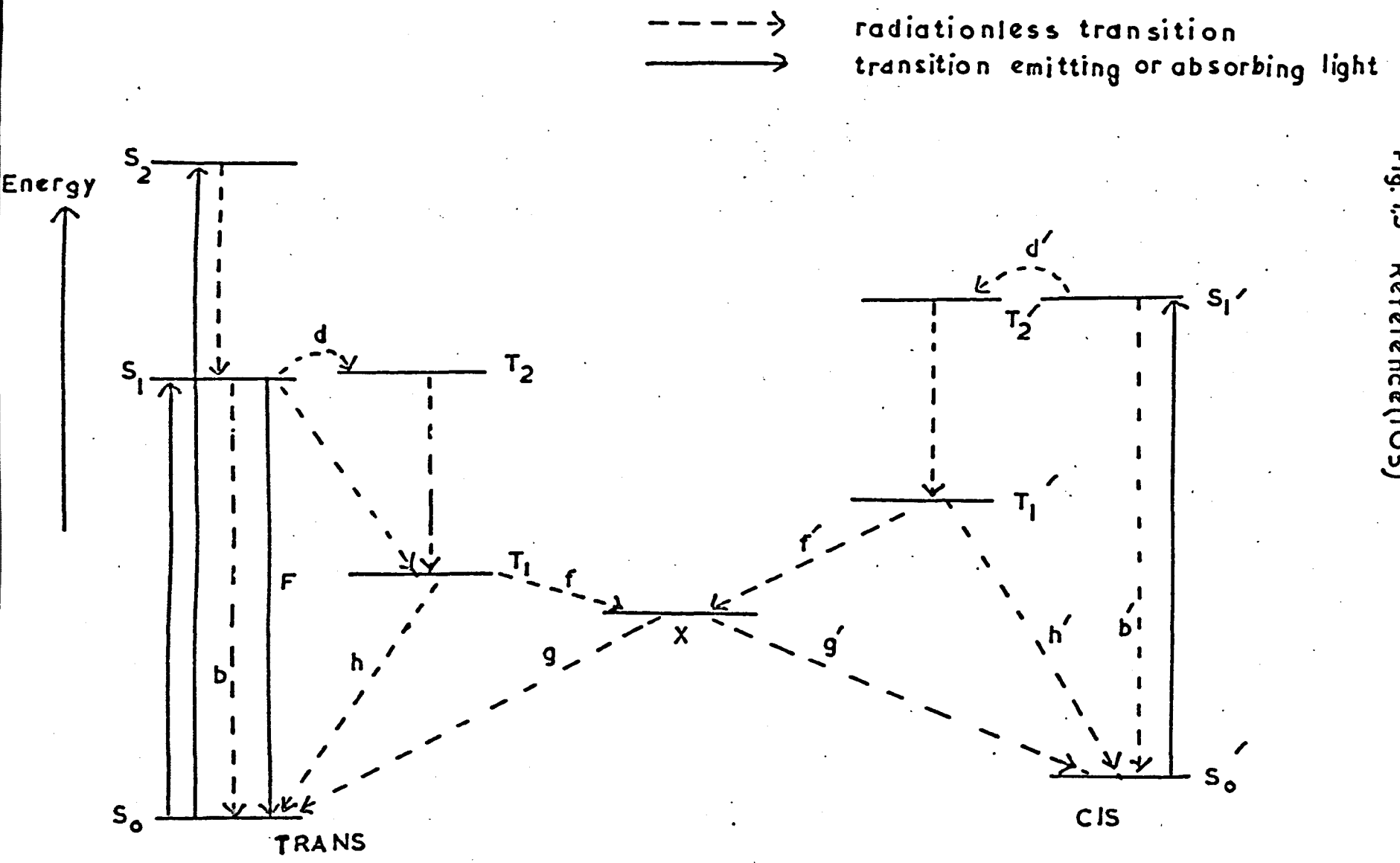

Fig. 1.5 Reference(105)

found that isomerisation under these conditions proceeds at ten times the rate in hydrocarbon solvents, though free iodine may have caused some catalytic effect in methyl iodide.

Theory predicts that perdeuteration should decrease the rate of radiationless transitions by inhibiting a kind of tunneling between the zero vibrational level of the excited state and high vibrational levels of the lower state.[109] Saltiel[110] found no deuterium effect on direct cis-trans isomerisation in the stilbenes, but since the energy gap between S_1 and available triplet states is very small, no deuterium effect on inter-system crossing is expected.[111] The Fischer mechanism described above accounts for the absence of a deuterium effect. However, Saltiel argued that a triplet mechanism is unlikely since azulene does not show the expected effect on direct isomerisation photostationary states.[112] If triplet states are involved then the slopes obtained from azulene quenching should depend on solvent viscosity. This was shown not to be the case in the direct isomerisation though it was the case in the photo-sensitised isomerisation.[113] This was explained by assuming that singlet energy transfer to azulene takes place over long distances in solution whilst triplet energy transfer requires approach to collisional diameters,[114] so that only the latter is viscosity dependent. Assuming singlet energy transfer to azulene, Saltiel et al.[113] derived the minimum distance of approach by experiment and found it to agree very well with that predicted by the Förster theory.[114]

The direct isomerisation of the stilbenes was then assumed to take place through rotation of the central bond in S_1 to a common

twisted singlet state p^1. ('phantom' singlet).

$$t^1 \rightarrow p^1$$
$$c^1 \rightarrow p^1$$
$$p^1 \rightarrow \mu t^o + (1-\mu)c^o$$

(c = cis, t = trans and μ is a constant)

It was suggested that a small activation energy of about 8kJ mol^{-1} for t^1 - p^1 rotation would account for the observed temperature effects and that the absence of trans-stilbene fluorescence from cis-stilbene[102] is accounted for if the energy of p^1 is low relative to t^1. The singlet mechanism for direct isomerisation is now generally accepted[115] though certain findings of Fischer et al. remain unexplained.

(ii) Photosensitised isomerisation

The photosensitised isomerisation of the stilbenes is of considerable interest. It was found that different triplet energy donors give rise to different photostationary state compositions[98, 116] (Fig. 1.6). Three types of measurement have been made: quantum yields of sensitised cis-trans isomerisation, measurement of photostationary state composition following prolonged irradiation and flash spectrophotometric measurements of the rate of decay of sensitiser triplets in the presence of isomerisable olefins. The following simple scheme can be applied :

Fig.1.6 Ref. (118)

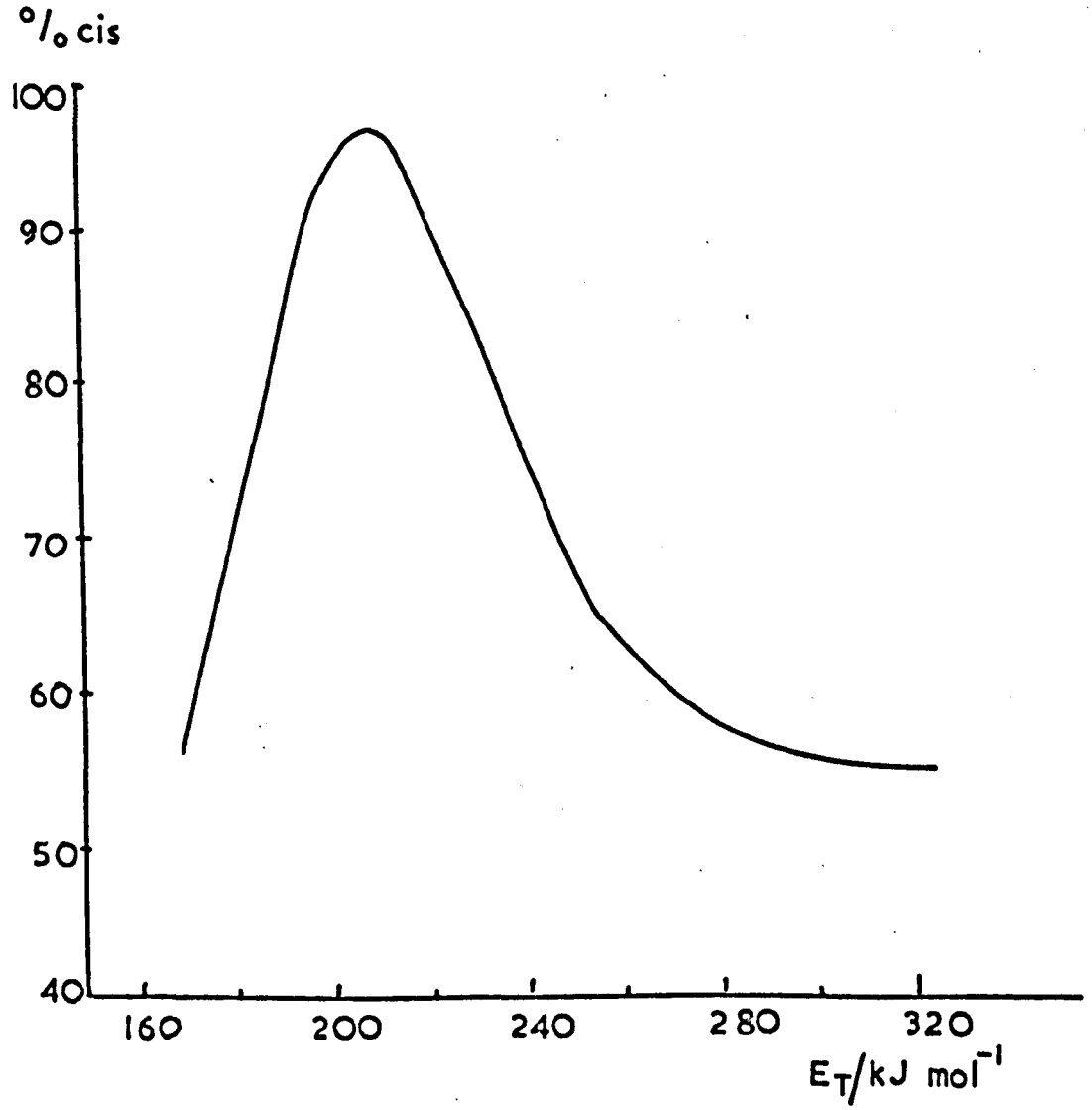

$D \rightarrow D^1$ excitation

$D^1 \rightarrow D + h\nu$ fluorescence, kf

$D^1 \rightarrow D^3$ inter-system crossing, kic

$D^3 + c \rightarrow D + T$
$D^3 + t \rightarrow D + T$ } energy transfer k_1 k_2

$T \rightarrow c$
$T \rightarrow t$ } decay to ground state kc kt

(D is the sensitiser, superscripts 1 and 3 indicating excited singlet and triplet states. c and t are the cis and trans isomers and T is a common twisted state). Data seem to indicate that there is a small barrier between transoid and non-planar (or cisoid) triplet states for the stilbenes though this does not appear to be the case with α-methylstilbene.

Applying stationary state theory :

$$[\text{cis}]/[\text{trans}] = (k_2/k_1) \times (k_c/k_t)$$

= excitation ratio x decay ratio

Sensitisers with triplet energy greater than cis (239 kJ mol^{-1}) and trans (210 kJ mol^{-1}) by at least 9 kJ mol^{-1} should transfer energy at the same diffusion-controlled rate to both isomers. If the decay ratio is independent of sensitiser, a constant high energy value for [cis]/[trans] should be obtained. As the sensitiser energy is varied between 239 and 210 kJ mol^{-1}, the mixture should become rich in cis due to the fall off in energy transfer to the cis isomer. As the energy falls below 210 kJ mol^{-1}, it is expected that the stationary state will again level off leading to an extremely cis rich mixture.

The actual experimental results shown in Fig. 1.6 do not obey this theory in the low energy region. The explanation originally

proposed by Hammond et al.[98] was that energy transfer can take place to cis stilbene to give a non-planar transoid excited triplet. This they called the phantom triplet since such transitions cannot be observed spectroscopically as they would violate the Franck-Condon principle. The process involved is so-called non-vertical energy transfer and is only considered to be important in flexible molecules having significantly different geometry in ground and excited states. The key postulate is that energy transfer with non-vertical excitation of the acceptor may occur when vertical transitions are forbidden for energetic reasons.

For the stilbenes the photostationary state becomes more trans rich as the concentration of the sensitiser is increased, for sensitisers of low triplet energy. Thus it appears that back transfer from the stilbene triplet to sensitiser gives the trans ground state. If the sensitiser concentration is kept constant, a similar increase in trans isomer in the photostationary mixture is observed as the concentration of added azulene is increased. This 'azulene effect' is independent of the sensitiser used demonstrating that the same species is being quenched in all cases. Since deactivation to the trans ground state is the result of quenching by azulene and sensitiser the geometry of the stilbene triplet was assigned as trans-planar, i.e. there is a minimum in the potential energy vs. twist curve near trans-planar geometry.[117]

Confirmation of this theory was obtained by Hammond and Herkstroeter.[118] They studied energy transfer rates by following the decay of sensitiser triplets with triplet-triplet absorption spectro-

scopy in flash photolysis experiments. It is found that the rates of energy transfer to the cis isomer fall off much more slowly with sensitiser triplet energy than is expected from energetic considerations. This fits in with the postulate of non-vertical energy transfer. With α-methylstilbene this process is inferred to be operative in both isomers.

The results for cis stilbene and both isomers of α-methylstilbene are best explained by invoking excitation to twisted excited states. Thus the term 'non-vertical excitation' is an appropriate one to describe the overall process. However, whether or not a non-vertical transition violating the Franck-Condon principle ever occurs is open to question. Such non-Franck-Condon phenomena are not needed to explain the results. They can be rationalised entirely on the basis of vibrationally 'hot bands' expected in the absorption spectra of the acceptor.[119] Furthermore, it is doubtful that the isolated molecule is an adequate model since relatively long times are involved in the non-vertical excitation process and should allow for vibronic coupling of the donor and acceptor. These possibilities are discussed by Lamola in his recent review of energy transfer processes.[117]

Non-vertical energy transfer has been invoked in other systems to explain results obtained in the photosensitised interconversion of quadricyclene and norbornadiene[120] and the cis-trans isomerisation of 1,2-diphenyl-cyclopropane.[121] However more recent studies have shown that the excited singlets of the sensitisers are involved.[122]

Saltiel[110] has shown that there is no loss in efficiency in the sensitised isomerisation of perdeuterostilbene compared with

stilbene. From this he concluded that the triplet decay ratio is not affected by deuteration. However measurements in glassy media at 77K show that perdeuteration increases the lifetime of stilbene triplets by 30%.[123] He also showed that the rate of decay from the twisted triplet state is sensitive to viscosity and temperature. From these results and those on the direct isomerisation, he deduces a possible potential energy diagram for the lowest excited electronic states of the stilbenes (Fig. 1.7(a)). Borrell and Greenwood[124] have carried out some self-consistent field M.O. calculations to predict the theoretical potential energy diagram for the stilbenes. Their results are shown in Fig. 1.7(b). The agreement between the two is good considering the assumptions involved in both cases. The major difference is the maximum in the triplet curve which is predicted by Saltiel close to trans-planar geometry and is absent in the theoretical curves. However, other calculations do predict this maximum.[125] As well as fitting in with the isomerisation results, the theoretical curves explain the fluorescence and phosphorescence behaviour mentioned above.

Apart from yielding some understanding of triplet energy transfer and the behaviour of excited states, the studies of cis-trans isomerisation have pointed to several useful applications two of which are described below:

(A) The change in cis-trans stationary state composition with the energy of the triplet excitation donor gives a 'chemical spectrum' of the substrate isomers (e.g. Fig. 1.6). Analysis of this spectrum can yield information about the triplet energies of the substrate

Fig. 1.7(a) Reference (110)

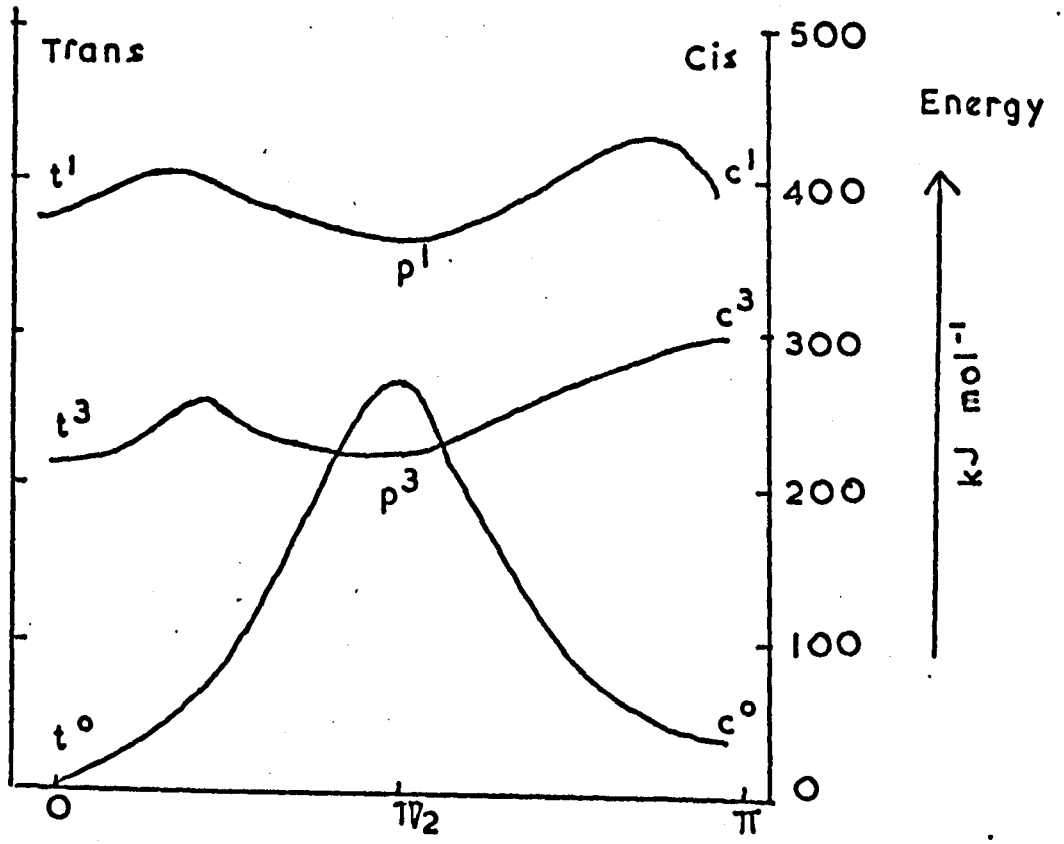

Fig. 1.7(b) Reference (124)

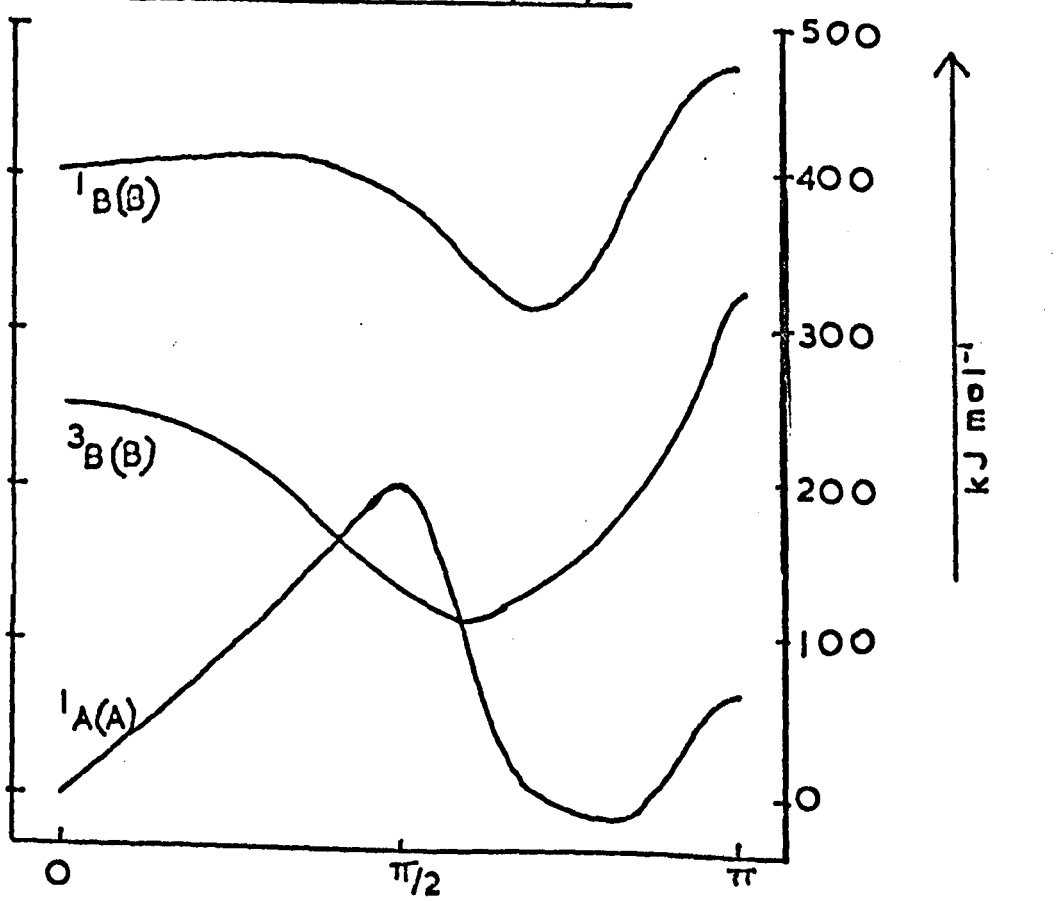

isomers.

(B) Lamola and Hammond[58] have shown that the quantum yield for photosensitised cis-trans isomerisation of an olefin is a function of three variables: the yield of sensitiser triplets produced by inter-system crossing, the efficiency of energy transfer to the olefin and the triplet decay ratio of the olefin triplet. Flash photolysis work has shown that triplet energy transfer is 100% efficient in most cases, even at low acceptor concentrations. If this is the case then it can be shown that the inter-system crossing yield is obtained by summing the quantum yields of isomerisation in each direction, thus :

$$\phi c + \phi t = \phi ic$$

(iii) Systems related to stilbene

Work on stilbene has stimulated studies of the photo-isomerisation of related systems. The isomerisation of azobenzene has been studied both experimentally and theoretically.[126, 127] Isomerisation seems to take place in the excited state which does not have an energy minimum in the twisted configuration. Saltiel et al.[128] have studied a model for the trans-excited state of stilbene by investigating the photochemistry of the indeno-inden,

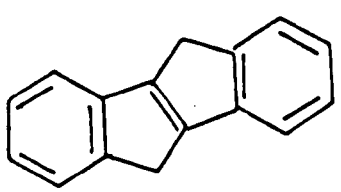

Results from this study show that the quantum yield of fluorescence is 0.94 and is independent of temperature in contrast to the

observations on trans-stilbene; but they are in agreement with a singlet mechanism.

The introduction of other aromatic moieties into the stilbene structure has been studied. The isomerisation of β-styrylnaphthalene[129] and 1,2-bis(4-pyridyl)ethylene[130 - 132] has been reported. In the latter case internal conversion from the excited singlet state to the ground state is found to be an efficient process and the direct isomerisation is thought to proceed via a triplet mechanism in contrast to the stilbenes. They suggest that the enhanced rate of internal conversion is due to the formation of an unstable ground state isomer which then returns slowly to the starting material. Such an unstable intermediate may be a valence tautomer of the olefin.[131]

Another study has followed concentration effects in the photochemical isomerisation of difuryl- and dithienyl - ethylene.[133] It was found that the trans/cis isomer ratio was dependent on the total concentration of substrate as was found with 4-nitro-4'-methoxystilbene. They interpreted their results in terms of collisional quenching of the twisted excited states by ground state trans molecules.

1.6(d) Photoisomerisation in Unsaturated Carbonyl Compounds

The photochemistry of enones and unsaturated diketones has been investigated in depth[134, 135] though kinetic studies of cis-trans isomerisation are few. The photochemistry of enones can be compared to that of a simple ketone or diene in that the reactions of the enone excited state can be expected to exhibit greater polar character

than that of the corresponding diene. Cis-trans isomerisation is a common and probably general primary process in α,β-unsaturated carbonyl compounds. In addition, ketones possessing a hydrogen atom on the carbon γ to the carbonyl group may undergo a variant of the Norrish type II reaction when intramolecular hydrogen abstraction is followed by deconjugation to form a β,γ -isomer. (See 1.3). This reaction seems to take place from the cis isomer of the starting compound. This deconjugation reaction is not general and several ketones give no evidence of this reaction. This lack of reactivity might result from a rapid relaxation to an appreciably twisted geometry in the triplet state. Alternatively it has been suggested that the unreactive ketones have n,π* excited triplets that decay very rapidly to relatively unreactive π,π* triplets.[136]

The gas phase photochemistry of pent-3-en-2-one has been studied and it was found that at 313 nm and temperatures up to 540K the only significant reaction is cis-trans isomerisation. The nature of the excited states involved is not clear.[137 - 139] The cis-trans isomerisation of enediones has also been noted, though not studied in any great detail.[140]

Many α,β-unsaturated acids and their derivatives undergo the primary process of cis-trans isomerisation. One of the earliest photochemical isomerisations observed was that of cinnamic acid.[141] This reaction has been studied in more detail recently and it is shown that the reaction can be brought about in the solid and liquid phases but in the former dimerisation to truxillic and truxinic acids

predominates.[142 - 144] The ultra-violet induced isomerisation of tiglic to angelic acid (2-methyl-2-butenoic acid) was first noted by Pelletier and McLeish[145] when powdered tiglic acid was irradiated with a 500W lamp for many hours, though no mechanistic study has been done on these compounds. Another compound that has been studied in this class is fumaric/maleic acid.[146]

Recently a certain amount of interest has been shown in the isomerisation of compounds containing a double bond out of conjugation with a suitable absorbing chromophore. Isomerisation can be brought about by intramolecular energy transfer if the chromophore is excited with a suitable wavelength. Such a compound is 1,1-dimethyl-1-benzoyl-2,4-pentadiene

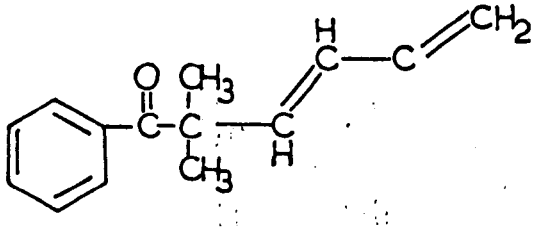

Leermakers et al.[147] showed that excitation of this compound with light of wavelength greater than 260 nm brings about excitation of the carbonyl moiety and then triplet intramolecular energy transfer to the diene function after rapid inter-system crossing. Cowan and Baum[148] have carried out a similar study of intramolecular energy transfer by following cis-trans isomerisation in the compound

shown below

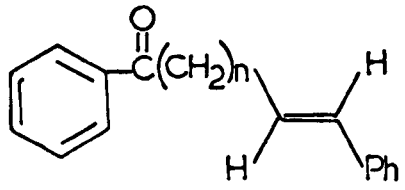

, where n= 1-4.

They found rate constants for intramolecular energy transfer varying from $7.2 \times 10^{10} s^{-1}$ when n = 1, to $3.3 \times 10^{9} s^{-1}$ when n = 4.

1.6(e) Photoisomerism in α,β-unsaturated esters

The cis-trans isomerisation of α,β-unsaturated esters has been studied as 'fall-out' from the well documented studies of photo-$\overset{de}{\wedge}$conjugation reactions to the β-γ-esters.[149 - 155]

In particular, Barltrop and Wills[155] studied the isomerisation of ethyl crotonate/isocrotonate.

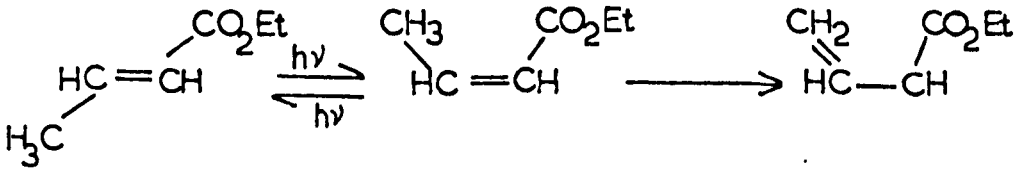

I II III

Irradiation of deoxegenated solutions of I in acetonitrile led firstly to a rapid interconversion of I and II and then, after an induction period, to a steady production of III. Irradiation of II gave similar results except that no induction period was observed. These results show that the cis isomer II is the precursor of III as

proposed by Kropp and Krause.[150] Experiments with benzophenone as sensitiser gave rapid equilibration of I and II but not III. Incomplete quenching of the geometrical isomerisation was observed with piperylene. They claimed that interconversion of the cis and trans isomers is a triplet state reaction whilst production of III probably goes via an excited singlet. It seems that the lowest excited single is n,π^* in nature due to the hump seen at the long wavelength edge of the main absorption peak (λ = 240 nm, ε = 50 $l.mol^{-1} cm^{-1}$)[156] and this is probably involved in the production of III. They proposed a cyclic mechanism for this bond migration.

Jorgenson and Gundel[152] in a simultaneous publication reported that ethyl 3,4,4-trimethyl-2-enoate isomerises rapidly and can then form either a cyclopropane derivative or a β,γ-isomer. They showed that these two products came from separate reaction paths starting with the two distinct isomers. The hydrogen abstraction reaction of these esters is much less dependent on the type of hydrogen involved than in the case of the corresponding ketones.[134] Following from this work Jorgenson[157] has published a comprehensive review of the photolytic behaviour of vinylcyclopropanecarboxylates of this type,

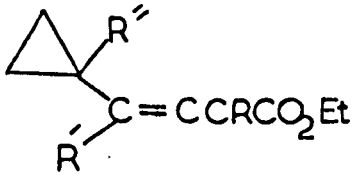

These esters are exceptionally reactive and give rise to six main classes of products under different conditions besides undergoing

simple isomerisation.

1.6(f) Theoretical work on unsaturated carbonyl systems

Although calculations on an α,β-unsaturated ester have yet to be carried out, some work has been done on the simplest of α,β-unsaturated carbonyl compounds: acrolein (acraldehyde, propenal, prop-2-en-1-al) McCullough et al.[158] carried out some C.N.D.O. - M.O[159] calculations on the ground state and lowest triplet states of acrolein to obtain curves of potential energy versus angle of twist about the double bond for the three states. They based their results on the bond lengths and angles quoted in a previous paper on the U.V. spectrum of acrolein[160] and their results are only approximate. However, it is clear from this work that the equilibrium geometry of the n,π* triplet should be planar whilst that of the π,π* triplet should be non-planar with respect to the CH_2 twisting coordinate by approx. 72°. Twisting should be accompanied by significant changes in the α-β bond length. It is also clear that the n,π* triplet is the lowest excited triplet state of planar acrolein though the gap between n,π* π,π* states decreases with twisting. This finding is in agreement with other calculations carried out by Zimmerman.[161]

In a very recent paper[162] Becker et al. announced the results of a theoretical and experimental study of acrolein. They carried out S.C.F. - M.O. - C.I.[163] calculations to derive the potential energy curves for the π,π* excited states of acrolein and also discussed the qualitative nature of the n,π* potential energy curves in the

light of experiments on fluorescence and phosphorescence spectra. They obtained potential energy curves as a function of twist about the central single bond and also about the terminal double bond. From these they deduced that photoisomerisation cannot occur around the single bond in either n,π^* or π,π^* states, but could occur around the double bond in the lowest π,π^* triplet state. In the latter case a potential energy minimum was found near 90° and degeneracy occurs with the ground state. They predicted that there is a crossover between triplet n,π^* and π,π^* states at around 20° of twist around the double bond and that at higher degrees of twist the π,π^* state becomes the lowest triplet state of the molecule. These results are in broad qualitative agreement with the more approximate findings of McCullough et al.[158] although the energy values in the two cases vary widely. Becker also found that the quantum yields of fluorescence and phosphorescence for acrolein were extremely low implying that excitation results in nearly complete internal conversion and/or photochemistry.

Although cis-trans isomerisation is not observable in acrolein, these results may provide a useful model for explaining the photochemistry of substituted enones and related compounds.

1.6(g) Summary and object of work

As can be seen from the above review, the combination of theoretical and experimental findings has led to a reasonable degree of understanding of the mechanisms of isomerisation in π,π^* systems. The potential energy versus twist diagram has been used successfully

to interpret the work on simple alkenes and has been of considerable help in the interpretation of the more complicated conjugated π,π^* systems such as stilbene. Less is known about the shape of these potential energy curves in n,π^* systems and the object of the present work was to try to obtain some quantitative results for the cis-trans isomerisation of such a system. A detailed study of the isomerisation reaction in a conjugated carbonyl system would provide the experimental basis for molecular orbital calculations of potential energy curves as has been done already for stilbene.

It was originally planned to extend the work of Stewart[137] on methyl propenyl ketone but this study was abandoned for the reasons outlined in Chapter 2. It was found that an amenable system for study was the conjugated ester, methyl tiglate and results for this compound are set out in Chapter 3.

REFERENCES TO INTRODUCTION

1. J.G. Calvert and J.N. Pitts, "Photochemistry", John Wiley, New York (1966).
2. N.J. Turro, "Molecular Photochemistry", W.A. Benjamin, New York (1965).
3. P.A. Leermakers, A.A. Lamola and N.J. Turro in, "Energy Transfer and Organic Photochemistry" Vol. XIV of Technique of Organic Chemistry (Ed. P.A. Leermakers and W. Weisberger), J. Wiley, New York (1969).
4. J.N. Pitts and J.K.S. Wan in "The Chemistry of the Carbonyl Group" (Ed. S. Patai), Interscience, London, (1966), 825 - 908.
5. C.H. Bamford and R.G.W. Norrish, J.Chem.Soc., 1504 (1935).
6. R.G.W. Norrish, Trans.Faraday Soc., 33, 1521 (1937).
7. R. Pieck and E.W.R. Steacie, Can.J.Chem., 33, 1304 (1955).
8. F.S. Wettack and W.A. Noyes, J.Amer.Chem.Soc., 90, 3901 (1968)
9. C.H. Bamford and R.G.W. Norrish, J.Chem.Soc., 1521 (1938).
10. R.S. Tolberg and J.N. Pitts, J.Amer.Chem.Soc., 80, 1304 (1958).
11. A. Zahra and W.A. Noyes, Dissertation, Rochester University (1964).
12. L.D. Hess and J.N. Pitts, Unpublished, See Ref.1.
13. N.C. Yang, A. Morduchowitz and D.H. Yang, J.Amer.Chem.Soc., 85, 1017 (1963).
14. A. Shönberg and A. Mustafa, Chem.Rev., 51, 1 (1952)
15. P.E. Eaton, J.Amer.Chem.Soc., 84, 2344 (1962)

16. D.R. Arnold in "Advances in Photochemistry", Vol. 6 (Ed. W.A. Noyes, G.S. Hammond, J.N. Pitts), Interscience, New York (1968), 301 - 418.

17. G. Büchi, C.G. Inman and E.S. Lipinsky, J.Amer.Chem.Soc., 76, 4327 (1954), and later papers.

18. N.C. Yang and M.J. Jorgenson, Tetrahedron Letters, 19, 1203 (1964).

19. J.N. Pitts and I. Norman, J.Amer.Chem.Soc., 76, 4815 (1954).

20. S. Cremer and R. Srinivasan, J.Amer.Chem.Soc., 87, 1647 (1965).

21. C.K. Johnson, B. Dominy and W. Reusch, J.Amer.Chem.Soc., 85 3894 (1963).

22. E. Ciamician and P. Silber, Ber., 33, 2911 (1900); 34, 1541 (1901).

23. C. Walling and M.J. Gibian, J.Amer.Chem.Soc., 87, 3361 (1965)

24. H.J.L. Bäckström and K. Sandros, Acta.Chim.Scand. 14, 48 (1960).

25. A. Beckett and G. Porter, Trans.Faraday Soc., 59, 2038 (1963).

26. J.A. Bell and H. Linschitz, J.Amer.Chem.Soc., 85, 528 (1963).

27. N.C. Yang and D-D.H. Yang, J.Amer.Chem.Soc., 80, 2913 (1958).

28. P.J. Wagner, J.Amer.Chem.Soc., 88, 5672 (1966).

29. P.J. Wagner, J.Amer.Chem.Soc., 89, 2903 (1967).

30. J.C.W. Chien, J.Amer.Chem.Soc., 89, 1275 (1967).

31. N.C. Yang and S.P. Elliott, J.Amer.Chem.Soc., 91, 7550 (1969).

32. D.B. Peterson and G.J. Mains, J.Amer.Chem.Soc., 81, 3510 (1959).

33. W. Davis and W.A. Noyes, J.Amer.Chem.Soc., 69, 2153 (1947).

34. G.R. McMillan, J.G. Calvert and J.N. Pitts, J.Amer.Chem.Soc., 86, 3602 (1964).

35. R. Srinivasan, J.Amer.Chem.Soc., 81, 5061 (1959).

36. V. Brunet and W.A. Noyes, Bull.Soc.Chim.France, 121 (1958).

37. R. Srinivasan, J.Amer.Chem.Soc., 84, 2475 (1962).

38. R.P. Borkowski and P. Ausloos, J.Phys.Chem., 65, 2257 (1961).

39. J.L. Michel and W.A. Noyes, J.Amer.Chem.Soc., 85, 1027 (1963).

40. R.E. Rebbert and P. Ausloos, J.Amer.Chem.Soc., 86, 4803 (1964).

41. P. Ausloos and R.E. Rebbert, J.Amer.Chem.Soc., 86, 4512 (1964).

42. P.J. Wagner and G.S. Hammond, J.Amer.Chem.Soc., 87, 4009 (1965).

43. P.J. Wagner and G.S. Hammond, J.Amer.Chem.Soc., 88, 1245 (1966).

44. P.J. Wagner and G.S. Hammond in Advances in Photochemistry, Vol.5, (Ed. W.A. Noyes, G.S. Hammond and J.N. Pitts), Interscience New York (1968), 94 - 104.

45. G.S. Hammond, P.A. Leermakers and N.J. Turro, J.Amer.Chem.Soc., 83, 2396 (1961).

46. P.J.W. Debye, Trans.Electrochem.Soc., 82, 265 (1942).

47. T.J. Dougherty, J.Amer.Chem.Soc., 87, 4011 (1965).

48. J.A. Barltrop and J.D. Coyle, Tetrahedron Letters, 3235 (1968).

49. F.S. Wettack, J.Phys.Chem., 73, 1167 (1969).

50. C. Walling and A. Padwa, J.Amer.Chem.Soc., 85, 1597 (1963).

51. C.H. Nicol and J.G. Calvert, J.Amer.Chem.Soc., 89, 1790 (1967).

52. K.H. Schulte-Elte and G. Ohloff, Tetrahedron Letters, 1143 (1964).

53. P.J. Wagner, J.Amer.Chem.Soc., 89, 5898 (1967).

54. D.R. Coulson and N.C. Yang, J.Amer.Chem.Soc., 88, 4511 (1966).

55. P.J. Wagner and A. Kemppainen, J.Amer.Chem.Soc., 90, 5896 (1968).

56. P.J. Wagner, Tetrahedron Letters, 1753 (1967(.

57. N.C. Yang, S.P. Elliott and B. Kim, J.Amer.Chem.Soc., 91, 7551 (1969).

58. A.A. Lamola and G.S. Hammond, J.Chem.Phys., 43, 2129 (1965).

59. N.C. Yang and E.D. Feit, J.Amer.Chem.Soc., 90, 504 (1968).

60. A. Meller, Mol. Photochem., 1, 257 (1969).

61. F.S. Wettack, G.D. Renkes, M.G. Rockley, N.J. Turro, and J.C. Dalton, J.Amer.Chem.Soc., 92, 1793 (1970).

62. R.E. Rebbert and P. Ausloos, J.Amer.Chem.Soc., 87, 5569 (1965).

63. P. Borrell and J. Sedlar, J.Chem.Soc., to be published

64. P. Borrell and J. Sedlar, Trans.Faraday Soc., 66, 1670 (1970).

65. J.S. Bradshaw, J.Org.Chem., 31, 237 (1966).

66. E. Wigner, Nachr.Akad,Wiss.Goettingen, IIa. Math.Physik.Chem. Abt., (1927).

67. D.F. Evans, J.Chem.Soc., 1351 (1957).

68. A. Terenin and V. Ermolaev, Trans.Faraday Soc., 52, 1042 (1956).

69. G.S. Hammond and W.M. Moore, J.Amer.Chem.Soc., 81, 6334 (1959).

70. A. Kearwell and F. Wilkinson in "Transfer and Storage of Energy by Molecules", Vol.1., (Ed. G.M. Burnett and A.M. North), Interscience, London (1969), 94 - 157, also R.B. Cundall, ibid, 1 - 56.

71. D.M.S. U.V. Atlas, Vol.IV, Butterworths, London (1968).

72. C. Ellis and A.A. Wells, "The Chemical Action of Ultraviolet Rays", Reinhold, New York (1941).

73. P. Borrell, Ann.Reports Chem.Soc., (London), 60, 62 (1963).

74. A. Schönberg, G.O. Schenck and O-A. Neumüller, "Preparative Organic Photochemistry", Springer-Verlag, Berlin (1968).

75. J.A. Barltrop and J.D. Coyle, J.Amer.Chem.Soc., 90, 6584, (1968).

76. R.B. Cundall in 'Progress in Reaction Kinetics', Vol.2. (Ed. G. Porter) Pergamon, London (1964), 167 - 208.

77. A.R. Olsen, Trans.Faraday Soc., 27, 69, (1931).

78. G.N. Lewis, T.T. Magel and D. Lipkin, J.Amer.Chem.Soc., 62 2973, (1940).

79. J.L. Magee, W. Shand and H. Eyring, J.Amer.Chem.Soc., 63 677, (1941).

80. R.S. Mulliken and C.C.J. Roothan, Chem.Rev., 41, 219, (1947).

81. D. Valentine, N.J. Turro and G.S. Hammond, J.Amer.Chem.Soc., 86, 4499, (1964).

82. H. Okabe and J.R. McNesby, J.Chem.Phys., 36, 601, (1962).

83. Z.R. Grabowski and A. Bylina, Trans.Faraday Soc., 60, 1131, (1964).

84. A.B. Callear and R.J. Cvetanovic, J.Chem.Phys., 24, 873, (1956).

85. R.B. Cundall and T.F. Palmer, Trans.Faraday Soc., 56, 1211, (1960).

86. R.B. Cundall and W. Tippet, Trans.Faraday Soc., 66, 350, (1970).

87. R.F. Borkman and D.R. Kearns, J.Amer.Chem.Soc., 88, 3467, (1966).

88. R. Srinivasan, J.Amer.Chem.Soc., 84, 3982, (1962).

89. O. Grummitt and F.J. Cristoph, J.Amer.Chem.Soc., 73, 3479, (1951).

90. J.H. Pinckard, B. Wille and L. Zeichmaster, J.Amer.Chem.Soc., 70, 1938, (1948).

91. G. Heller, Ber., 72, 1858, (1939).

92. J. Saltiel, L. Metts and M. Wrighton, J.Amer.Chem.Soc., 92, 3227, (1970).

93. H.L. Hyndman, B.M. Monroe and G.S. Hammond, J.Amer.Chem.Soc., 91 2852, (1969).

94. J. Saltiel, L. Metts and M. Wrighton, J.Amer.Chem.Soc., 91, 5684 (1969).

95. S. Boué and R. Srinivasan, J.Amer.Chem.Soc., 92, 3226,(1970).

96. R. Srinivasan and S. Boué, Tetrahedron Letters, 203, (1970).

97. R. Srinivasan, Advances in Photochemistry (See Ref. 1.6) 4, 119, (1966).

98. G.S. Hammond, J. Saltiel et al., J.Amer.Chem.Soc., 86, 3197 (1964).

99. G.S. Hammond, N.J. Turro and P.A. Leermakers, J.Amer.Chem.Soc., 83, 2396, (1961).

100. R, Hurley and A.C. Testa, J.Amer.Chem.Soc., 92, 211, (1970).

101. J. Saltiel in 'Survey of Progress in Chemistry', Vol. 2, (Ed. A.F. Scott) Academic Press, New York (1964), 256.

102. H. Dyck and D.S. McClure, J.Chem.Phys., 36, 2326 (1962).

103. S. Malkin and E. Fischer, J.Phys.Chem., 68, 1153, (1964).

104. F. Aurich, M. Hauser, E. Lippert and H. Stegemeyer, Z. Phys. Chem. N.F., 42, 123, (1964).

105. D. Gegiou, K.A. Muszkat and E. Fischer, J.Amer.Chem.Soc., 90, 3907, (1968).

106. K.A. Muszkat, D. Gegiou and E. Fischer, J.Amer.Chem.Soc., 89, 4814, (1967).

107. D. Gegiou, K.A. Muszkat and E. Fischer, J.Amer.Chem.Soc., 90, 12, (1968).

108. G. Fischer, K.A. Muszkat and E. Fischer, Israel J.Chem., 6, 965, (1968).

109. G.W. Robinson and R. Frosch, J.Chem.Phys., 37, 1962, (1962).

110. J. Saltiel, J.Amer.Chem.Soc., 90, 6394, (1968).

111. D.L. Beveridge and H.H. Jaffé, J.Amer.Chem.Soc., 87, 5340, (1965).

112. J. Saltiel, E.D. Megarity and K.G. Kniepp, J.Amer.Chem.Soc., 88, 2386, (1966).

113. J. Saltiel and E.D. Megarity, J.Amer.Chem.Soc., 91, 1265, (1969).

114. A.A. Lamola, p.37 in Ref. 3.

115. W.M. Horspool in 'Photochemistry, Vol. 1., Specialist Periodical Reports of the Chemical Society (Ed. D. Bryce-Smith) London, (1970), 236

116. L.M. Stephenson and G.S. Hammond, Angew. Chem., 8, 261, (1969).

117. A.A. Lomola, pp. 60 - 70 in Ref. 3.

118. W.G. Herkstroeter and G.S. Hammond, J.Amer.Chem.Soc., 88, 4769, (1966).

119. A. Bylinda, Chem.Phys.Letters, 1, 509, (1968).

120. G.S. Hammond, N.J. Turro and A. Fischer, J.Amer.Chem.Soc., 83, 4674, (1961).

121. G.S. Hammond, P. Wyatt, C.D. DeBoer and N.J. Turro, J.Amer.Chem. Soc., 86, 2532, (1964).

122. S. Murov, R.S. Cole and G.S. Hammond, J.Amer.Chem.Soc., 90, 2959, (1968).

123. W.G. Herkstroeter and D.S. McClure, J.Amer.Chem.Soc., 90, 4522, (1968).

124. P. Borrell and H.H. Greenwood, Proc.Roy.Soc., A298, 453, (1967).

125. C.H. Ting and D.S. McClure, unpublished; quoted in Ref. 110.

126. P.P. Birnbaum and D.W.G. Style, Trans.Faraday Soc., 50, 1192, (1954).

127. G. Zimmerman, L.Y. Chow and V.J. Paik, J.Amer.Chem.Soc., 80, 3528, (1958).

128. J. Saltiel, O.C. Zafiriou, E.D. Megarity and A.A. Lamola, J.Amer.Chem.Soc., 90, 4759, (1968).

129. G.S. Hammond, S.C. Shim and S.P. Van, Mol. Photochem, 1, 89 (1969).

130. D.G. Whitten and M.T. McCall, Tetrahedron Letters, 2755, (1968).

131. D.G. Whitten and M.T. McCall, J.Amer.Chem.Soc., 91, 5097, (1969).

132. D.G. Whitten, J.W. Happ et al., J.Amer.Chem.Soc., 92, 3499, (1970).

133. A.A. Zimmerman, C.M. Orlando, M.H. Gianni and K. Weiss, J.Org. Chem., 34, 73, (1969).

134. N.C. Yang and M.J. Jorgenson, Tetrahedron Letters, 19, 1203, (1964).

135. M.J. Jorgenson and N.C. Yang, J.Amer.Chem.Soc., 85, 1698, (1963).

136. P.J. Wagner and G.S. Hammond pp. 120 - 121 in Ref. 44.

137. N.D. Stewart, M.Sc.Thesis, Keele University, (1965).

138. L.D. Hess and J.N. Pitts, unpublished.

139. R.S. Tolberg and J.N. Pitts, J.Amer.Chem.Soc., 80, 1304, (1958).

140. R. Ramasseul and A. Rassat, Bull.Soc.Chim.France, 2218, (1963).

141. R. Stoermer, Ber., 44, 637, (1911).

142. M.D. Cohen and G.M.J. Schmidt, J.Chem.Soc., 1966, (1964).

143. S. Lindenfoss, Arkiv for Kemi, 12, 267, (1958).

144. M.B. Hocking, Can.J.Chem., 47, 4567, (1969).

145. S.W. Pelletier and W.L. McLeish, J.Amer.Chem.Soc., 74, 6292, (1952).

146. A.R. Olsen and F.L. Hudson, J.Amer.Chem.Soc., 55, 1410, (1933).

147. P.A. Leermakers, J-P. Montillier and R.D. Rauh, Mol.Photochem., 1, 57, (1969).

148. D.O. Cowan and A.A. Baum, J.Amer.Chem.Soc., 92, 2153, (1970).

149. M.J. Jorgenson, Chem.Communications, 137, (1965).

150. P.J. Kropp and H.J. Krause, J.Org.Chem., 32, 3222, (1967).

151. K.J. Crowley, J.Amer.Chem.Soc., 85, 1210, (1963).

152. M.J. Jorgenson and L. Gundel, Tetrahedron Letters, 4991, (1968).

153. C.R. Judge, Part II Thesis, Oxford, (1967).

154. R.R. Rando and W. von E. Doering, J.Org.Chem., 33, 1671, (1968).

155. J.A. Barltrop and J. Wills Tetrahedron Letters, 4987, (1968).

156. W.D. Closson, S.F. Brady and P.J. Orenski, J.Org.Chem., 30, 4026, (1965).

157. M.J. Jorgenson, J.Amer.Chem.Soc., 91, 6432, (1969).

158. J.J. McCullough, H. Ohrodynk and D.P. Santry, Chem.Communications 11, 570, (1969).

159. C.N.D.O. stands for complete neglect of differential overlap. See J.A. Pople and G.A. Segal, J.Chem.Phys., 44, 3289, (1966). and references therein.

160. J.C.D. Brand and D.G. Williamson, Disc.Faraday Soc., 35, 184, (1963).

161. H.E. Zimmerman, R.W. Binkley, J.J. McCullough and G.A. Zimmerman, J.Amer.Chem.Soc., 89, 6589, (1967).

162. R.S. Becker, K. Inuzuka and J. King, J.Chem.Phys., 52, 5164, (1970).

163. S.C.F. - M.O. - C.I. stands for self consistent field - molecular orbital - configuration interaction. See J.A. Pople, Trans.Faraday Soc., 49, 1375, (1953).

2. EXPERIMENTAL

As described earlier, the experiments were divided into two broad sections: those on cis-trans isomerisation and those on the Type II reactions of ketones. The main link between these two topics was the experimental technique used. Consequently, the techniques used for both parts of this work are described together in this chapter.

2.1 Introductory work on ethylidene acetone

The original plan for this research project was to continue work on the photochemical cis-trans isomerisation of ethylidene acetone (pent-3-en-2-one, E.A.) started by N.D. Stewart in this research group.[1] To do this, it was necessary to isolate, in reasonable purity, the cis and trans isomers of this compound. As ethylidene acetone is not available from Chemical suppliers, it was obtained as a sample kindly provided by B.P. Chemicals Ltd., who make it as an intermediate. The starting material was extremely impure, containing at least 12 appreciable impurities. In this material E.A. was present as 98% trans. Fractional distillation on a Towers D.T.520 distillation unit removed many impurities and a fraction boiling between 118 - 125°C contained mainly E.A. as the trans isomer with a small amount of cis and other impurities.

Attempts were made to purify the distillate by preparative gas chromatography using Polypropylene Glycol (4.6 m.), SE30 Silicone gum (4.6 m.) and Polyethylene Glycol adipate (4.6 and 9.2 m.) columns.

All these attempts proved only partially successful - the limit of purity was 98% trans. Very efficient fractional distillation was tried using a Nester-Faust NFT-60 Annular Spinning-Band distillation unit operating at a high reflux ratio (30:1). The prolonged boiling of the mixture caused considerable thermal decomposition and vacuum distillation proved inefficient. However, by this method, a mixture enriched in the trans isomer was obtained, which was then further purified by preparative gas chromatography (on P.P.G. at 140°C). This gave about 99% pure trans.

The original mixture was enriched in the cis isomer by photolysis in the Hanovia reactor (See section 2.5), which also increased other impurities. Attempts were made to isolate the cis isomer by Spinning-Band distillation and preparative chromatography but these failed to produce more than 90% cis. Samples of the 99% trans sealed in capillary tubes were stored in a refrigerator for several weeks over a vacation period. Upon sampling it was found that an appreciable conversion to the cis had taken place. At this stage, the project was abandoned in favour of a study of the methyl tiglate/angelate system.

2.2 Materials

2.2(a) Solvents

(i) Cyclohexane was purified from the technical grade material supplied by B.D.H. Limited. Olefinic impurities were removed by fast stirring with concentrated sulphuric acid until the acid washings were clear. It was then separated, washed with 5% NaOH and then water, finally drying overnight over anhydrous $CaCl_2$. The resulting product was passed down a 1 metre column of silica gel to remove aromatic impurities. The remaining liquid was then rectified on a Vigreux column collecting between 81 and 82°C. Purity was checked on a P.E.G.A. column in the V.P.C. No measurable impurity was seen and the liquid was transparent in the U.V. to below 250 nm.[2]

(ii) Ethanol

The method used for purification[2] was to heat 95% ethanol under reflux with KOH (20gm/litre) and $AgNO_3$(10gm/litre). After 1 hr., the flask was shaken thoroughly and left overnight, before filtering. The filtrate was dried over anhydrous $CaCl_2$ and distilled on a Towers D.T.520 fractionating column collecting between 78 and 79°C (Lit 78.3°C). The pure ethanol was stored over freshly regenerated Linde 4A molecular sieve. Purity was checked on the V.P.C. and U.V., the only impurity being a trace of methanol which was ignored.

(iii) Methanol

B.D.H. Limited G.P.R. grade methanol was rectified on the Towers column and the middle fraction boiling at 64.5°C was collected which was 99.7% pure (V.P.C.).

(iv) Benzene

B.D.H. Limited 'Analar' grade was distilled before use, collecting at 79.7°C. Purity was checked on the V.P.C.

(v) Ethyl Iodide

Commercial ethyl iodide was shaken with $Na_2S_2O_3$ solution and then water to remove free iodine. The product was dried over $CaCl_2$ and then distilled at 72°C, storing over mercury in an amber glass bottle in the dark.

(vi) Cyclohexene [2]

B.D.H. reagent grade cyclohexene was shaken with portions of a fresh solution of pure ferrous sulphate until the aqueous solution no longer turned brown, in order to remove organic peroxides. The cyclohexene was then separated and dried over $CaCl_2$ before distilling under nitrogen with a Vigreux column. The product was checked for purity on the V.P.C. and stored under nitrogen in the dark. The purity of the cyclohexene stored in this way was periodically checked with starch-iodide paper and when necessary, it was re-purified as described above. It was found that, despite precautions, the compound formed per oxides very quickly and had to be re-purified practically every week during use.

2.2(b) Substrates

(i) Methyl Tiglate (2-carbomethoxy-2-butene)

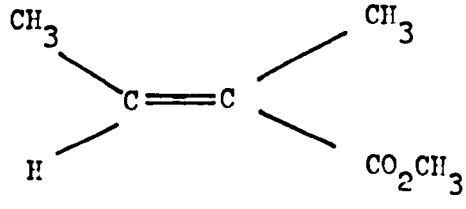

was not available commercially and was prepared from tiglic acid. Koch-Light Ltd., tiglic acid was esterified, by a classical method, by refluxing for approx. 12 hrs. in methanol with a trace amount of concentrated sulphuric acid as a catalyst. This gave a cloudy solution of the ester in methanol. The solution was shaken with sodium bicarbonate solution until neutral to litmus, when the organic layer was extracted by shaking with portions of ether. The combined ethereal extracts were dried over $CaCl_2$ and distilled at 33°C to remove most of the ether. The remaining liquid was finally purified by preparative gas chromatography (See Section 2.12(a)). The resulting methyl tiglate was dried over anhydrous Na_2SO_4 and stored in a fridge. It was more than 99% pure by V.P.C. analysis. It is a clear liquid with a fruity odour B.Pt.139.5°C/766 mm. D_4^{20} 0.9468, [3]

(ii) Methyl Angelate

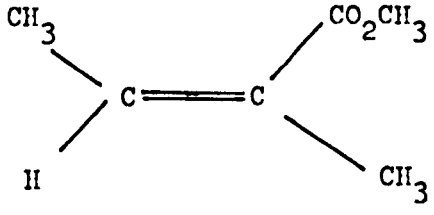

As with the tiglate, this ester was not available commercially and also angelic acid is extremely expensive. Consequently, it was synthesised by photochemical means.

A solution of about 5 ml. of crude methyl tiglate, prepared, but not purified as above, dissolved in 100 ml. of cyclohexene was photolysed in the preparative photolysis vessel using a Hanovia Ltd., medium pressure mercury lamp. (See Section 2.5). After about 12 hrs.

the composition of the mixture had reached around 40% methyl angelate. At this stage, the photolyte, was concentrated under vacuum on a Büchi 'Rotavapor' rotary evaporator until the solvent had been largely removed. The methyl angelate and tiglate present in the residue were separated and purified by preparative gas chromatography (See Section 2.12(a)). By these means 99% pure methyl angelate was obtained with the main impurity being methyl tiglate. The product was dried, sealed in an ampoule and stored in a refrigerator. Methyl angelate is a stable colourless liquid with an odour of rotten apples. B.Pt.127.7°/764 mm D_4^{20} 0.9413. [3]

The identities of the compounds prepared as methyl angelate and tiglate were confirmed by spectral analysis (see later).

(iii) Methyl n-propyl ketone (2-pentanone)

B.D.H. laboratory reagent 2-pentanone was found to contain many impurities, particularly acetone and other ketones. These were removed by rectification three times on the Towers distillation unit collecting at 102 - 103°C with a reflux ratio of 1:4 and a jacket temperature of 62°C. The final product was stored in an amber glass bottle in a refrigerator and was more than 99.9% pure. (V.P.C.).

(iv) Methyl iso-butyl ketone (4-methyl-2-pentanone), methyl hexyl ketone (2-octanone), methyl n-amyl ketone (2-heptanone), methyl n-butyl ketone (2-hexanone) were supplied by B.D.H. Ltd., or Koch-Light Ltd., and were distilled before use, as for 2-pentanone.

2.2(c) Other Chemicals

(i) Paramagnetic Salts

Manganese, nickel and chromic chlorides were B.D.H. reagent grade and were used as the hydrates.

Copper sulphate was 'Analar' grade.

All were used without further purification.

(ii) Quenching Olefins

Piperylene (trans 1,3-pentadiene) and cis hept-2-ene were both supplied by Koch-Light Ltd., and were rectified before use. Heptene was rectified on the Spinning-Band column.

(iii) Photosensitisers

Benzophenone, anthraquinone, naphthalene, benzil, pyrene, biphenyl and azulene were all Koch-Light puriss grade and were recrystallised from suitable solvents before use. Acetophenone was B.D.H. reagent grade distilled before use.

(iv) Miscellaneous

Acetone was B.D.H. reagent grade and was redistilled. 1-Pentene was used without purification (Koch-Light puriss) Ethylene glycol was B.D.H. commercial grade and was redistilled.

Sources of other chemicals used are specified in the text.

2.3 Light Sources

Three different types of mercury arc lamp were used. These were the low, medium and high pressure mercury lamps.

2.3(a) Low Pressure arc

This lamp was used for irradiating capillaries in the merry-go-round apparatus (See Section 2.7). It was manufactured by Hanovia Ltd. and consisted of a U-tube 14 cm. long by 2.5 cm. across made from 8 mm. 'spectrosil' tubing. It was provided with an electrode at each end and was powered by a step-up transformer from the mains. The lamp was rated at 70 watt and the starting current was 1 amp. In such lamps, the mercury vapour pressure is low (c.a.10^{-3}mm) as they operate near room temperature. Under these conditions, nearly all the radiation is concentrated in the lines at 253.7 and 185.0 nm., corresponding to the transitions $^3P_1 \rightarrow {}^1So$ and $^1P_1 \rightarrow {}^1So$ in the mercury atom. The lower wavelength was cut out by the acetic acid solution used and then the lamp was considered as a monochromatic source of 254 nm. radiation. The major disadvantage of this source was that the actual emitting area of the lamp was very large, making optical arrangement difficult. However, it is a very stable source of ultra-violet light.

2.3(b) Medium Pressure arc

This lamp was a Hanovia UVS 220 W. arc powered by a transformer and intensity stabilising device. The light intensity of this source was found to be effectively constant. The lamp was mounted in a brass housing similar to that used for the high pressure lamp (q.v.) and was cooled by a stream of air directed onto the quartz envelope. In this type of lamp the operating temperature is higher and hence the

Fig. 2.1

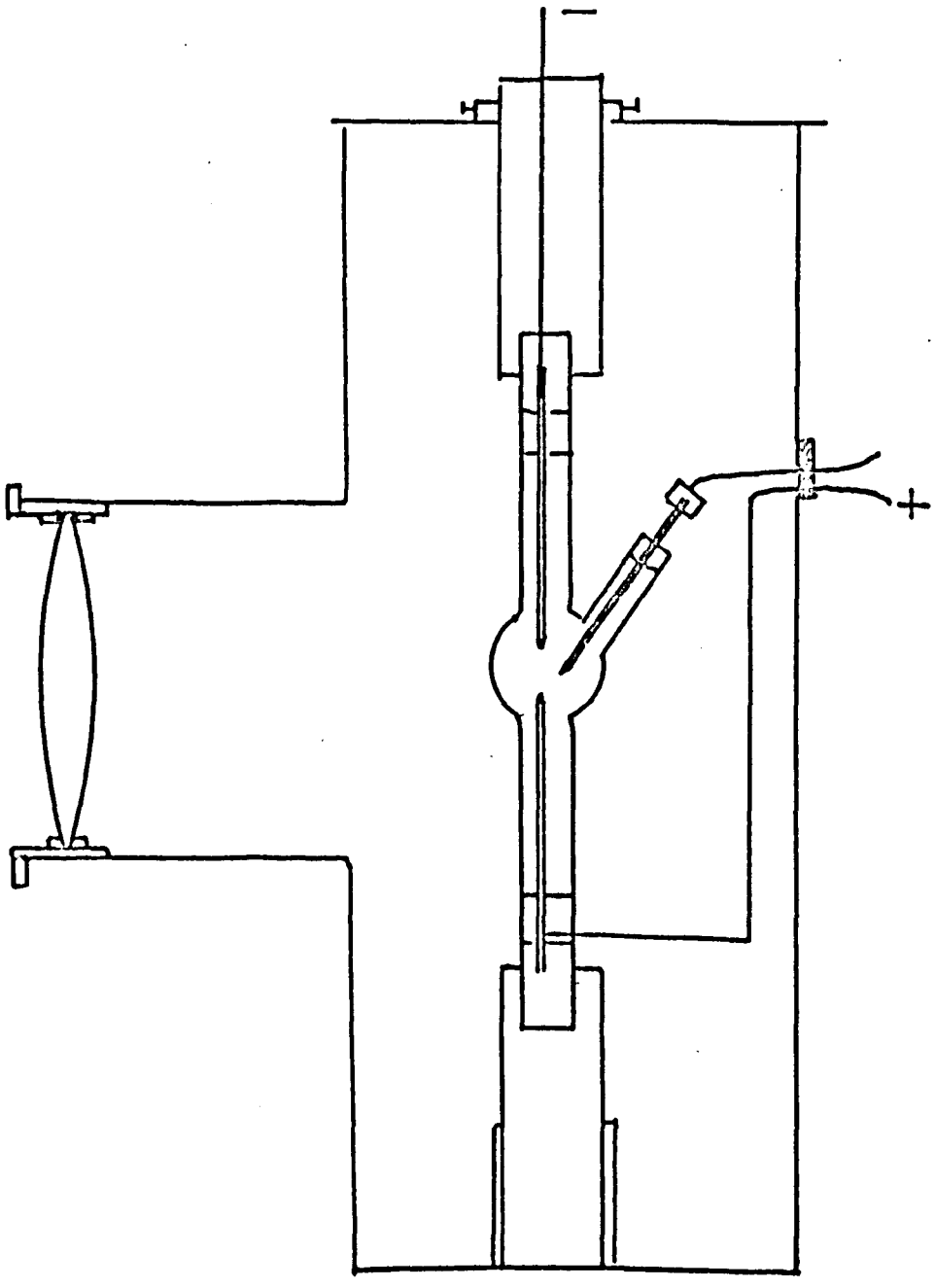

pressure inside the envelope is about 1 atmosphere. Under these conditions many mercury atoms are excited to higher states and undergo many transitions not involving the ground state, resulting in many more lines, which are subject to some pressure-broadening. The medium pressure lamp was similar in its spectrum to the high pressure lamp and though less intense, it was more stable with a longer operating lifetime.

A Hanovia 100 W. medium pressure lamp was used for large scale photolyses in the immersion well apparatus (See Section 2.5).

2.3(c) High Pressure arc

These sources operate at higher temperatures and pressures of up to 100 atmospheres or more. Temperature and pressure-broadening of the spectral lines is greater and a higher intensity of continuum is also present, as compared to the other mercury lamps. The sharp line at 254 nm. is missing in these lamps due to re-absorption of the resonance radiation.

The lamp used was a Wotan HBO 500 W. arc (Osram Limited Germany) powered by a transformer and fitted with a push-button starter. The lamp was mounted on asbestos supports in a brass housing coated with graphite on the inside. The beam was collimated by a 7 cm. diameter 'spectrosil' lens with the arc at its focal point (10 cm.) is shown in Fig. 2.1. The lifetime of the lamp was 250 hrs. and care was taken to avoid too frequent starting of the lamp which caused a decrease in the lifetime. As the light intensity decayed somewhat with time, a check was kept on the intensity.

2.3(d) Measurement of Spectral Distribution

In the course of another investigation, in collaboration with Dr. J. Sedlar, an apparatus was built to measure the spectral distribution of various ultra-violet light sources. This consisted of a Hilger and Watts D.285 prism monochromator into which a beam of light from the lamp, housed in an asbestos box, was directed. A Phillips 9662B quartz-jacketed photomultiplier was mounted in a light-tight housing at the outlet of the monochromator, and was kept at a constant voltage by a series of 120V. batteries. The whole apparatus was mounted rigidly on a bench. By scanning the spectrum with the prism turntable, a graph of photomultiplier current, read on a microammeter, against wavelength was constructed. This was then corrected for changing photomultiplier response by calibrating the photomultiplier at 3 wavelengths, isolated by optical filters from high intensity lamps, against a ferrioxalate actinometer. The resulting data gave an accurate picture of the spectral distribution of the light emitted from each lamp, from 240 nm. up to the visible range of the spectrum.

The output of a typical medium pressure mercury lamp (100 W.) is shown in Fig. 2.2 together with that of a typical low pressure lamp (6 W. lamp-emission observed from 4 cm. tube length). The latter is taken from Ref.4. The spectrum of a high pressure lamp is similar to that of a medium pressure lamp (see above).

Fig. 2.2 Medium pressure lamp

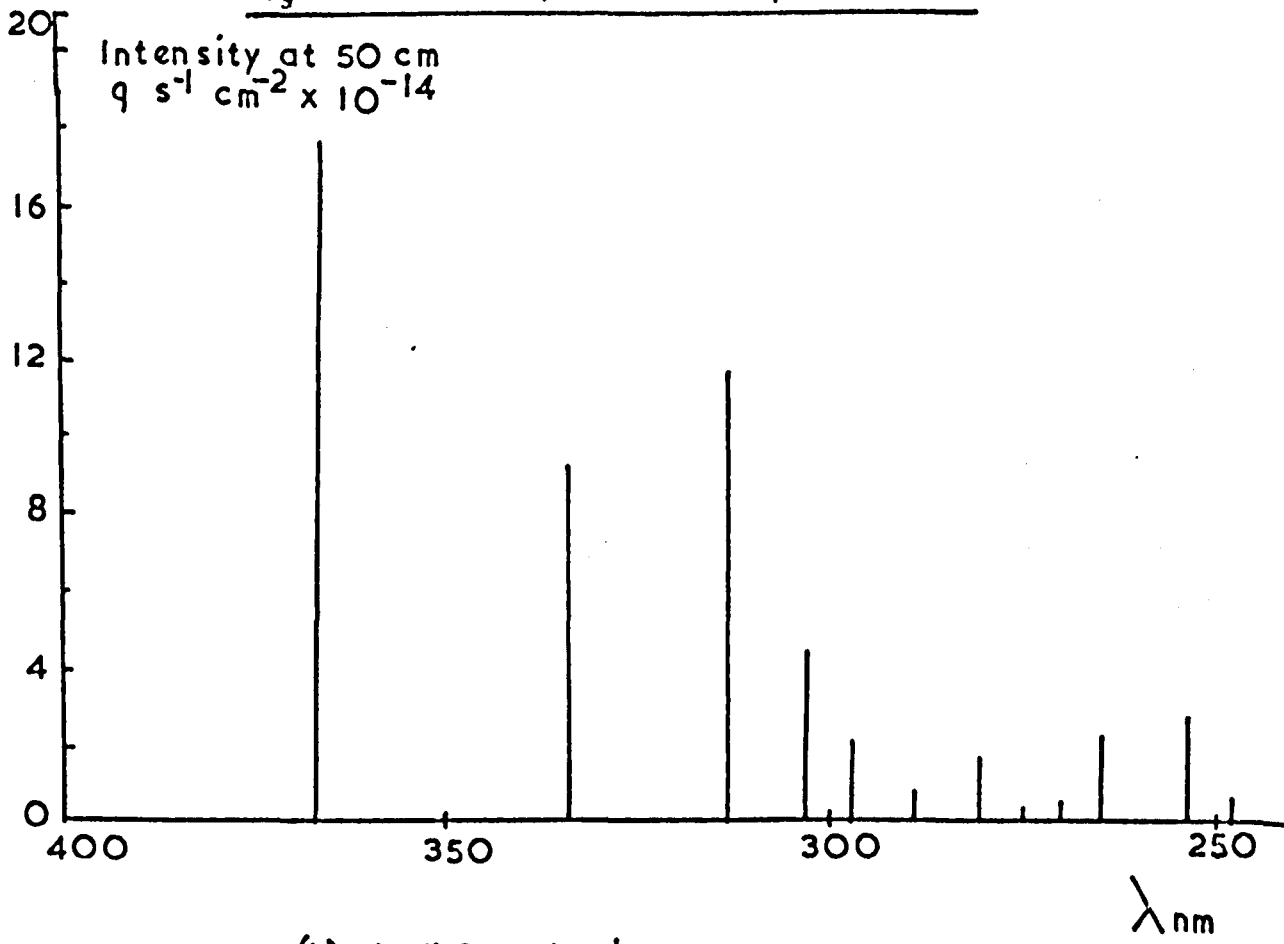

(b) Low pressure lamp

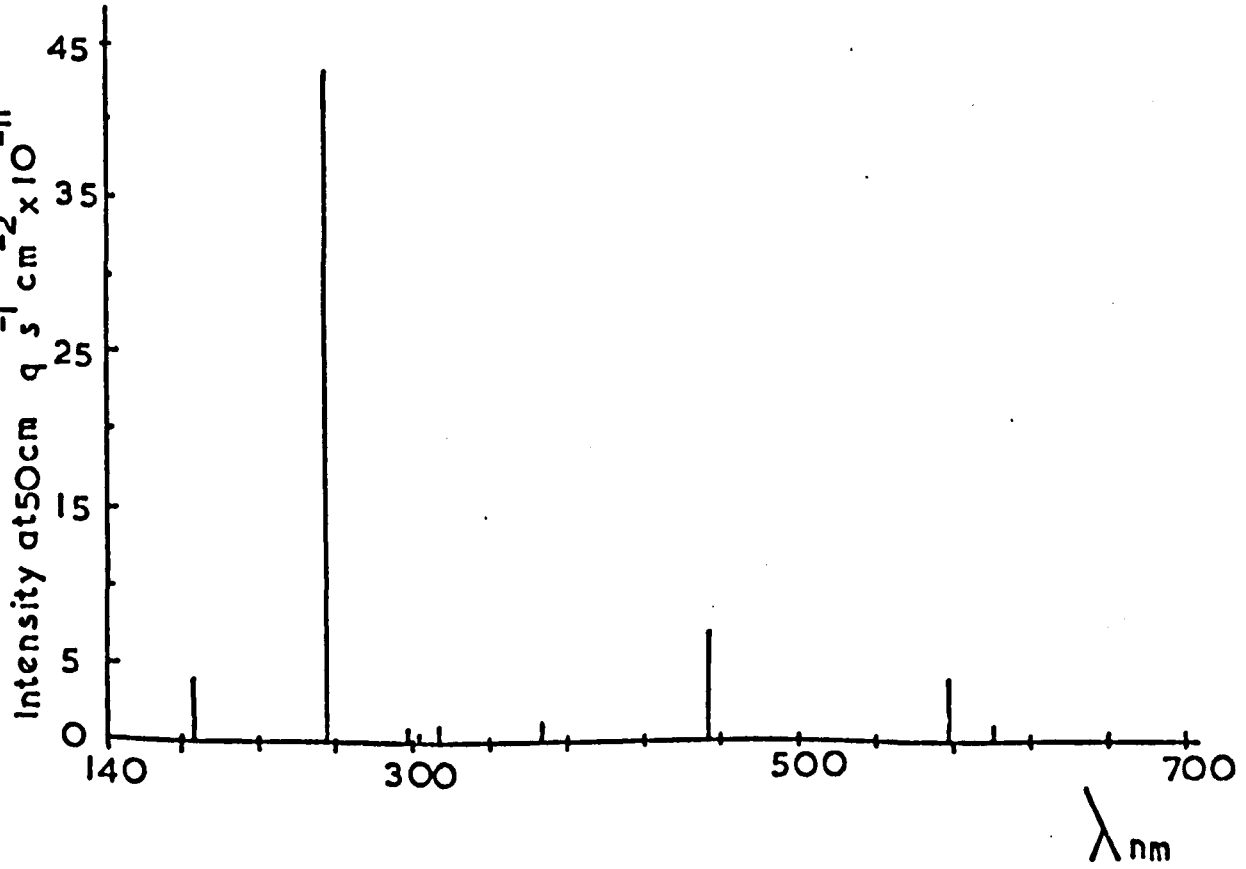

2.4 Optical Filters

Optical Filters were used, in conjunction with the high and medium pressure mercury lamps, to isolate particular lines in their spectra. Both chemical and interference filters were used. Their transmissions were checked on the SP.800 spectrophotometer before use.

2.4(a) Interference Filters

These were supplied by Barr and Stroud Ltd. and were of the metal dielectric narrow-band type. Filters were used which transmitted the lines at 254, 313 and 366 nm., cutting-off all other regions of the ultra-violet. Transmission spectra for these filters are shown in Figs. 2.3(a), (b) and (c).

2.4(b) Chemical Filters

Certain chemical filters were used where interference filters were either not available, or gave too low transmission. An effective filter was found to be a combination of 2 pieces of 2 mm. thick Chance-Pilkington OX7 glass with a 5 cm. path length quartz cell filled with dry Cl_2 gas at 1 atmosphere.[4] This filter transmitted the region around 254 nm. and was found to be quite stable. It also transmitted above 400 nm.

A combination of a 1 cm. path length quartz cell filled with a solution of potassium chromate, (0.2g./litre) in 0.05N NaOH, with a 2 mm. thick piece of OX7 glass was found to be an extremely effective peak transmission filter for the 313 nm. mercury line. Peak transmission was 50% at 313 nm. with a band width of 21 nm. at 25% transmission. This filter was used in conjunction with the high pressure mercury lamp and was completely stable (transmission unchanged

Fig. 2.3(a,b)

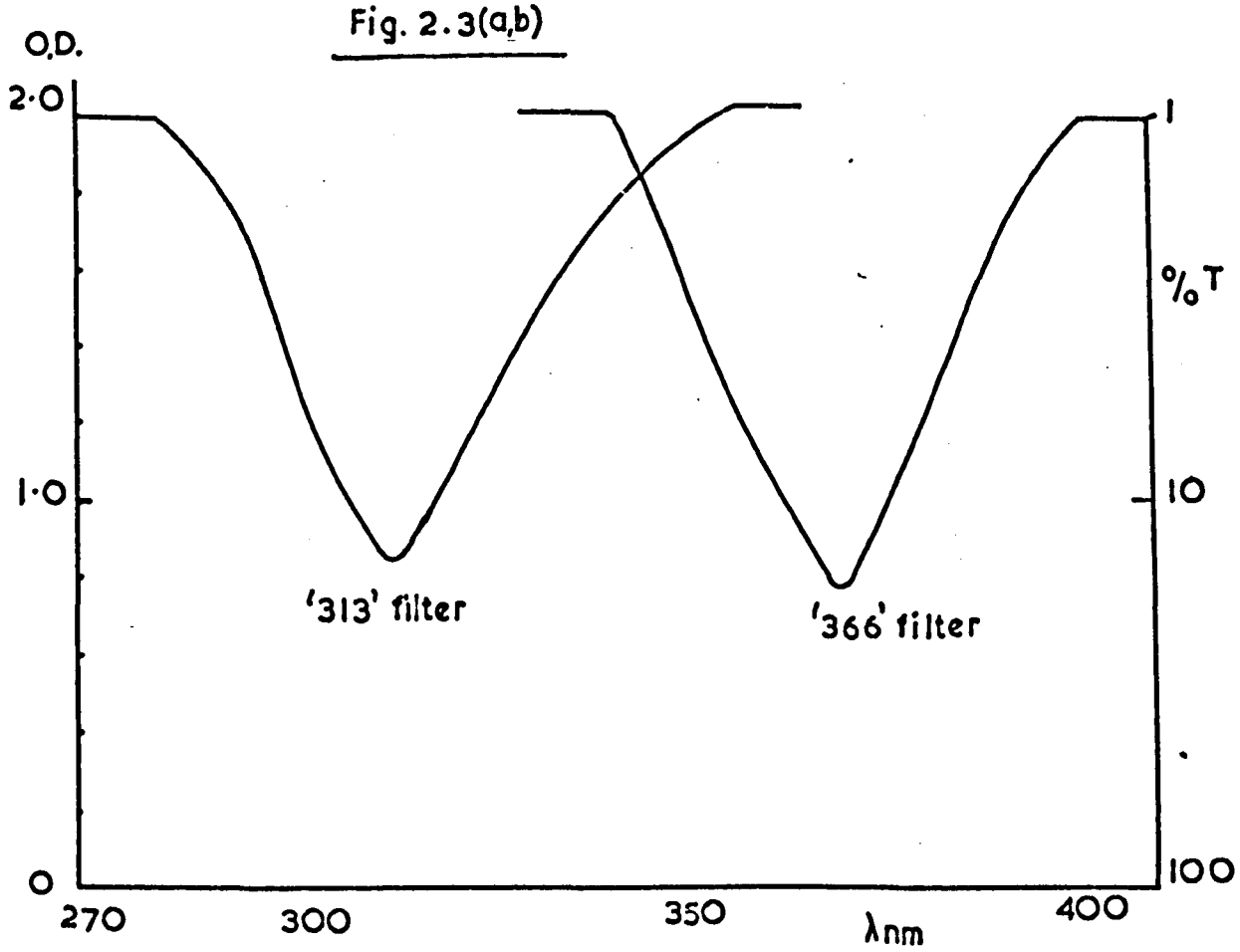
O.D.
2·0
1·0
0
1
%T
10
100
'313' filter
'366' filter
270
300
350
400
λnm

23(c)

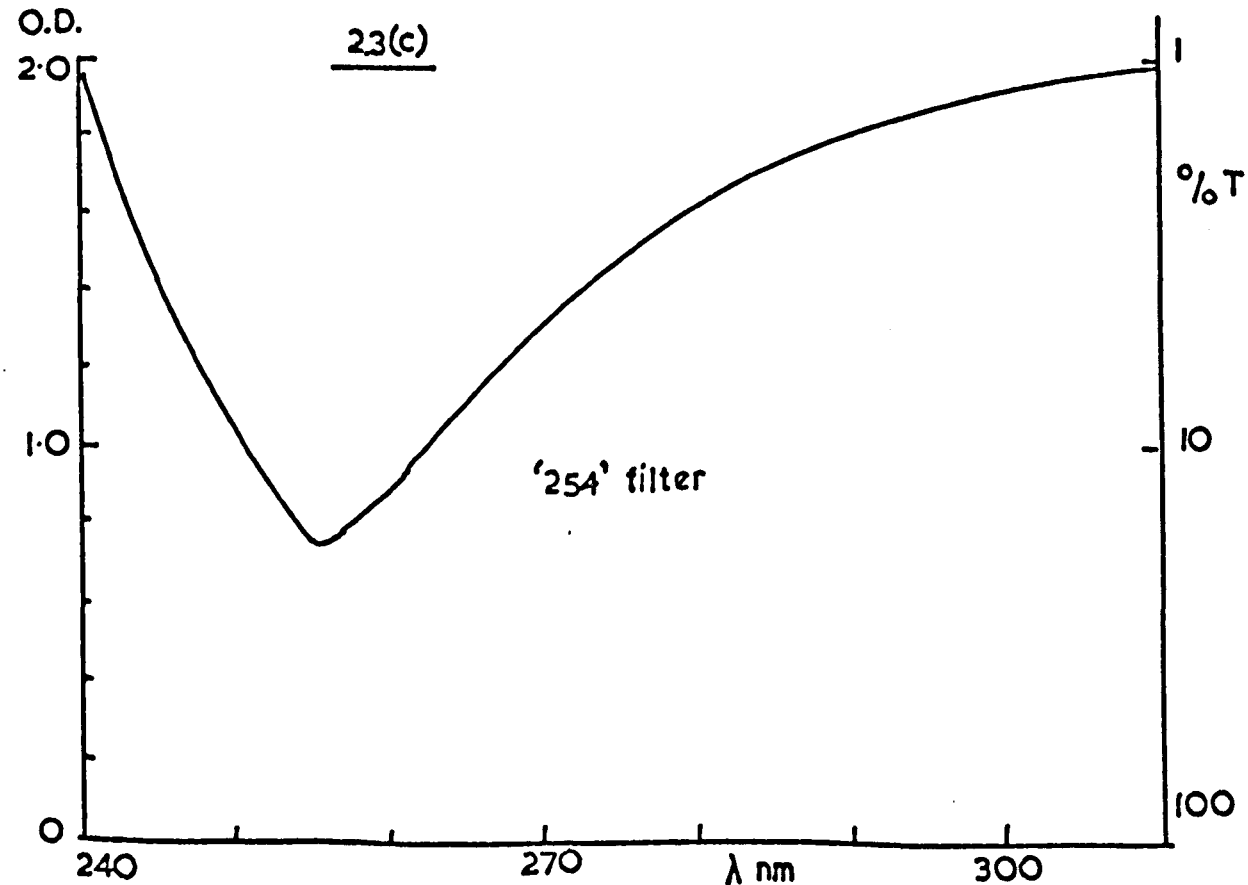
O.D.
2·0
1·0
0
1
%T
10
100
'254' filter
240
270
λ nm
300

after 50 hrs. irradiation). Although chromate solutions have been used for these purposes before,[5] it is believed that this is the first time that this combination has been used.

Spectra, taken on the SP.800, for these two chemical filters are shown in Figs. 2.3(d) and (e).

Fig. 2.3(d) Chromate filter

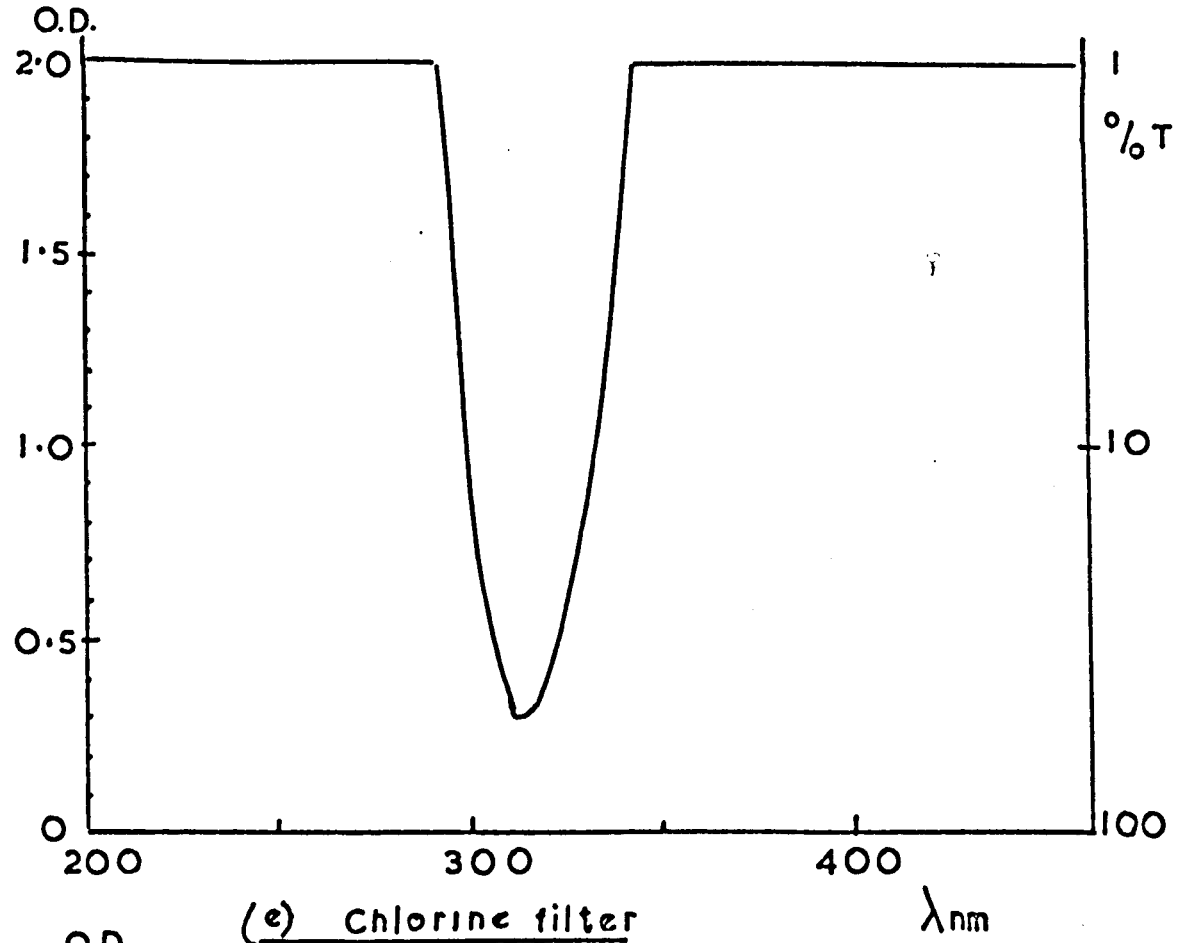

(e) Chlorine filter

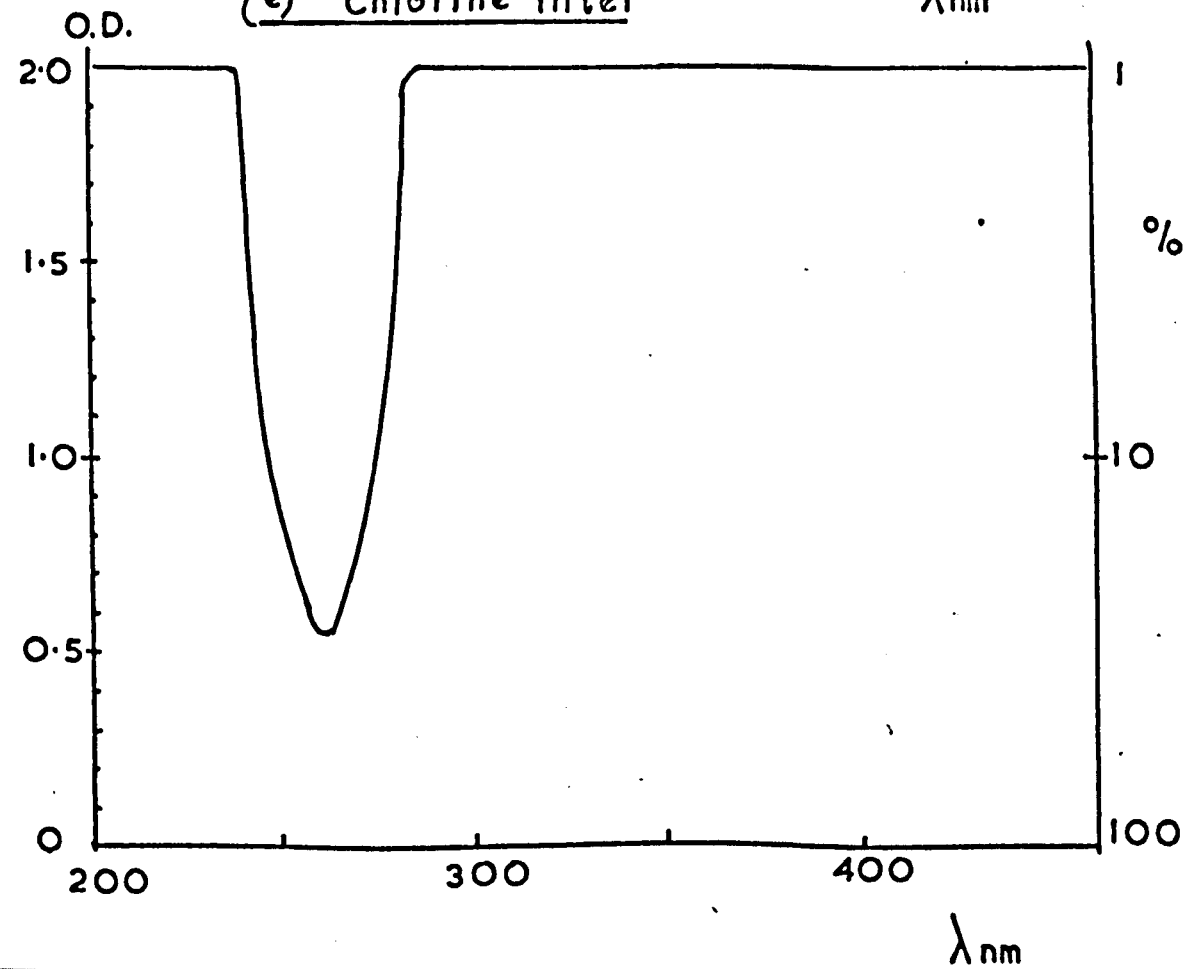

2.5 Preparative Photolysis Apparatus

The apparatus used is shown in Fig. 2.4. The vessel was designed to fit around a Hanovia Ltd., immersion-well photolysis apparatus, housing a 100 W. medium pressure Hg lamp. Water was circulated between the two-piece synthetic quartz envelope for cooling and air was circulated inside the well to remove ozone. The outer vessel held some 100 ml. of liquid to be photolysed, which was stirred by a 'teflon'-sheathed paddle and magnetic stirrer. Nitrogen could be bubbled through the solution via the fine bore delivery tube and out via the side tube, which could be attached to either a mercury sealed exit or to a gas collection head filled with di-butyl phthalate for collecting gaseous products. A rubber serum cap was fitted for taking samples during the course of the photolysis. The usual procedure was to flush the solution with a fast flow of nitrogen for about 15 mins., before sealing-off the apparatus and photolysing.

For larger volumes of solution a special 3-necked 1 litre flask was provided by Hanovia with a central socket to fit the immersion-well.

Fig. 2.4

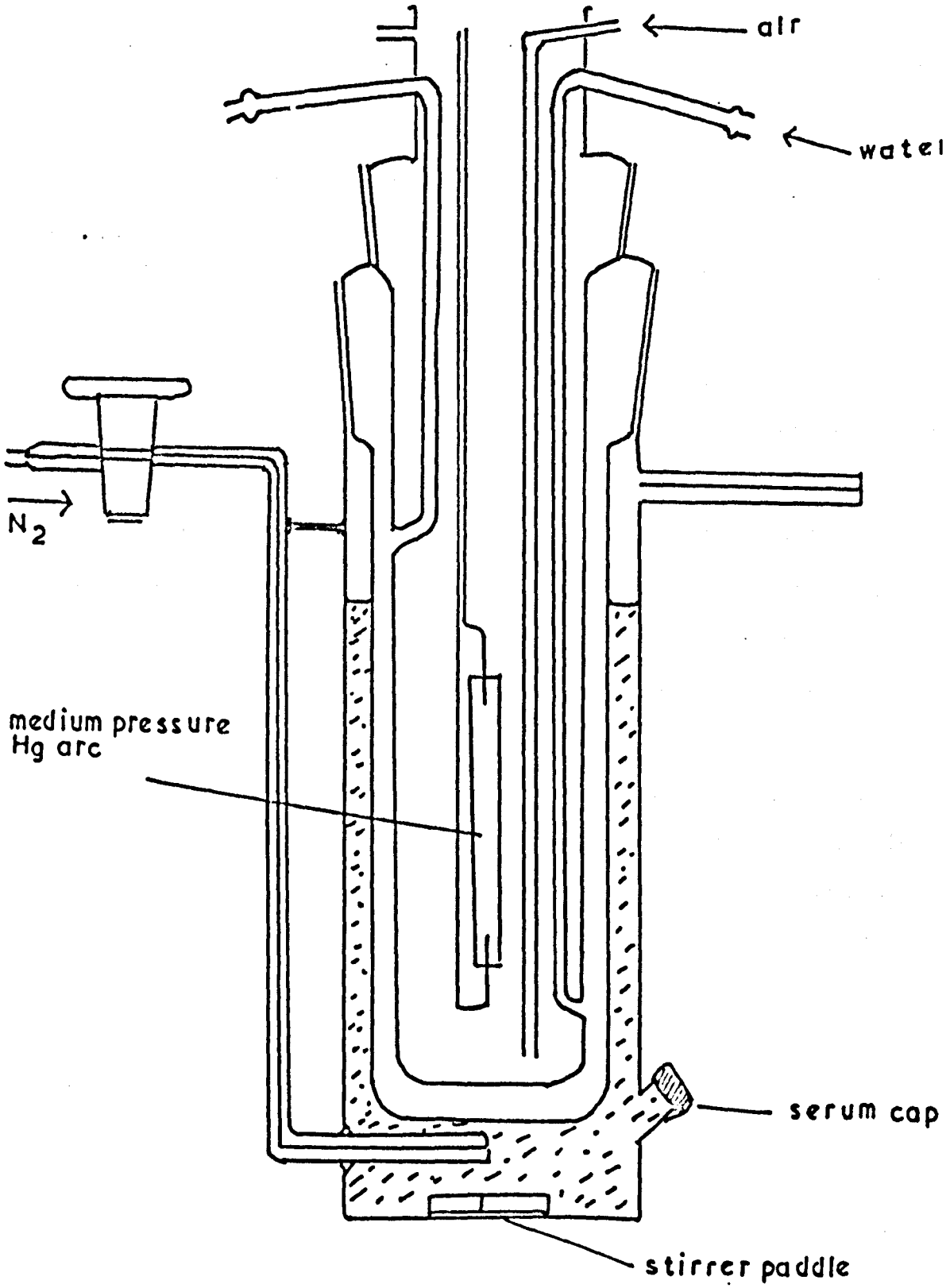
air
water
N_2
medium pressure
Hg arc
serum cap
stirrer paddle

2.6 Low Temperature Photolysis

The experiments tried at low temperatures were unsuccessful (See Results chapter), but I shall briefly explain the apparatus used. This was the Jencon's 'Spectro-Dewar' (See Fig. 2.5i). The solution to be photolysed was de-gassed on the vacuum line and then distilled into the special 3-windowed quartz cell, attached to the vacuum line by a 8 mm. quartz to pyrex graded seal. The cell was then sealed-off with a torch, just above the graded seal, so that it could be introduced into the brass conduction block at the bottom of the inner part of the dewar. The dewar was then assembled and evacuated to 'black vacuum', making sure that the windows of the cell were in line with those on the outer part of the dewar. The contents of the cell were then cooled by filling the dewar with a liquid refrigerant so that conduction cooled the cell. The outer windows did not mist up as they remained at room temperature. The liquid in the cell was then photolysed by placing the apparatus in front of a suitable light source.

The major disadvantage of this technique is that sampling is not continuous. Therefore, all rate curves must be constructed one point at a time. As light intensity reaching the cell is low, this is an extremely laborious job.

Fig. 2.5(i) Spectro-Dewar

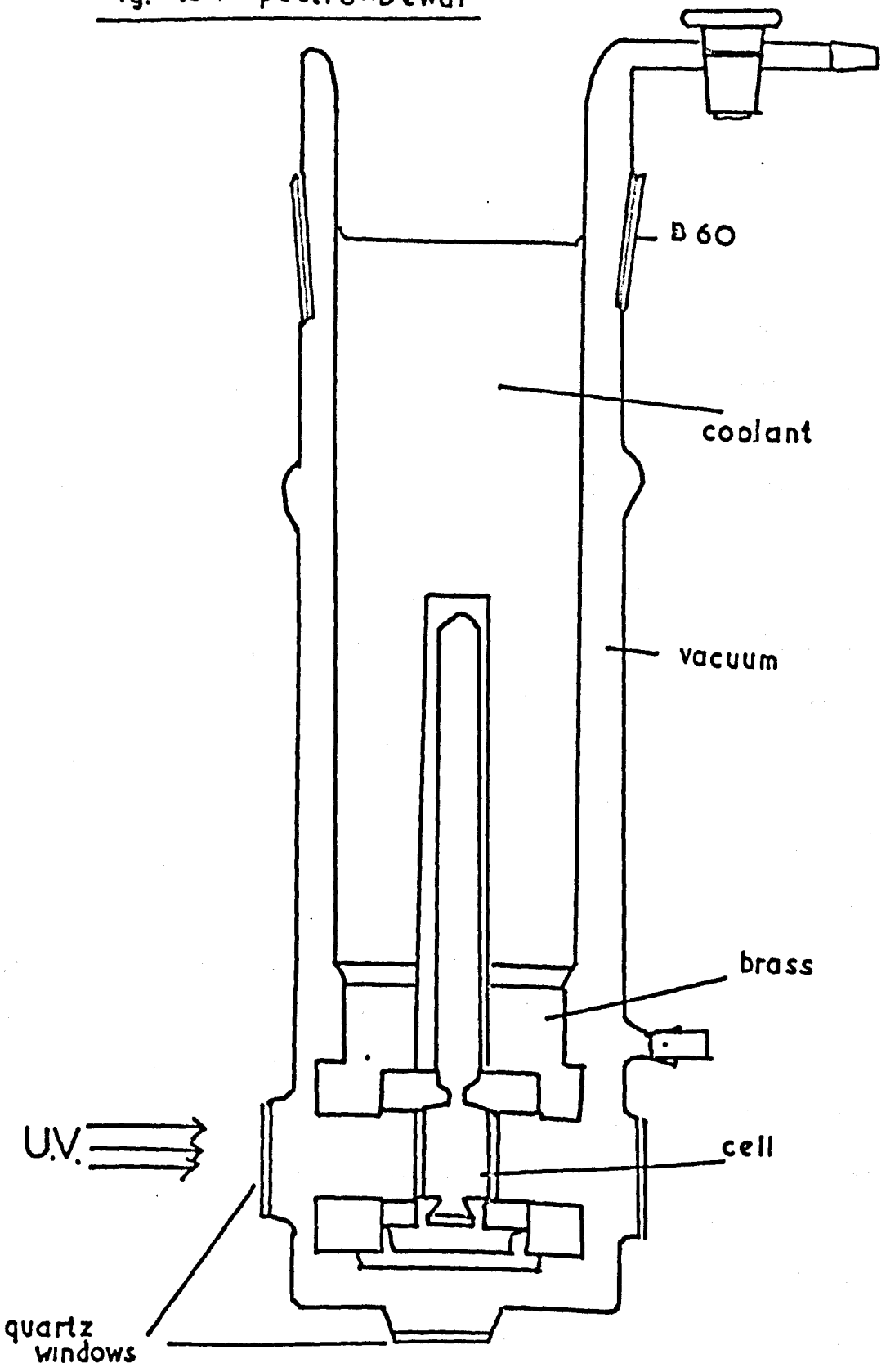

2.7 The Capillary Technique

The idea of using small quartz capillaries as photolysis vessels was first suggested by Porter and Volman.[6, 7, 8] Their technique was refined by Sedlar[9] and further amendments to this method are outlined below. The advantages of using small sealed tubes are that only small quantities of reactant need be prepared and that all products can be analysed. Various methods of filling such tubes in the absence of oxygen (a triplet quencher) have been devised.

2.7(a) Filling under Nitrogen

(i) In this method a known amount of oxygen-free solution was introduced into a 1 mm i.d. quartz capillary tube (Thermal Syndicate Ltd.) of wall thickness 0.5 mm., and sealed-off under a nitrogen atmosphere.

About 1 ml. of the solution to be studied was placed in a small glass tube fitted with a silicone rubber serum-bottle cap (Perkin-Elmer Ltd.) and a finely drawn side-arm about 5 cm. long (See Fig. 2.5(a)). Nitrogen, from the purification line (See Section 2.8(b)), was bubbled through the solution via a fine bore hypodermic needle, 11.5 cm. in length, attached to the nitrogen supply tube with a compression coupling and 'Araldite' cement (C.I.B.A. Ltd.). The nitrogen flow was around 50 ml./min. and the solution was cooled in ice to minimise evaporation of the solvent. After 15 - 20 mins. the side-arm was sealed-off with a small flame, the nitrogen flow stopped and the needle removed. The solution was now assumed to be oxygen-free, and was not kept in this tube for more than 24 hrs. before use.

Fig. 2.5(iii)

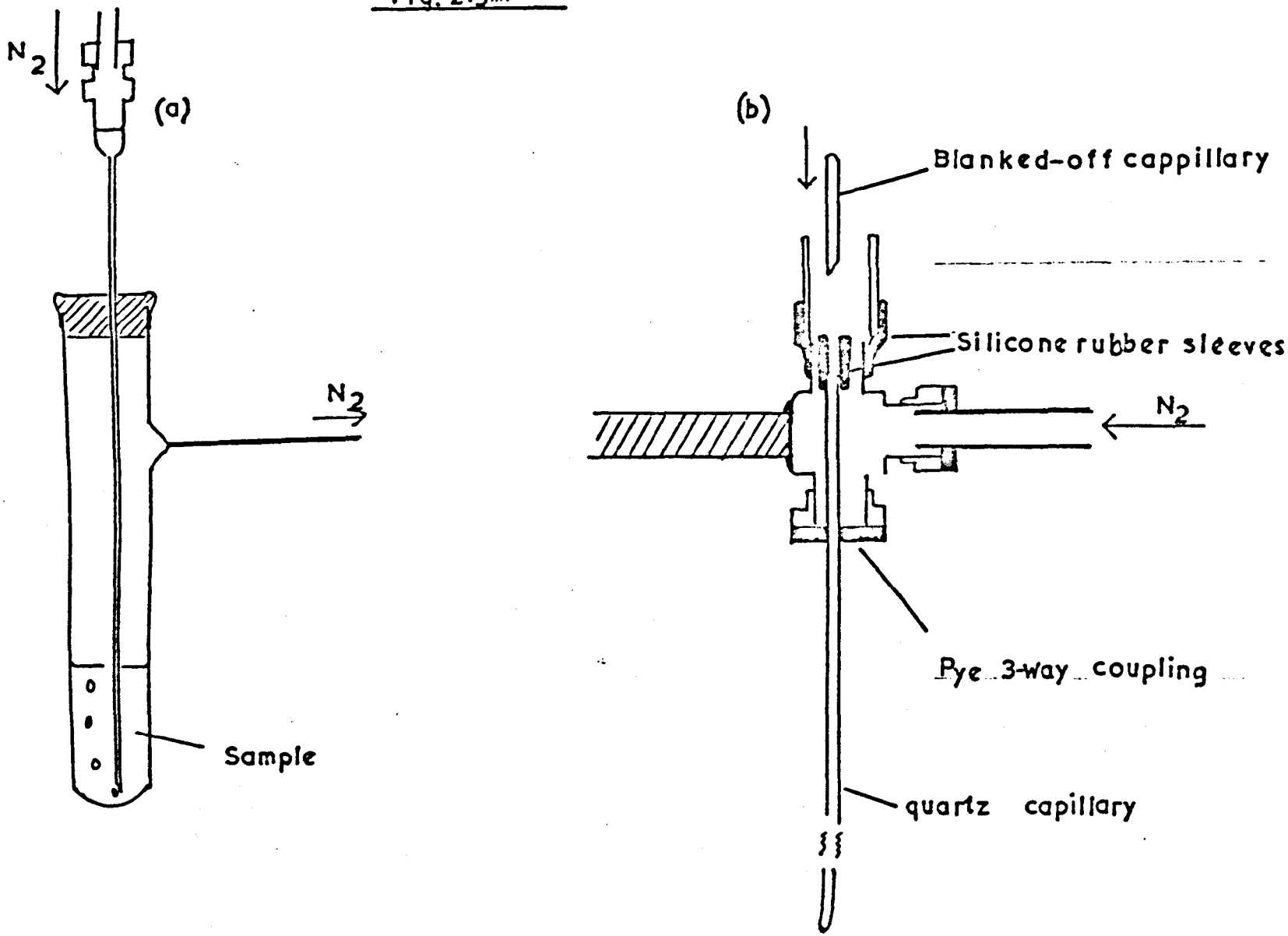
N2
(a)
N2
Sample
(b)
Blanked-off cappillary
Silicone rubber sleeves
N2
Pye 3-way coupling
quartz capillary

The device used for filling capillaries is shown in Fig. 2.5(b). It consisted of a Pye 3-way compression coupling (for 3.2 mm. o.d. tubing) mounted in a retort stand, by means of a rod to which it was fixed by 'Araldite'. A length of 3.2 mm. nylon tubing was attached to one arm of the coupling supplying a fast flow of pure nitrogen. The top arm of the coupling was extended with a short length of glass tubing and P.V.C. sleeve. The bottom arm was fitted with a silicone rubber disc, through which a piece of quartz capillary tubing was pushed, forming a gas-tight septum.

The length of capillary (about 8 cm.) was first rounded-off at each end by a hot flame. To one end was attached a 1 cm. length of 2 mm. i.d. silicone rubber tubing and the other end was pushed into the coupling from the top until it was in the position shown in the diagram. The top of the coupling was blanked-off with a piece of Apiezon Q-compound so that all the nitrogen flow was directed down the tube. After a few minutes, the bottom of the tube was sealed-off with the cone of an oxygen/gas torch whilst the blanking plug was removed. The tube was now full of nitrogen and protected from the air by a flow of nitrogen out of the mouth of the coupling. A long-needled microlitre syringe was flushed with nitrogen by pumping the piston up and down with the needle in the nitrogen supply, and then quickly used to sample 15µls of solution from the reservoir to the capillary through the protective stream of nitrogen around the neck of the coupling. After filling, the tube was sealed by pushing a plug, made from sealed capillary tube, into the top of the silicone rubber sleeve. This was done under nitrogen. The filled tube was then

removed from the top of the coupling and the plug pushed home to form a tight seal. The operation was then repeated until a batch of 5 or 6 tubes, all filled with the same solution, had been prepared. Filled tubes were stored in a refrigerator to avoid exposure to stray U.V. light.

(ii) Other Methods of Filling under Nitrogen

All samples filled under nitrogen were filled by the technique (i). However, other techniques were first devised and later discarded. Clearly, the method described above is open to criticism, in that it is not easy to exclude all oxygen from the samples by these means. I shall describe the unsuccessful methods tried, in the hope that it may be possible to modify them in future.

The first method described was due to Sedlar who had some success in using it.[9] In this method, the liquid sample was de-gassed on a vacuum line by freeze-thaw cycles and then stored over a nitrogen atmosphere. The vessel used for this procedure was a 50 ml. round-bottomed flask with its neck drawn-out and attached via a 'teflon' tap to a B14 socket (and hence to the vacuum line). A side arm was fitted ending in a Wade compression coupling which was securely attached with 'Araldite' and whose open end was closed with a silicone rubber chromatograph septum. The liquid was introduced, de-gassed and, whilst still frozen, nitrogen was admitted and the tap closed. When the liquid thawed a slight positive pressure of nitrogen was present in the vessel and this enabled liquid to be forced up into a microlitre syringe introduced through the septum. The liquid was then discharged into a quartz capillary as in (i), only in this case, the liquid was frozen

down and the tube sealed by fusion, after the walls had been dried by a fast flow of nitrogen from a syringe needle.

This method was tried with a solution of methyl tiglate in cyclohexane, but was rejected, as it was found that the septum swelled in the vapour and blocked the syringe needle every time it was pushed through the coupling. The positive pressure of nitrogen was dangerous and the vessel exploded on one occasion. The method of sealing the tubes by fusion, though clearly the best in theory, was not possible with these solutions. This was because the tiglate seemed to be absorbed on the walls of the tube and charred when attempts were made to seal the tube. This was despite apparent drying with a nitrogen flow. However, this method has been used successfully with solutions that do not attack the septum and are not absorbed onto the quartz walls.[9] Another filling method was developed as an alternative. It made use of the apparatus shown in Fig. 2.6. The solution was placed in the tube, with the long delivery tube sealed, and de-gassed as above, on the vacuum line. The liquid was then allowed to thaw, and nitrogen was introduced at atmospheric pressure. The tip of the delivery tube was then broken open and the sample capillary placed over the delivery tube, so that a fast flow of nitrogen flushed all the air out of the tube, which was then sealed. The capillary was held in the 3-way coupling, described earlier.

The whole arrangement was then tilted by 90° around the cone and socket joint until liquid had been forced, by the nitrogen flow, into the fine bore side-arm attached to the delivery tube. When the apparatus was returned to the vertical position, this quantity of liquid was

Fig. 2.6

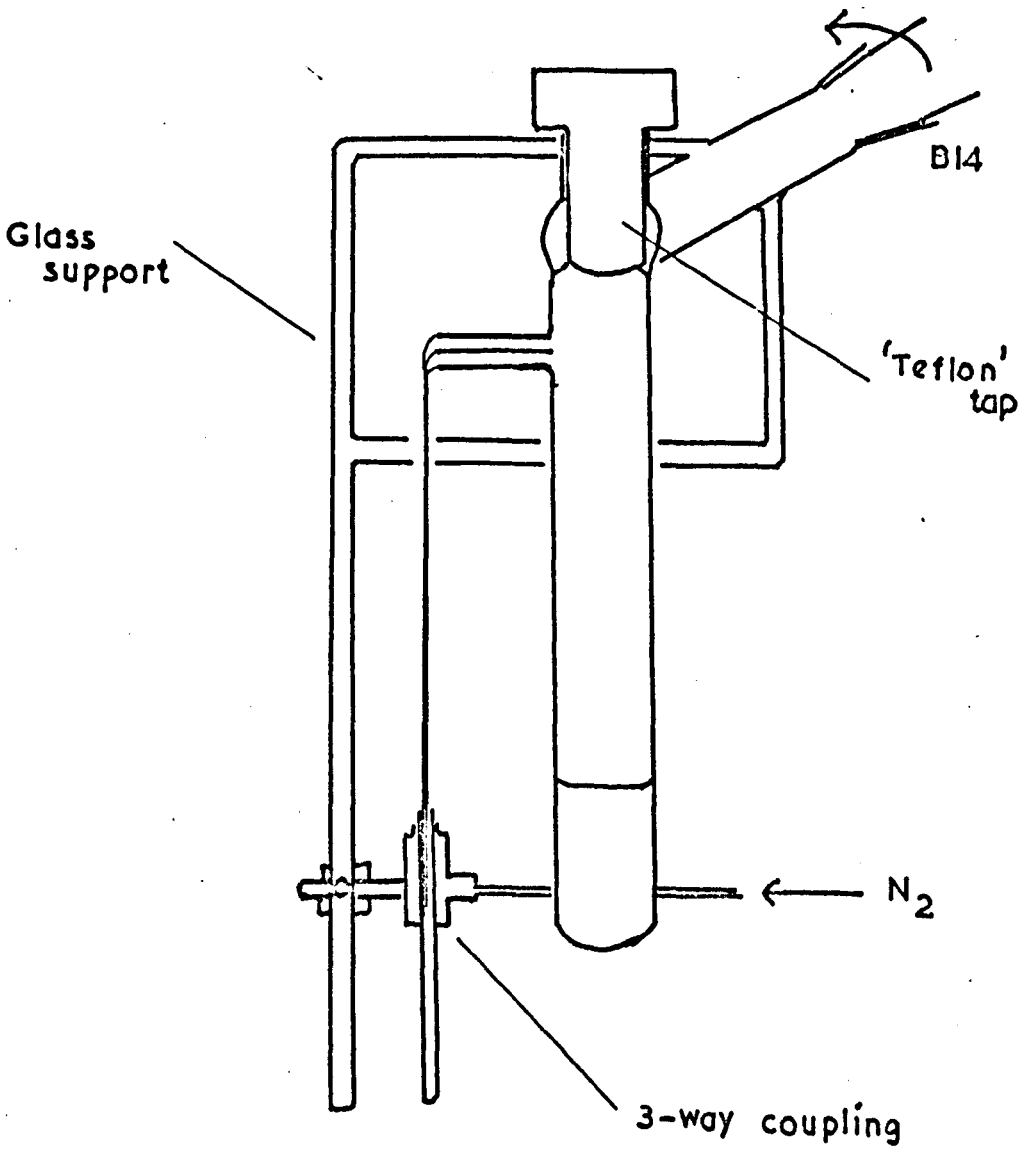

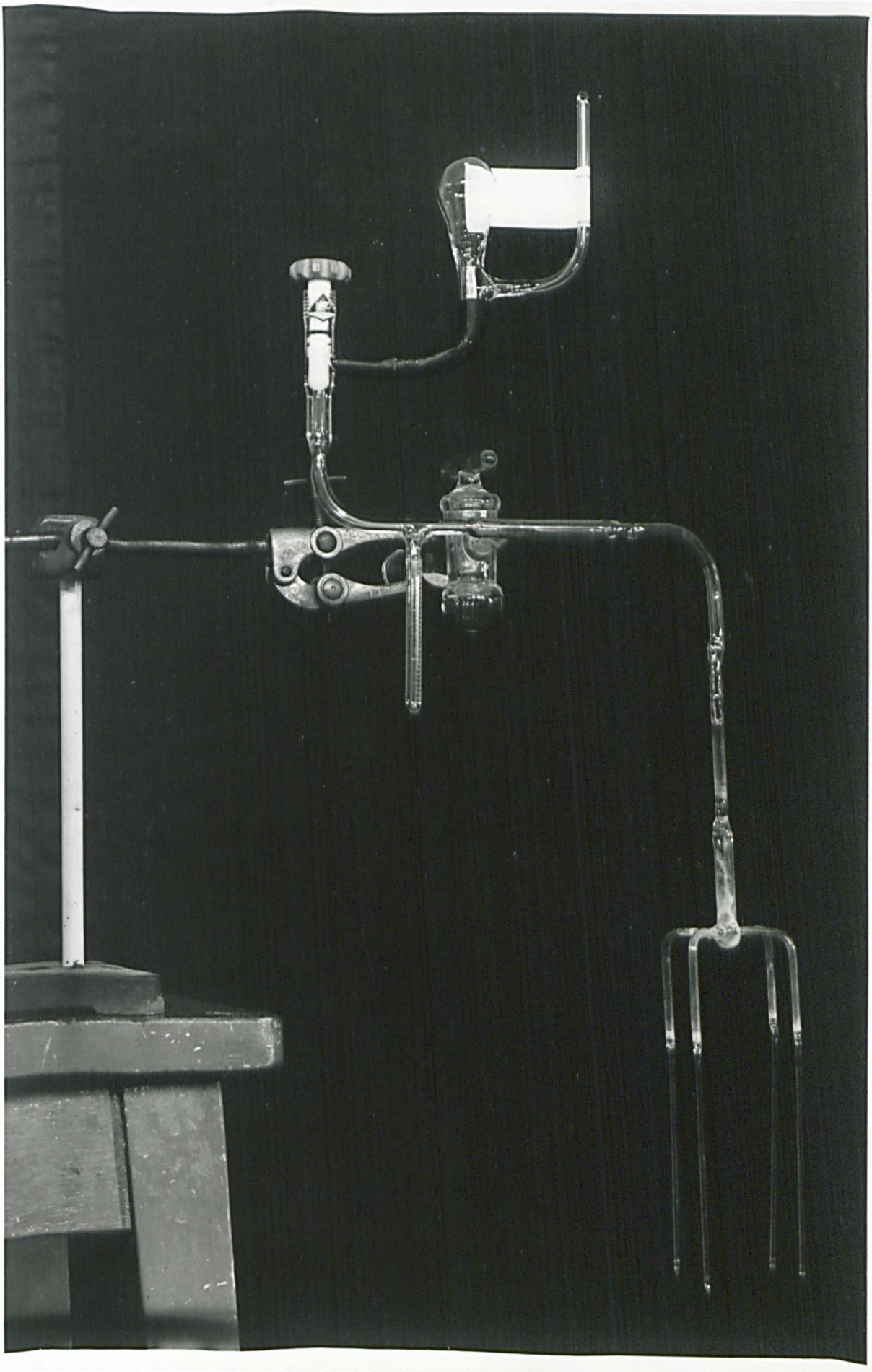

ejected into the capillary. The sample tube was then sealed by fusion, after lowering from the delivery tube. Apart from the disadvantages in the sealing method, this method worked satisfactorily. Its major disadvantage was that the whole arrangement was too elaborate and each sample took a considerable time to prepare. The apparatus was delicate and difficult to make. However, this method was probably the most efficient way of excluding air from the samples with nitrogen, as it avoided the use of a syringe to transfer liquid. Due to its complicated nature, this method was not used to obtain any of my results.

2.7(b) Filling under Vacuum

The technique used here was first described by Borrell & Sedlar[9] The apparatus used is seen in the photograph. The filling arm consisted of a reservoir connected, via a greaseless tap, to a graduated tube cut from a 1 ml. graduated pipette and, via a 5 mm. quartz to pyrex graded seal (Jencon's Limited) to a 4-way joint and four 10 cm. long quartz capillaries. The whole arm was connected through a T-joint and tap to a cone and socket joint attached to the vacuum line. The joint was held together by springs. (In the photograph the main tap is of the ground glass type. This was later replaced by a 'teflon' greaseless tap). Several greaseless taps were tried. All relied on 'teflon'to make the seal. The most successful were found to be those manufactured by Quickfit Limited ('Rotaflo') and Fischer & Porter Limited, though the latter were rather expensive.

Liquid was placed in a removable trap attached to the vacuum line and de-gassed roughly by a freeze-thaw cycle. It was then distilled into the filling arm with both taps open, in the position with

the capillaries pointing upwards. The de-gassing process was then completed and the liquid was finally frozen down and the arm pumped down, until no coloured discharge was seen with a 'Tessla' vacuum tester, when the taps were shut. The arm was then rotated through 180° so that the capillaries were pointing downwards. With the main tap shut, the reservoir tap was opened slowly so that a measured quantity of liquid ran down into the graduated tube (c.a. 80µls). The reservoir was then sealed off, and the liquid was distilled into the capillaries, by cooling above a solid CO_2/acetone cooling bath in a large dewar. After freezing the tubes down in liquid nitrogen the main tap was opened and 'black' vacuum re-established. The capillaries were then sealed-off with an oxygen/natural gas torch (Carlisle Ltd. N.J.). Goggles were worn during all quartz working operations. A new set of tubes was blown onto the stubs of the last set, after removing the filler arm from the vacuum line. The reservoir remained sealed-off and de-gassed for a considerable time. It was protected from the U.V. glare of quartz-blowing by masking with black P.V.C. tape.

Difficulties were experienced with the distillation process. Uneven filling of the tubes was common and this leads to uneven concentrations between tubes. It was found virtually impossible to sample exactly the same concentration into each tube though the differences were usually small. Factors influencing the distillation were :-

(i) Tube length - all tubes had to be the same length

(ii) Speed of distillation - if distillation was too fast then the concentration differences were great.

(iii) Constriction at sealing point - if a tube was sealed-on with a slight constriction at the joint, then distillation into that tube was much slower than into the others. The sealing process was critical and extremely difficult to do properly.

(iv) Temperature differential - if a 'dry ice'/acetone cooling bath was used then the distillation was more even than if liquid nitrogen was used.

Clearly, these differences of distillation were irrelevant if the liquid had only one component, as in the case of methyl propyl ketone actinometry. However, they lead to considerable inaccuracies with a mixture of components with widely differing boiling points such as methyl tiglate and cyclohexane. The system for which this method was originated by Dr. Sedlar, that of acetone and cyclohexene[10] (both very volatile) was particularly suitable for this technique.

2.7(c) Measurement of capillary diameter

To check the internal diameter of the capillary tubes a measured length of mercury was weighed in a capillary. A typical measurement was :-

Mercury length	=	4.25 cm.
Wt. of mercury	=	0.4548g.
Volume of mercury	=	0.03357 c.c.[11]
Radius of tube	=	0.05015 cm.
Diameter	=	1.003 cm.

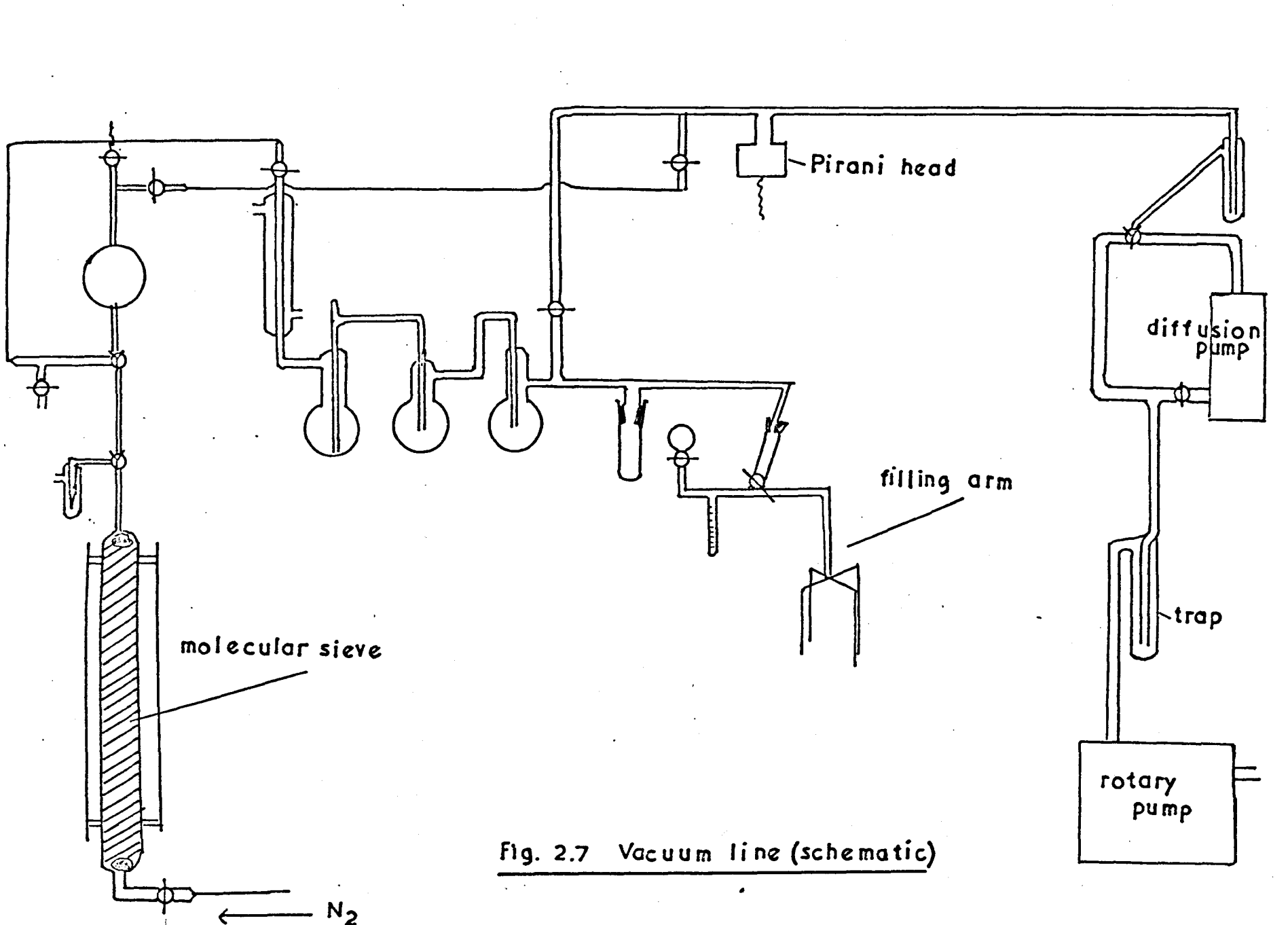

Fig. 2.7 Vacuum line (schematic)

The diameter of each batch of tubing was checked and was found to vary by $\pm$ 5% only. The wall thickness quoted as 0.5 mm. varied by a greater degree, but this was ignored.

2.7(d) Vacuum Line

A vacuum line was constructed for use with the vacuum filling of capillaries and was also used for other experiments. (See Fig. 2.7). This line was of conventional design. Pumping was by an Edwards Ltd. ED.35 rotary oil pump backing an N.G.N. Electrical Ltd. oil diffusion pump using Edwards 702 silicone fluid. Except for the filling arm, ground glass taps were used (Laboratory Glassware Manufacturers Ltd.) with Edwards high vacuum silicone grease as lubricant. These were periodically cleaned with pentane and regreased to avoid contamination from vapour absorbed by the grease. A nitrogen line was built into the vacuum system with a 0.5 m. purification column of Linde 4A molecular sieve to absorb moisture and grease. This column was regenerated at 180°C, by passing a calibrated current through 'nichrome' windings with nitrogen flowing. The source of nitrogen was a cylinder of B.O.C. Ltd. 'white spot' nitrogen. Springham spring-loaded taps and Pye compression couplings were used on the nitrogen line. The supply line was 3.2 mm. o.d. nylon pressure tubing.

An Edwards G5C-2 2-range Pirani head and gauge were used to assess the absolute vacuum. This was better than 10^{-2} N./m.^{2}, which was considered satisfactory for de-gassing purposes. An Edwards Type 2 H.F. Tester was used to detect leaks and as a rough guide to vacuum. 'Black vacuum' with this instrument is quoted as less than 5.3×10^{-2} N./m.^{2}. This was usually taken to be an acceptable vacuum.

Care was taken to exclude mercury from the vacuum system.

2.7(e) Photolysis of Capillaries

(i) Water thermostat

The apparatus used is shown in Fig. 2.8. It consisted of a black-painted brass tank of about 10 l. capacity. It was filled with clean tap water and maintained at a constant temperature by means of an immersion heater (Electrothermal Ltd., 400 W.) connected to a contact thermometer and relay. For maintaining temperatures near ambient, cold water was circulated through a 3 m. coiled copper pipe immersed in the tank. The tank was stirred slowly by a glass paddle and stirrer motor. By these means the temperature of the bath could be maintained to within $\pm$ 1°C.

Two 2 mm. thick 'spectrosil' windows were mounted in the walls of the tank and the samples, fixed in a holder, were mounted on a brass beam running across the tank between the windows. The windows were 5 cm. in diameter and were sealed into the tank by threaded mountings and O-rings. The tank was covered by a lid to keep out dust and the water was changed regularly to maintain the transparency of the optical train. The capillary holder is shown in Fig. 2.9. It was made from a block of aluminium and was painted black, to reduce reflections. It held 6 capillary tubes and was so shaped that the columns of liquid in the tube were positioned in the middle of the light beam. The tubes were held in 2 mm. square grooves by a rubber grip. A shutter device was made from a brass disc and was mounted on the support beam between the window and the samples. Each tube was loosely held in the holder

Fig. 2.8

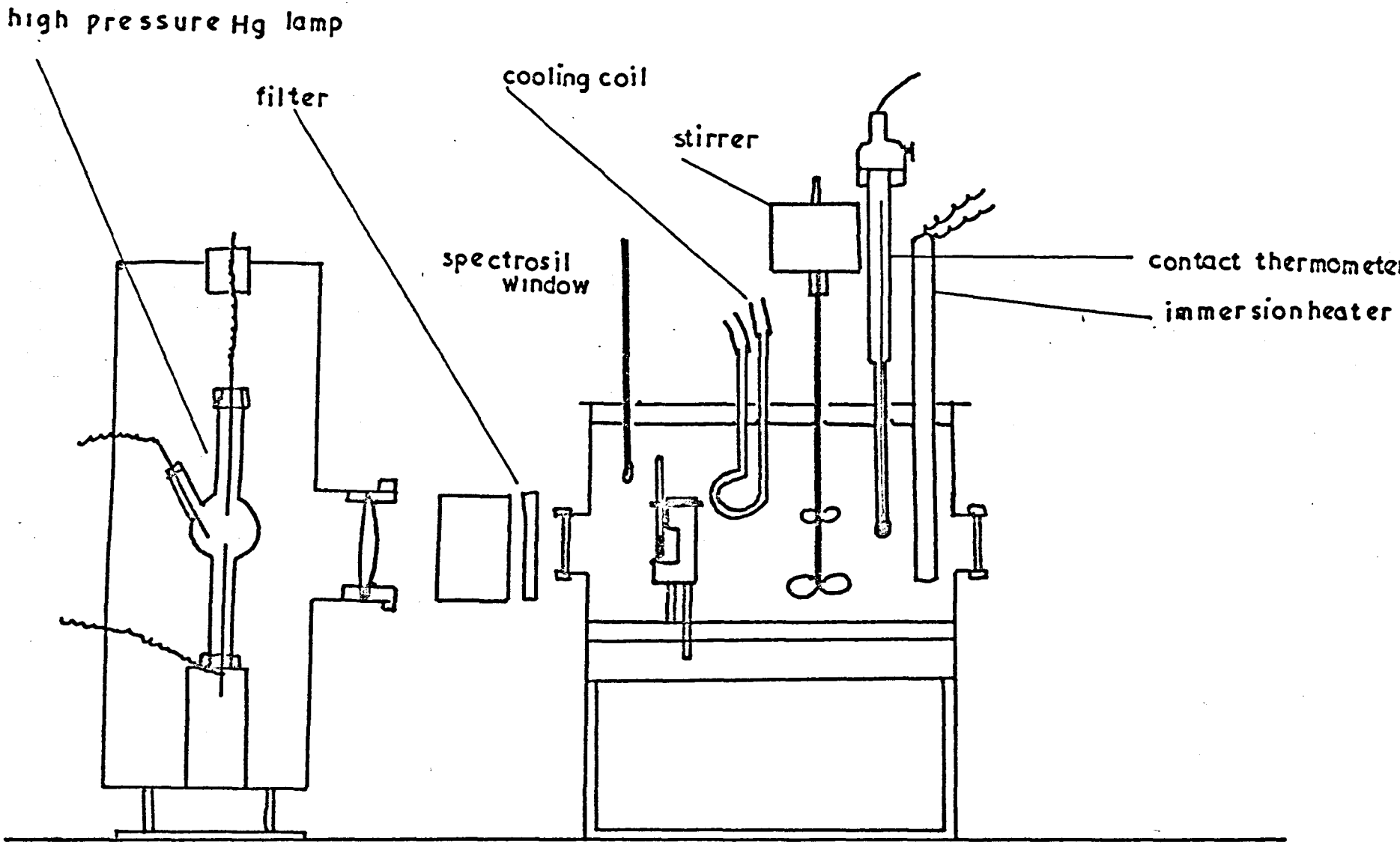
high pressure Hg lamp
filter
cooling coil
stirrer
spectrosil window
contact thermometer
immersion heater

Fig. 2.9

(a) Front view showing one capillary

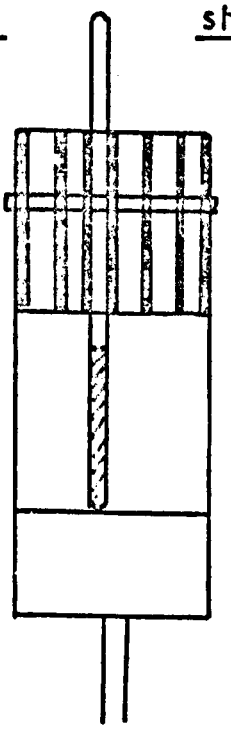

(b) Side view

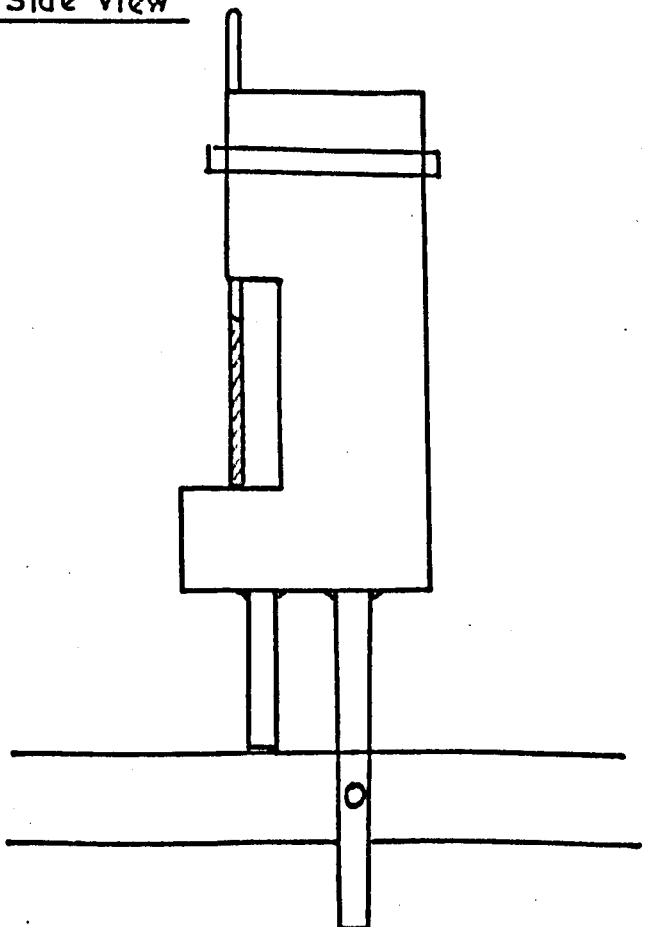

to enable individual tubes to be taken out after known times.

Using the high pressure lamp, Sedlar found that a high degree of consistency from tube to tube could be obtained and this was borne out in this work. It was essential to have a nearly parallel and uniform beam of light for these experiments and so only the high pressure lamp, with its near point source, could be used. Attempts were made to monitor the decay of the lamp with a photomultiplier and microammeter mounted behind the other window, but these were not very successful. The improvement of this method of monitoring was neglected when the semi-micro technique was adopted in place of the capillary method.

(ii) Photolysis on "merry-go-round" apparatus

For photolysis of capillaries with the low pressure mercury lamp at 253.7 nm., a rotating photolysis apparatus was constructed. (The name "merry-go-round" was first used by Moses at the California Institute of Technology, See Ref.2). This was necessary, as the large size of the source otherwise made even illumination impossible. See Fig. 2.10. Tubes were mounted in a rubber retaining ring on the inside of a rotating cylinder made from a length of 'alkathene' pipe (15 cm. long, 9 cm. in diameter), perforated with holes for good air circulation. The cylinder was mounted on an electric stirrer motor and the whole arrangement was enclosed in an asbestos box, fitted with a fan, contact thermometer, heater and relay for temperature control. Suspended from the top of the box and inside the rotating cylinder, was the lamp enclosed in a double quartz jacket taken from a Hanovia

Fig. 2.10

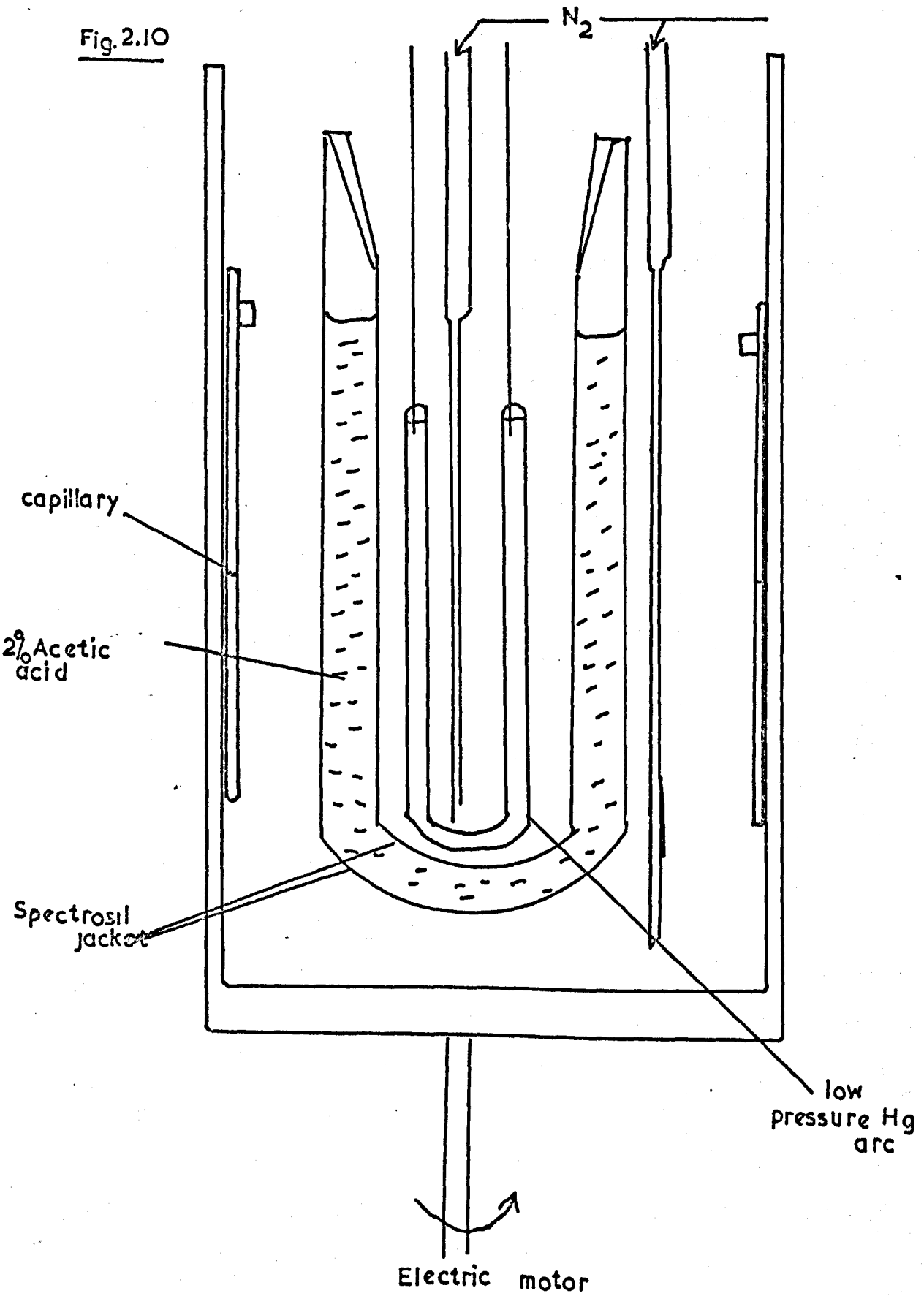
N_2
capillary
2% Acetic acid
Spectrosil jacket
low pressure Hg arc
Electric motor

immersion-well apparatus. (See Sections 2.3(a) and 2.5). The 3 mm. thick annular space between the quartz envelopes was filled with a solution of 20% acetic acid to absorb unwanted 185 nm. light. This solution was changed regularly and showed a drop of 15% in concentration after 15 hrs. irradiation. A slow flow of nitrogen was passed through a hypodermic needle into the cavity containing the lamp and also into the cylinder containing the tubes, to prevent ozone formation and the consequent absorption of 254 nm. light.

At a constant speed setting of 40 revolutions per min. each tube on the cylinder wall saw the same aspect of the lamp 100 times in under 3 min. and, since no irradiations were shorter than this, the averaging of illumination was considered adequate. This was borne-out by experiment when two identical tubes gave idential degrees of conversion after the same time (20 mins.); within sampling error on the chromatograph.

The lamp was allowed to warm up for 15 mins., before placing any samples on the drum.

2.7(f) Analysis of Capillary Samples

Attempts to sample the whole contents of the capillary after reaction into the V.P.C. with a steel plunger device were not successful as the tubes were too strong and the volume to large. No attempt was made to get round this difficulty, as gaseous products were not seen in most of this work. The tubes were broken open and sampling was by means of a syringe. This could be done with a repeatability of $\pm$ 2% (found by injecting many aliquots of the same sample).

2.8 Semi-micro Technique

2.8(a) Optical System and Cell

The apparatus used is seen in Fig. 2.11 and the photograph. It was designed in collaboration with Dr. J. Sedlar. In this case, the photolysis vessel was a cylindrical, water-jacketed 'spectrosil' cell, supplied by Ross Scientific Ltd. (Type 50) which is shown in Fig. 2.12. The path length of this cell was 10 mm. and the optical surface area 1.30 $cm.^2$. The inner cell was surrounded by an annular water jacket and the whole vessel was fitted with a B7 socket. The cell was attached to a glass neck via a B7 cone, which was sealed at the top by a rubber serum cap. Pure nitrogen from the nitrogen purification line (See Sect. 2.8(b)) was passed into the cell by means of a stainless steel hypodermic needle, sealed into the side arm of the neck by 'Araldite'. An exit tube carried the nitrogen away to the atmosphere via a capillary pressure head flowmeter filled with di-butyl phthalate. With a slow flow of nitrogen, the cell was therefore sealed to the air.

The cell and bubbling-arm were mounted in a V-shaped piece of plywood on an Ealing Optical Instruments optical bench, 0.5m. long. The optical bench was mounted firmly on a wooden base in line with the beam from a mercury arc lamp (high, or medium pressure) fixed in a brass housing. The cell was thermostated by means of an electric circulation pump (Charles Austen Ltd.) and a constant temperature bath controlled by a Tecam temperature control unit. Interference or chemical filters were mounted in appropriate holders on the bench and

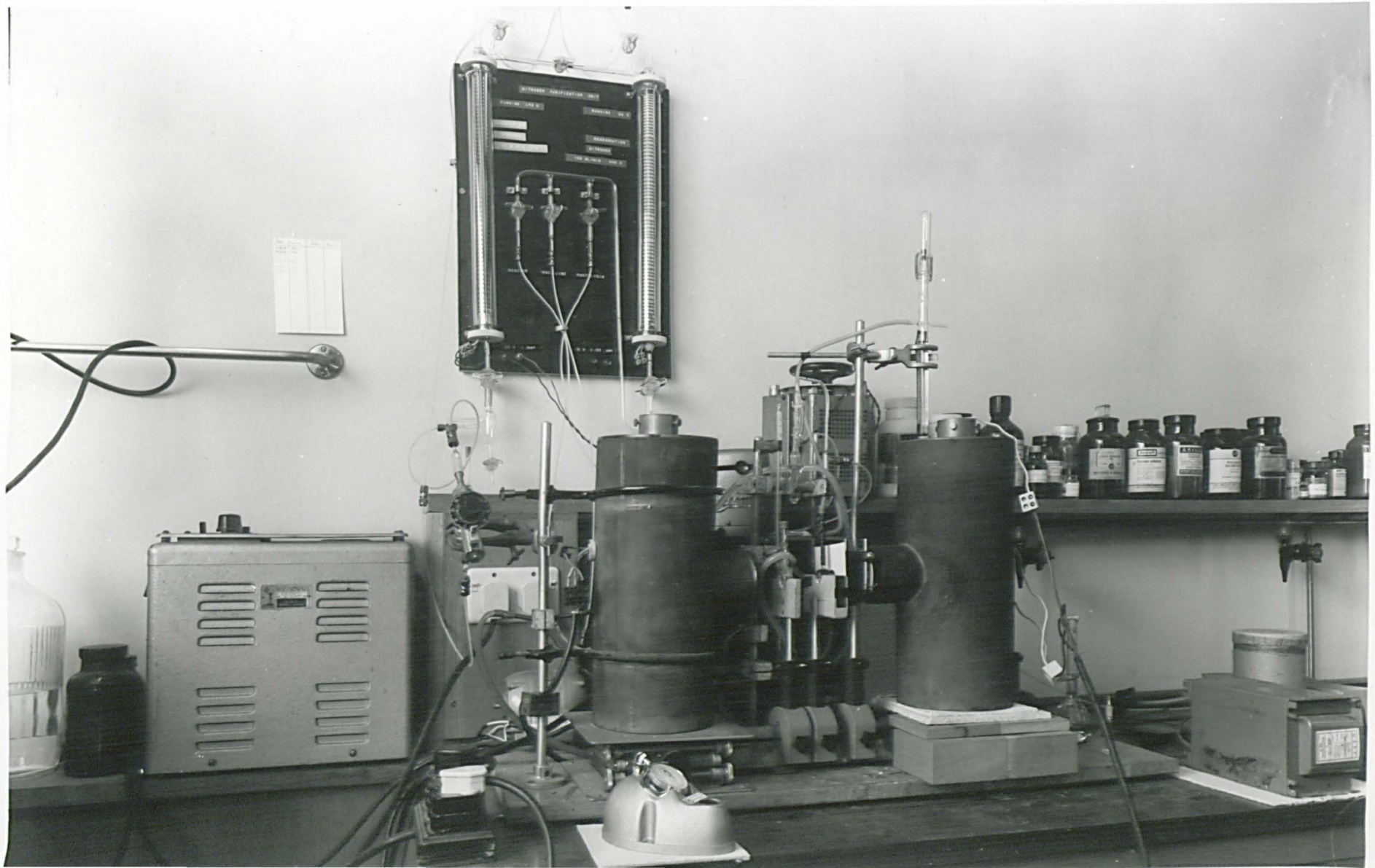

Fig. 2.11

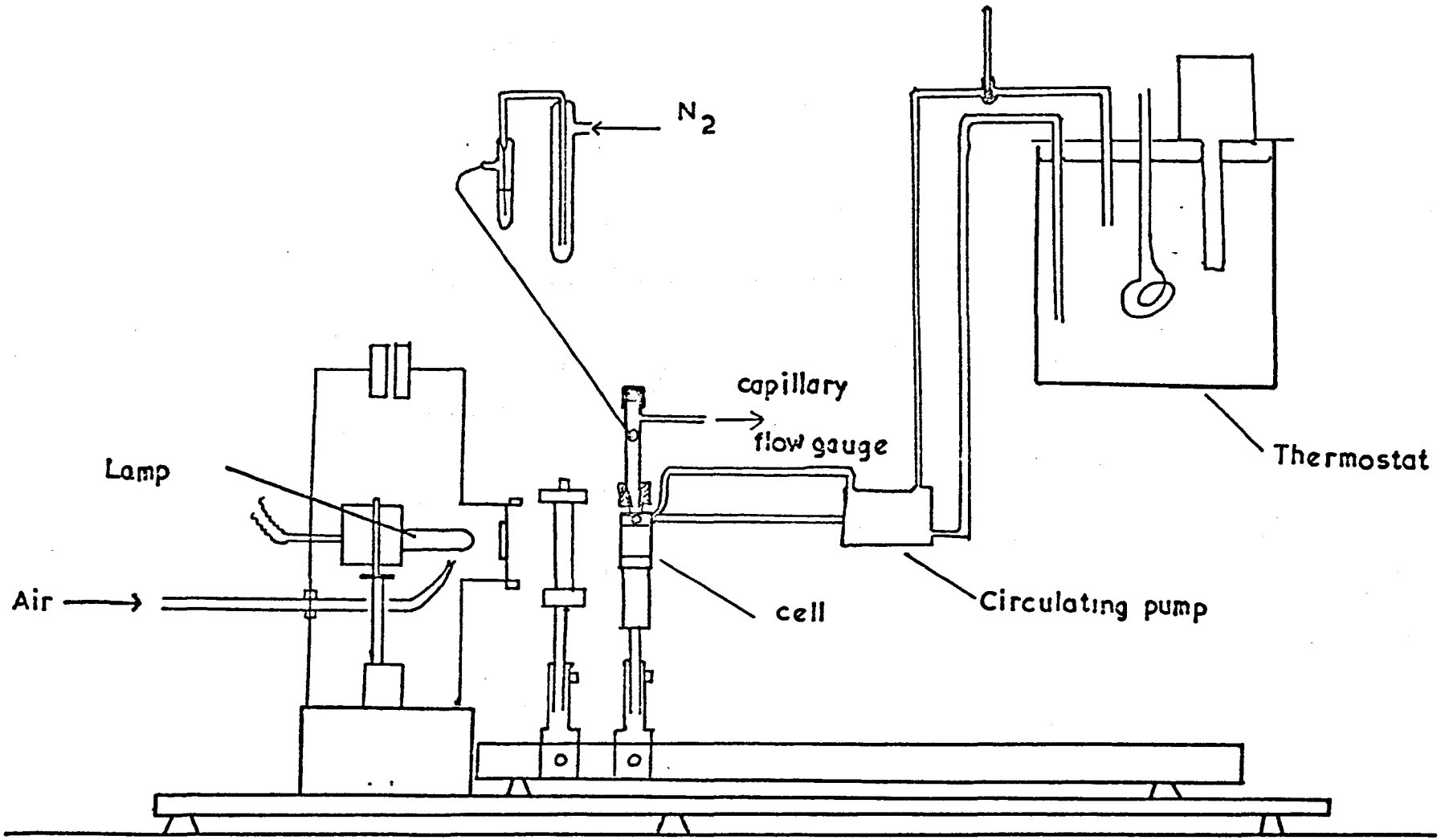
N2
capillary
flow gauge
Thermostat
Lamp
Air
cell
Circulating pump

Fig. 2.12

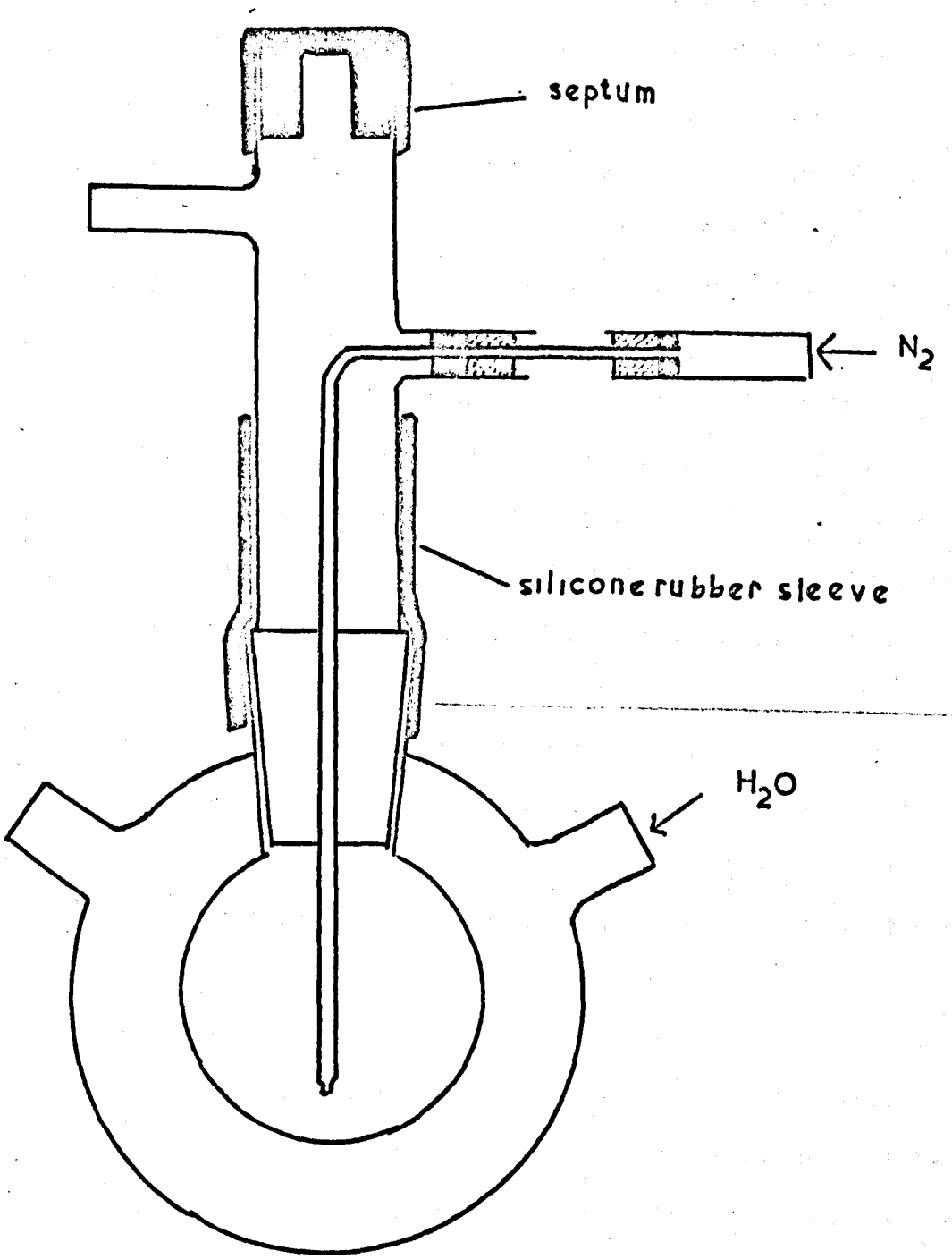

the optics were lined-up by sighting with two centering-pins. A piece of OX7 glass was mounted in the aperture of the lamp housing to act as a heat shield and to cut down visible radiation.

The cell was filled with solution by means of a long-needled syringe and was fixed to the bubbling arm using a greased silicone rubber sleeve to ensure a good seal around the cone and socket joint. The serum cap was then replaced and nitrogen bubbled through the solution at a rate of around 10 ml./min. for 0.5 hr. After this period, the flow was reduced to about 1 ml./min., which was just sufficient to stir the solution and exclude O_2. Samples were taken away for analysis with a Shandon-Terumo UMS10, 11.5 cm. needled syringe. The nitrogen was first passed through a glass bubbler, filled with solvent, to saturate the stream of gas entering the cell and, hence, reduce solvent loss. This bubbler was thermostated with the same water-flow used for the cell, so that the nitrogen was saturated at the same temperature as the sample vessel. After each run the cell was cleaned with chromic acid and distilled water. The needle was cleaned regularly and the serum cap exchanged on every run.

This method was found to be quite satisfactory for photolyses of up to 5 hr. duration. Above this time, evaporation of solvent became significant. The method was also unsatisfactory for volatile products and very volatile solvents. With solutions containing a high proportion of dissolved solid, care had to be taken to prevent blockage of the needle, with crystals of solute.

2.8(b) Nitrogen Purification

The apparatus is shown in Fig. 2.13. It consisted of two parallel glass columns, 25 mm. in diameter and 47 cm. long, surrounded by glass jackets 40 mm. in diameter. Inside the jacket, each column was wound with approx. 50 turns of 'nichrome' wire. The jackets were attached to the columns by means of specially-made asbestos rings and connecting rods. Nitrogen was passed up the first column, down the second and was finally distributed to its destination by means of a manifold of three taps. All taps were spring-loaded (Springham Ltd.).

The first column was packed with activated copper on Kieselguhr[13] and was heated, during use, to 170°C, by passing a pre-set current through the nichrome wire, controlled by a Variac rheostat. The packing for this column was made by depositing copper hydroxide on Kieselguhr[14] (B.D.H., acid purified) and then heating to give cupric oxide. This was powdered and packed into the column, when it was activated by passing a stream of hydrogen at 170°C, collecting water in the trap at the base of the column. This gave a deep violet packing in the column which, as it becomes exhausted, changes to yellow-brown. The column was regenerated by the same method, when ½ the column had changed colour. Care was taken, as the finely divided copper is pyrophoric in air.

The other column was packed with Linde 4A Molecular Sieve (B.D.H. Ltd.) to remove moisture from the de-oxegenated gas. This was also activated at 180°C by passing nitrogen up the column and trapping the water. It was used at room temperature and periodically re-generated.

Fig. 2.13

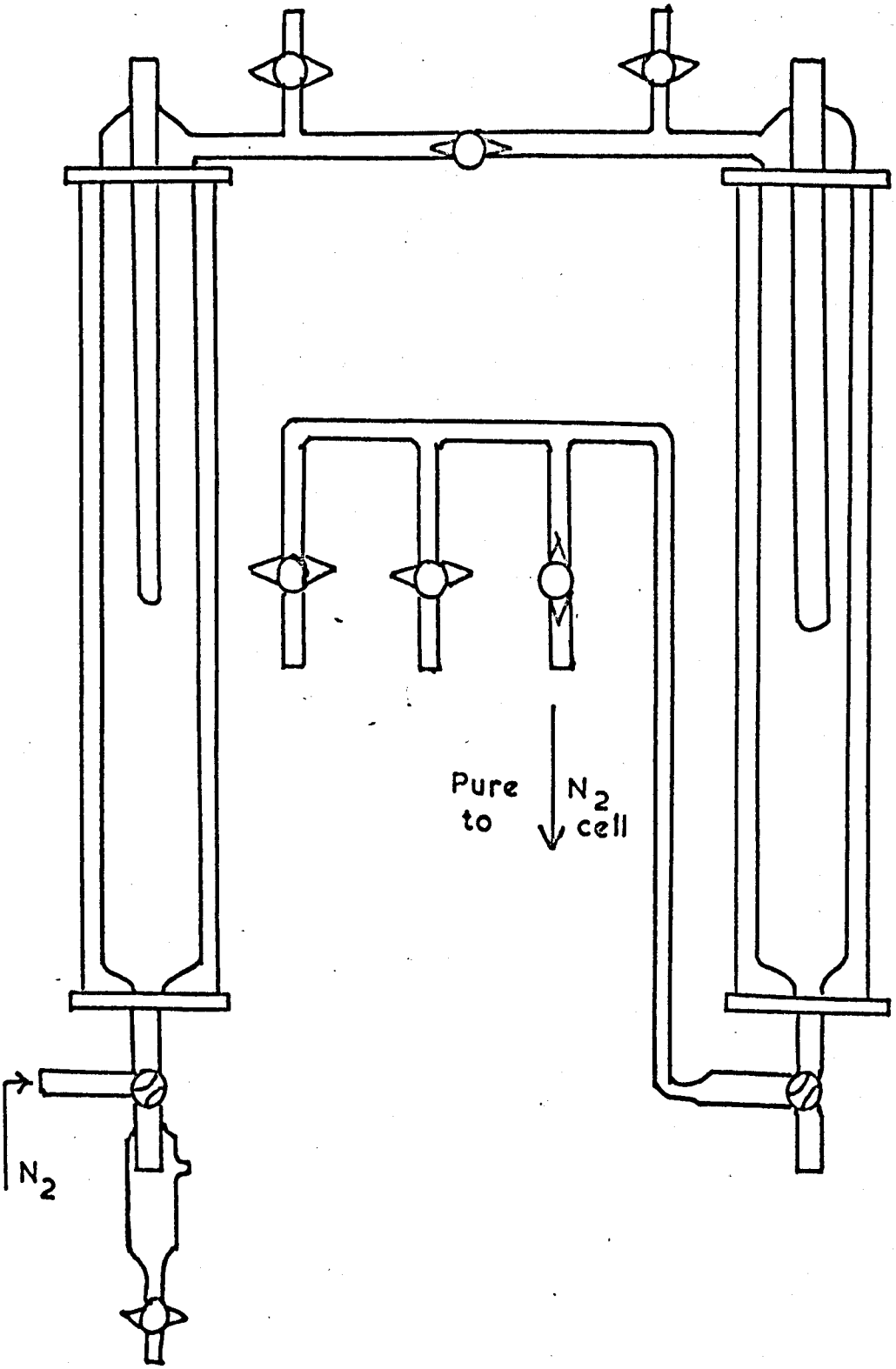

The nitrogen used for these purposes was B.O.C. 'white-spot' nitrogen claimed to contain no more than 10 p.p.m. of oxygen and other impurities. Clearly, with a continuous flow of even this small concentration of oxygen through the photolyte, appreciable quenching effects might be seen. After purification on this line, oxygen concentration should be below 0.4 p.p.m.,[13] though this was never verified. The gas flow was controlled by an Edwards needle valve mounted between the cylinder and the purification line.

2.9 Actinometry

The method of Hatchard and Parker was used to determine the absolute intensity of the light sources.[15, 16, 17] This relies upon the production of Fe^{2+} ions from a sulphuric acid solution of potassium ferrioxalate, $K_3Fe(C_2O_4)_3$ when irradiated with light of a wavelength between 250 and 577 nm. The Fe^{2+} ions are then complexed with 1,10-phenanthroline and analysed colorimetrically. The quantum yield of this reaction has been well established and was taken as 1.25 at 254 nm., 1.24 at 313 nm. and 1.21 at 366 nm. (25°C).[17]

Pure solid reactant was prepared by mixing 3 volumes of 1.5M. $K_2C_2O_4$ solution and 1 vol. of 1.5M. $FeCl_3$ solution. The precipitated potassium ferrioxalate was recrystallised from warm water and dried in air. It was stored in the dark in an amber glass bottle. A 0.006M solution of the solid in 0.1N. H_2SO_4 was used and this was also stored in the dark, without decomposition. 1 cm. of this solution absorbed 99% of incident light up to 390 nm. The solution was handled in the dark using only a red photographic safelight (Ilford F904).

As recommended, the SP500 spectrophotometer was calibrated at 510 nm., to find the extinction coefficient of the red phenanthroline -iron complex, by making up standard solutions. The value found was $\varepsilon = 1.15 \times 10^4$ litres $mole^{-1}$ cm^{-1} (compared to 1.11×10^4 Ref. 17).

To determine the light intensity incident upon a cell, the cell was filled with the actinometer solution and photolysed for a known time, eliminating as much as possible of the stray light. The solution was stirred with a slow stream of O_2-free N_2 from a fine

glass capillary. After photolysis the solution was shaken and 0.5 ml. was drawn out using a special pipette. To this was added 1.0 ml. of 0.1% 1,10-penanthroline solution, 4.5 ml. of 0.1N sulphuric acid and 2.5 ml. of oxalate buffer, the whole being made up to 10 ml. in a volumetric flask. Concurrently, a blank was made up with the unexposed solution. After developing in the dark for 45 mins., the optical density of the solution was measured against the blank at 510 nm. in 1 cm. photometer cells in the SP500. The intensity of the illumination was worked out from the formula below :-

$$I = \frac{(O.D)\ v_1 v_3 \times 6.023 \times 10^{20}}{\varepsilon l v_2 t s\ \phi_\lambda}\ q.sec.^{-1}cm.^{-2}$$

where v_1 = volume of photolysis cell; ml.

v_2 = volume of aliquot; 0.5 ml.

v_3 = volume of flask; 10 ml.

ε = extinction coeff.; 1.15×10^4 $l.mole^{-1}cm.^{-1}$

l = path length of photometer cell; 1.0 cm.

t = photolysis time; secs.

s = irradiated area of cell; $cm.^2$

ϕ_λ = quantum yield for actinometer, at wavelength λ

O.D. = Optical Density

For the water-jacketed cell arrangement, the same cell was used for actinometry. The bubbling-arm was replaced by a short length of glass tube with a B7 cone fitting into the cell and supporting it in

the same position. A long glass capillary was used as bubbler.

With the capillary technique, it was not feasible to fill capillaries with the light-sensitive solution, so the quantum yield of acetone production from pure 2-pentanone was used as a secondary actinometer. This was then measured against ferrioxalate actinometry in a larger cell (See Results Section).

2.10 Comparison of capillary and semi-micro techniques

In the course of this work the advantages and disadvantages of both techniques were discovered. They are listed here, as a summary.

2.10(a) The capillary technique had the following advantages over the semi-micro technique :-

(i) Complete absence of O_2, under vacuum, is ensured.

(ii) It is possible to follow the concentration of all products, as the capillary is a small closed system. This includes volatile products difficult to see in other techniques.

(iii) Only small quantities of reactant are needed.

(iv) High % conversions are obtained in short times.

(v) Capillary samples can be photolysed at any reasonable temperature.

Its disadvantages were :-

(i) Samples difficult to prepare.

(ii) The capillary is an ill-defined optical system.

(iii) No continuous sampling - must use one tube per point.

(iv) Uncertainty in composition if filled under vacuum. See 2.7(b).

(v) No stirring of solution. This may be important with concentrated solutions.

(vi) Actinometry difficult.

2.10(b) Against these the semi-micro technique has the following advantages :-

(i) Well defined optical system.

(ii) Well stirred, by nitrogen.

(iii) Continuous sampling.

(iv) Solutions of solids easy to handle. These cannot be handled with the vacuum capillary technique.

(v) Actinometry direct and simple.

Its disadvantages are :-

(i) Loss of volatile components; particularly gaseous products.

(ii) Limited temperature range; 15 - 90°C with water.

(iii) Approx. 100x lower conversion, for the same intensity, as capillary sample of same reactant.

(iv) Questionable exclusion of oxygen as compared to vacuum capillary method, though always assumed that O_2 was excluded.

(v) Danger of contamination from needle in certain solvents. This was noticed, for instance, when it was found that the needle produced more ferrous ions in a ferrioxalate actinometer solution than did the incident light. Contamination could be reduced by fitting a piece of quartz over the needle with an inert plastic sleeve.

2.11 Spectra

2.11(a) Mass Spectrometry

The mass spectrometer used was a Perkin-Elmer-Hitachi RMU6(E) single focusing instrument. (Resolution up to 6000). This was used in conjunction with a Pye 104 analytical gas chromatograph, via a Watson-Biemann helium separator. The columns used were 3.2 mm. o.d. and 1.5 m. long, and used a helium carrier gas. The instrument was equipped with a mass marker but this could not be used when coupled to the V.P.C. as the scan time was too long. A Honeywell 'Visicorder' photographic recorder was used to record spectra. Mass units were counted by turning up the sensitivity until a peak corresponding to every mass number was seen. Direct injection facilities were available for gas, liquid and solid samples.

2.11(b) Ultra-Violet Spectra

The spectrophotometer used mostly was a Pye-Unicam SP800A linear wavelength automatic scanning machine. (190 - 700 nm.). Liquid samples were usually contained in a pair of optically-matched, 10 mm. path length 'spectrosil' cells fitted with 'teflon' stoppers. (Unicam).

For actinometry (See Section 2.9), the older SP500, manual scan, spectrophotometer was used. At 510 nm., it was used with the tungsten lamp, blue filter and shutter in position 1.

2.11(c) Infra-Red Spectra

Three instruments were used at different times. They were the Perkin-Elmer 357 and Pye-Unicam SP200G grating spectrophotometers and the Perkin-Elmer 137 prism machine.

The samples used were thin films held between polished sodium chloride plates.

2.11(d) N.M.R. Spectra

The spectrometer was a Perkin-Elmer model R10 60 $Mc.sec^{-1}$ machine. The spectrometer was used only on its simplest mode of operation. Spectra were run in CCl_4 solution with T.M.S. as marker.

2.12 Gas Chromatography

2.12(a) Preparative Gas Chromatography

A Pye 105 automatic preparative chromatograph was used. (See Section 2.2(b)). The column used was a glass spiral of tubing 0.95 cm. o.d. and 4.6 m. long, packed with 15% Polypropylene Glycol (P.P.G.) on Chromosorb W (Perkin-Elmer Ltd.). The flow rate was set at 150 ml./min. and the column temperature 145°C, for optimum separation of the esters. When optimum conditions had been reached, the chromatograph was set on programmed automatic operation, when a continuous plastic tape operated the machine through a compressed air servo system. Injection was automatic and controlled by a pressure head of nitrogen operating on a 50 ml. reservoir of substrate. Collection was automatic and pure components were collected in coiled glass traps cooled in a freezing bath of solid CO_2/acetone. (-78°C).

A flame ionisation detector fed from a 100:1 stream splitter was connected to a Servoscribe recorder.

2.12(b) Analytical Gas Chromatography

(i) Description

The analytical machine used for all experiments was a Pye Series 104, Model 24 gas chromatograph. This was fitted with a dual flame analyser. The oven temperature could be programmed. A Vitatron linear/logarithmic UR400/1 flat-bed 10 mV recorder was used. This was fitted with 8 chart drive speeds.

The carrier gas was B.O.C. 'white-spot' nitrogen and the flames were supplied with hydrogen and compressed air, the hydrogen

being passed through molecular sieves before use. Gas lines were of 3.2 mm. nylon (air and N_2) or copper (H_2) tubing, using Pye compression couplings.

Liquid samples were injected into the column by means of a microlitre syringe. Various types were tried. Most samples were taken with a Shandon-Terumo UMS10G 10µl syringe with an 11.5 cm. needle. A Hamilton 10µl (701-N) syringe with a 5 cm. needle was also used. The syringe was cleaned after use by flushing with ether and drying on a water pump.

(ii) Columns

Various column packings were used for different separations. These were packed into 4 mm.-bore Pyrex glass, or stainless steel, columns coiled into a circle of 17.8 cm. diameter and of three standard lengths:1.5, 2.1 and 5.5 m. The mesh size of the packing was usually 80:100 and the columns were pre-heated, where necessary. Different flowrates, from 50-100 ml./min., were used in different separations and were set using a bubble flowmeter.

(iii) Calibration

The machine was calibrated for each compound on each column by, either injecting different volumes of a standard solution of the compound from a syringe, or by injecting the same volume of different standard solutions. The latter were prepared volumetrically in most cases. A calibration graph was plotted of peak height (measured in cm. with a ruler) vs. amount injected. Conditions were chosen,

such that the peak to be measured was as sharp as possible and well resolved from other peaks. The graph was usually a straight line, though, in some cases, it became a curve when large amounts were injected and the flame overloaded. Typical calibration graphs are shown in Fig. 2.14 - 2.16. Other calibration factors are tabulated below. Note that when a column was used for long periods at high temperatures it was recalibrated from time to time.

The following columns were used for analytical purposes:

Stationary Phase	Abbreviation	% Loading	Column Length metres
Polyethylene glycol adipate	PEGA	10	2.7
Apiezon L	APL	10	2.7
Polypropylene glycol	PPG	10	1.5
Di-nonyl phthalate	DNP	10	1.5
Bis-methoxy ethyl adipate	EA	20	1.5

The first three columns were used at several different temperatures. Calibration factors for each set of conditions are given overleaf. The heading 'sensitivity' is the number of cm peak height multiplied by the amplifier attenuation factor corresponding to one mole of substance injected. This is worked out from the

gradient of the calibration graph.

Compound	Column	Operating Temp. °C.	Nitrogen flow ml min^{-1}	Sensitivity cm mol^{-1} x 10^{-12}	
Methyl Tiglate	PEGA	100	50	1.63	*
Methyl Tiglate	PEGA	100	50	2.31	*
Methyl Angelate	APL	150	50	2.58	
Acetone	PEGA	100	50	2.48	
Acetone	PEGA	80	50	1.71	
1-Pentene	PPG	100	60	3.37	
1-Pentene	PPG	80	60	3.29	
Acetone	PPG	100	60	1.67	
Acetone	PPG	80	60	1.05	
2-Octanone	PEGA	150	50	5.45	
4-Methyl-2-pentanone	PPG	100	60	0.99	
2-Pentanone	PPG	80	60	0.537	
Acetone	DNP	70	55	0.857	
2-Pentanone	APL	130	50	2.59	
Acetone	APL	130	50	2.16	

Column calibrations ... continued

Compound	Column	Operating Temp. °C.	Nitrogen Flow ml min^{-1}	Sensitivity cm mol^{-1} x 10^{-12}
2-Pentanone	PPG	100	60	0.909
Acetone	EA	100	75	0.82
2-Pentanone	EA	100	75	0.79
2-Octanone	PPG	150	60	0.833
2-Octanone	APL	130	50	0.676
Cyclohexene	PEGA	70	50	1.04 *
Acetone	DNP	60	50	0.254

* Calibration graphs curved at higher concentrations. Figure quoted is from linear part of calibration graph.

Certain sensitivities quoted changed with time and new calibrations were carried out. The corrected values are used in calculation of results where necessary.

Fig. 2.14 is the calibration graph for methyl tiglate on PEGA at 100°. Fig. 2.15 is the curve for methyl angelate under the same conditions.

Fig. 2.16 shows a typical linear calibration curve for acetone on PEGA at 100°.

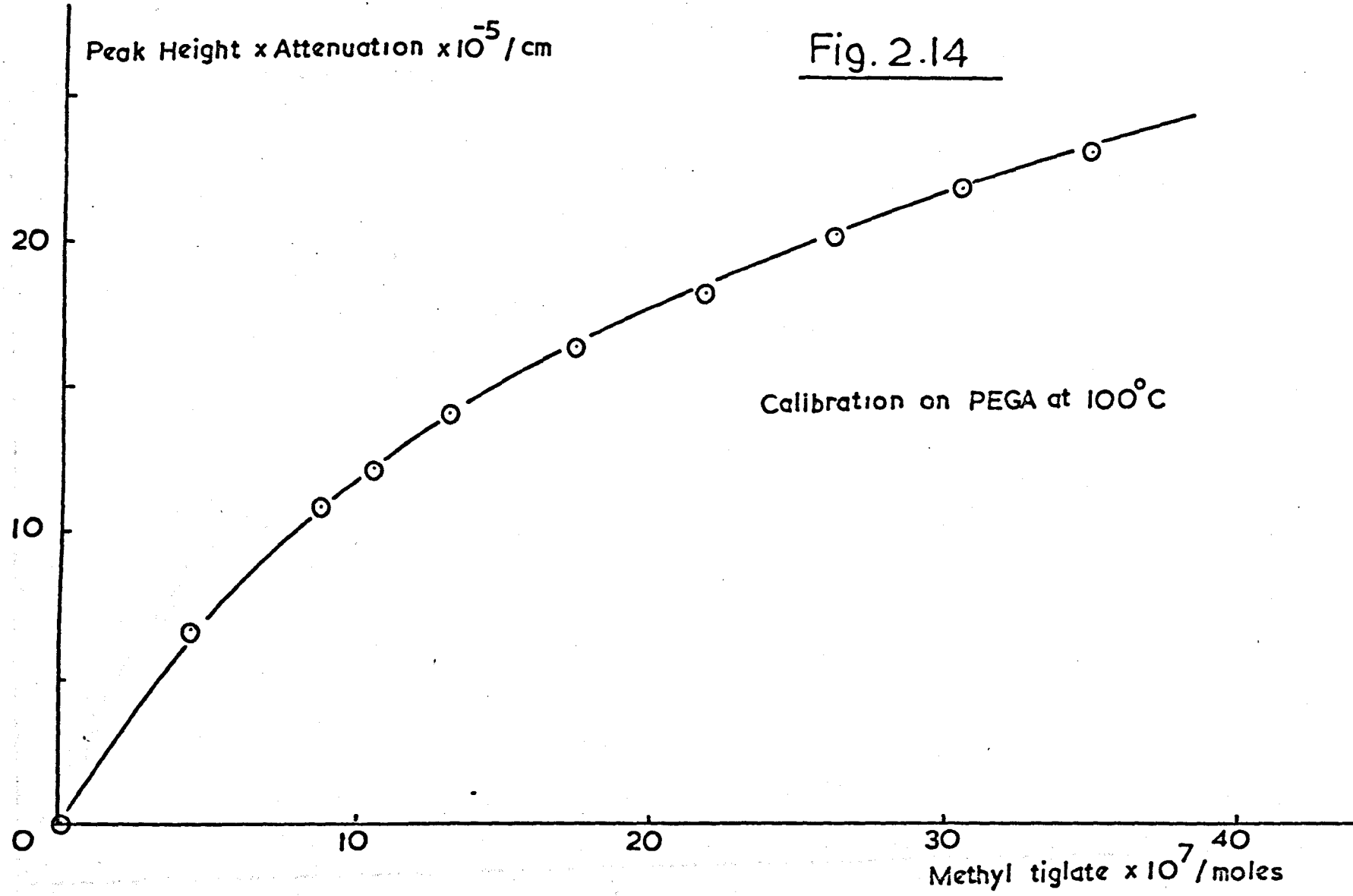
Peak Height x Attenuation x 10^{-5} / cm
Fig. 2.14
20
10
0
10
20
30
40
Calibration on PEGA at 100°C
Methyl tiglate x 10^{7} / moles

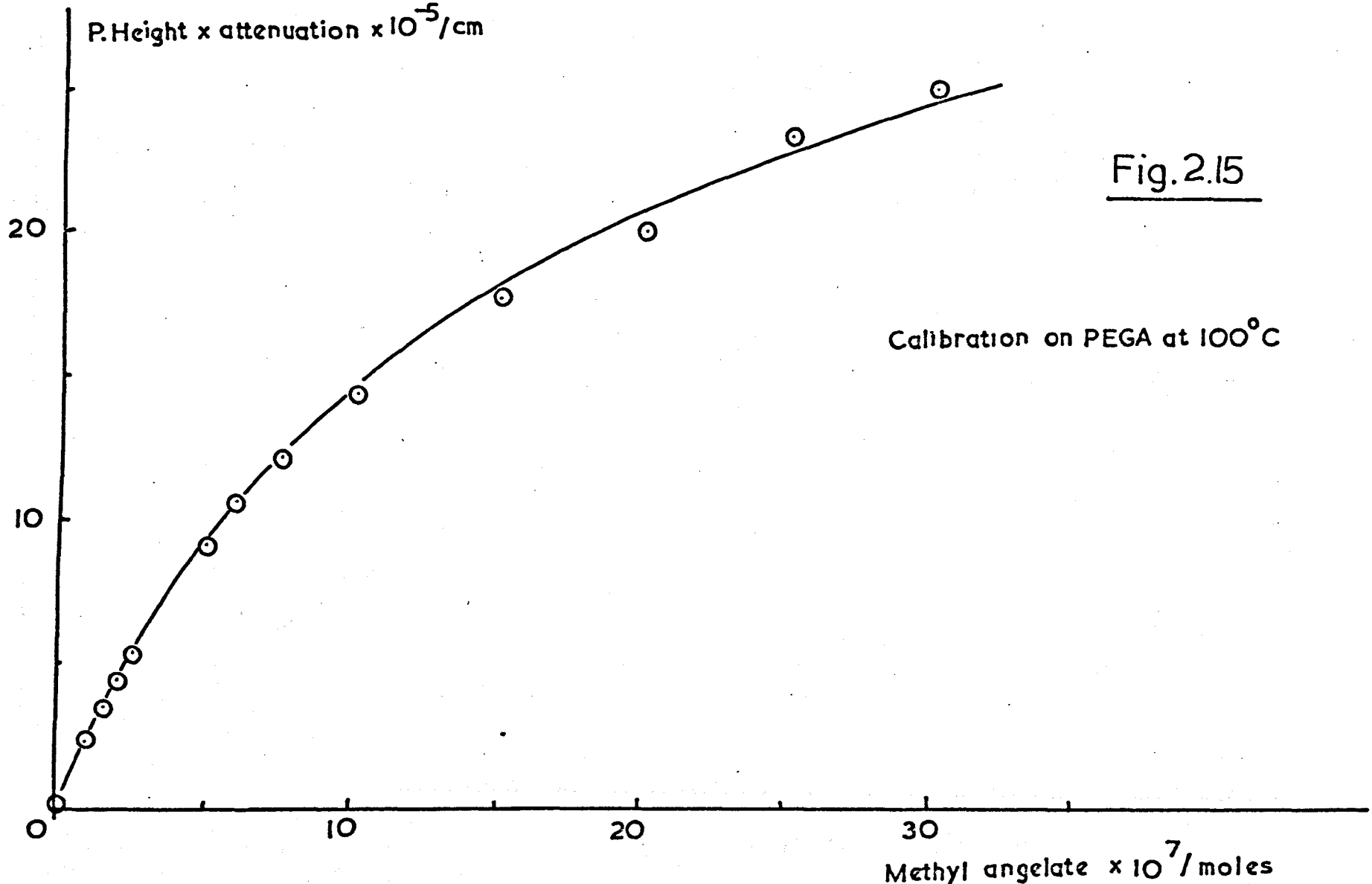

Fig. 2.15

Calibration on PEGA at 100°C

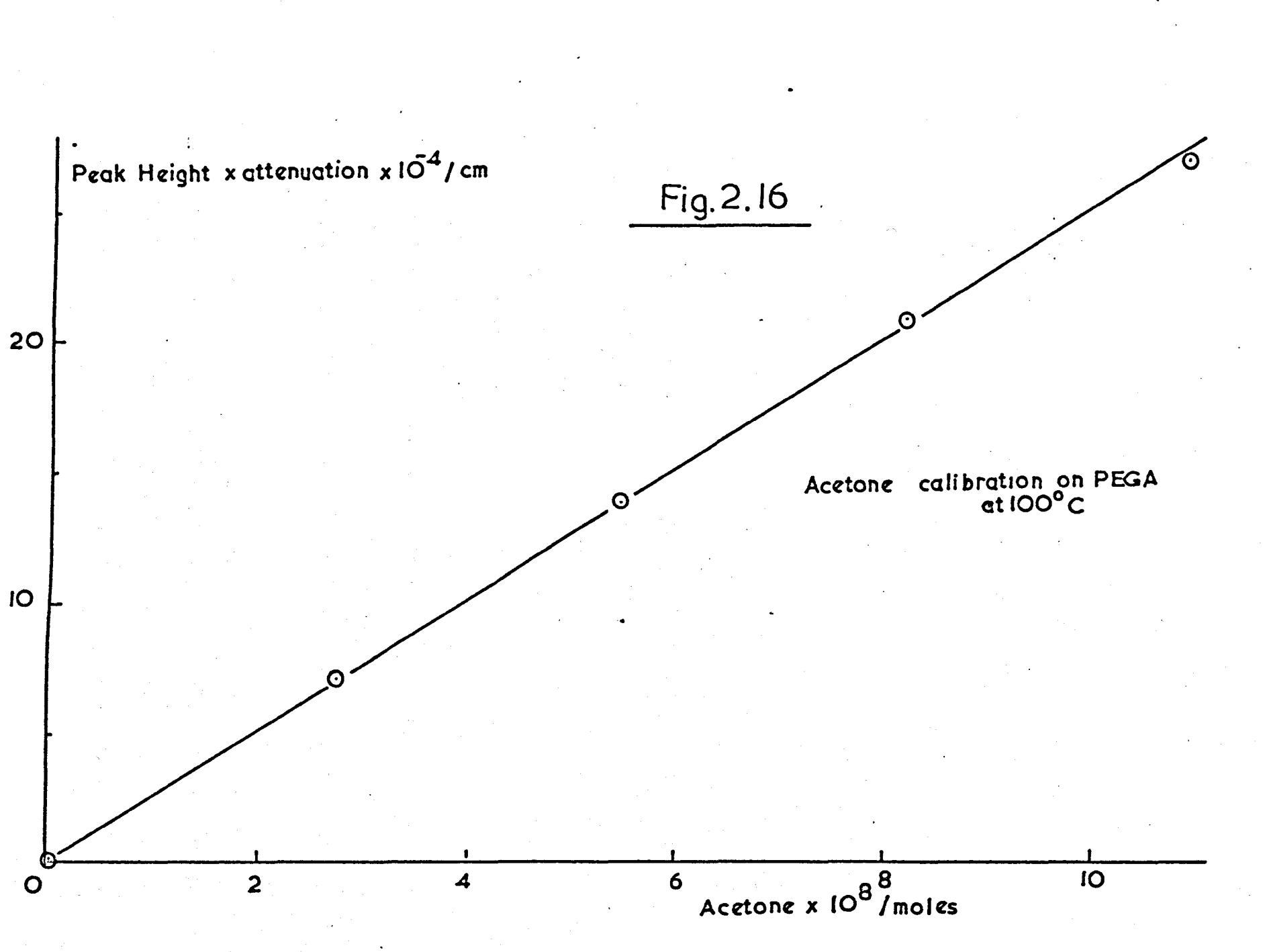
Peak Height x attenuation x 10^{-4} / cm
Fig. 2.16
20
10
0
2
4
6
8
10
Acetone calibration on PEGA at 100°C
Acetone x 10^{8} / moles

REFERENCES TO CHAPTER 2.

1. N.D. Stewart, M.Sc.Thesis, Keele University (1965).
2. D.D. Perrin, W.L.F. Armarego, D.R. Perrin, "Purification of Laboratory Chemicals, Pergammon (1966).
3. Eyre and Spotiswoode Ltd., "Dictionary of Organic Compounds", 4th Ed.
4. C.A. Parker, "Photoluminescence of Solutions", Elsevier, (1968).
5. M. Kasha, J.Optical Soc. of America, 38, 929 (1949).
6. K. Porter and D.H. Volman, Photochem. Photobiol. 1, 267 (1962).
7. K. Porter and D.H. Volman, Bull.Soc.Chim.Belges, 71, 831 (1962).
8. K. Porter and D.H. Volman, J.Amer.Chem.Soc., 84, 2011 (1962).
9. P. Borrell and J. Sedlar, J.Sci.Instrum., 2, 439 (1969)
10. P. Borrell and J. Sedlar, Trans. Faraday Soc., 66, 1670 (1970).
11. "Handbook of Chemistry and Physics", Chemical Rubber Co., 45th Ed., (1964).
12. N.J. Turro and A.A. Lamola "Energy Transfer and Organic Photochemistry", Chap.IV. Vol XIV In the series, "Technique of Organic Chemistry" Ed. Leermakers and Weissberger, (1969).
13. R.E.Dodd and P.L. Robinson, "Experimental Inorganic Chemistry", Elsevier, (1954).
14. F.R. Meyer and G. Rounge, Angew. Chem., 52, 637 (1939).
15. J.G. Calvert and J.N. Pitts, "Photochemistry", J. Wiley (1966).
16. C.A. Parker, Proc.Roy.Soc., A220, 104, (1953)
17. C.G. Hatchard and C.A. Parker, Proc.Roy.Soc., A235, 518 (1956).

3. PHOTOISOMERISATION: RESULTS

3.1 Spectra

U.V., I.R., N.M.R. and mass spectra of methyl tiglate and the isomer produced by preparative photolysis of methyl tiglate (Section 2.2(b)) were taken as confirmation of structure. These spectra are shown in Figs. 3.1 to 3.7. It can be seen by inspection of these spectra[1] that the compound prepared from methyl tiglate is indeed the cis isomer, methyl angelate. ('Cis' here refers to the two bulkiest groups being on the same side of the double bond). Spectra were obtained as described in Section 2.11.

The ultra-violet extinction coefficients for the two isomers are tabulated below. They were measured in cyclohexane solutions prepared by quantitative dilution.

Compound	λmax. nm	εmax. $l.mol^{-1}cm^{-1}$	ε_{254} $l.mol^{-1}cm^{-1}$
Methyl Tiglate	216.5	10.5×10^3	130
Methyl Angelate	218	7.85×10^3	174

In a polar solvent, ethanol, the maxima of the U.V. absorption peaks are very slightly shifted to the red and the peak is broadened slightly. There is no sign of a weak n-π^* transition in either solvent. In ethanol λmax. for methyl tiglate is at 218 nm and

for methyl angelate λmax. = 219 nm. As in cyclohexane the long wavelength tail of the spectrum extends further for methyl angelate than tiglate. No extinction coefficients were measured in ethanol. The only quoted values concerning the absorption spectra of methyl tiglate and methyl angelate are for ethanol solution when higher values for εmax. were obtained[2] :

methyl tiglate : λmax. = 215 nm, $\varepsilon = 1.12 \times 10^4$ $l.mol^{-1}cm^{-1}$

methyl angelate: λmax. = 217 nm, $\varepsilon = 9.1 \times 10^3$ $l.mol^{-1}cm^{-1}$

Although these values are slightly different from those above the qualitative trend is the same.

Fig.3.1 Methyl tiglate U.V.

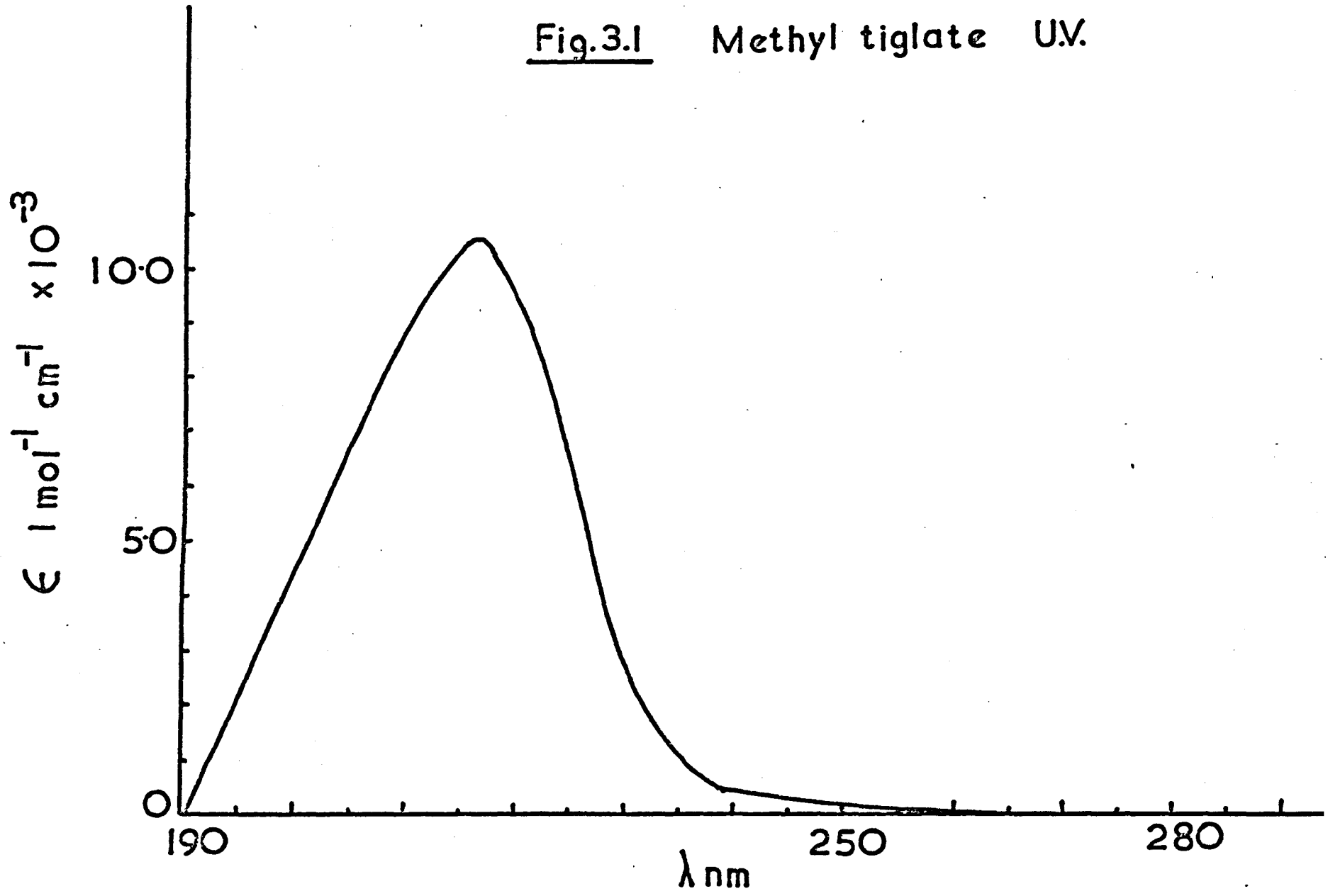

Fig. 3.2 Methyl angelate U.V.

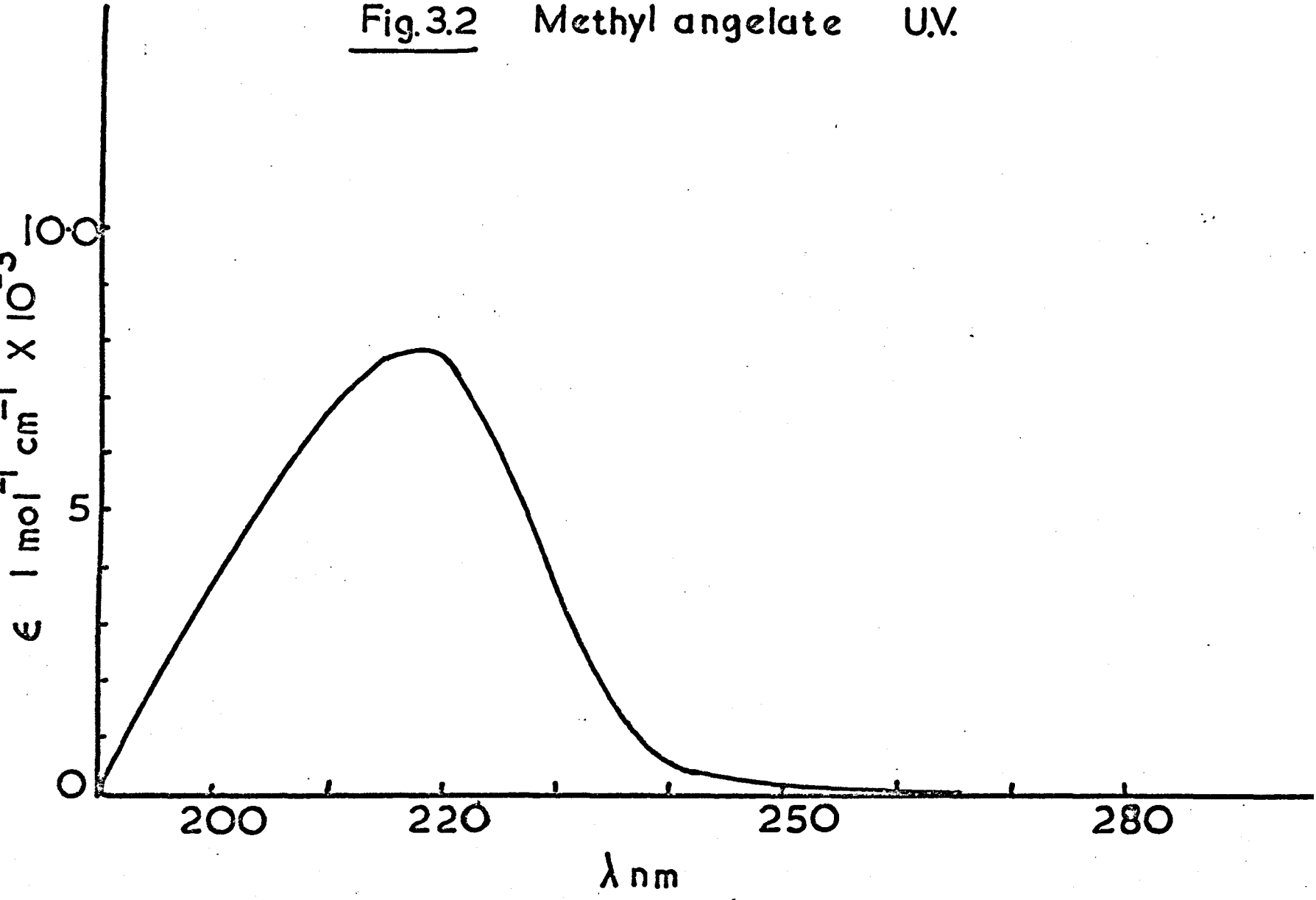

Fig. 3.3

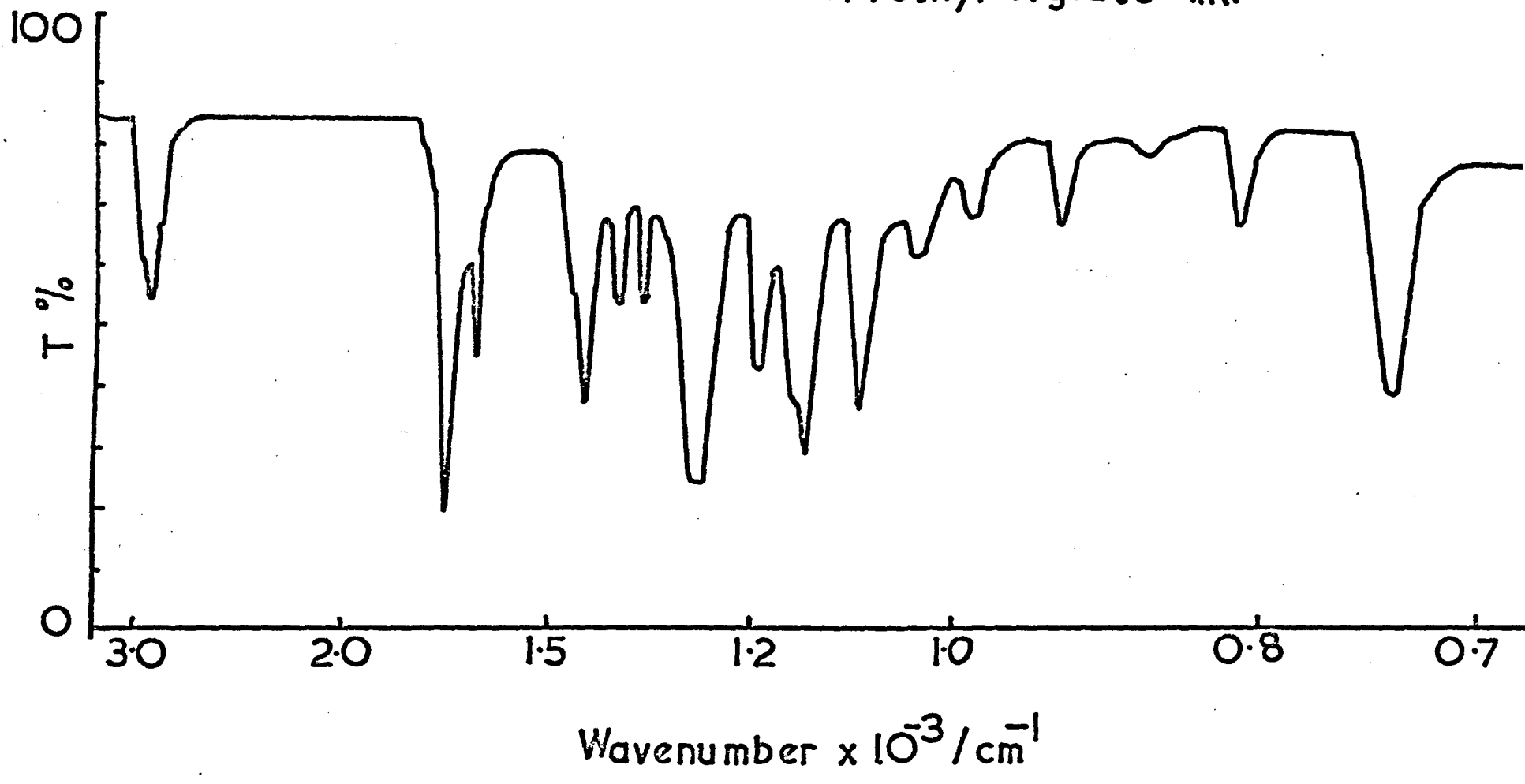
Methyl tiglate I.R.
100
T %
0
3·0
2·0
1·5
1·2
1·0
0·8
0·7
Wavenumber x 10⁻³ / cm⁻¹

Fig. 3.4

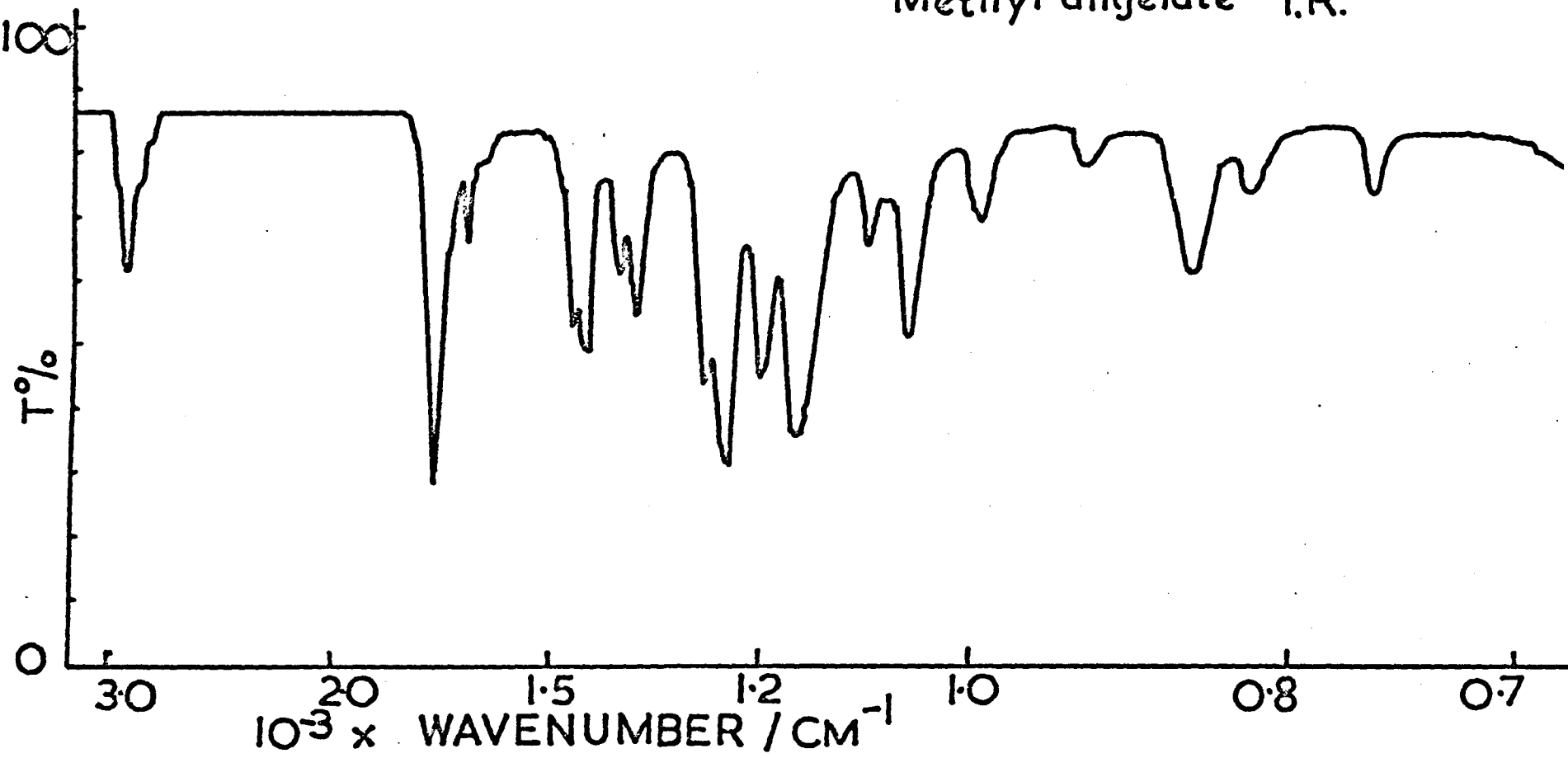
Methyl angelate I.R.
100
T%
0
3·0
2·0
1·5
1·2
1·0
0·8
0·7
10⁻³ x WAVENUMBER / CM⁻¹

Fig. 3.5 Methyl angelate: Mass spec.

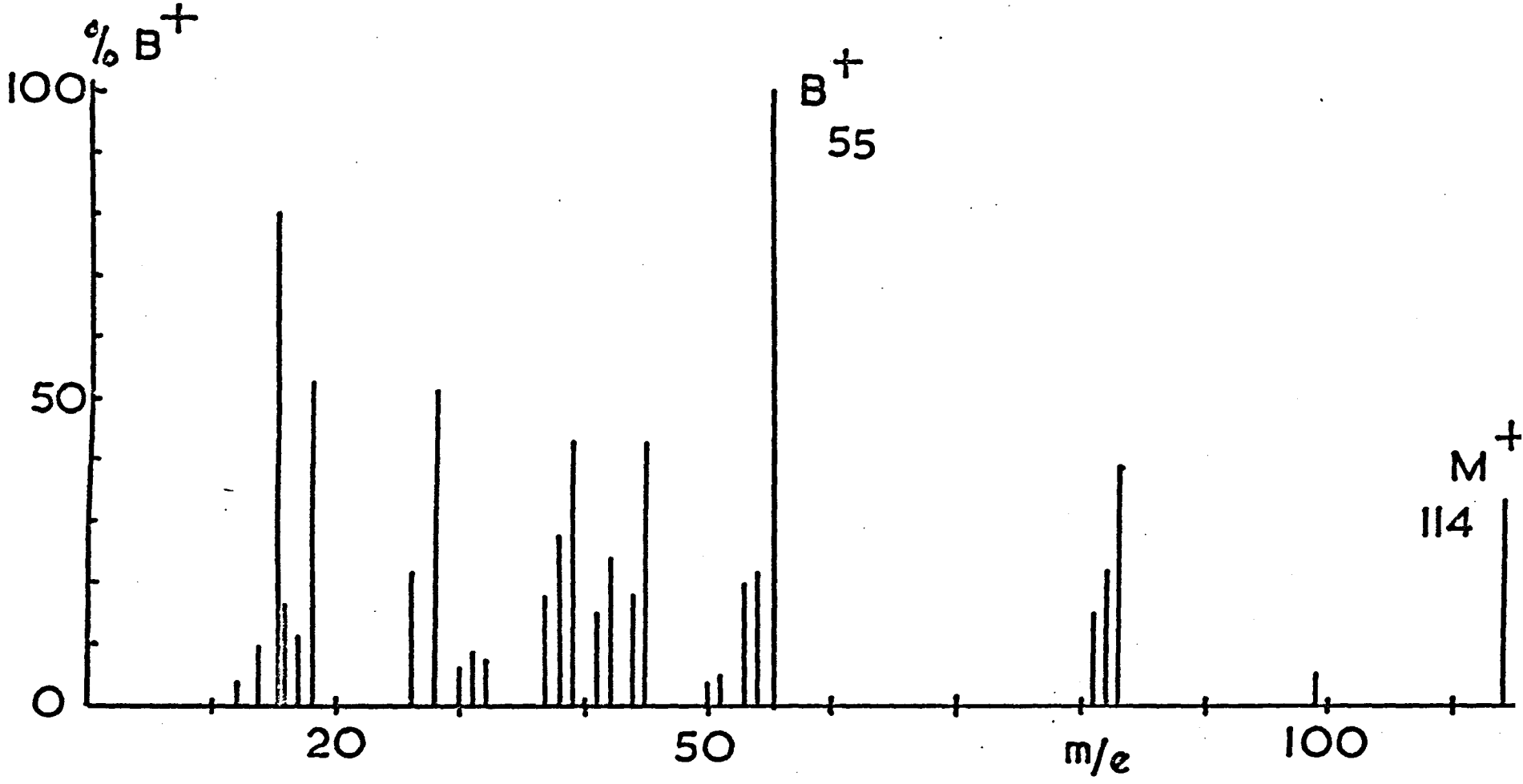

Fig.3.6 Methyl tiglate : Mass spec.

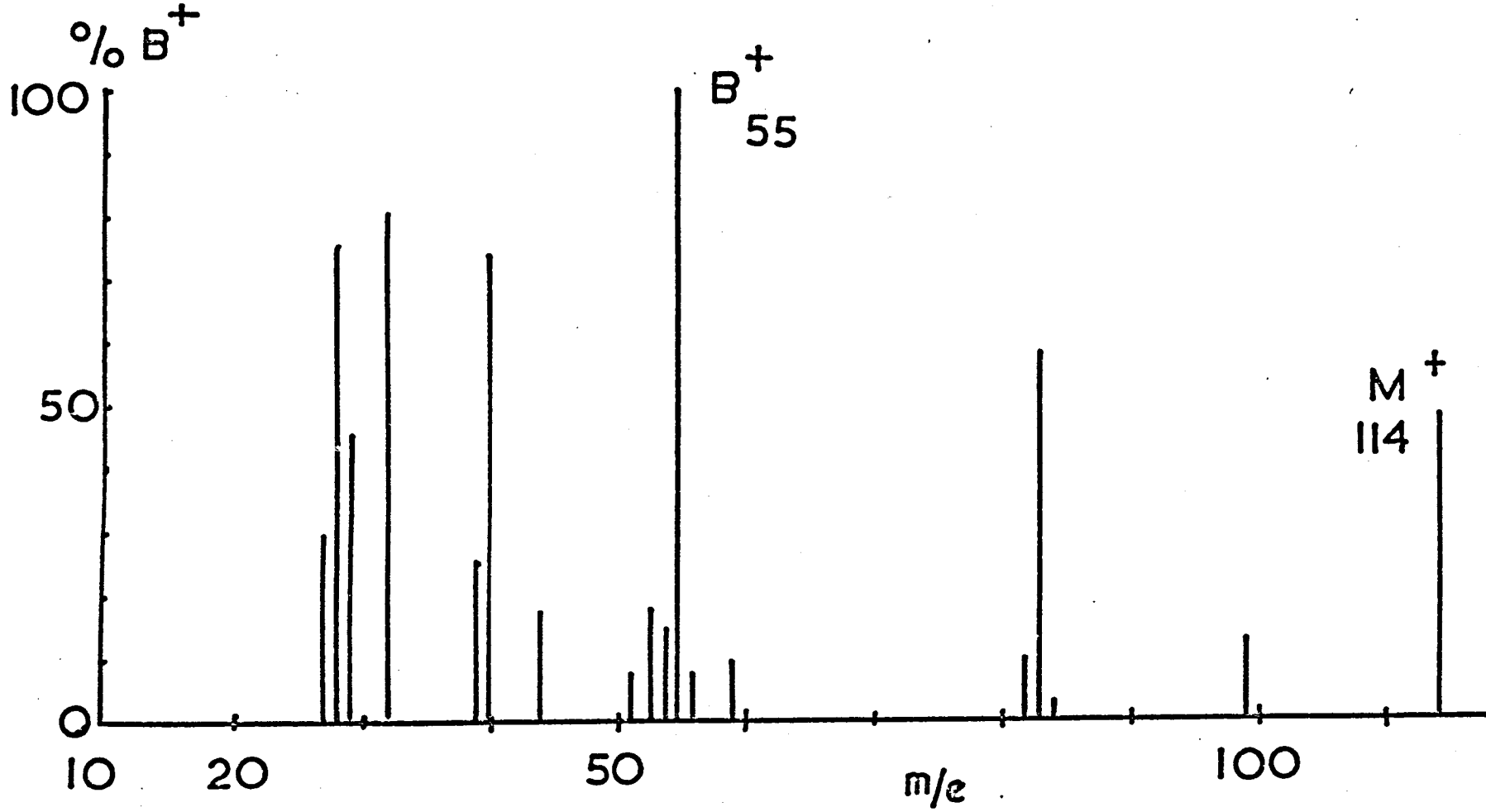

Fig. 3.7

Methyl angelate. N.M.R.

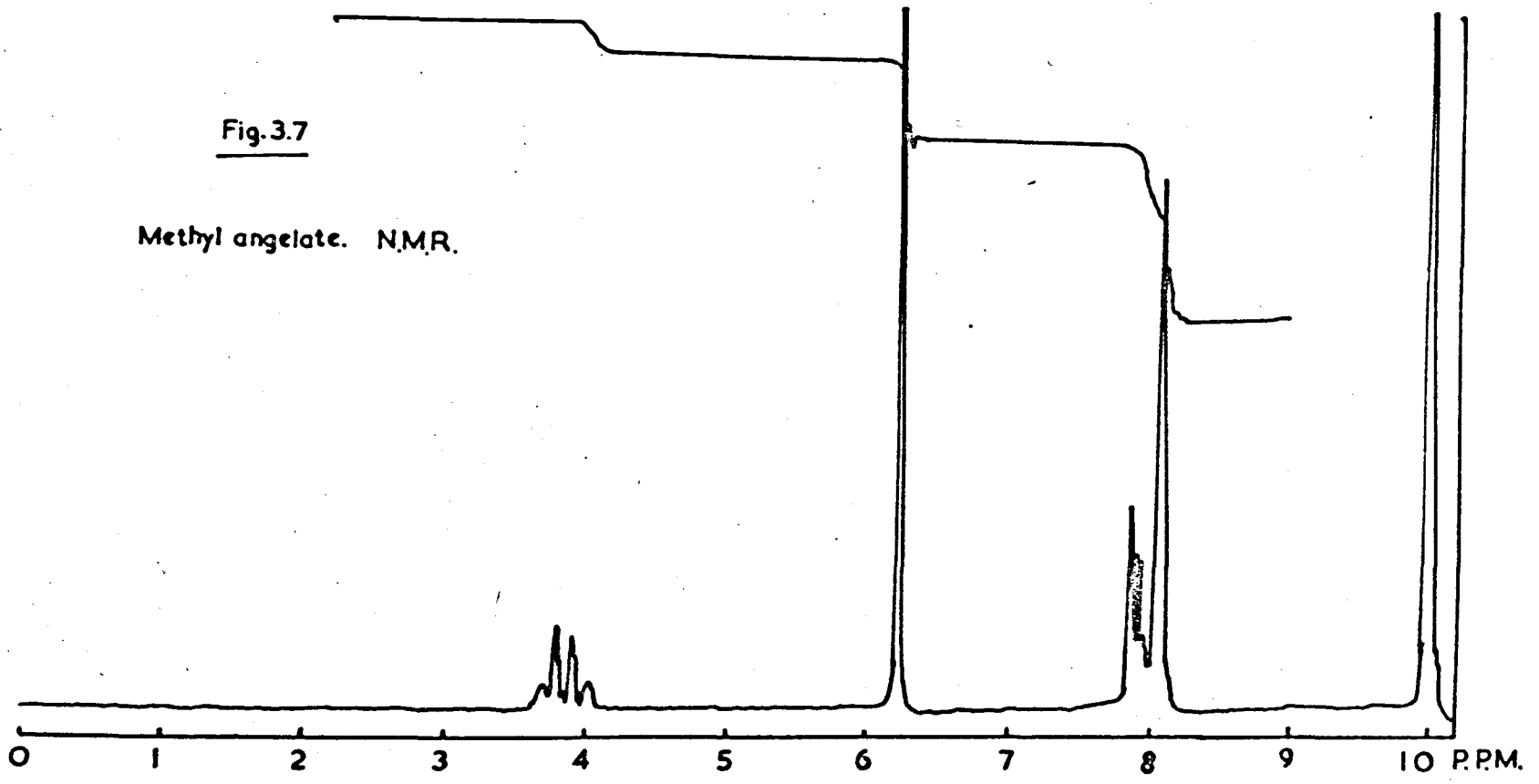

3.2 Preliminary Photolysis

As a preliminary experiment, capillary tubes were filled under vacuum with a 10% solution of methyl tiglate in cyclohexane, the methyl tiglate having been purified by preparative gas chromatography as described in Section 2.2(b). The tubes were photolysed for 10 to 300 min with the unfiltered high pressure mercury lamp at 25°C. The reaction mixture was analysed on PEGA columns at 100°C by injecting 1 microlitre samples. A typical chromatograph trace is shown in Fig. 3.8. As photolysis time increased, the peak corresponding to methyl tiglate, (I), dropped and the peak (II) appeared. This was shown to be methyl angelate by preparative scale photolysis as already described. Under these chromatograph conditions the retention time for methyl angelate was 3.4 min and for methyl tiglate 5.2 min. A further peak, (III), with a shorter retention time (2.6 min) was slowly produced and this built up to an appreciable concentration after long irradiation. The other small peak shown in Fig. 3.8 was an impurity present in all these solutions and did not change with time. Fig. 3.9 shows a plot of these results. The results are only qualitative as the peak heights are not corrected for detector sensitivity. As can be seen, the methyl angelate is produced quickly at first but is then consumed to produce the product (III) after prolonged irradiation.

In another experiment starting from methyl angelate, methyl tiglate was produced rapidly and (III) was produced linearly with time; there being no induction time as was observed with methyl tiglate. Such an experimental curve is shown in Fig. 3.10. Note

Fig.3.8

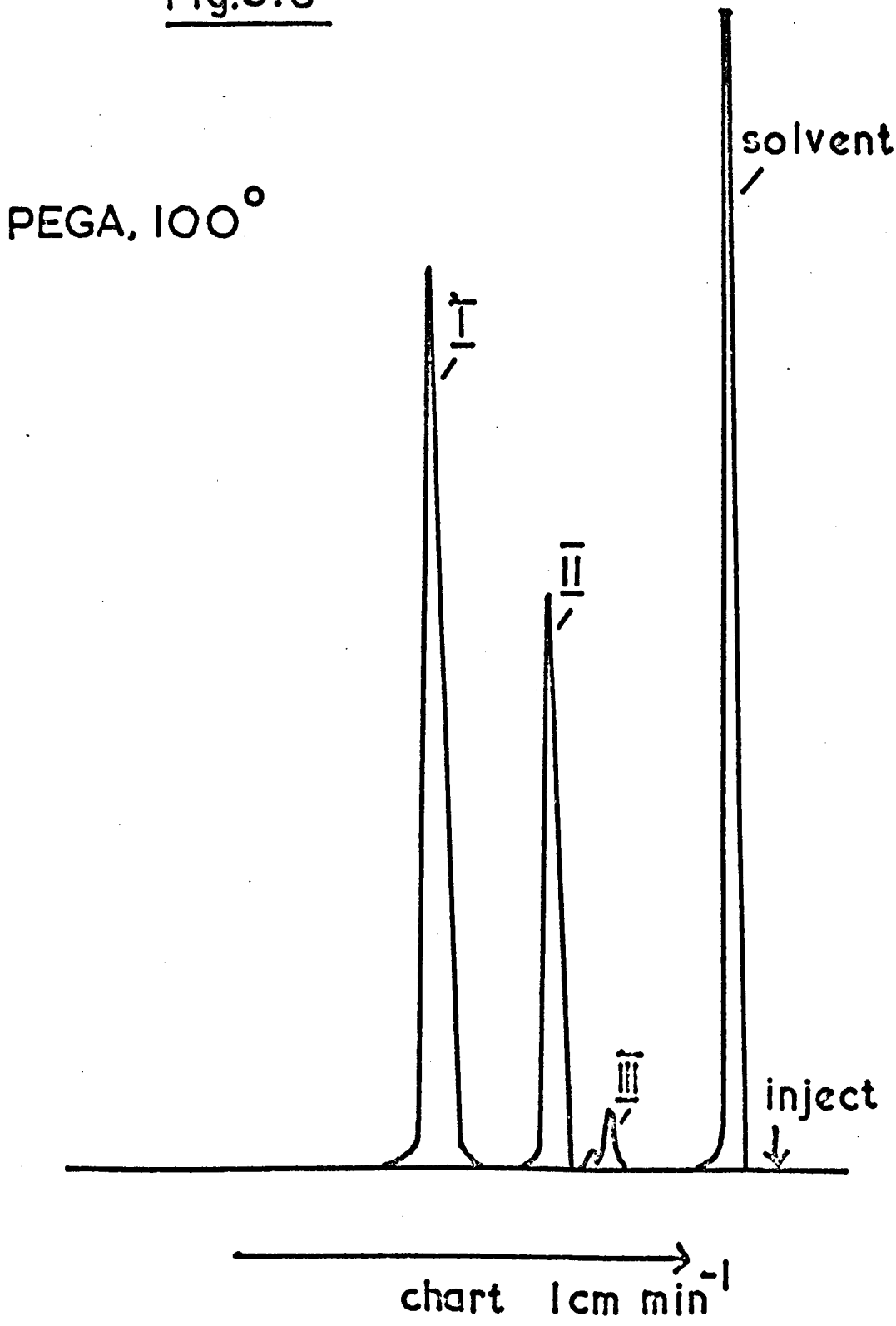

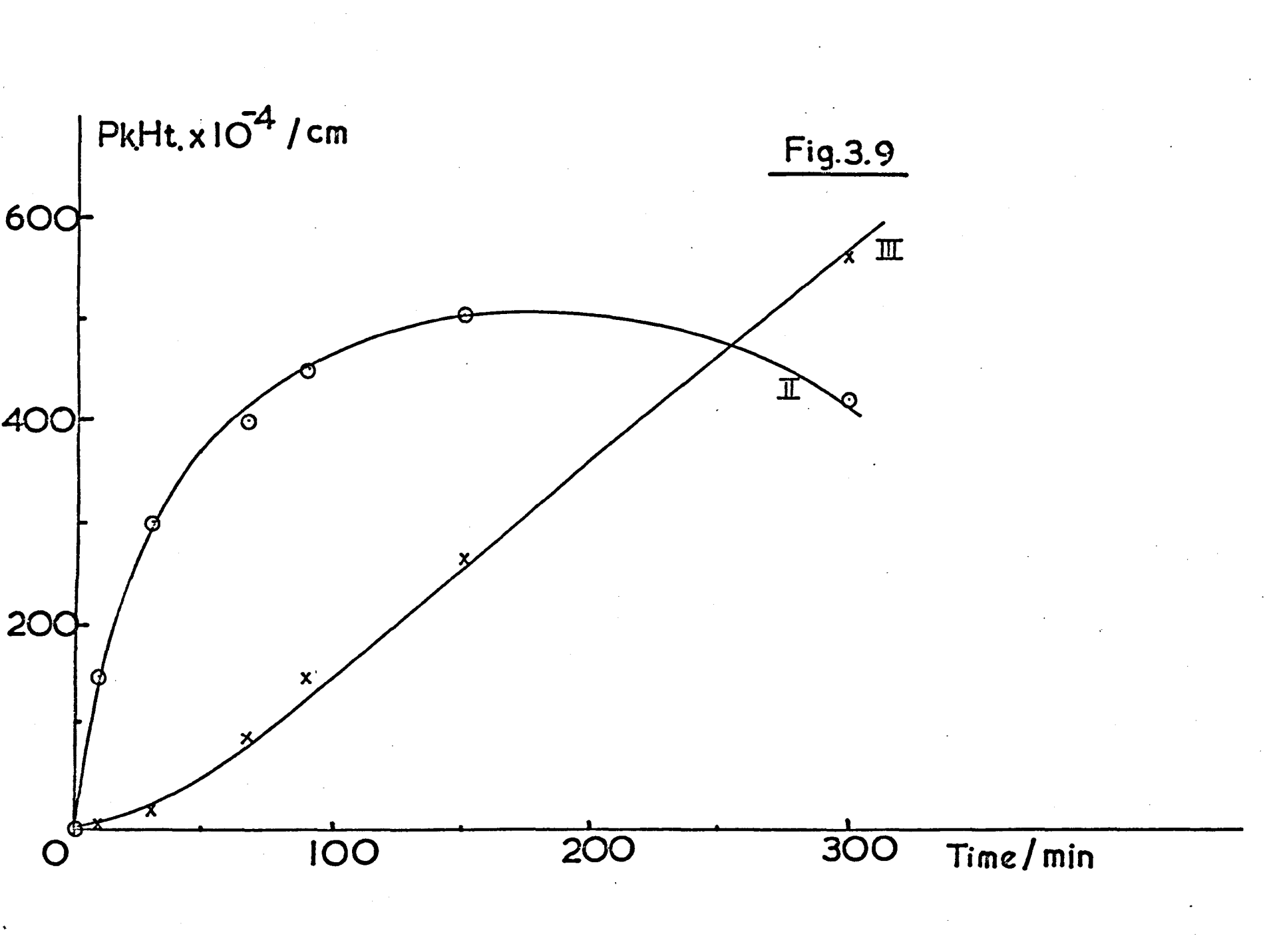

Fig. 3.9

Fig 3.10

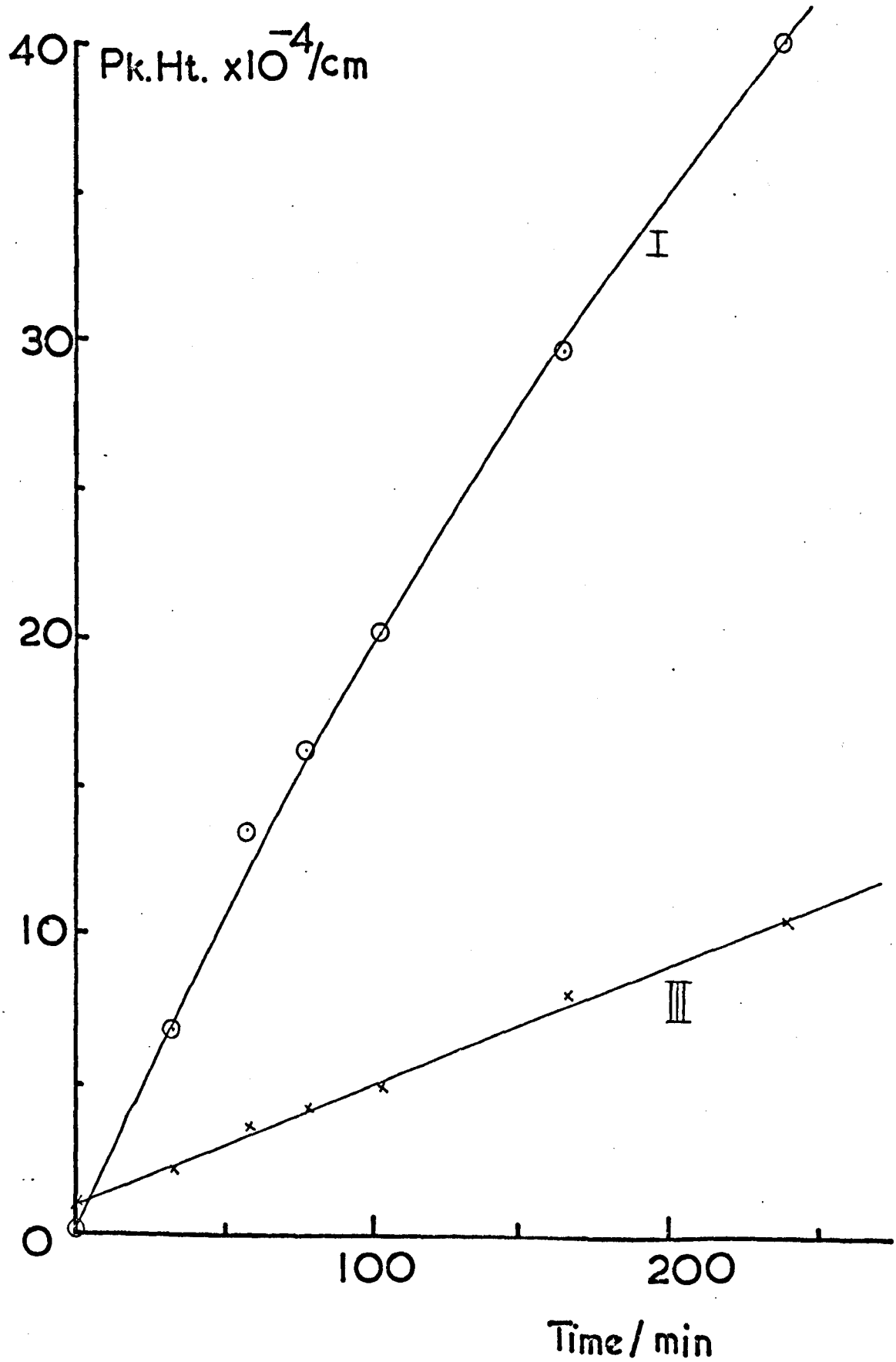

that the conditions used in this experiment were different from those used to obtain Fig. 3.9. These points were obtained by irradiating capillaries filled under vacuum on the merry-go-round apparatus using monochromatic light. In both cases no other products were detected on the gas chromatograph other than those mentioned.

3.3 The Nature of Product III

A small volume of 10% methyl angelate solution in cyclohexane was photolysed for 4 hours with the unfiltered high pressure lamp. The resulting mixture of angelate, tiglate and unknown was analysed on the mass spectrometer and coupled gas chromatograph (See Section 2.11) so that a mass spectrum of the compound (III) was obtained. This is shown in Fig. 3.11. To confirm the structure of (III) a preparative photolysis of a 10% solution of crude methyl tiglate in pentane was carried out. After 24 hours the reaction mixture contained an appreciable amount of (III) and this was then separated from the other isomers and impurities by preparative gas chromatography, using a PPG column at 145°C. About 0.5 ml of compound (III) was isolated and was found to be about 95% pure; the other 5% being mainly methyl angelate. It was not possible to remove all the latter as the two compounds were eluted very close together on the chromatograph.

N.M.R. and I.R. spectra of (III) are shown in Figs. 3.12 - 13. A U.V. spectrum was also taken but this was merely a spectrum of the methyl angelate impurity. (i.e. $\lambda max.$ = 218 nm and $\varepsilon = 10^4$ assuming 5% solution of methyl angelate). No other absorption bands were seen in the U.V. This is consistent with (III) being a deconjugated isomer of methyl tiglate as a non-conjugated ester would absorb only very weakly above 200 nm and would be obscured by traces of conjugated impurity. From analysis of the mass spectrum, N.M.R. and I.R. spectra it seems that the unknown compound is the β,γ-

Fig. 3.11 Mass spec. $CH_2=CH-CH(CO_2CH_3)(CH_3)$

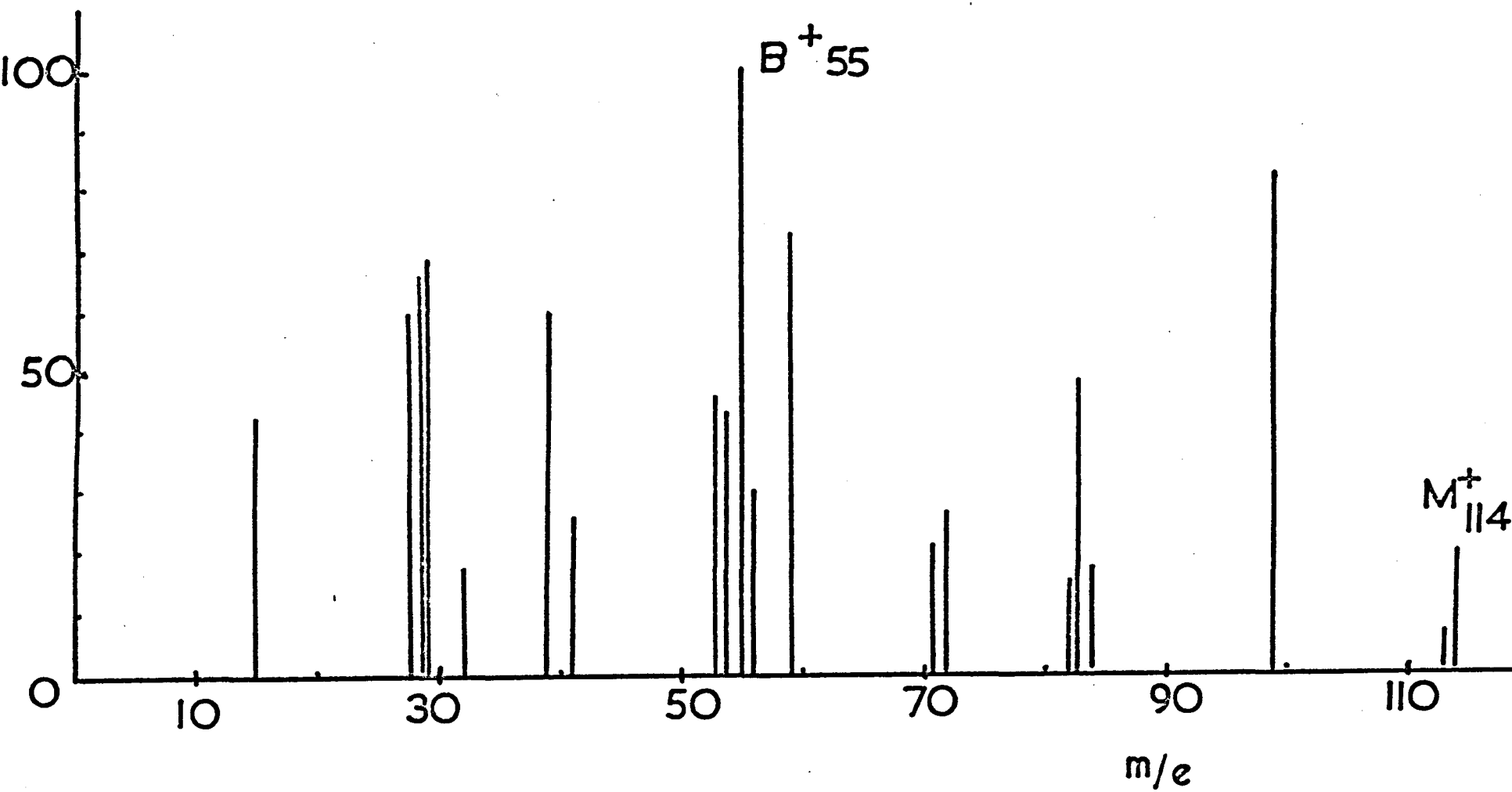

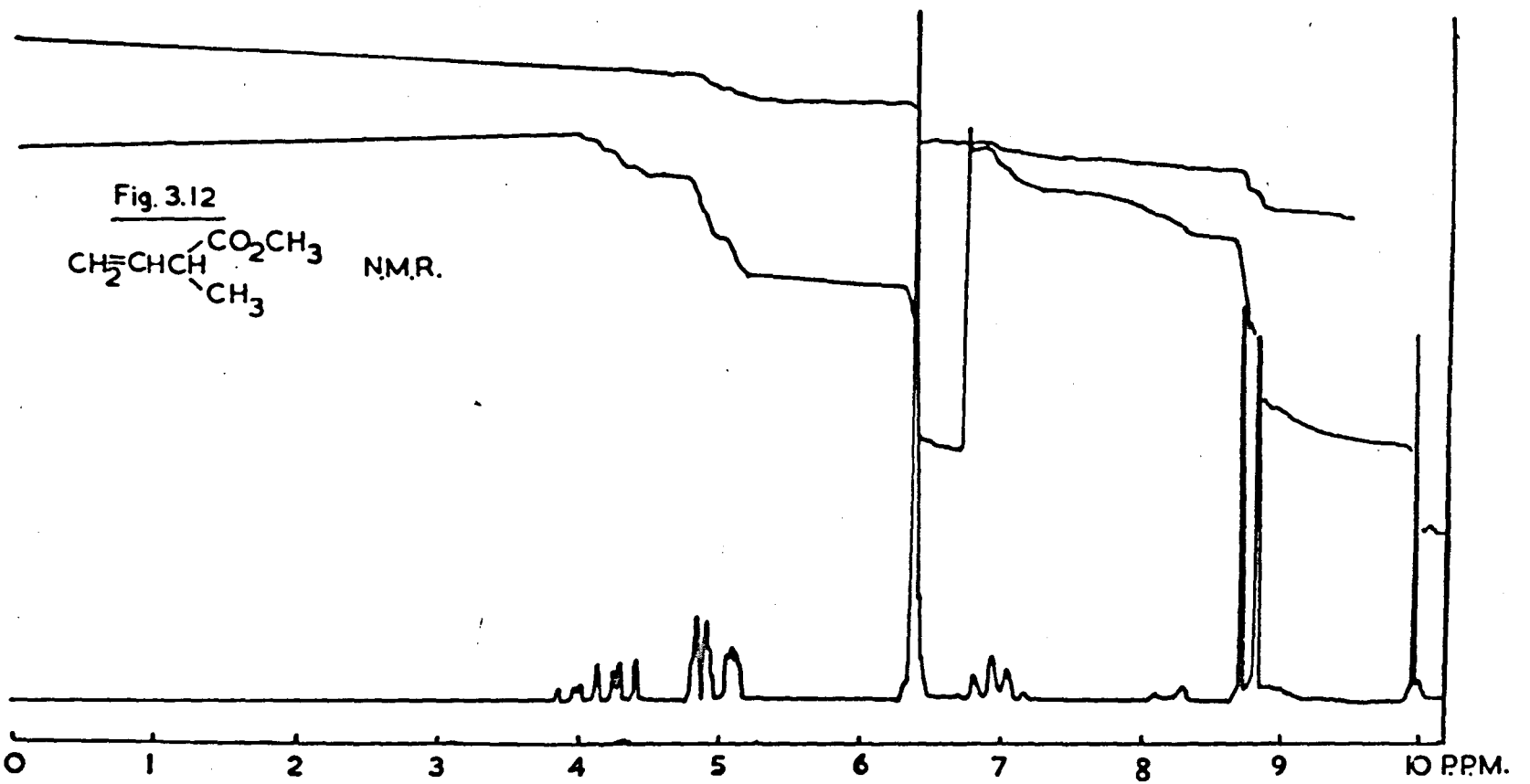
Fig. 3.12
CH2=CHCH(CO2CH3)CH3
N.M.R.
0
1
2
3
4
5
6
7
8
9
10 P.P.M.

Fig. 3.13 I.R. of $CH_2=CH-CH(CO_2CH_3)(CH_3)$

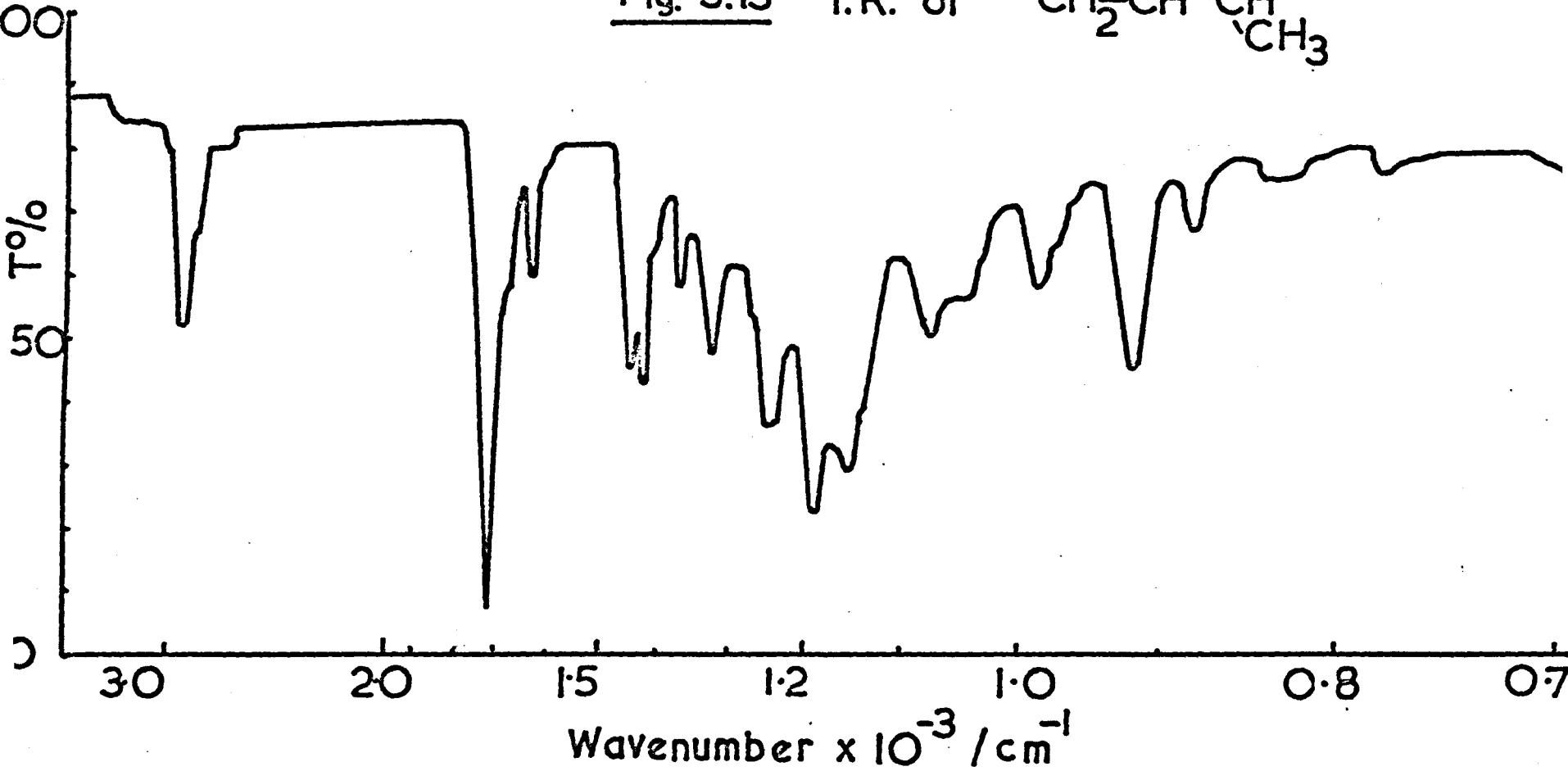

unsaturated ester formed by de-conjugation of the π system.

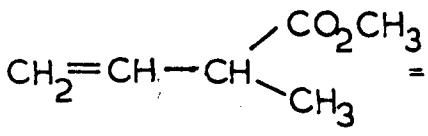

= III

(3-carbomethoxy-but-1-ene)

Comparing the mass spectra of (III) with those of methyl angelate and methyl tiglate it is apparent that the unknown is an isomer of these two. The main difference between the mass spectrum of (III) and of methyl angelate is the increased abundance of the fragment with m/e = 59. This can be assigned to loss of the carbomethoxy group which is no longer conjugated to the double bond. The position of the carbonyl stretching mode in the infra-red supports the idea that the ester carbonyl is no longer conjugated.

The N.M.R. spectrum confirms that the structure is as shown above and not :

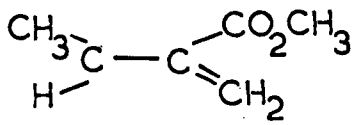

This follows from the position of the multiplets corresponding to single protons. The triplet at 7τ is assigned to the proton attached to the α-carbon and the multiplet at 4.2 τ is assigned to the proton attached to the β-carbon. In the alternative structure there is only one single proton.

From plots 3.10 and 3.9 it is clear that the percursor of this β,γ-unsaturated ester is methyl angelate and not the tiglate.

As a guide to the mechanism of this reaction a 10% solution of methyl angelate in MeOD (Koch-Light, 'puriss') was photolysed at 254 nm in the semi-micro apparatus and the resulting de-conjugated product was analysed on the coupled V.P.C. - mass spectrometer. The spectrum obtained is shown in Fig. 3.14. It can be seen that the molecular ion and base peak are increased by one mass unit compared to those of (III). The spectrum is consistent with the incorporation of a deuterium atom on the α-carbon atom. (This is discussed in Chapter 5.).

3.5 Photolysis of 313 nm

The U.V. spectrum of a 5% solution of methyl tiglate in cyclohexane (by volume) was taken. There appeared to be some absorption of 313 nm though this was probably due to traces of impurity in the ester. As a check, this solution was photolysed for 3h in the semi-micro apparatus using the medium pressure lamp and 313 nm interference filter. There was no change in the initial small concentration of methyl angelate present. It was therefore concluded that the absorption was due to an impurity which did not sensitise the reaction. This is borne out by the observation that if the absorption was due to methyl tiglate the extinction coefficient would be less than 1 $l.mol^{-1}cm^{-1}$, which is unlikely.

Fig.3.14 Mass spec.of $CH_2=CH-C(CO_2CH_3)(CD_3)CH_3$

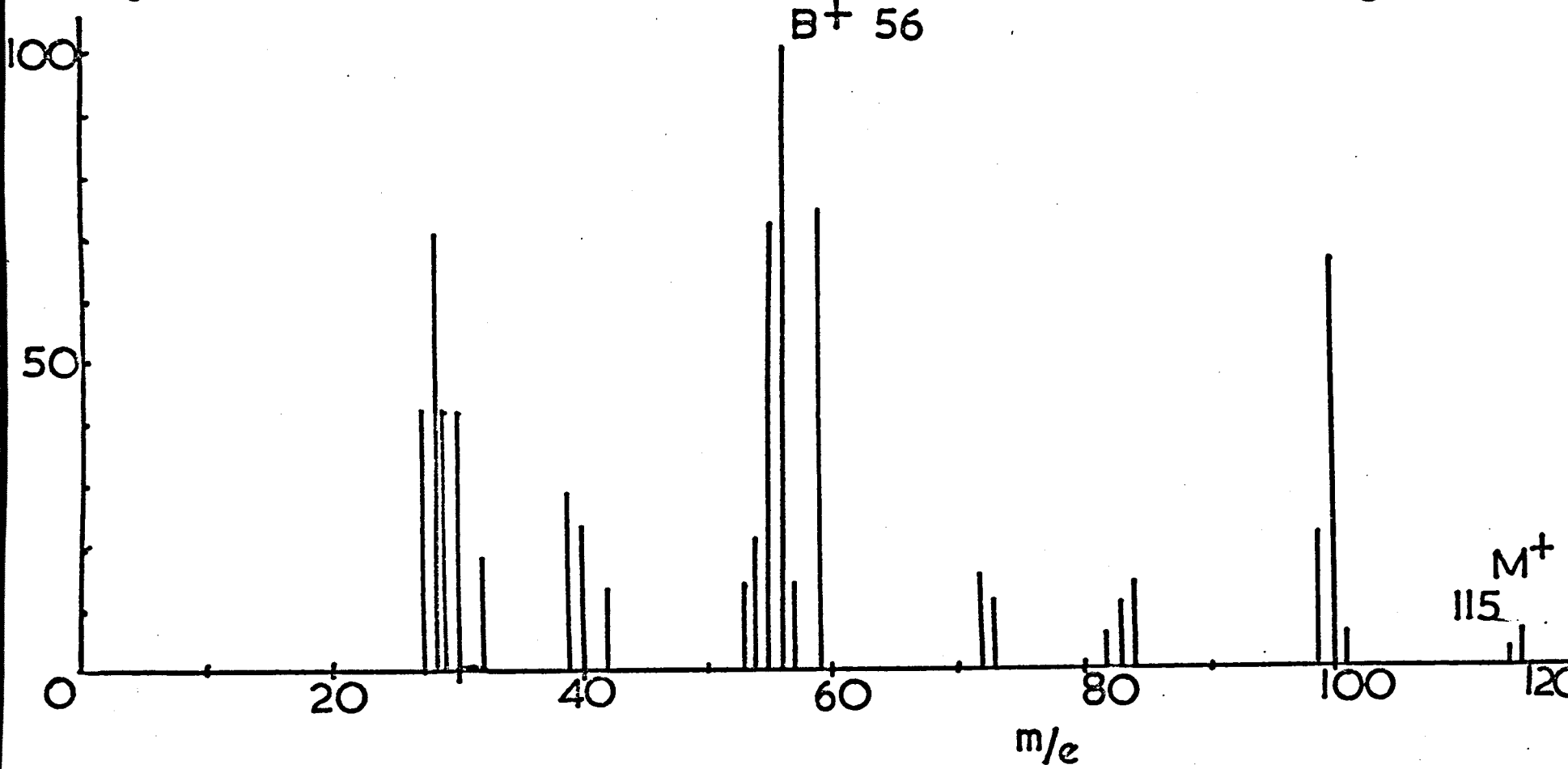

3.4 Thermal Isomerisation

Samples of pure methyl tiglate in quartz capillary tubes under vacuum were heated in the oven of a Pye 104 gas chromatograph for known lengths of time in an attempt to follow the first order thermal isomerisation in the same way as Calvin and Alter did with stilbene derivatives.[3] This oven represented an accurate air thermostat with a range from room temperature up to 400°C and a temperature constant to within ± 1°C. At 100°C there was no apparent reaction after 18 h. The same was true over the same time at 175°C. When the tubes heated to 303°C there was 7% conversion after 92 h. However, at this temperature the contents of the tube were present as a vapour at very high pressure so that measurements under these conditions were probably irrelevant to solution work at room temperature. Apart from methyl tiglate, several other unidentified products were observed in the samples heated for long periods at this temperature. Similar experiments starting with methyl angelate were equally unsuccessful and no further attempts were made to study the thermal reaction. Clearly the energy barrier to rotation around the double bond is considerable.

3.6 Actinometry in Capillaries

In order to determine the quantum yields of processes taking place on the merry-go-round apparatus it was first necessary to determine the quantum yield of the secondary actinometer used, methyl propyl ketone (2-pentanone). This was carried out under nitrogen on the semi-micro apparatus at 25°C using the medium pressure lamp and 254 nm interference filter. The intensity of the light incident of the cell was first determined by ferrioxalate actinometry as described in Section 2.9. Three actinometric determinations were made.

Time of Illumination min.	Optical Density of Phenanthroline Solution
20	0.250
20	0.260
20	0.248
Average =	0.253

The cell dimensions were measured with a vernier scale and the volume was determined by weighing.

Cell volume	=	1.26 cm^3
Path length	=	1.0 cm
Surface area of face	=	1.26 cm^2

Using the formula quoted in 2.9 the measured light intensity at 254 nm = $\underline{1.77 \times 10^{14} \text{ quanta } s^{-1} cm^{-2}}$.

Without changing the position of the cell, the actinometer solution was replaced with pure 2-pentanone which was photolysed under a stream of pure nitrogen after purging of oxygen for 30 min. Acetone production was followed by injecting 1 microlitre aliquots onto PEGA at 100°C. The resulting data is shown in Fig. 3.15

Time, min	Peak Ht, Acetone, cm
0	35
60	300
98	550
213	1220
334	1790

Gradient of straight line plot = 5.28 cm min^{-1}

Sensitivity = 2.48×10^{12} cm mol^{-1}

∴ Acetone formed per cell per minute = 2.68×10^{-9} mol

∴ Quantum yield of acetone formation from 2-pentanone = 0.121

Sedlar[4] found a value of 0.123 for the same quantum yield at 313 nm. In gas phase work, Wettack and Noyes[5] found that this quantum yield was virtually independent of wavelength between 313 and 254 nm though their value was somewhat higher. There is no reason to expect the quantum yield of such a reaction to be the same in both pure liquid ketone and the gas phase at relatively low pressures. The value of 0.121 was

Fig.3.15

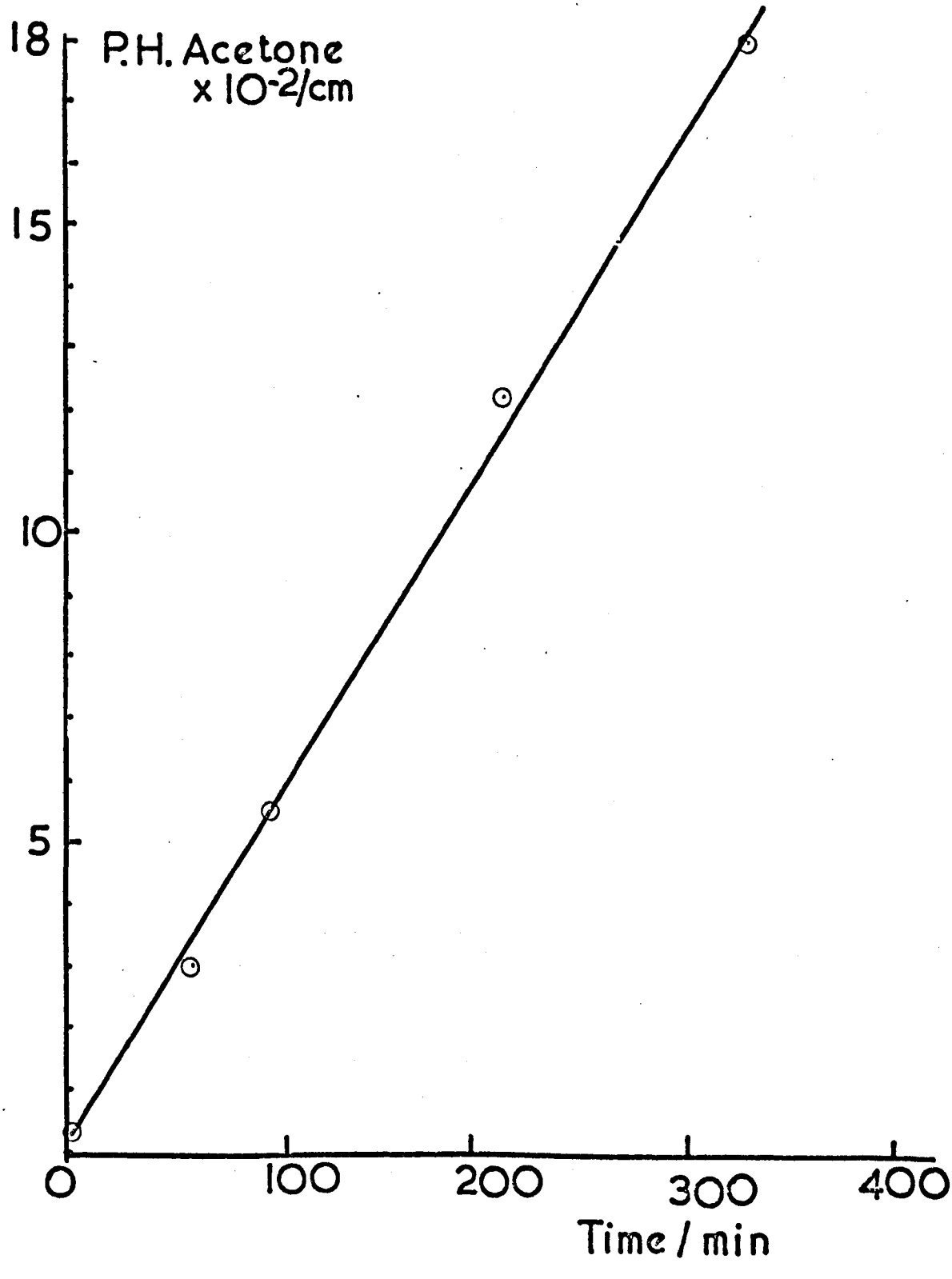

therefore used to calculate all quantum yields in capillaries.

The extinction coefficient of 2-pentanone at 254 nm was measured to be 8.56 $l.mol^{-1}cm^{-1}$. Therefore, applying Beer's Law, the optical density of a 0.025 cm column of pure 2-pentanone is 2.1, i.e. absorbs >99% of incident light. From simple geometrical considerations it can be shown that parallel chords of length 0.25 mm enclose 99.3% of the area of a circle 1.0 mm in diameter. If capillary tubes of 1.0 mm internal diameter are assumed to be perfectly circular in cross-section, then it is clear that 99% of A_a sample of pure pentanone in such a capillary will absorb 99% of incident light at 254 nm. Applying the same arguments, the minimum concentration of methyl tiglate that can be assumed to be absorbing 100% of incident light is 0.5 mol $l.^{-1}$ in a capillary tube.

In order to measure the quantum yield of isomerisation in capillaries the amount of acetone produced from 2-pentanone was determined after measured irradiation times on the merry-go-round. The quantum yield of isomerisation was then calculated from the expression ,

$$\phi = \frac{0.121 \times \text{moles of product formed per minute per microlitre}}{\text{moles of acetone formed per minute per microlitre}}$$

Pentanone actinometer tubes were photolysed periodically during the experiments with the merry-go-round apparatus. The rate of production of acetone was found to vary randomly about an average value of 1.59×10^{-9} mol $min^{-1}\mu l^{-1}$. The reasons for this variation were not clear though a certain amount of inaccuracy was caused by decomposition

in the stored tubes which were filled at one time and kept in a refrigerator. This was corrected for by measuring a control tube with every photolysis, but may not have been completely eliminated as a source of error. It was assumed that the lamp delivered a constant output after a short warm-up period but variations may have been caused by ageing of the acetic acid filter, although this was changed regularly. The average value for the rate of acetone production was used in calculations and this corresponds to an intensity of 1.0×10^{16} quanta $s^{-1}cm^{-2}$ on the surface of the rotating cylinder.

3.7 Photolysis on Merry-go-Round, Temperature Variation

A series of quartz capillary tubes were filled with a solution of methyl tiglate in pure cyclohexane under vacuum. These tubes were then photolysed on the merry-go-round (Section 2.7(e)) at three temperatures, 26°, 35° and 50°C to see if temperature had any effect on the quantum yield of isomerisation. The concentration was chosen so that all incident light was absorbed by the solution. For low conversions to methyl angelate the formation of the de-conjugated ester was unimportant and was not followed in these experiments.

The acetic acid filter solution was changed regularly to maintain a constant intensity. Without this filter, a similar rate of isomerisation was seen but several unidentified new products were seen with retention times on PEGA greater than methyl tiglate. With the filter 185 nm light was cut off (checked on SP800) and these other products were not formed.

As has already been mentioned in Section 2.7 difficulties arose in uniform filling of the capillaries by the vacuum filling method. Within a batch of tubes filled with a given solution of methyl tiglate in cyclohexane there was found to be a considerable variation in concentration. Once filled a tube could not be analysed until after photolysis, when it was broken open and sampled on the gas chromatograph. This variation was found to be ± 10%. Consequently all experiments involving capillary tubes filled by this method were subject to considerable random variation in composition which combined with a sampling error (estimated at ± 3%

by injecting repeated samples of the same solution) led to high scatter in the results. However these results are included as the semi-micro method was not developed until later in the work and, despite large errors, they give a fair quantitative picture of the system.

3.7(a) Photolysis at 25°C

Concentration of methyl tiglate = 1.04 Molar in cyclohexane.

Analysis on PEGA at 100° with 1 microlitre aliquots (see sensitivity curves).

Fig. 3.16

Photolysis time min	Peak Ht. Angelate cm x 10^{-4}	Peak Ht. Tiglate cm x 10^{-4}	gm Angelate x 10^{5}	gm Tiglate x 10^{5}	Total Isomers gm x 10^{5}	% Angelate Total
10	6.0	116	0.28	11.0	11.28	2.5
20	14.2	119	0.67	11.4	12.07	5.5
40	22.4	115	1.0	10.9	11.9	8.4
60	35.0	110	1.7	10.2	11.9	14.3
135	56.0	100	3.0	8.8	11.8	25.4
200	77.0	92	4.5	7.8	12.3	36.6

N.B. In the above table, as in all following results, 'peak height' includes the attenuation factor of the detector. It will be referred to by the abbreviation P.H. in following tables.

Fig.3.16

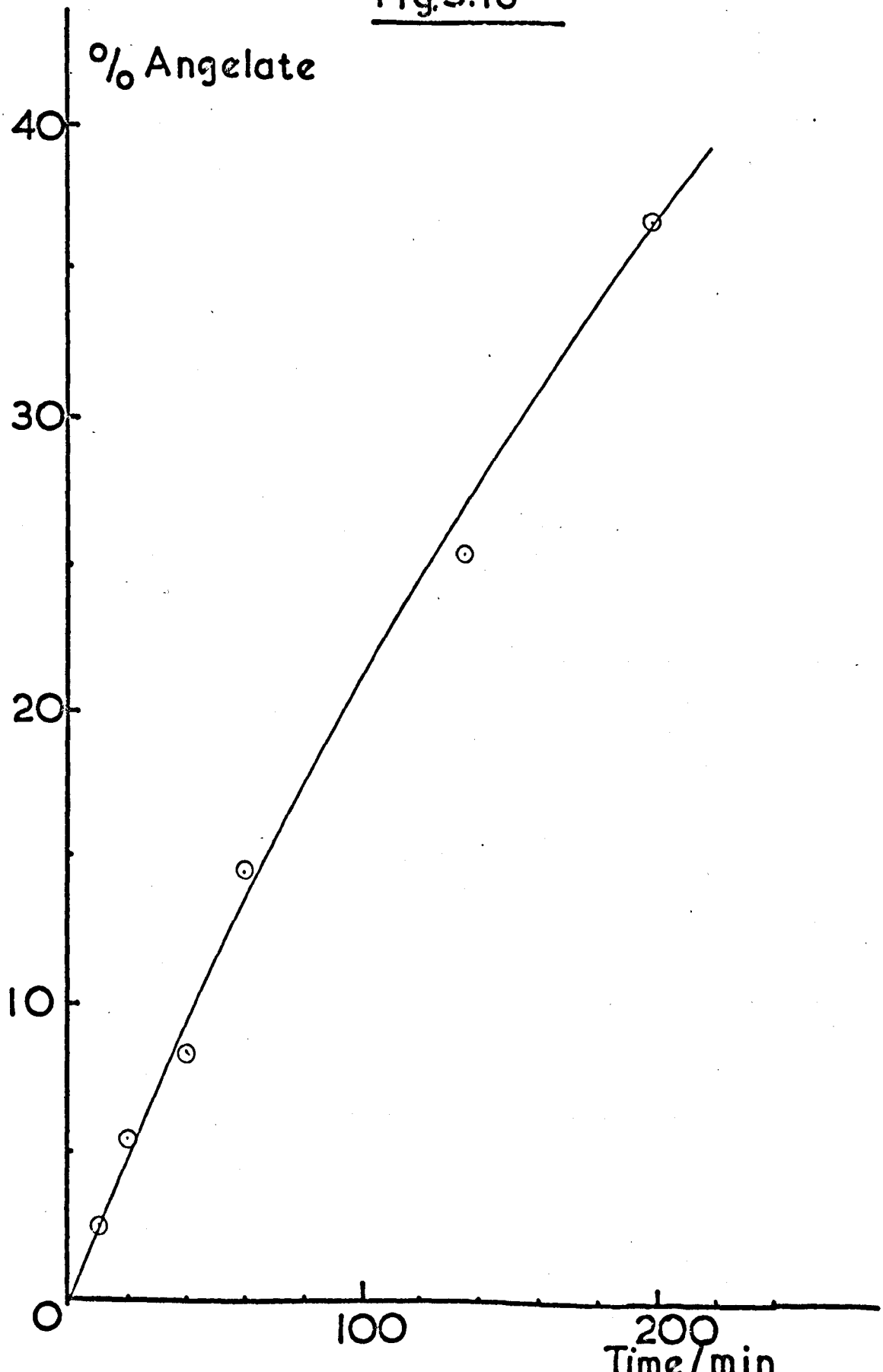

The last oolumn expresses the amount of angelate produced as a percentage of the sum of angelate and tiglate measured in each tube to smooth out variations due to variations in initial concentration. Note that in this case mole % and gramme % are the same thing as the molecular weight of angelate and tiglate is the same.

3.7(b) Photolysis at 35°C

Initial tiglate concentration = 1.07 Molar. Analysis as in (a)

Fig. 3.17

Time min	P.H. Angelate cm x 10^{-4}	P.H. Tiglate cm x 10^{-4}	gm Angelate x 10^{5}	gm Tiglate x 10^{5}	Total Isomers gm x 10^{5}	% Angelate Total
5	3.12	122	0.14	12.0	12.14	1.1
10	6.4	126	0.30	12.6	12.9	2.3
15	11.0	126	0.52	12.6	13.12	4.0
20	15.0	124	0.71	12.2	12.93	5.8
25	16.6	120	0.79	11.6	12.4	6.4
35	22.2	116	1.07	10.4	11.47	9.3
60.5	36.0	114	1.7	10.8	12.5	13.6
120	60.0	97.5	3.2	8.5	11.7	27.3
180	72.0	91.0	4.1	7.7	11.8	34.7
250	82.0	89.0	4.8	7.4	12.2	39.3
300	86.0	83.0	5.2	6.8	12.0	43.3

Fig. 3.17

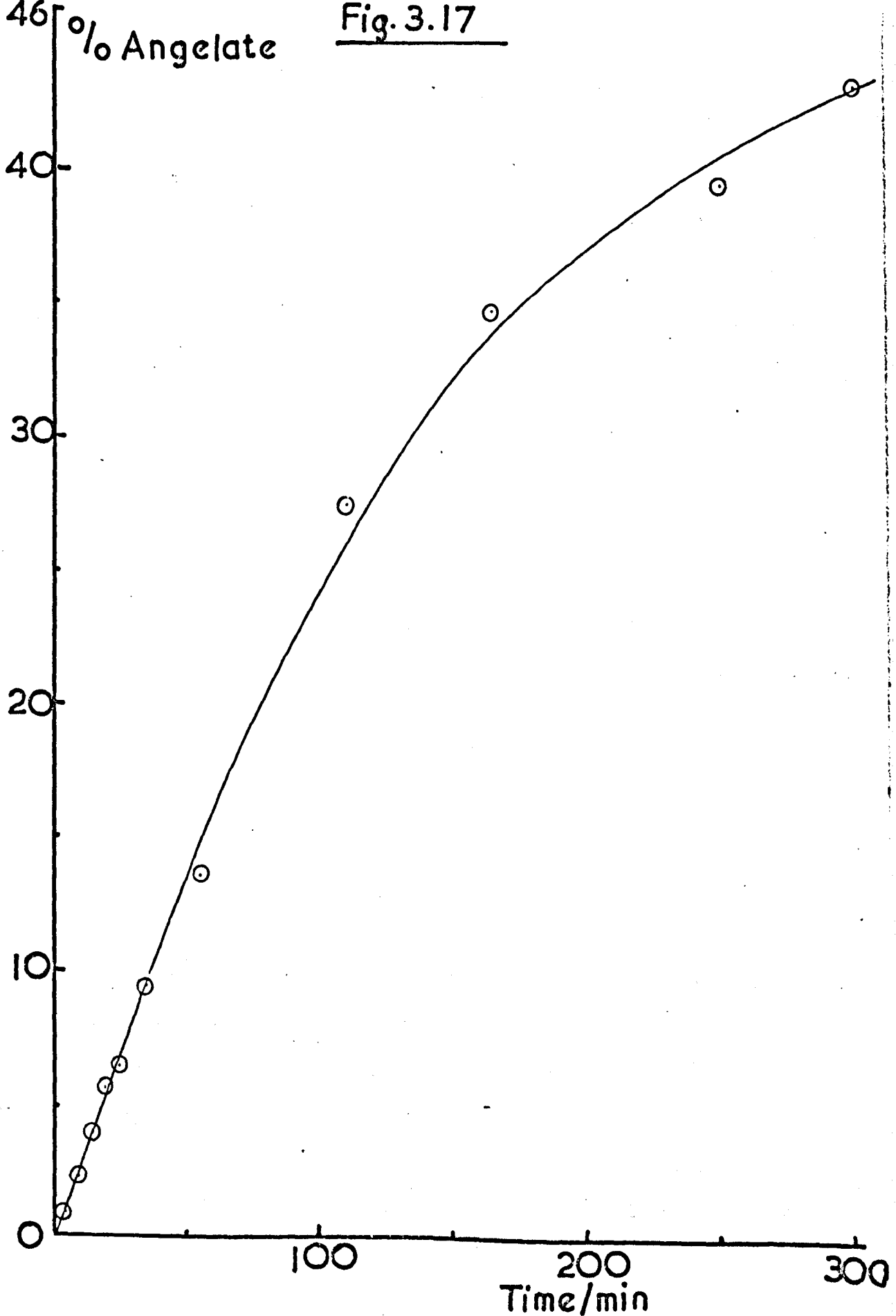

3.7(c) Photolysis at 50°C

Initial tiglate concentration = 1.12 Molar.

Analysis as in (a)

Fig. 3.18

Time, min	P.H. Angelate cm x 10^{-4}	P.H. Tiglate cm x 10^{-4}	gm Angelate x 10^5	gm Tiglate x 10^5	Total Isomers gm x 10^5	%Angelate Total
13	10.0	124	0.47	12.2	12.67	3.7
20	15.8	128	0.75	12.8	13.55	5.5
29	20.8	123	0.90	12.0	12.90	7.0
42	24.0	130	1.1	13.2	13.31	8.3
48	35.0	112	1.7	10.4	14.0	14.0
60	41.0	123	2.0	12.0	12.1	14.3
90	47.0	108	2.4	9.9	12.3	19.5
120	59.0	99	3.1	8.7	11.8	26.3

3.7(d) Summary

The quantum yields are obtained from the initial slopes of the plots of percentage angelate against time of photolysis. (Figs. 3.16 - 3.18). The curvature shown by these plots is presumably due to the back reaction, angelate to tiglate. The determination of the initial slope was simplified by plotting reciprocals. It was found that for low conversions there existed a

Fig. 3.18

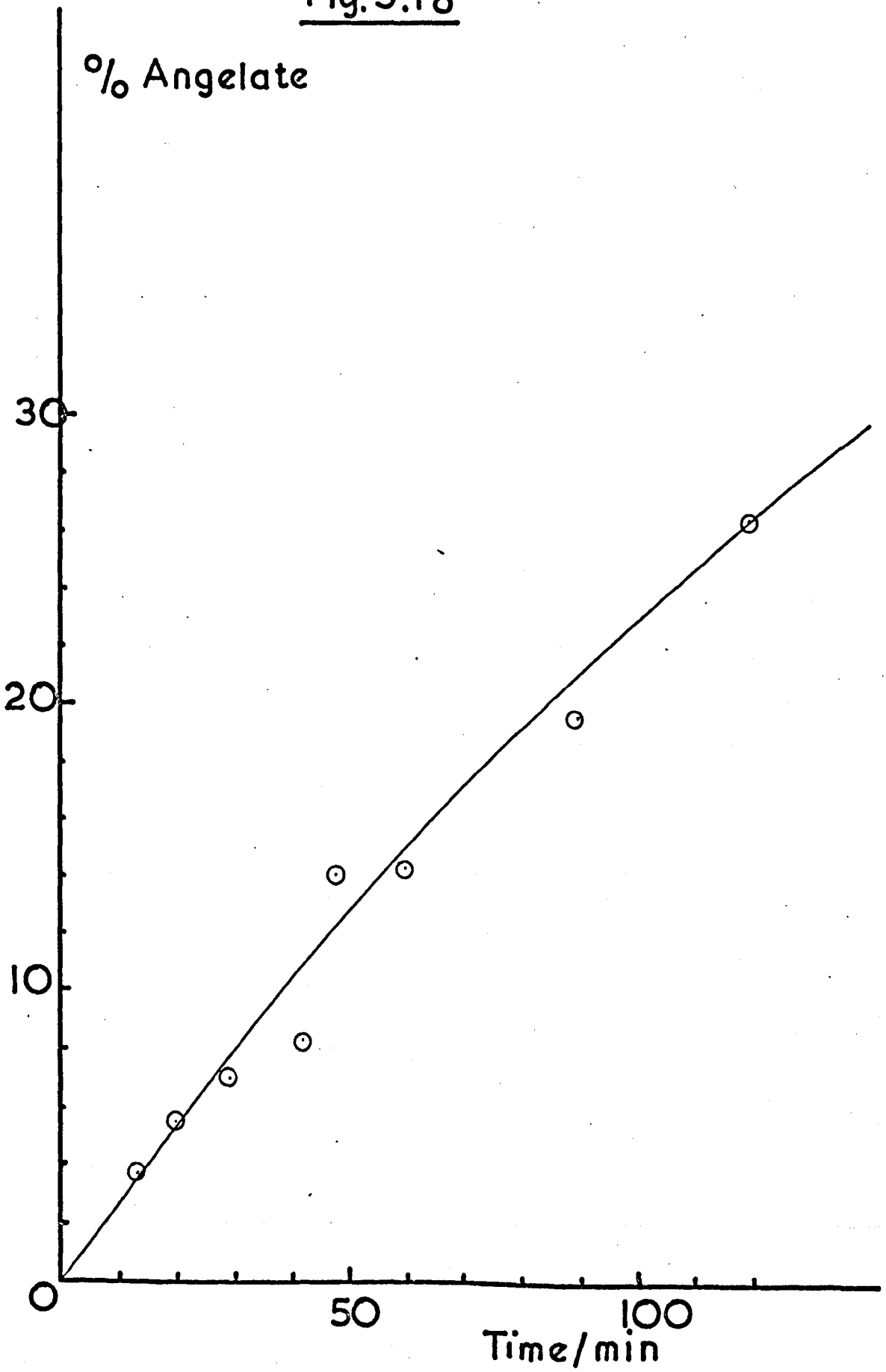

linear relationship between the reciprocal of the time and the reciprocal of the % angelate formed.

$$\text{i.e.} \quad \frac{1}{A} = \frac{a}{t} + b$$

where A = % angelate formed, t = time and a and b are constants

$$\text{rearranging,} \quad \frac{dA}{dt} = \frac{a}{(a + bt)^2}$$

∴ Initial slope when t = 0 is given by :

$$\frac{dA}{dt} = \frac{1}{a}$$

This is the reciprocal of the slope of the reciprocal plot so that the initial slope can be obtained from the linear plot. Such a reciprocal plot for the results at 35°C is shown in Fig. 3.19 where the reciprocal points are taken from the best curve through the original data. The results are tabulated below :

Initial concentration of tiglate mol $l.^{-1}$	Temperature °C	Initial Slope % min	Rate of production of angelate, mol $min^{-1} \mu l.^{-1}$	ϕ
1.04	26	0.260	0.270×10^{-8}	0.206
1.07	35	0.264	0.282×10^{-8}	0.216
1.12	50	0.265	0.297×10^{-8}	0.226

The quantum yields were calculated from an assumed intensity of

Fig. 3.19

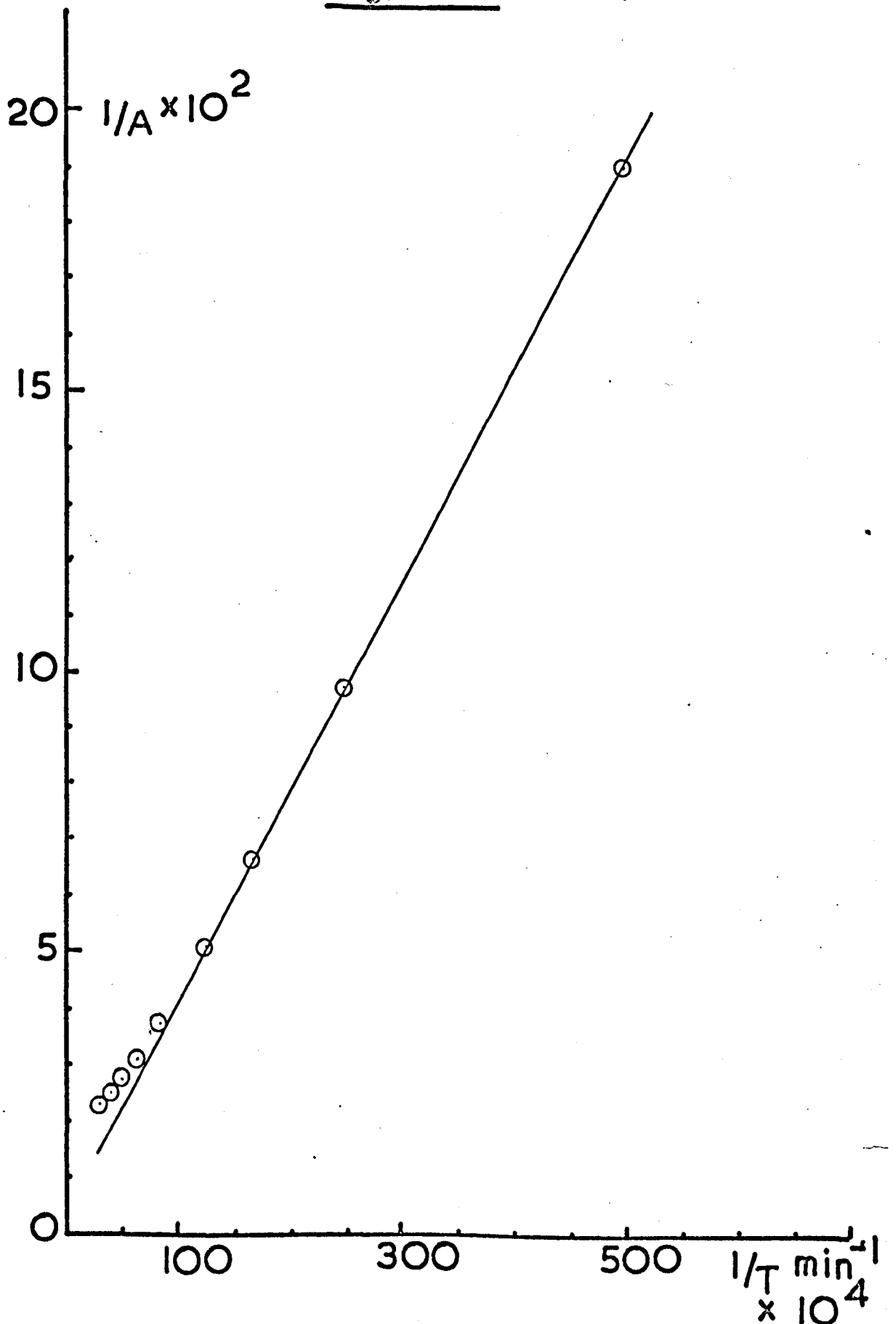

1.0×10^{16} q s^{-1} cm^{-2} as explained in 3.6. The observed variation in ϕ corresponds to an activation energy of about 1 kJ mol^{-1}. However, bearing in mind the experimental errors involved from various sources, it is possible that this variation is spurious.

3.8 Photolysis on Merry-go-Round, Concentration Dependence

The influence of concentration of methyl tiglate on the rate of isomerisation at 35°C was investigated by photolysing a series of tubes filled under vacuum on the merry-go-round apparatus as in 3.6. All analyses were on PEGA at 100°C with 1 microlitre aliquots.

3.8(a) 0.510 Molar methyl tiglate Fig. 3.20

Time min	P.H. Angelate cm x 10^{-4}	P.H. Tiglate cm x 10^{-4}	gm Angelate x 10^{5}	gm Tiglate x 10^{5}	Total Isomers gm x 10^{5}	% Angelate Total
15	8.9	71.0	0.35	5.5	5.85	6.0
31	16.6	65.5	0.7	5.0	5.7	12.3
43	25.2	68.5	1.1	5.2	6.3	17.5
71	34.0	60.5	2.0	4.5	6.5	30.8
107	35.0	52.0	2.1	3.8	5.9	35.6
127	40.5	47.0	2.0	3.4	5.4	37.0
150	44.0	45.0	2.6	3.2	5.8	44.8
226	52.5	41.5	3.2	2.9	6.1	52.5

Fig. 3.20

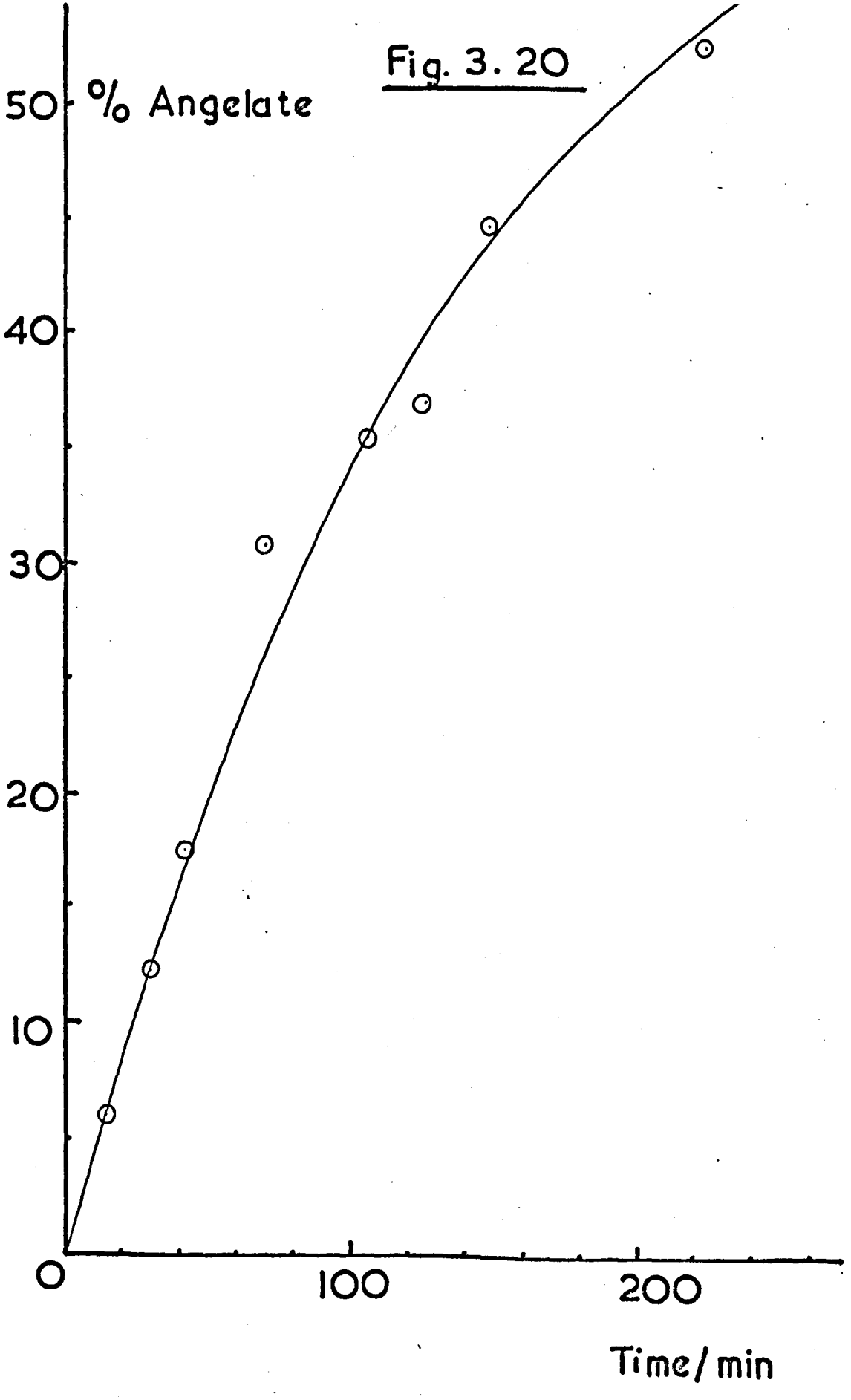

3.8(b) 2.20 Molar methyl tiglate Fig. 3.21

Time min	P.H. Angelate cm x 10^{-4}	P.H. Tiglate cm x 10^{-4}	gm Angelate x 10^5	gm Tiglate x 10^5	Total Isomers gm x 105	% Angelate Total
20	14.0	194	0.55	27.8	28.3	1.9
35	31.6	178	1.5	23.6	25.1	6.0
75	47.0	178	2.3	23.6	25.9	8.9
87	48.5	172	2.5	22.0	24.5	10.2
148	69.5	166	3.9	20.4	24.3	16.0
186	88.0	156	5.4	18.0	23.4	23.1
268	105	150	6.9	17.0	23.9	28.9

3.8(c) 2.67 Molar Methyl tiglate Fig.3.22

Time min	P.H. Angelate cm x 10^{-4}	P.H. Tiglate cm x 10^{-4}	gm Angelate x 10^5	gm Tiglate x 10^5	Total Isomers gm x 10^5	% Angelate Total
30	17.6	196	0.75	28.6	29.3	2.5
58	30.5	202	1.4	30.2	31.6	4.4
81	38.0	196	1.8	28.6	30.4	5.9
101	47.5	194	2.4	28.0	30.4	7.9
130	55.5	192	2.9	27.4	30.3	9.6

Fig.3.21

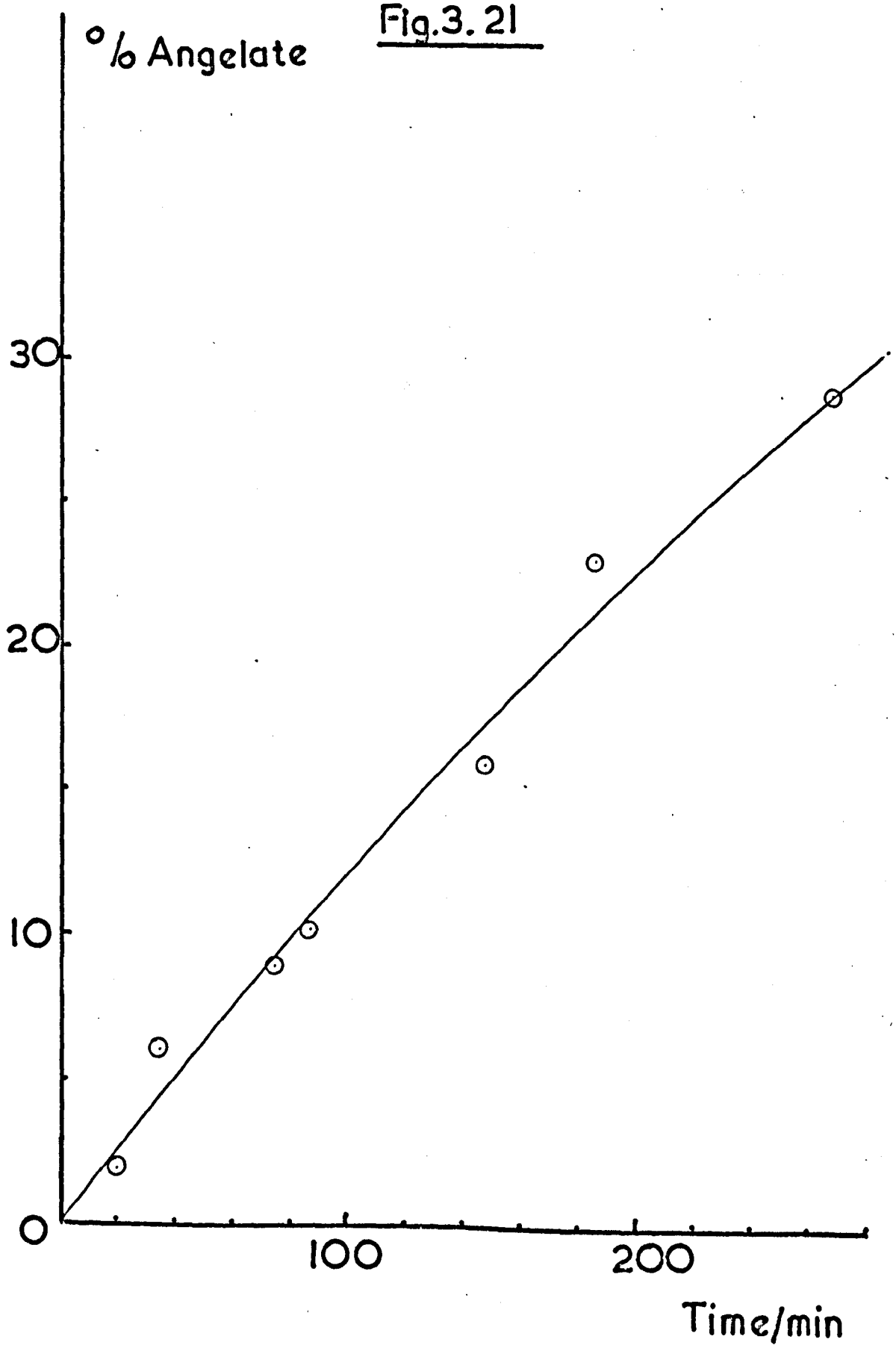

Fig. 3.22

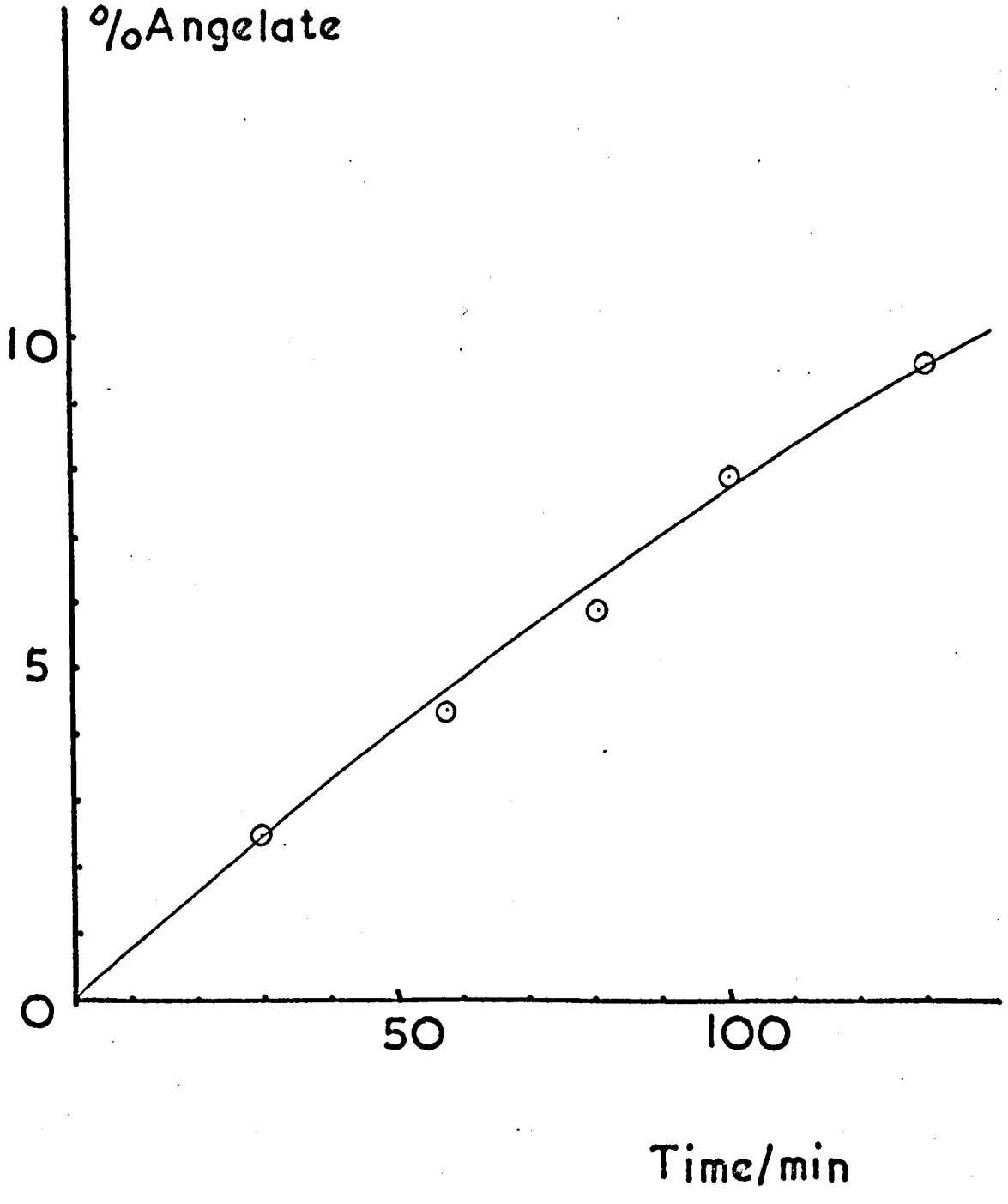

3.8(d) 3.33 Molar methyl tiglate Fig. 3.23

Time min	P.H. Angelate cm x 10^{-4}	P.H. Tiglate cm x 10^{4}	gm Angelate x 10^{5}	gm Tiglate x 10^{5}	Total Isomers gm x 10^{5}	% Angelate Total
18	10.2	220	0.48	36.4	36.9	1.3
40	24.0	214	1.17	34.4	35.6	3.3
65	33.0	214	1.67	34.4	36.1	4.6
80	40.0	220	2.09	36.4	38.5	5.4
168	82.0	220	4.8	36.4	41.2	11.6
256	106	208	7.0	32.4	39.4	17.8

3.8(e) Summary

As in 3.7 initial slopes were measured and quantum yields were determined using the intensity calculated in 3.6. These are tabulated below

Temp. °C	Initial Concentration of Tiglate Molar	Initial Slope % min^{-1}	Rate of formation of angelate mol min^{-1} microlitre^{-1} x 10^{8}	ø
35	0.510	0.431	0.220	0.166
35	1.07	0.264	0.282	0.216
35	2.20	0.106	0.233	0.178
35	2.67	0.091	0.243	0.184
35	3.33	0.07	0.233	0.178

Fig. 3. 23

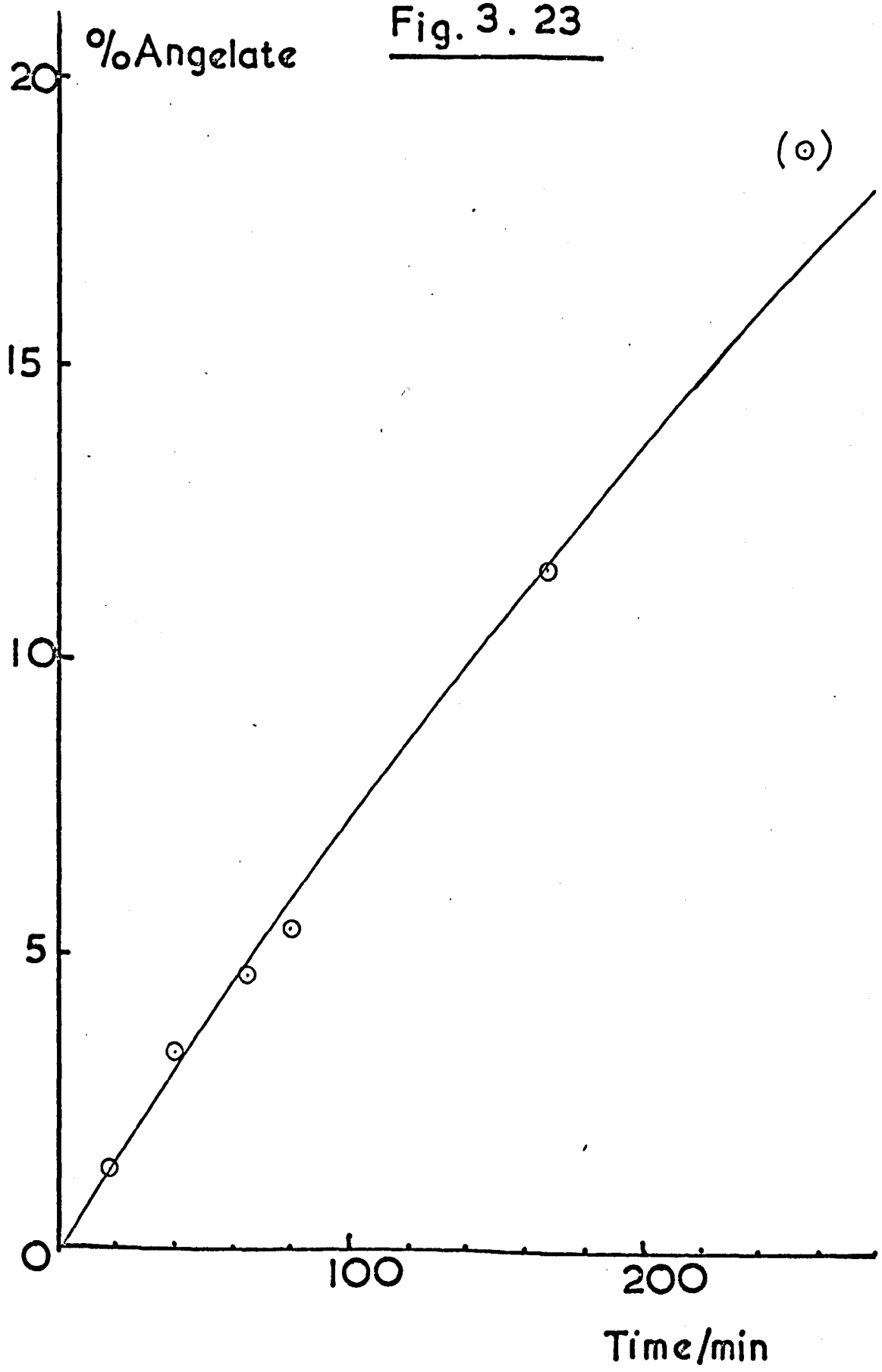

3.9 Semi-Micro Apparatus; Variation of Concentration

The results in 3.8 suggested that there may be a concentration dependence but they were not sufficiently reliable to deduce anything from them. When the semi-micro technique was devised it was decided to repeat these results. Various concentrations of methyl tiglate were photolysed in this apparatus (See Section 2.8) using the medium pressure lamp and 254 nm interference filter. Under these conditions conversions were very low and no curvature was observed on the production versus time graphs. A small concentration effect was observed due to evaporation of the solvent after long photolysis times. This was corrected for by scaling to the peak height of a small impurity peak used as an internal standard. By this means good straight line plots were observed.

3.9(a) 3.51×10^{-2} Molar methyl tiglate

Analysis on PEGA at 100° using 1 microlitre samples.

Photolysis temperature = $35^{\circ}C$.

Intensity measured by ferrioxalate = 1.77×10^{14} q $s^{-1} cm^{-1}$

Fig. 3.24

Time min	P.H. Angelate cm x 10^{-2}
0	6.5
30	7.5
80	8.7
120	10.5
154	11.9
200	13.2

Fig. 3.24

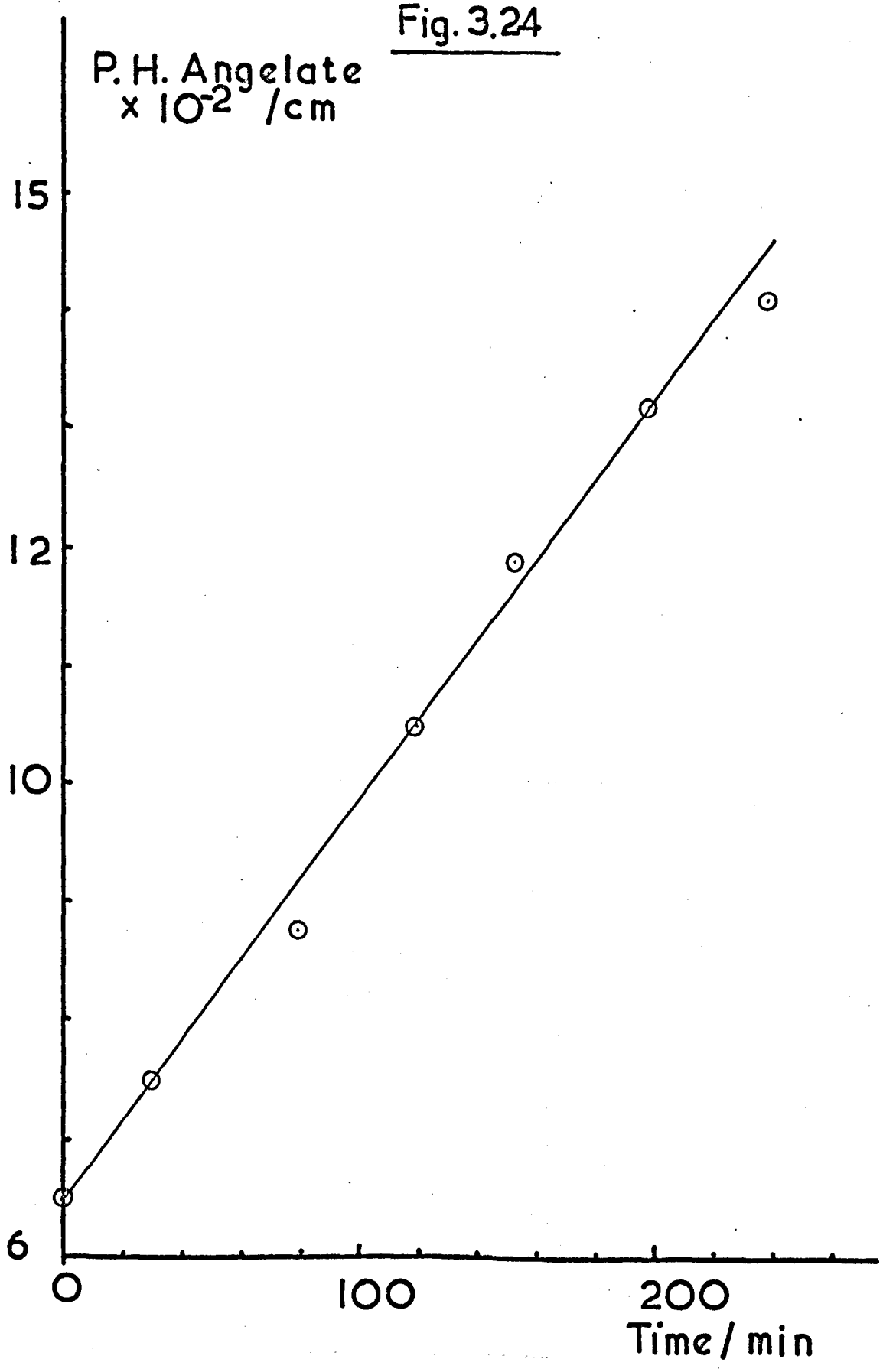

3.9(b) 0.360 Molar methyl tiglate

35°C. Analysis as in (a). Cell position altered and intensity changed to 1.05×10^{14} q $s^{-1}cm^{-2}$ as measured by ferrioxalate actinometry.

Fig. 3.25

Time min	P.H. Angelate cm x 10^{-2}
0	0.34
30	1.0
43	1.2
50	1.6
68	1.9
93	2.4
121	3.0
142	3.4

3.9(c) Molar methyl tiglate

35°C. Analysis as in (a). Intensity as in (b).

Fig. 3.26

Time min	P.H. Angelate cm x 10^{-2}
3	1.4
53	2.5
102	3.7
154	5.2
201	5.8
231	6.8

Fig. 3.25

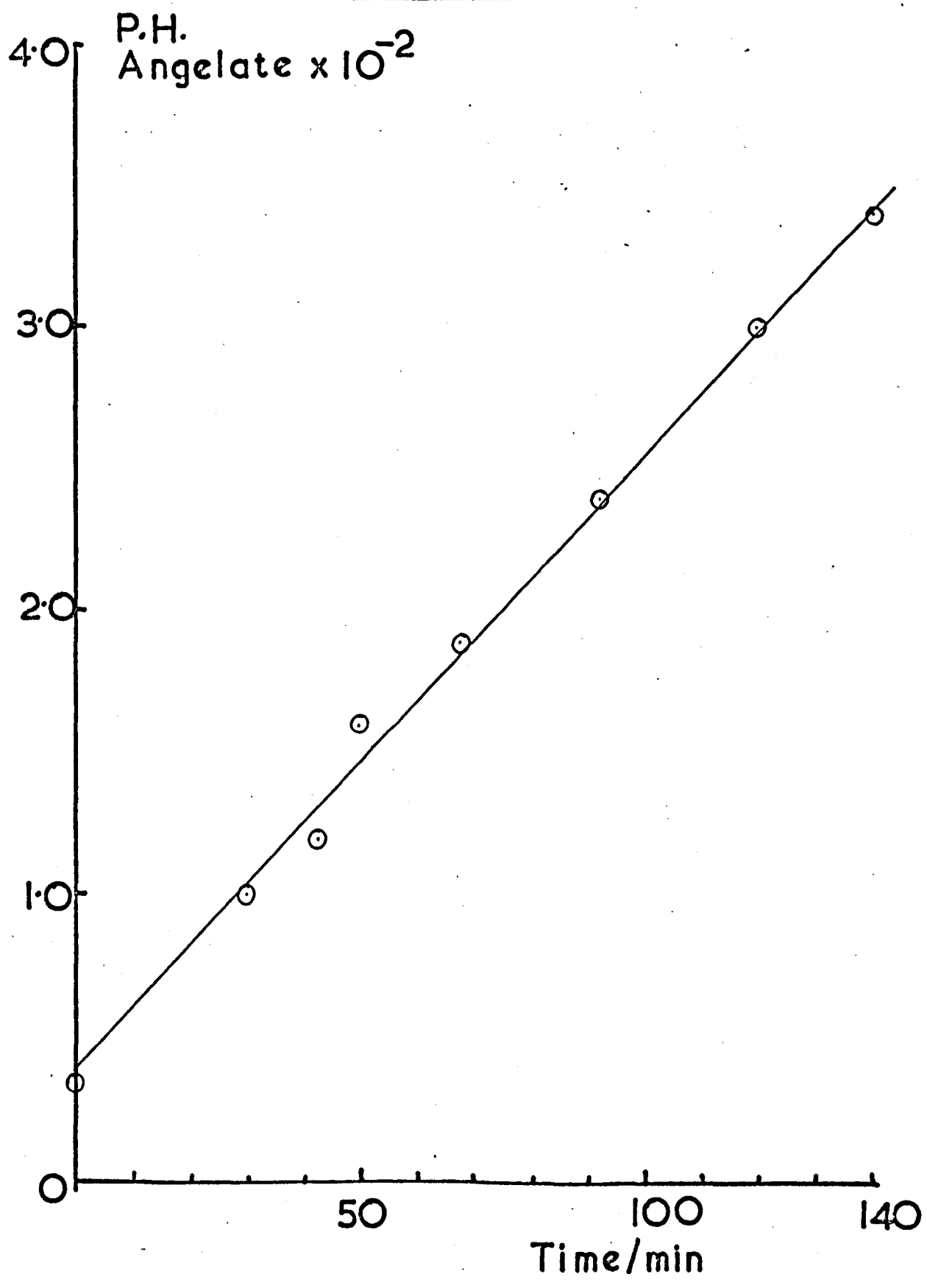

Fig.3.26

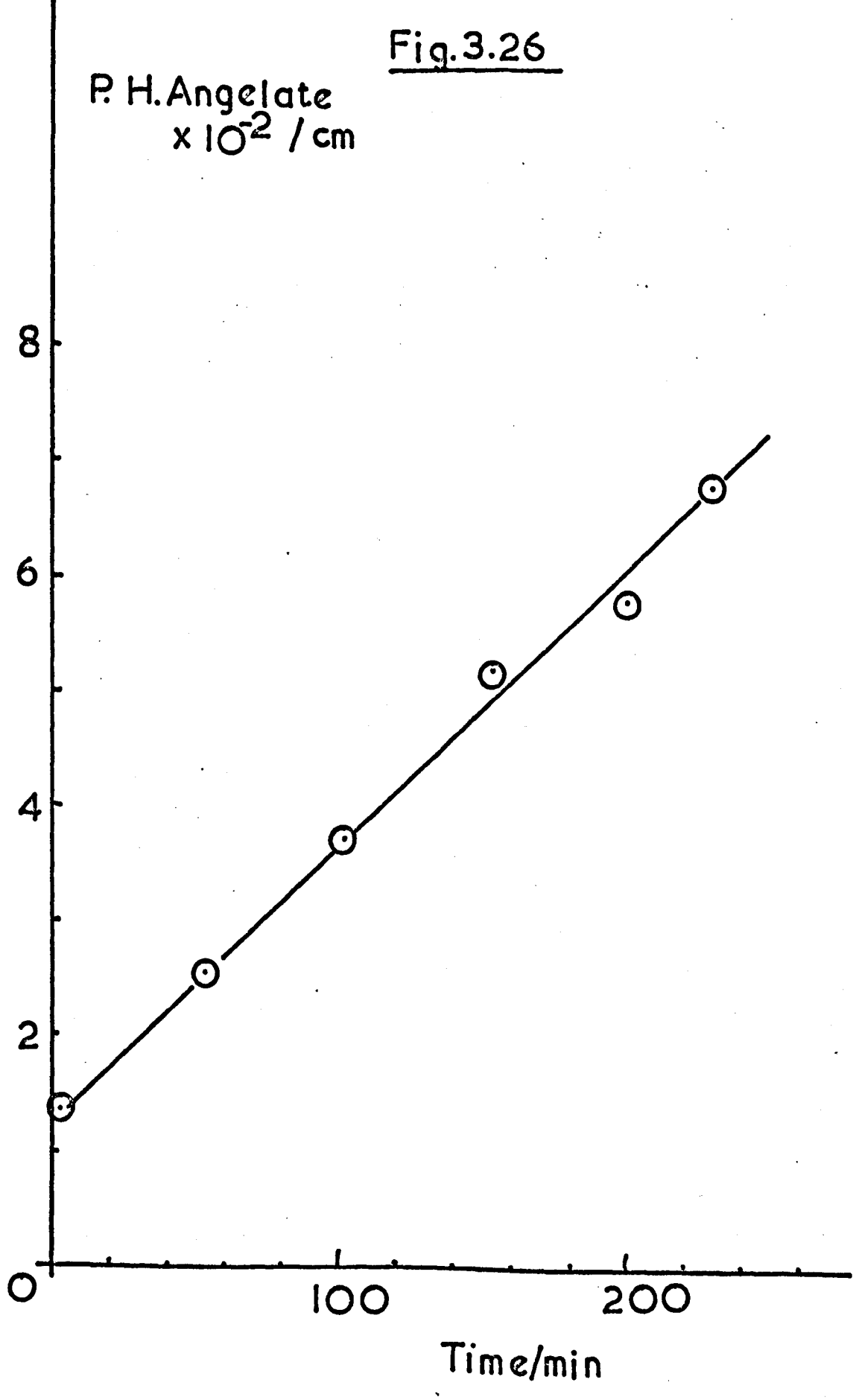

3.9(d) 1.96 Molar methyl tiglate

As (c).

Fig. 3.27

Time min	P.H. Angelate cm x 10^{-2}
0	6.6
40	7.4
82	8.4
102	8.75
139	9.6

3.9(e) Summary

Using the tabulated chromatograph sensitivity (Section 2.12), the quantum yields were calculated using the intensities measured. These are tabulated below.

Initial Tiglate Concentration Molar	Intensity q $s^{-1}cm^{-2}$ x 10^{-14}	Slope of Production Graph cm $min^{-1}\mu l^{-1}$	ϕ
0.0351	1.77	3.37	0.083
0.36	1.05	2.20	0.091
1.04	1.05	2.40	0.098
1.96	1.05	2.16	0.090

There appears to be no variation of quantum yield with concentration. The average value measured in this apparatus is found to be 0.090 ± 0.003

Fig. 3.27

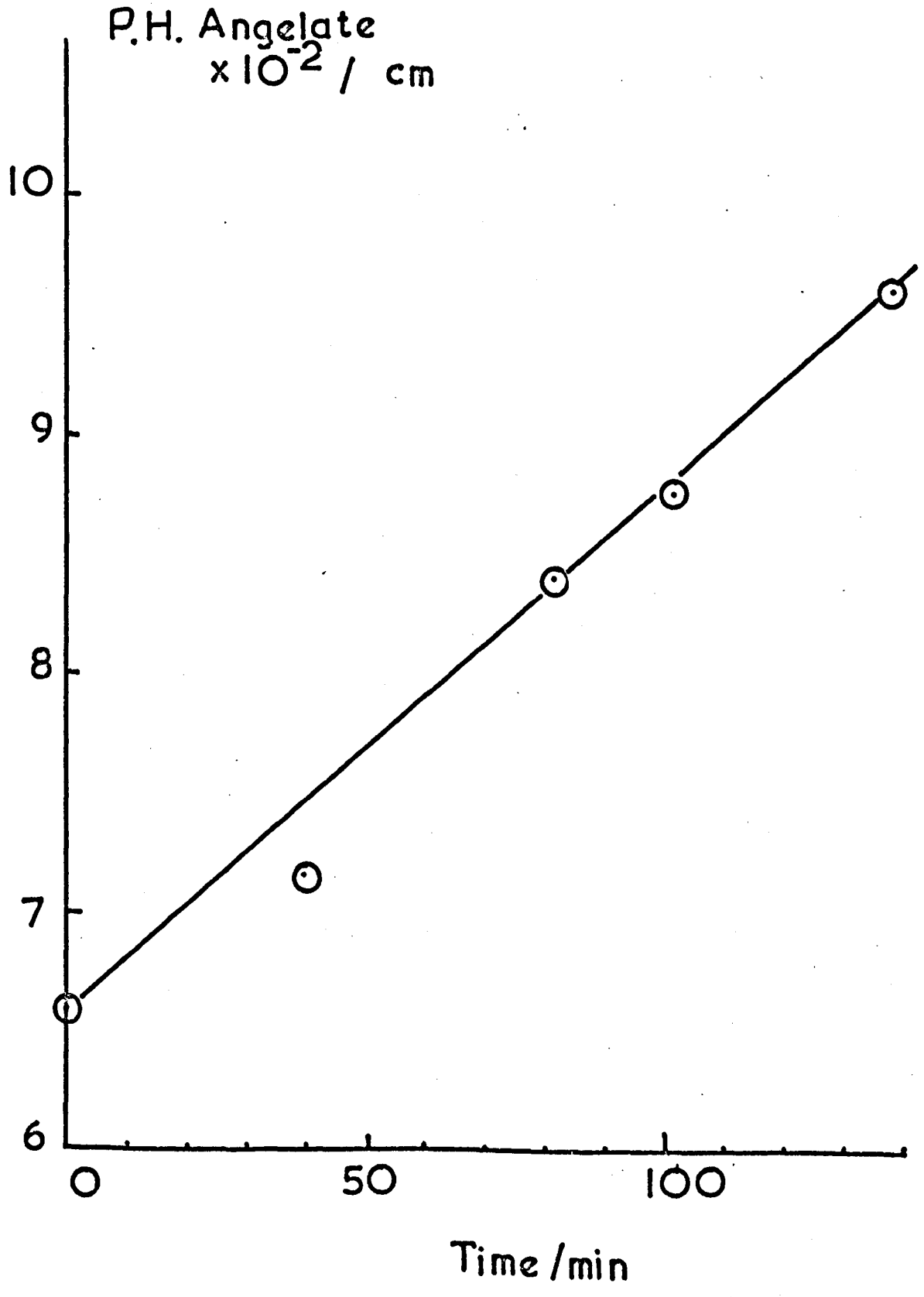

3.10 Effect of Solvent

A solution of methyl tiglate 0.42M in purified ethanol was photolysed in the semi-micro apparatus at 35°C to see if a hydroxylic solvent had any effect on the quantum yield of isomerisation at 254 nm.

Analysis on APL at 150°C with 1 microlitre samples.

Intensity = 1.05×10^{14} q $s^{-1} cm^{-2}$

Fig. 3.28

Time min	P.H. Angelate cm x 10^{-2}
0	0
48	1.0
90	2.2
125	2.8
152	3.4
177	4.2

Slope = 2.30 cm min^{-1}

∴ Rate of production of angelate = 0.89×10^{-12} mol $\mu l^{-1} min^{-1}$

∴ $\underline{\phi = 0.086}$

This is, within experimental error, the same as the value found in cyclohexane.

Fig. 3.28

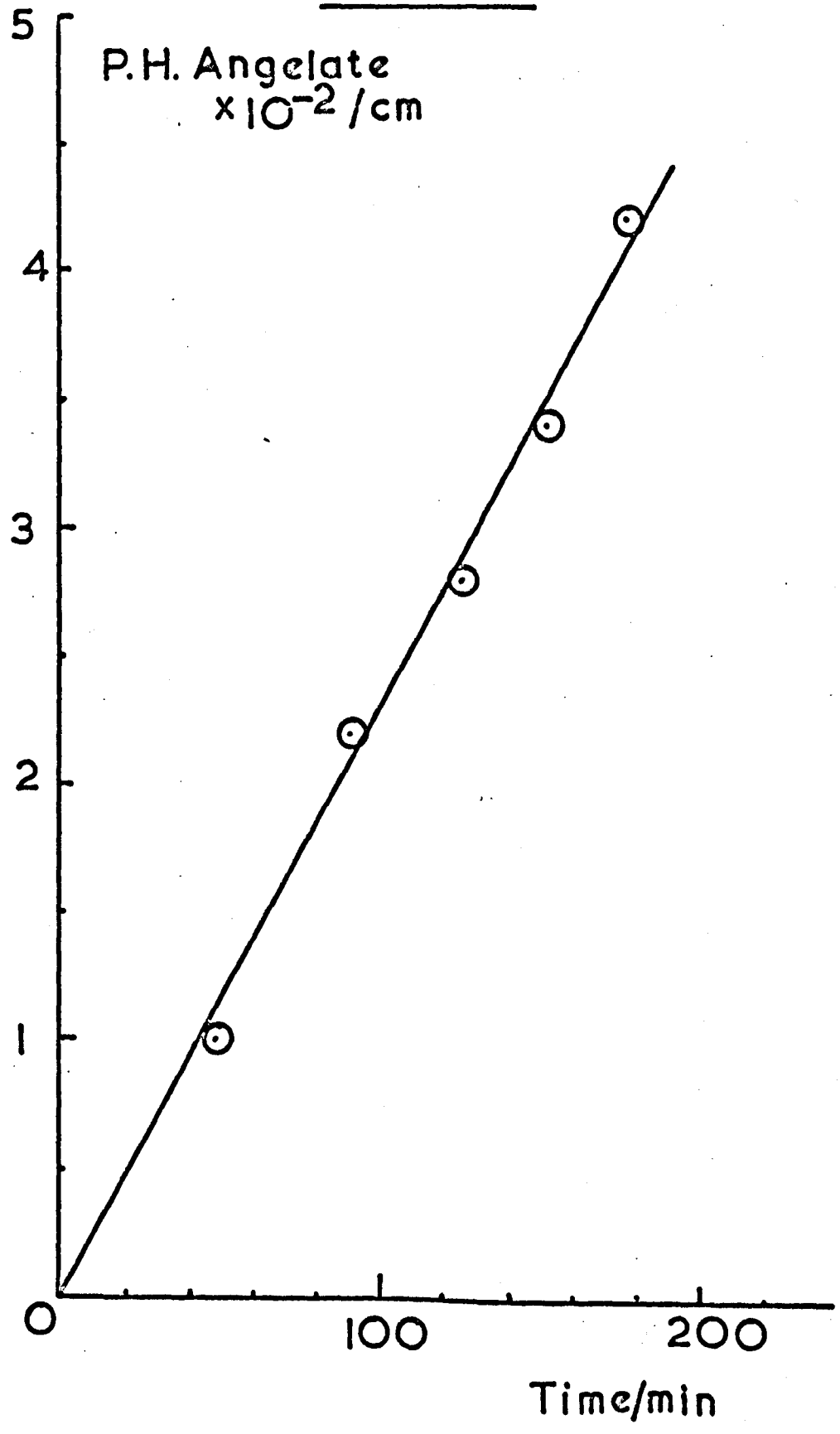

3.11 Low Temperature Photolysis

As described in Section 2.6 an attempt was made to measure the quantum yield of isomerisation at low temperatures. A solution of methyl tiglate, 0.42M in ethanol, was degassed on the vacuum line and sealed into the special cell. It was then photolysed for 315 min at 195K (acetone and solid CO_2) with a small spiral low pressure mercury lamp mounted in a housing, fitted with a quartz window and flushed with nitrogen. When opened and analysed the amount of angelate present was given by a peak height of 1.4×10^3 cm per microlitre on PEGA at $100^{\circ}C$. This was such a low conversion that it was difficult to measure with accuracy as the solvent peak overlapped the methyl angelate peak to some extent. A control was run at room temperature under the same conditions and this gave a peak height of angelate = 7.0×10^3cm after 1320 min. When the errors are taken into consideration it would seem that the reduction in temperature had little, or no effect on the quantum yield. Further attempts to study the effect of low temperatures were abandoned.

3.12 Methyl Angelate to Methyl Tiglate Isomerisation

A sample of pure methyl angelate was prepared and identified as previously described (Sections 2.2 and 3.1). Solutions of this compound in cyclohexane were photolysed by both capillary and semi-micro techniques to determine the quantum yield of the reverse isomerisation.

3.12(a) 1.75×10^{-2} mole litre^{-1} methyl angelate

35°C. Analysis on PEGA at 100°C. Semi-micro technique. Intensity = 1.77×10^{14} q $s^{-1}cm^{-2}$.

Fig. 3.29

Time min	P.H. Angelate cm
0	0
35	47.9
65	60.5
109	106.5
135	138
167	168

Production of (III) negligable.

$\phi = 0.0324$

As in the case of the reverse reaction the values found in capillaries were higher than this. They are set out below.

3.12(b) 1.83 Molar methyl angelate and 1.10 Molar methyl angelate

Analysis as in (a). Merry-go-round at 35°C. Intensity as in 3.6.

The sensitivity was measured approximately for compound (III) on PEGA at 100°C as being 2.2×10^{12}cm mol^{-1}.

Fig. 3.29

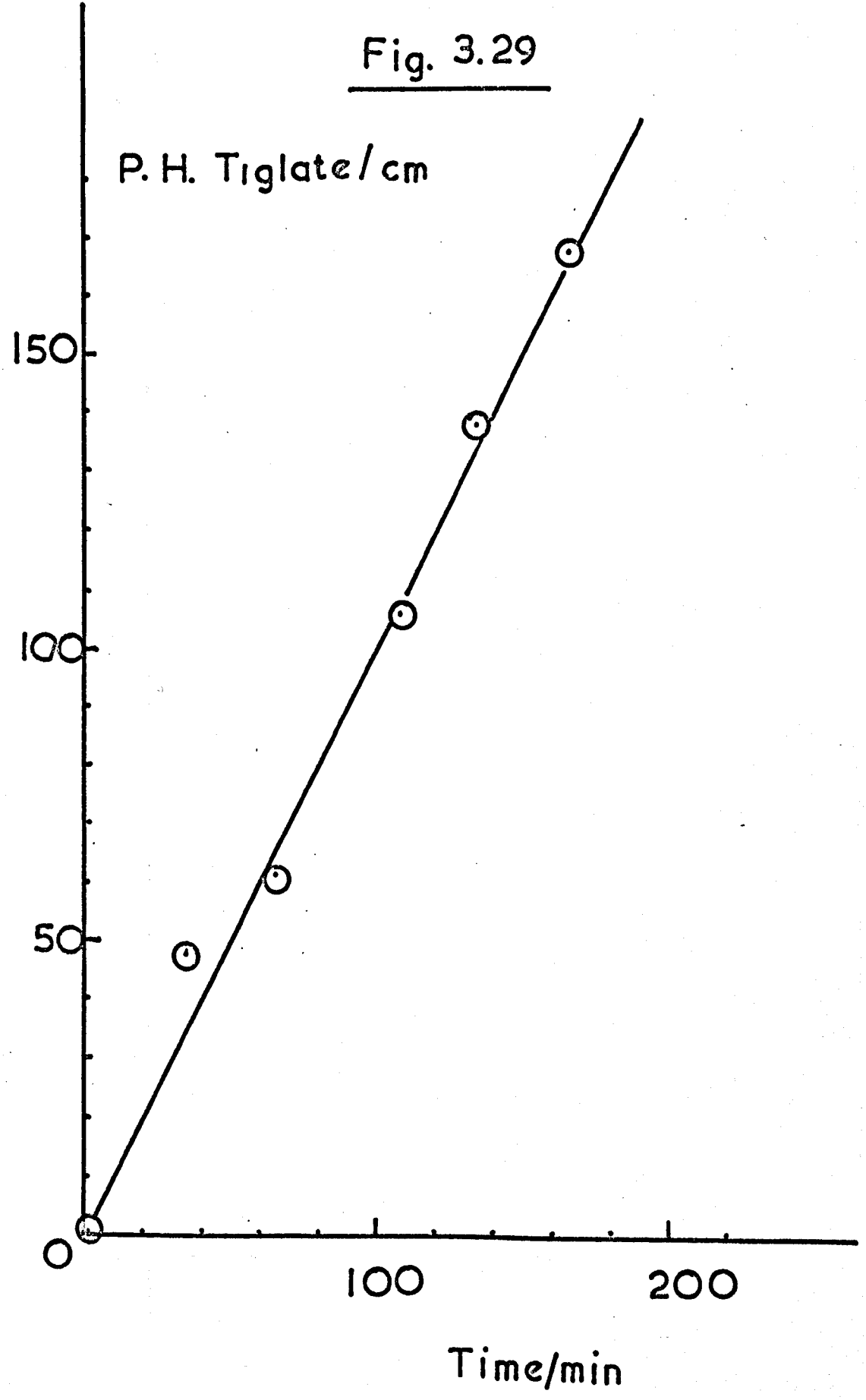

Time min	Initial molarity of methyl angelate	P.H. Angelate cm x 10^{-4}	P.H. Tiglate cm x 10^{-4}	gm Angelate x 10^5	gm Tiglate x 10^5	gm (III) x 10^5	Total Isomers gm x 10^5	% Tiglate Total	%(III) Total
0	1.83	196	0.1	20.8	0.01	0.08	20.9	0.05	0.38
15	1.83	202	3.7	21.8	0.23	0.11	22.1	1.04	0.49
30	1.83	195	5.5	20.5	0.35	0.15	20.9	1.67	0.72
45	1.83	202	8.3	21.8	0.55	0.17	22.5	2.44	0.76
58	1.83	200	8.9	21.5	0.60	0.19	22.3	2.69	0.85
98	1.83	190	14.4	19.4	0.97	0.26	20.7	4.68	1.26
0	1.10	152	0.1	12.6	0	0.05	12.6	0	0.40
33	1.10	147	6.8	11.9	0.42	0.11	12.4	3.4	0.89
58	1.10	138	13.5	10.7	0.90	0.19	11.9	7.6	1.59
78	1.10	146	16.2	11.5	1.10	0.22	12.8	8.6	1.72
103	1.10	145	18.4	11.6	1.27	0.25	13.1	9.7	1.91
166	1.10	134	28.6	10.0	2.05	0.41	12.4	16.5	3.30
240	1.10	127	40.0	9.3	2.81	0.55	12.7	22.2	4.33

Figs. 3.30, 3.31.

Fig. 3.30

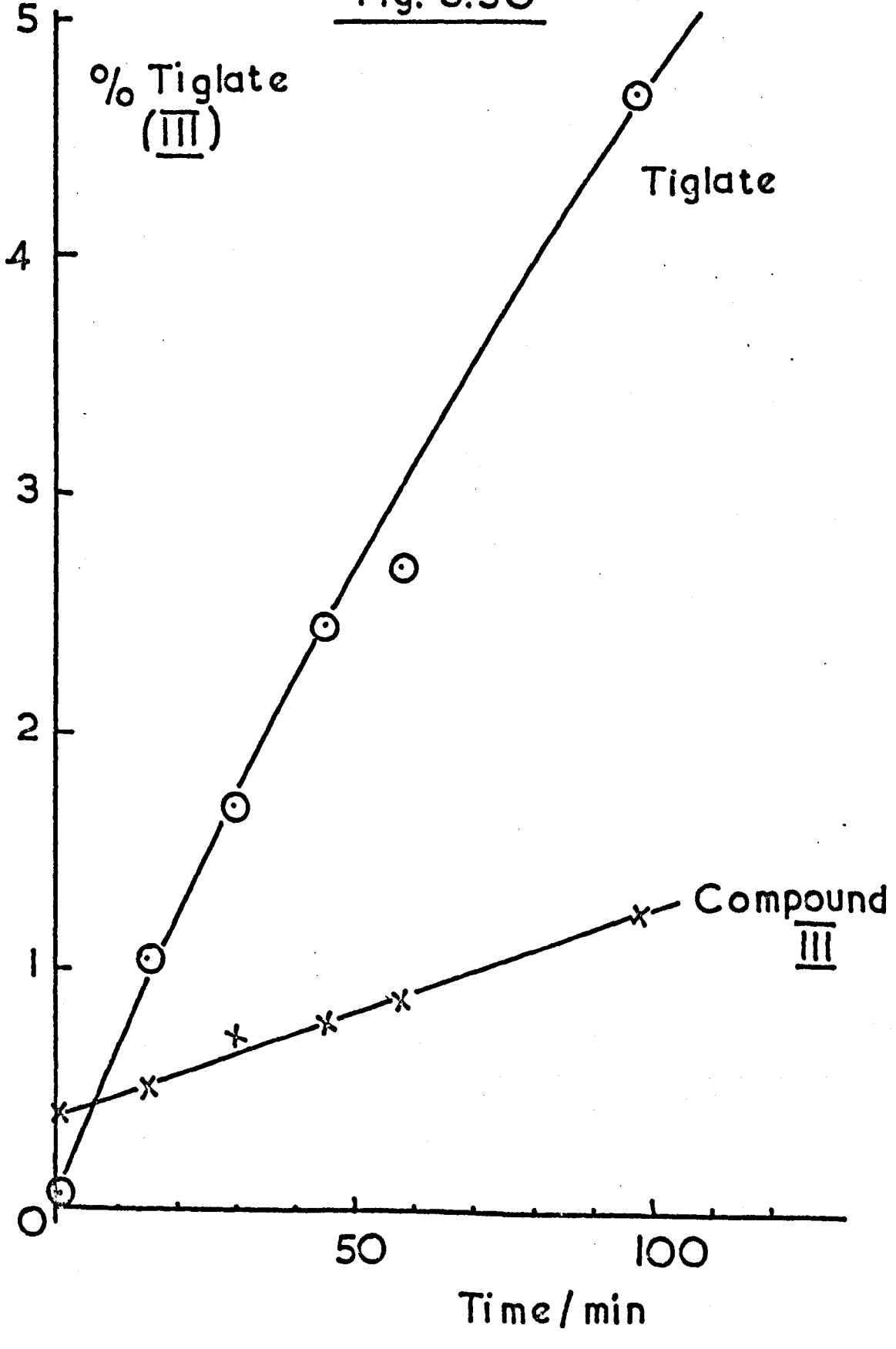

Fig. 3.31

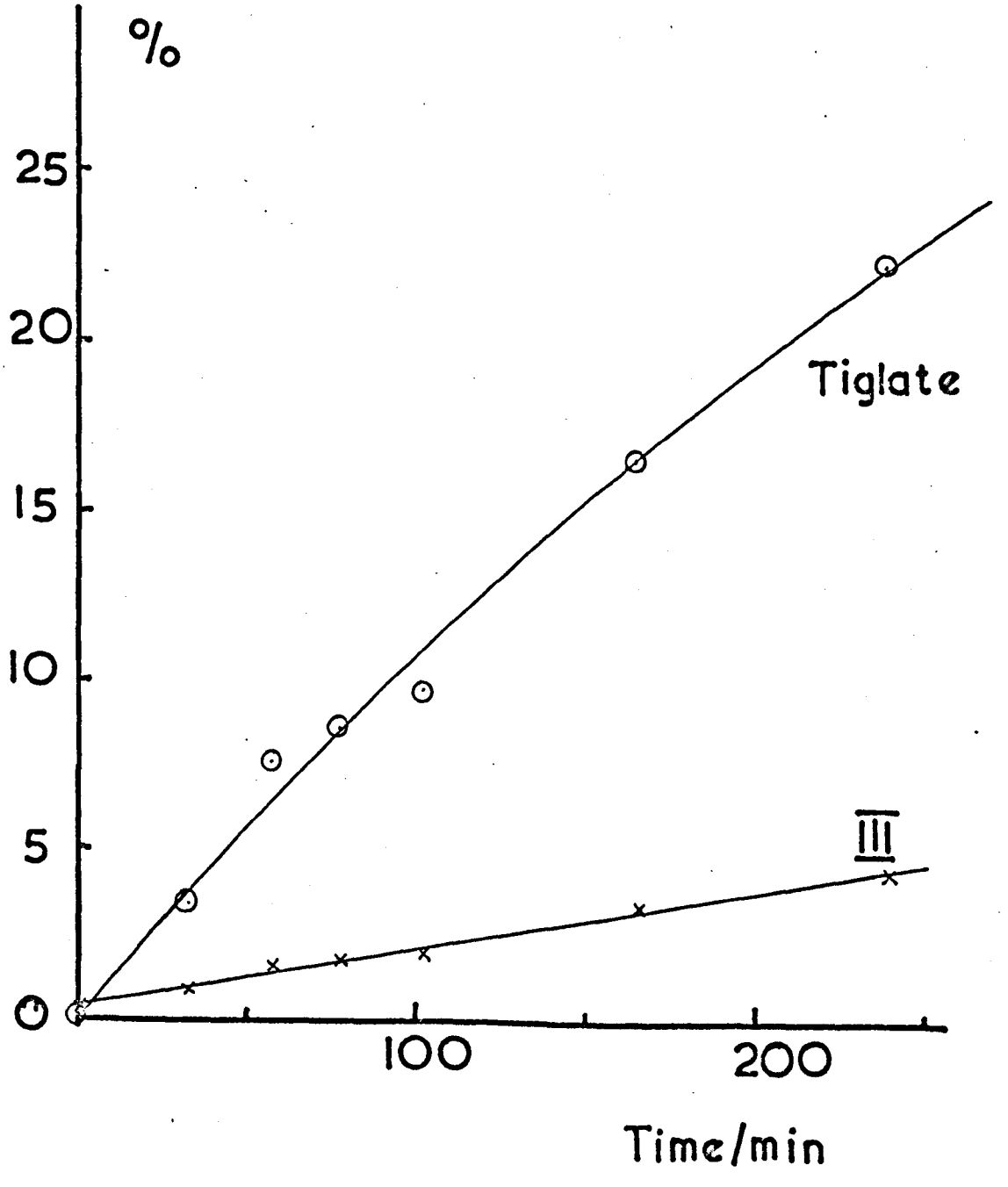

3.12(c) Summary

From Figs. 30 and 31 the following quantum yields were calculated.

Initial conc. of Angelate, M	Initial Slope of Tiglate Production % min^{-1}	Initial Slope of III Production % min^{-1}	ø Ang.→ Tig.	ø Ang.→ III
1.83	5.8×10^{-2}	0.85×10^{-2}	0.081	0.0119
1.10	11.4×10^{-2}	1.65×10^{-2}	0.095	0.0138

Although these values differ considerably from the value obtained in (a) it is observed that the ratio of the quantum yield of isomerisation to that of de-conjugation is the same in both cases above, 6.8.

3.13 Photosensitisation - Preliminary experiments

3.13(a) A solution of 0.614 mol litre^{-1} methyl tiglate in cyclohexane containing 20% (by volume) acetophenone was photolysed at 313 nm with the medium pressure lamp and interference filter in the semi-micro apparatus. 1 microlitre portions were analysed on PEGA at 100°.

Fig. 3.32

Time min	P.H. Angelate cm x 10^{-2}
0	16.5
30	31.5
60	47.5
87	57.8
227	127
243	138

3.13(b) The same solution was then photolysed with the 366 nm filter in the same experimental arrangement.

Fig. 3.33

Time min	P.H. Angelate cm x 10^{-2}
0	146
63	228
104	285
126	320
155	350
207	420

Fig. 3.32

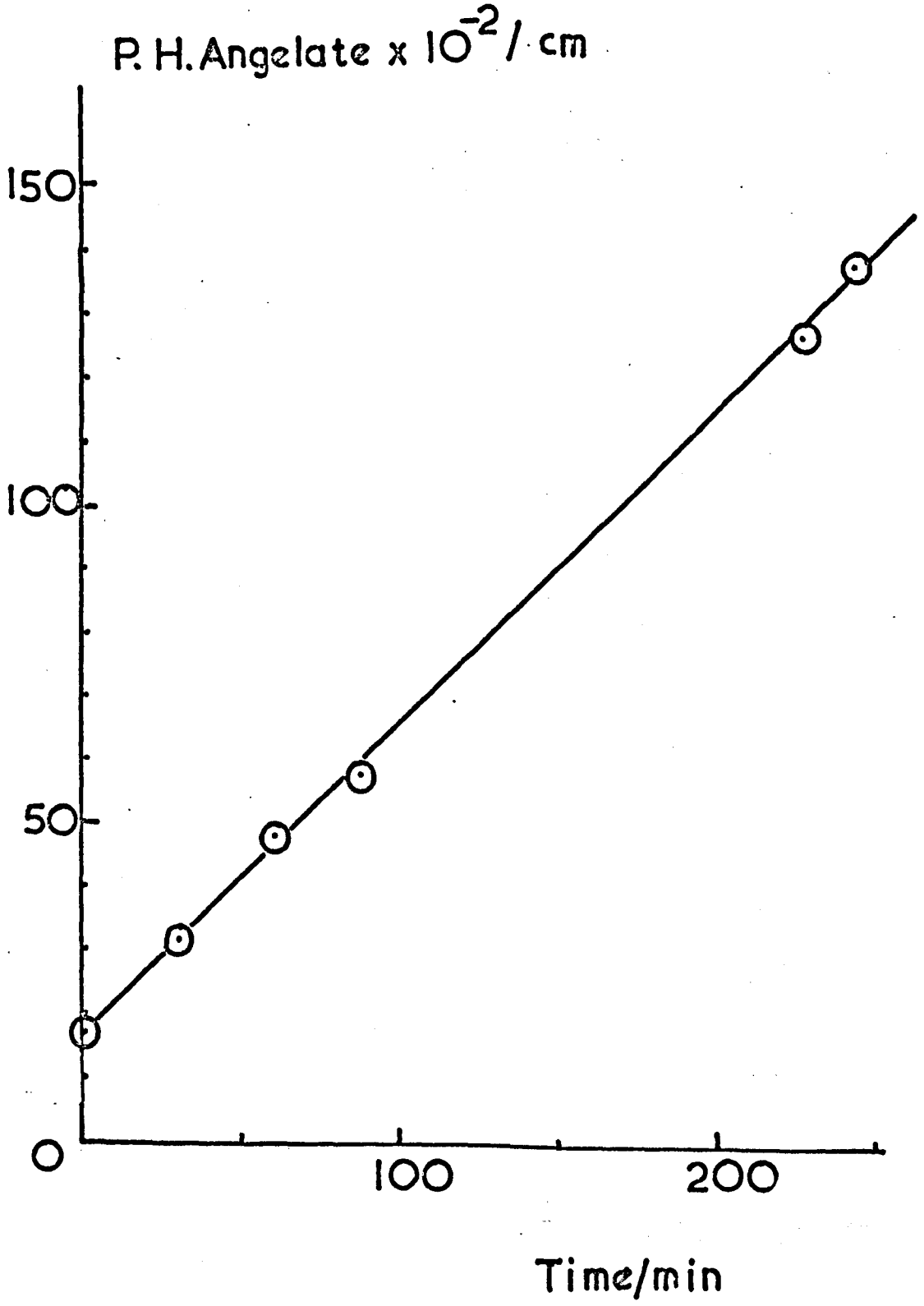

Fig. 3.33

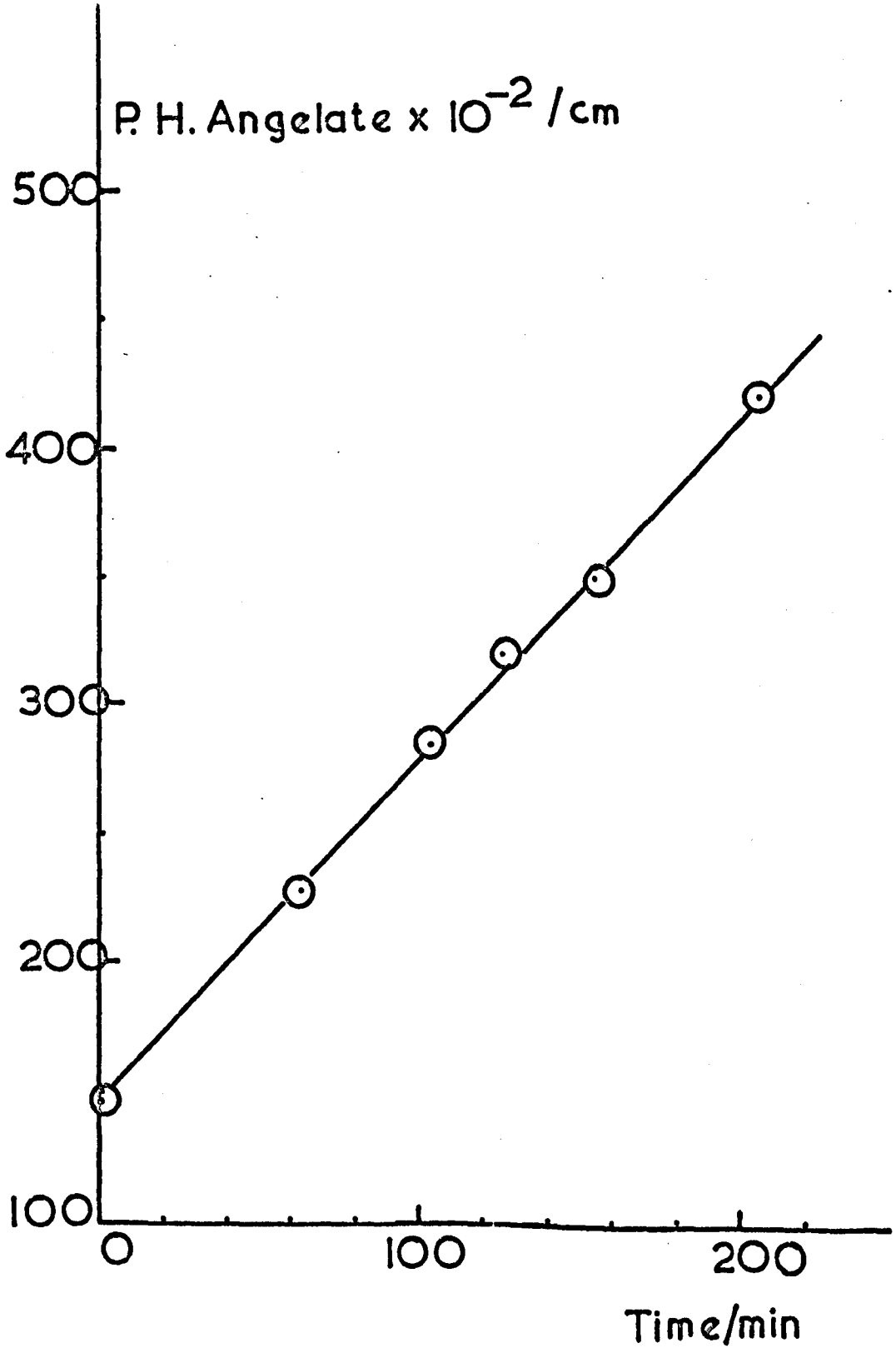

This solution was then photolysed for a further 16h, by which time the angelate represented about 10% of the total ester concentration. No trace of compound (III) was seen even at the maximum possible sensitivity of the detector. It was concluded that (III) is not formed in the photosensitised reaction. The results above show that it is a genuine photosensitised reaction as methyl tiglate does not itself absorb at either wavelength.

The intensity at 313 and 366 nm was not measured but that at 254 nm = 1.77×10^{14} q $s^{-1}cm^{-2}$. If the ratios of intensities was as was later determined then I313 = 8.0×10^{14} q $s^{-1}cm^{-2}$ and I366 = 22.5×10^{14} q $s^{-1}cm^{-2}$. From the slopes of Figs. 3.32 and 3.33 the quantum yields are therefore 0.267 and 0.257 respectively.

3.14 Absorption Spectra in Ethyl Iodide

In an attempt to get some approximate measure of the triplet energy of methyl tiglate, the U.V. spectrum was recorded in freshly distilled ethyl iodide (10% solution). In such a heavy atom solvent singlet to triplet transitions become possible due to perturbation effects (See for example Ref.6). A weak absorption band was seen on the long wavelength end of the ethyl iodide cut-off which was shown to be due to the methyl tiglate. The onset of this absorption was at 400 nm. No such absorption was observed in the same strength solution in hydrocarbon solvents, though it could possibly have been caused by traces of impurity in the ester. 400 nm corresponds to an energy of 300 kJ mol^{-1} (71.5 kcals mol^{-1}). As a check on this experiment it was found that the onset of absorption of benzophenone corresponded to a triplet energy of 292 kJ mol^{-1} as compared to the published value of 289 kJ mol^{-1} from phosphorescence measurements.

This result suggests that the triplet energy of methyl tiglate is around 300 kJ mol^{-1}. This is of the order expected and fits in with photosensitisation results described overleaf. The reliability of this energy is open to question, however, due to the fact that the ethyl iodide is absorbing strongly at the position of the methyl tiglate absorption seen.

3.15 Benzophenone photosensitisation

Photolysis of a solution, 2.78 x 10^{-2}M methyl tiglate and 0.394 M Benzophenone in cyclohexane. Photolysis at 25°C on semi-micro apparatus at 366 nm. Analysis of 1 microlitre samples on PEGA at 100°C.

Fig. 3.34

Time min	P.H. Angelate cm x 10^{-2}
0	10.2
44	34.5
71	50.5
88	58
104	67
126	74
143	87
232	116
294	160

Slope of production curve = 51 cm min^{-1}
Intensity measured by ferrioxalate = 15.70 x 10^{14} q $s^{-1}cm^{-2}$
∴ Quantum yield = 0.141

To obtain a value for the photostationary state a small amount of methyl angelate was added to this solution so that the total concentration of ester was 4.2 x 10^{-2} mol $litre^{-1}$. The solution was then photolysed for a further 189 min when a constant composition was obtained. This stationary composition was 52.9% tiglate.

Fig. 3. 34

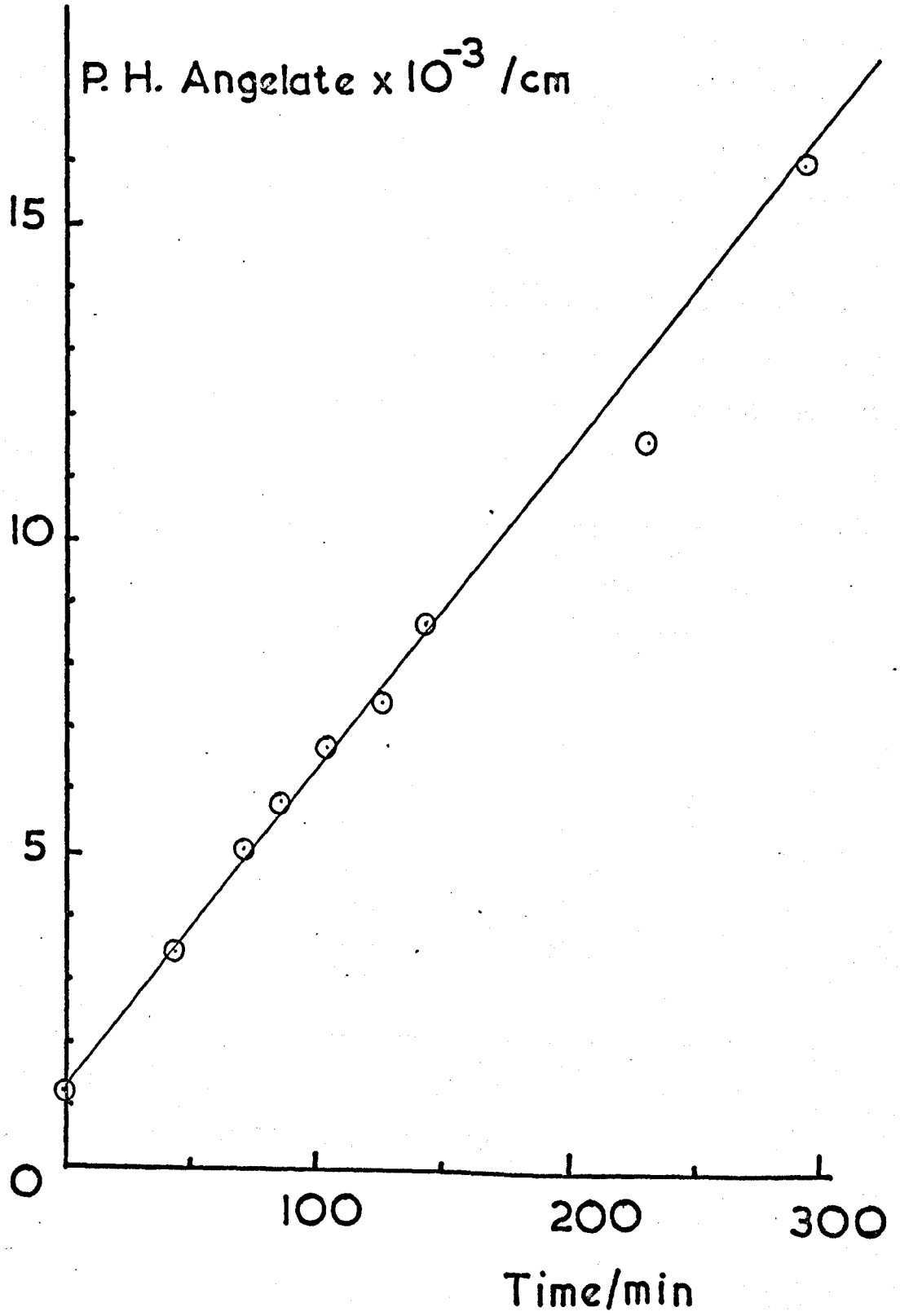

3.16 Other Sensitisers

Other compounds of different triplet energy were tried as sensitisers for the isomerisation. Biphenyl (E_T = 275 kJ mol^{-1}), naphthalene (E_T = 254), benzil (E_T = 224) and pyrene (E_T = 204) were all tried under conditions where they absorbed all incident light at 313 nm. None of them acted as photosensitisers and no reaction was observed. Acetone (E_T = 330 mol^{-1})[8] was found to be an effective photosensitiser. A solution containing 6.6 x 10^{-2} mol $litre^{-1}$ methyl tiglate and 1.37 mol $litre^{-1}$ acetone was photolysed at 313 nm and 25°C on the semi-micro apparatus. Analysis on PEGA at 100°C.

Fig. 3.35

Time min	P.H. Angelate cm x 10^{-2}
4	0.4
25	7.0
41	12.2
78	22.5
102	30.0
124	36.0
171	45.5
178	50.5
218	62.0

Intensity = 4.74 x 10^{14} q $s^{-1}cm^{-2}$

Slope = 28.5 cm min^{-1} $\therefore$ ϕ = 0.260

Fig. 3.35

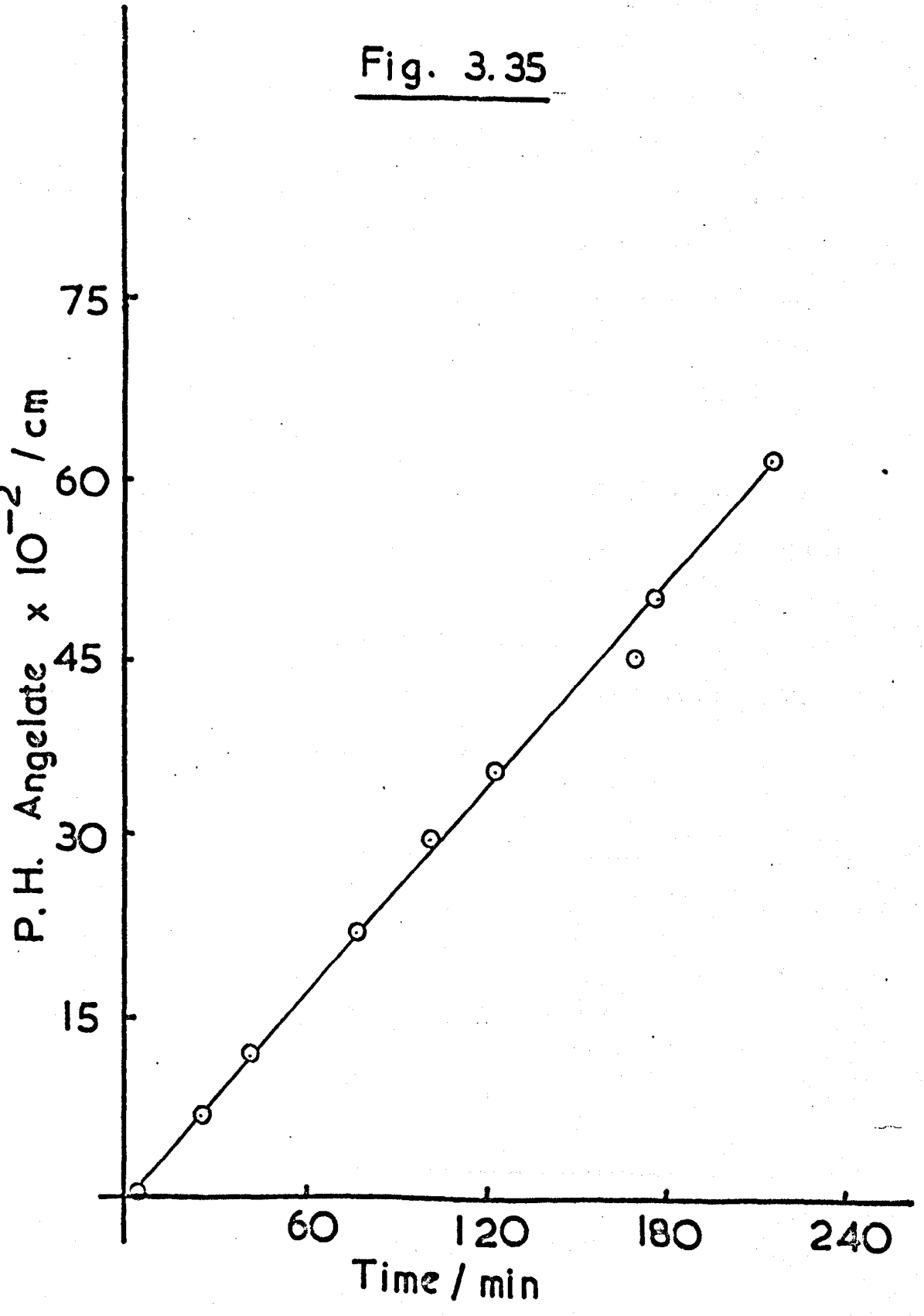

In order to find the photostationary state with acetone, the intensity was increased by illuminating the cell from both sides using the high pressure lamp and another 313 nm interference filter as an additional source of light. In this way the light entering the cell was increased tenfold and equilibrium conditions were reached much more quickly. The photostationary composition of the above solution was found to be 50.3% methyl tiglate. In the same way, that of a solution of 6.6×10^{-2} mol litre^{-1} methyl tiglate in 10% acetophenone in cyclohexane was measured to be 49.8% tiglate.

9, 10 - Anthraquinone (E_T = 263 kJ mol^{-1})[7] was found to be an inefficient photosensitiser for the isomerisation. A solution containing 2 mgm of anthraquinone (9.6×10^{-4} mol litre^{-1}) in 10 mls of a 6.6×10^{-2} M solution of methyl tiglate was photolysed at 313 nm in the semi-micro apparatus at 25°C. Analysis on PEGA at 100°C.

Time min	P.H. Angelate cm x 10^{-2}
0	0
139	3.5
167	4.0
202	5.0
243	6.25
260	6.5
303	7.5

Slope = 2.5 cm min^{-1} µl^{-1}

Intensity = 5.61 q s^{-1}cm^{-2} ∴ Ø = 0.019

It was noticed that the production of two unknown side-products proceeded at about 10 times the rate of isomerisation. These products were probably oxetanes. The low quantum yield of isomerisation reflects this side reaction. The exact nature of the addition products was not investigated.

3.17 Attempts at Quenching Photosensitisation

A series of experiments was planned to try to determine the dependence of photostationary state composition on azulene concentration in the benzophenone photosensitised reaction. The concentrations were arranged so that the benzophenone was absorbing more than 90% of the light. When such an experiment was carried out it was found that after 8h illumination at 313 nm the methyl tiglate and angelate had both been consumed to an extent that the total ester concentration was less than 10% of the initial concentration. The original deep blue colour of the azulene had also been dissipated and a light blue fluorescence was noticed on irradiation at 313 nm. At least three new product peaks were seen on the chromatograph. The same reaction was observed at 366 nm. This series of experiments was therefore abandoned. When naphthalene was used instead of azulene a similar reaction leading to depletion of the ester was observed and no stationary state could be established. No attempt was made to identify the products of these complex reactions.

3.18 Effect of Benzophenone Concentration on the Photosensitised Isomerisation

As part of a more detailed study of the benzophenone sensitised isomerisation it was decided to investigate the effect of benzophenone concentration on the isomerisation, if any.

1 x 10^{-2}M solutions of methyl tiglate in cyclohexane were made 0.5 to 4 x 10^{-2}M in benzophenone and photolysed at 313 nm and 25°C in the semi-micro apparatus. Analysis was on PEGA at 100°C, using 1 microlitre samples. Due to breakage, a new cell was used. This was 1.0 cm path length and 1.302 cm^3 in volume.

Fig. 3.36

Time min	P.H. Angelate cm x 10^{-2}	Concentration of benzophenone mol $l.^{-1}$ x 10^2
0	1.6	4.0
39	6.0	4.0
137	16.5	4.0
223	22.5	4.0
348	30.5	4.0
0	0.8	2.0
56	6.2	2.0
99	9.5	2.0
134	14.0	2.0
149	14.5	2.0
233	19.4	2.0

Fig. 3.36 - continued

Time min	P.H. Angelate cm x 10^{-2}	Concentration of benzophenone mol $l.^{-1}$ x 10^{2}
0	1.4	1.0
45	4.6	1.0
68	5.4	1.0
86	7.0	1.0
114	8.2	1.0
209	12.8	1.0
253	13.8	1.0
267	14.5	1.0
0	1.4	0.5
18	2.4	0.5
45	4.4	0.5
63	4.8	0.5
75	5.2	0.5
90	6.6	0.5

These data are shown in Figs. 3.36 - 37.

The results are summarised overpage.

Fig. 3.36

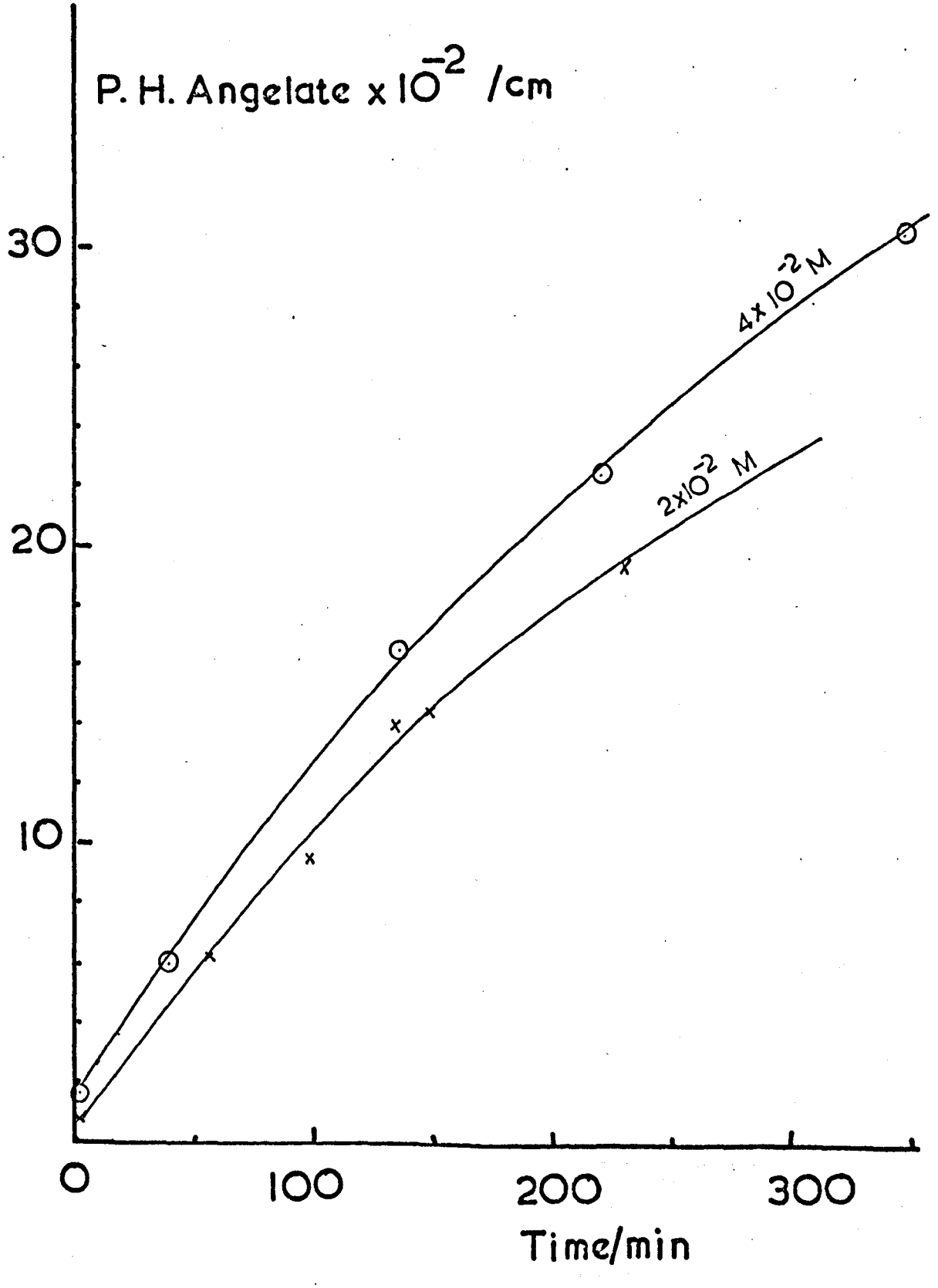
P. H. Angelate x 10⁻² /cm
30
20
10
0
100
200
300
Time/min
4x10⁻² M
2x10⁻² M

Fig. 3.37

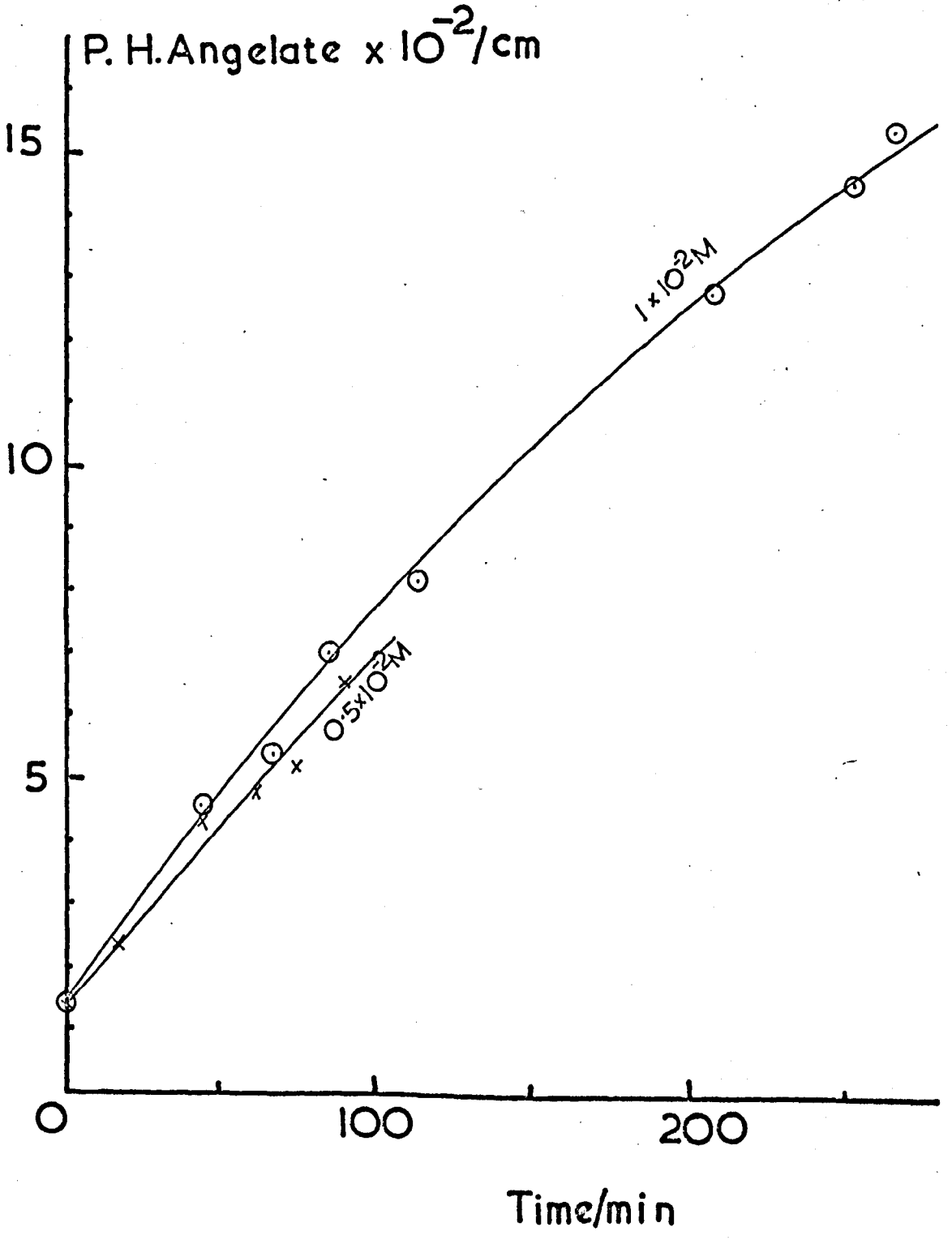
P. H. Angelate x 10^{-2}/cm
15
10
5
0
100
200
Time/min
1×10^{-2}M
0.5×10^{-2}M

Molarity of Benzophenone x 10^2	Slope cm min^{-1}	Absorbance of solution	% Light Absorbed	Scaled Slope cm min^{-1}
0.5	5.6	0.30	49.9	11.2
1.0	7.6	0.60	74.9	10.1
2.0	10.1	1.20	93.7	10.75
4.0	11.7	2.40	99.6	11.7

In the above table it can be seen that if the rates are scaled to 100% absorption of the incident light they approximate to a constant value. The variation is due to the difficulty in measuring the initial slopes of the rate plots which are curved. (Probably due to consumption of benzophenone by side reactions). Absorbances (optical densities) were measured on the SP800.

3.19 Effect of Ester Concentration on Benzophenone Photosensitised Isomerisation

3.19(a) Solutions of methyl tiglate 1.33 to 6 x 10^{-2} molar in 0.5 x 10^{-2} molar benzophenone in cyclohexane were photolysed at 25°C and 313 nm in the semi-micro apparatus. Analysis was on PEGA at 100°. Intensity as in 3.18 = 5.61 x 10^{14} q $s^{-1}cm^{-2}$.

Time min	P.H. Angelate cm x 10^{-2}	Initial Concn. of Tiglate mol $l.^{-1}$ x 10^{2}	Time min	P.H. Angelate cm x 10^{-2}	Initial Concn. of Tiglate mol $l.^{-1}$ x 10^{2}
0	1.6	2.0	0	6.2	4.0
71	9.27	2.0	59	14.0	4.0
137	13.6	2.0	73	15.2	4.0
158	16.0	2.0	98	18.0	4.0
221	21.9	2.0	217	31.5	4.0
240	22.1	2.0	489	60.0	4.0
0	7.6	6.0	0	1.4	1.33
57	19.0	6.0	24	3.8	1.33
76	21.0	6.0	127	10.5	1.33
98	26.0	6.0	178	14.5	1.33
111	28.5	6.0	208	17.5	1.33
135	31.7	6.0	229	19.0	1.33

Rate plots for these 4 concentrations are shown in Fig. 3.38. Taken with the result from Section 3.18 these give five values of the rate of isomerisation for different concentrations of methyl tiglate.

Fig. 3.38

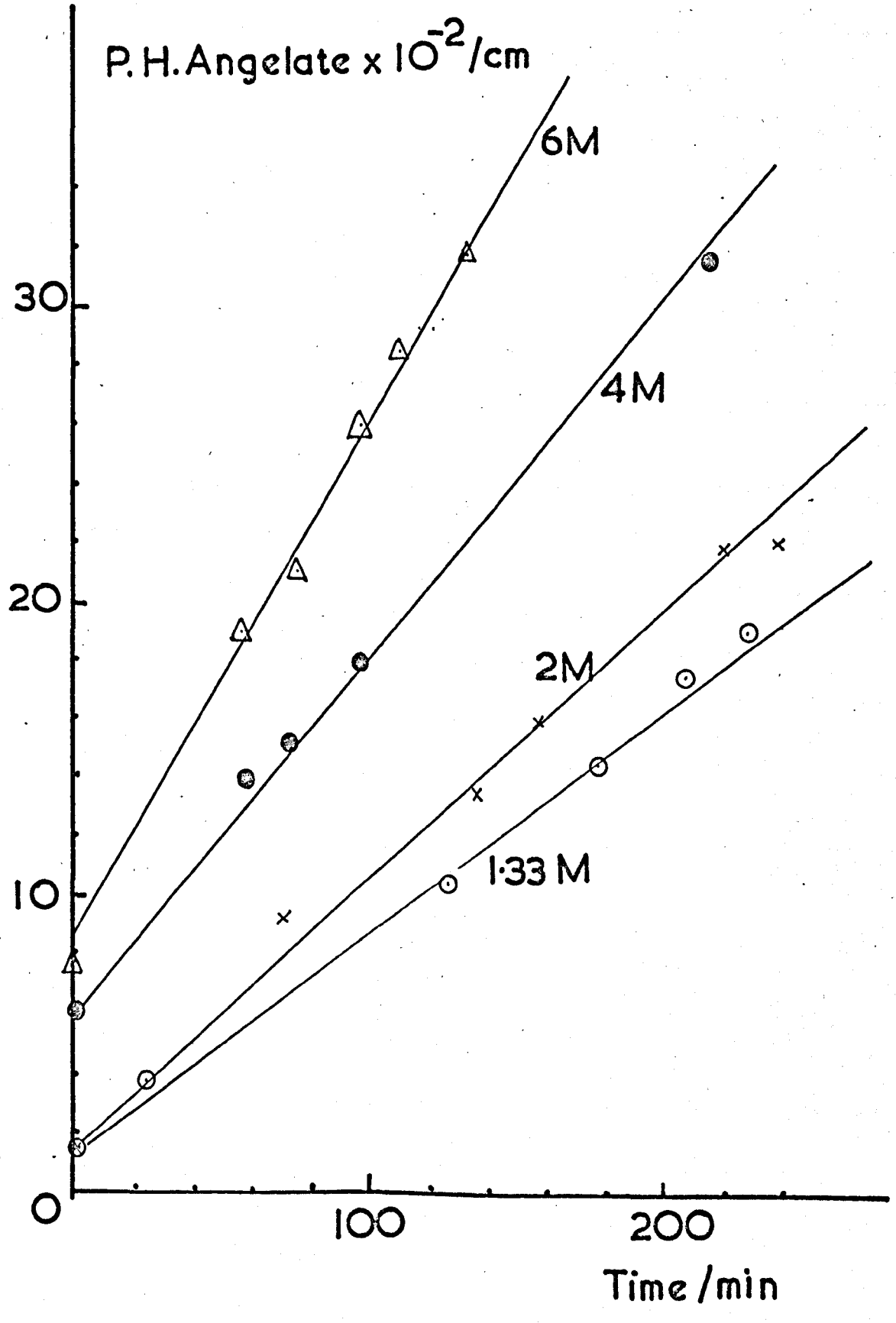

Concentration of Tiglate mol $l.^{-1}$ x 10^2	Slope cm min^{-1}	Rate of Production of Angelate mol $min^{-1}\mu l.^{-1}$ x 10^{12}
1	5.6	2.42
1.33	7.4	3.20
2	9.1	3.94
4	12.1	5.24
6	17.1	7.40

3.19(b) A similar series of experiments was carried out with methyl angelate as the starting isomer. As before the benzophenone concentration was 0.5 x 10^{-2} mol $l.^{-1}$ and the conditions were as above.

Time min	P.H. Angelate cm x 10^{-2}	Initial Concentration of Tiglate mol $l.^{-1}$ x 10^2
0	0.25	1.0
44	3.5	1.0
62	4.0	1.0
77	4.4	1.0
91	5.6	1.0
137	8.0	1.0

Time min	P.H. Angelate cm x 10^{-2}	Initial Concentration of Tiglate mol $l.^{-1}$ x 10^{2}
0	1.6	2.0
37	5.0	2.0
56	7.4	2.0
78	8.4	2.0
90	9.6	2.0
250	23.0	2.0
0	0.75	4.0
15	2.4	4.0
37	5.0	4.0
68	8.2	4.0
82	11.6	4.0
102	13.6	4.0
119	15.6	4.0
0	2.0	1.33
27	3.8	1.33
45	4.4	1.33
66.5	6.0	1.33
81	6.5	1.33
96	7.75	1.33
136.5	11.0	1.33

Time min	P.H. Angelate cm x 10^{-2}	Initial Concentration of Tiglate mol $l.^{-1}$ x 10^{2}
0	0	0.83
25	1.5	0.83
39	2.0	0.83
46	2.2	0.83
64	2.8	0.83
88	4.0	0.83
125.5	6.0	0.83

These data are shown in Fig. 3.39

Concentration of Angelate mol $l.^{-1}$ x 10^{2}	Slope cm min^{-1}	Rate of Production of Tiglate mol $min^{-1}\mu l.^{-1}$ x 10^{12}
0.826	4.7	2.88
1.0	5.8	3.56
1.33	6.7	4.10
2.0	8.9	5.45
4.0	12.6	7.72

Fig. 3.39

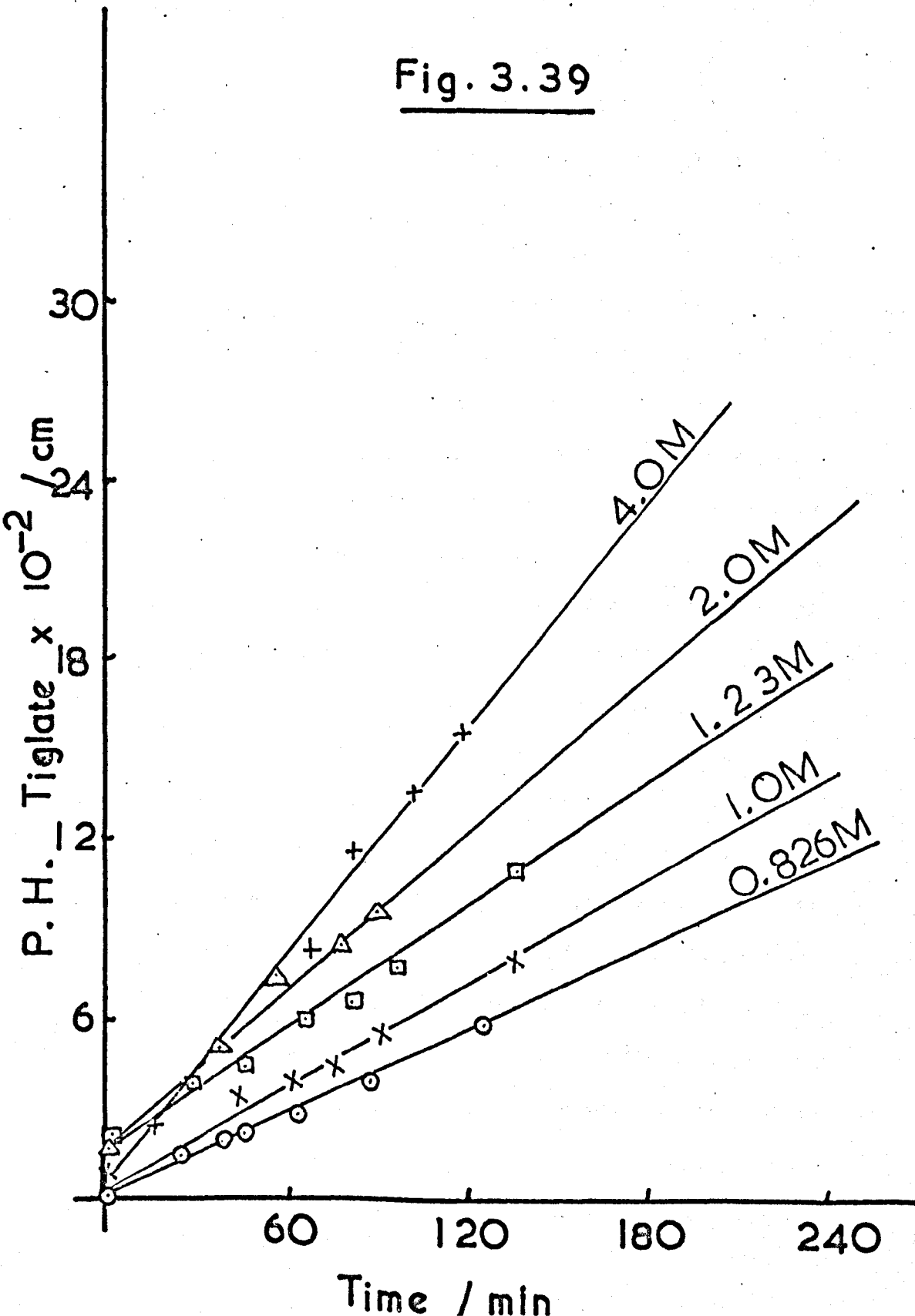
P. H. Tiglate x 10^{-2} /cm
30
24
18
12
6
60
120
180
240
Time / min
4.0M
2.0M
1.23M
1.0M
0.826M

3.20 Addition Products with Benzophenone

It was noticed that photolysis of solutions containing methyl angelate or tiglate and benzophenone as photosensitiser formed two side products which were eluted on the PEGA columns (100°C) after 9.5 and 11.5 min respectively. (Under the same conditions, the retention times of methyl angelate and tiglate are respectively 3.4 and 5.2 min). Comparing the rates of production of these peaks it seems that the first peak is formed more quickly from methyl angelate than from methyl tiglate, but that the second peak is produced at similar rates from both isomers. When the temperature was raised to 50°C it was observed that the rate of isomerisation went down and the rate of production of other products went up. A third peak with a retention time of 13.4 min appeared after long photolysis times though this was produced more slowly than the other peaks.

A reaction mixture containing these three products were analysed using the V.P.C. coupled to the mass spectrometer with an SE30 column. As all three compounds were present in minute amounts (approx. 10^{-4} mol $ml.^{-1}$) the mass marker could not be used and so the m/e values quoted may be subject to a certain error. All the three compounds had the same molecular weight of 296, corresponding to one molecule of benzophenone plus one molecule of methyl tiglate. If they are referred to as A, B and C in increasing order of retention times then the most abundant peaks in their mass spectra are listed below.

A 296, 295, 249, 210, 197, 182, 183, 184, 171, 168, 139, 125, 113,

109, 108, 107, 103, 99, 95, 94, 85, 81, 75, 67, 53, 39, 32, 28.

Base peak = 171

B 296, 295, 265, 249, 242, 210, 182, 183, 170, 167, 159, 142, 141 129, 117, 115, 111, 105, 91, 83, 77, 55, 41, 32, 28

Base peak = 105

C 296, 295, 249, 205, 183, 184, 165, 167, 153, 128, 115, 105, 89, 75, 50, 32, 28

Base peak = 183. Also many metastable peaks.

These fragmentation patterns are difficult to interpret but peak B can be assigned as the oxetane,

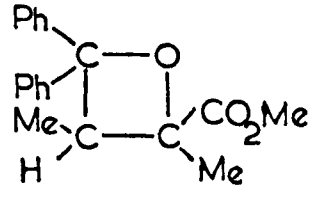

C may be the other geometrical isomer (cis-trans) of B produced by slow interconversion from B. The nature of A is obscure though it may be a Diels-Alder type adduct in which a six-membered ring is formed. Graphs of peak height against time for this peak indicate that it is formed very quickly from the angelate but is not photostable.

3.21 Quenching Experiments

Several difficulties were encountered when it was attempted to study the quenching of the direct isomerisation by the addition of compounds with low triplet energies that could act as energy acceptors from the triplet state of the ester. Since the main absorption band of the esters are so far into the blue most compounds known to possess low triplet levels absorb strongly in the same region. Commonly used quenchers such as dienes cannot be used as they have extinction coefficients at 254 nm greater than that of the esters. Most other common quenching agents also absorb at 254 nm. Simple olefins such as 1-heptene and cyclohexene were purified until transparent at 254 nm. However, when added to solutions of methyl tiglate and sealed into capillaries under vacuum neither compound quenched the isomerisation as far as could be seen. The experiment with cyclohexene was repeated in the semi-micro apparatus but again no quenching or other reaction was observed. The same was true with the reverse isomerisation.

It was shown by Porter and Wright[9] that paramagnetic ions reversibly quench the excited triplet states of many molecules. They suggested that this takes place through catalysed inter-system crossing with overall spin conservation[10] and showed that the rate constants for quenching were independent of magnetic susceptibility. These ions will also quench the excited singlet states of organic molecules but as these are generally much shorter lived in solution this will be less important. Solutions of a series of such compounds were

made up in ethanol and it was found solutions of $NiCl_2 . 6H_2O$ and $MnCl_2 . 4H_2O$ were transparent at 254 nm. Other paramagnetic species tried were either insufficiently soluble in ethanol or not transparent at this wavelength.

Quenching experiments were carried out using ethanolic solutions of Ni^{2+} and Mn^{2+} at 254 nm. The semi-micro technique had to be used and consequently conversions were low. Ethanol, being a polar solvent, was eluted from the column with considerable tailing so that the methyl angelate produced from the isomerisation of methyl tiglate was largely obscured by the solvent tail. Other columns were tried and PPG was found to be better but even with this column the measurements were very inaccurate. Ethylene glycol was tried as a solvent to remove the problem of tailing but this solvent was not sufficiently volatile to give reproducible sampling at temperatures low enough to give good separation of the isomers. Temperature programming was too lengthy to allow samples to be taken at small time intervals. The solution eventually adopted was to use the full mercury arc using only the OX7 glass as a filter. In this way, conversions high enough to be measured in ethanol despite tailing were obtained. It was unlikely that the quencher was absorbing much of the light under these conditions as the OX7 glass removed most of the very short wavelengths.

The results for Mn^{2+} quenching under these conditions are given below.

Solutions 1.67×10^{-2} mol litre^{-1} methyl tiglate, photolysed with full arc at 25°C in semi-micro apparatus. Analysis on PEGA at

100°C. 1 microlitre samples.

Fig. 3.40

Time min	P.H. Angelate cm x 10^{-2}	Concentration of Mn^{2+} mol $l.^{-1}$
0	0	0
11.5	3.4	0
25	9.5	0
30	11.5	0
38.5	14.0	0
47	16.0	0
55	20.0	0
0	0	0.205
24	6.5	0.205
38	10.0	0.205
51.5	14.0	0.205
76	19.0	0.205
82	24.7	0.205
96	25.9	0.205
0	0	0.103
14	4.0	0.103
32	8.5	0.103
68	17.5	0.103
76	21.5	0.103
82	22.5	0.103
90	24.75	0.103

Fig. 3.40 continued

Time min	P.H. Angelate cm x 10^{-2}	Concentration of Mn^{2+} mol $l.^{-1}$
0	0	0.0164
29	9.0	0.0164
35	10.2	0.0164
44.5	13.8	0.0164
53	15.7	0.0164
60	17.6	0.0164
80.5	24.9	0.0164
101	30.5	0.0164

From Fig. 3.40

Concentration of Mn^{2+}, Molar	Slope cm min^{-1}	Rate of Production of angelate mol $min^{-1}\mu l^{-1} \times 10^{-11}$
0	37.0	1.60
0.0164	30.6	1.33
0.103	27.4	1.19
0.205	26.8	1.16

When the semi-micro apparatus was used with a stream of air bubbling through the solution instead of oxygen a similar degree of quenching was observed. Same solution of tiglate as above, analysis on PEGA at 100°C.

Fig.3.40

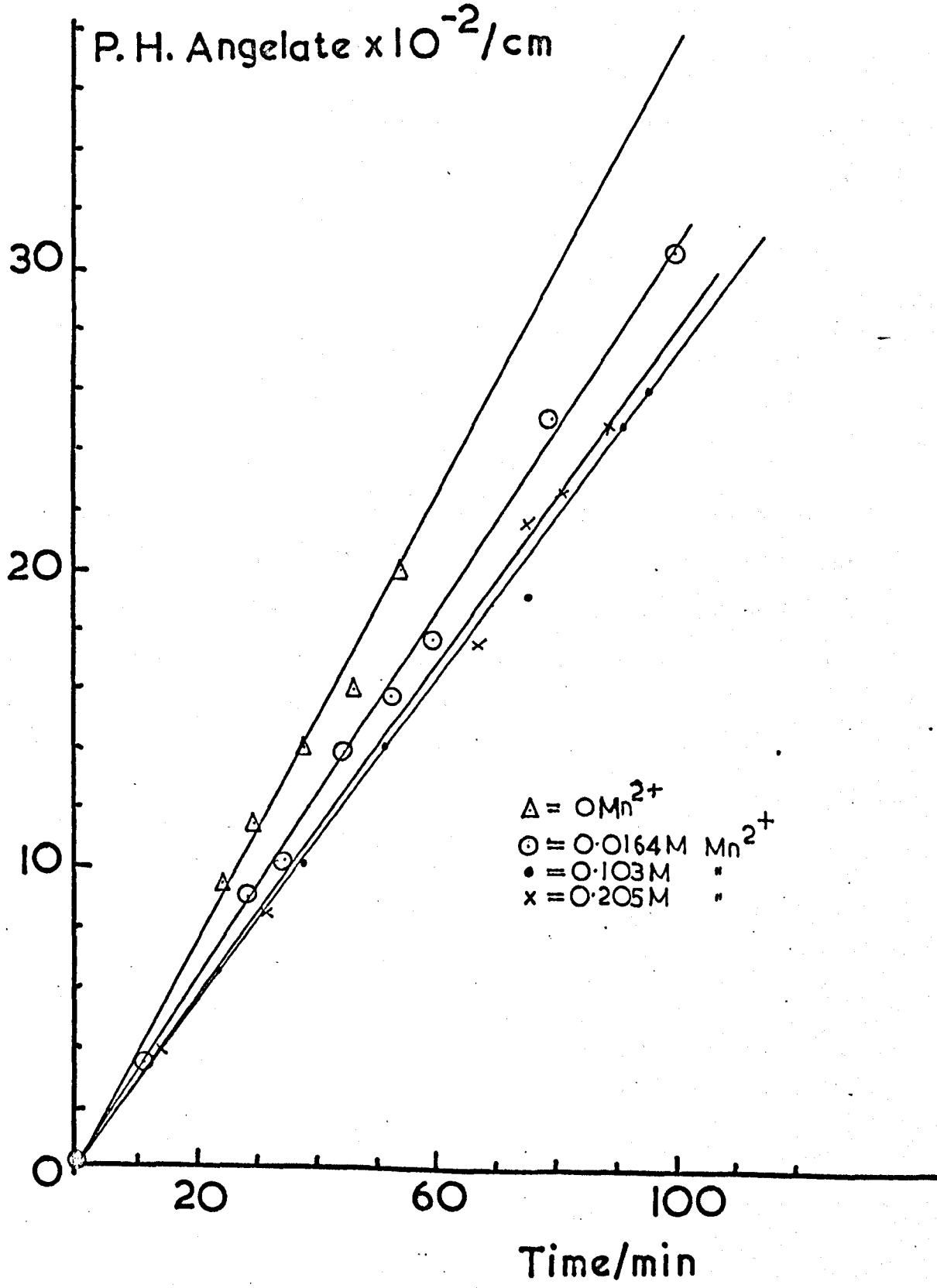
P. H. Angelate x10^{-2}/cm
30
20
10
0
20
60
100
Time/min
△ = 0 Mn^{2+}
⊙ = 0·0164 M Mn^{2+}
• = 0·103 M "
x = 0·205 M "

Time min	P.H. Angelate cm x 10^{-2}
14	3.6
22	6.0
30	6.5
49	13.0
83	21.5
96.5	27.0

This gives a slope of 26.4 cm min^{-1} which is about the same as the limiting quenching observed with manganese ions above.

Using 254 nm light and nickel chloride as quencher the only reliable result obtained was that for a 4.16 x 10^{-2}M solution of methyl tiglate 1.84 x 10^{-2}M in $NiCl_2$ the quantum yield was reduced to 0.068 as compared with 0.090 with no added nickel.

3.22 Summary of Results

1. The quantum yield of methyl tiglate to angelate isomerisation was measured as 0.090 ± 0.003 in cyclohexane solution at 25°C and 254 nm. It was found to be independent of initial ester concentration and change of solvent. Ø increased by 9.7% from 26°C to 50°C. There was no photolysis at 313 nm.

2. The quantum yield of isomerisation for methyl angelate to tiglate was measured as 0.032 at 35°C and 254 nm.

3. The β,γ-unsaturated isomer was produced as a product of photolysis in the direct isomerisation but not on photosensitised isomerisation. Methyl angelate was established as precursor for this product. Deuterium was incorporated on photolysis in MeOD.

4. The isomerisation was photosensitised by carbonyl compounds with high triplet energies: acetone, acetophenone, benzophenone and 9,10-anthraquinone. No sensitisation was observed with biphenyl, benzil, naphthalene and pyrene. The composition of the photostationary state mixture was 50% methyl tiglate using acetone and acetophenone as photosensitisers and 53% tiglate using benzophenone. Photosensitisation by benzophenone and anthraquinone was accompanied by compound formation.

5. The quantum yield of photosensitised isomerisation using benzophenone was found to be independent of benzophenone concentration but increased with increasing ester concentration (q.v.).

6. The triplet energy of methyl tiglate was estimated at 300 kJ mol^{-1} from the absorption spectrum in ethyl iodide.

7. Thermal isomerisation was extremely slow at 175°C. At 303°C, 7% conversion from tiglate to angelate was observed after 92h heating in sealed tubes.

8. Photoisomerisation from tiglate to angelate at 254 nm was partially quenched by oxygen and paramagnetic ions. Using the full medium pressure mercury arc, the limiting degree of quenching was measured as 28% using oxygen at atmospheric pressure and 0.2 mol litre^{-1} Mn^{2+}.

REFERENCES TO CHAPTER 3.

1. R.M. Silverstein and G.C. Bassler 'Spectrometric Identification of Organic Compounds', Wiley, New York, (1963).
2. 'Organic Electronic Spectral Data', Vol V, (Ed. J.P. Phillips, R.E. Lyle and P.R. Jones) Interscience, New York, (1960).
3. M. Calvin and H.W. Alter, J.Chem.Phys., 19, 768, (1951).
4. P. Borrell and J. Sedlar, J.Sci.Instrum., 2, 439, (1969).
5. F.S. Wettack and W.A. Noyes, J.Amer.Chem.Soc., 90, 3901, (1968).
6. G.S. Hammond, S.C. Shim and S.P. Van, Mol.Photochem, 1, 89, (1969).
7. J.G. Calvert and J.N. Pitts 'Photochemistry' Wiley, New York, (1966) pp. 297 - 298.
8. N.J. Turro, J.C. Dalton and D.S. Weiss in 'Organic Photochemistry' Vol.2 (Ed. O.L. Chapman), M. Decker, New York, (1969), p.1 - 63.
9. G. Porter and M.R. Wright, Disc.Faraday Soc., 27, 18, (1957).
10. A. Kearwell and F. Wilkinson in 'Transfer and Storage of Energy by Molecules', Vol.I (Ed. G.M. Burnett and A.M. North) Wiley, London, (1969) p.144.

4. QUENCHING OF PHOTOELIMINATION: RESULTS

4.1 U.V. Absorption Spectra

The U.V. absorption spectra of the three ketones studied are shown in Fig. 4.1. The spectra shown are all taken in cyclohexane as solvent. The relevant extinction coefficients are tabulated below.

Compound	λ max. nm	ε max. $l.mol^{-1}cm^{-1}$	ε 313 $l.mol^{-1}cm^{-1}$
2-pentanone	282	19.8	5.35
2-octanone	282.5	21.0	5.92
4-methyl-2-pentanone	283.5	19.3	6.33

The spectra were also taken in benzene solution to try and detect any differences.

Compound	λ max. nm	ε max. $l.mol^{-1}cm^{-1}$	ε 313 $l.mol^{-1}cm^{-1}$
2-pentanone	282	22.6	5.13
2-octanone	282.5	21.8	4.96
4-methyl-2-pentanone	284	22.0	6.08

Fig. 4.1

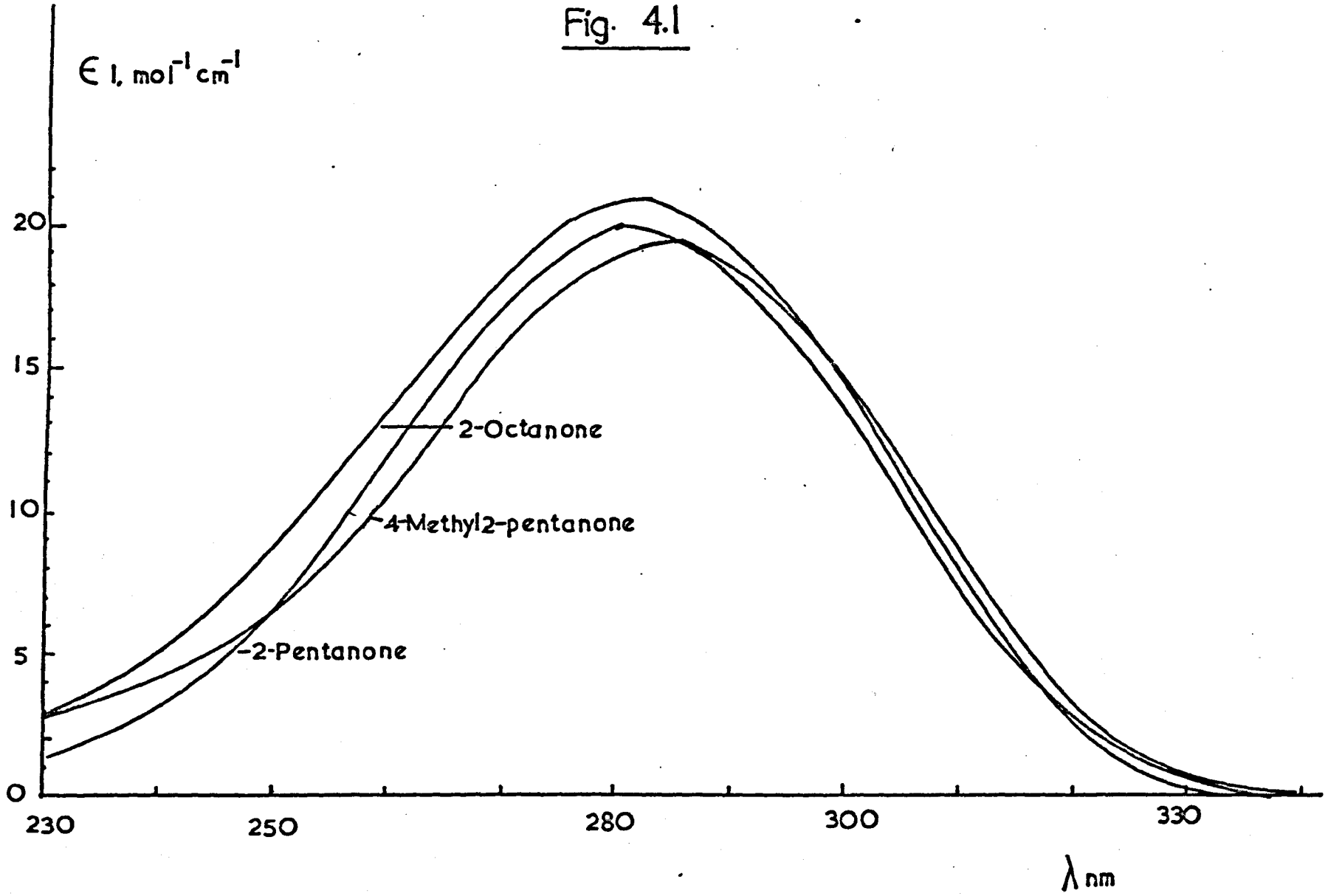
ε l. mol⁻¹ cm⁻¹
20
15
10
5
0
2-Octanone
4-Methyl2-pentanone
2-Pentanone
230
250
280
300
330
λ nm

The effect of changing the solvent from cyclohexene to benzene is to 'sharpen' the peak corresponding to the n-π^* transition reducing the absorption at 313 nm whilst increasing that at the maximum. The position of the maximum remains unchanged. If these hydrocarbon solvents are replaced by a more polar solvent the absorption band is shifted to shorter wavelengths as with all n-π^* transitions. For 2-pentanone the size of this shift is 7 nm in ethanol and 6.5 nm for n-butanol.

4.2 Photolysis of Pure Liquid Ketones

A series of aliphatic ketones containing γ-hydrogen atoms was photolysed at 313 nm and 25°C in the pure liquid state. The semi-micro apparatus was used and acetone production was followed by gas chromatography using one microlitre aliquots. The light source used was the high pressure mercury lamp together with the OX7 glass/potassium chromate solution filter. (See Sections 2.3 and 2.4). The results are tabulated below.

Ketone	Time min	P.H. Acetone cm x 10^{-2}	Ketone	Time min	P.H. Acetone cm x 10^{-2}
A	0	4.5	D	0	20.5
A	15.5	72	D	10	43.0
A	23.5	108	D	22	77.0
A	39.5	200	D	37	120.0
A	51	280	D	129.5	385
B	0	28	E	0	3.0
B	13.5	51	E	20	72
B	38	92	E	71	190
B	61	115	E	79	220
B	73	135	E	101	275
B	125.5	215	E	158	407.5
			E	161.6	425
C	0	14			
C	18	85			
C	44	210			
C	58	272.5			
C	95.5	437.5			

Fig. 4.2

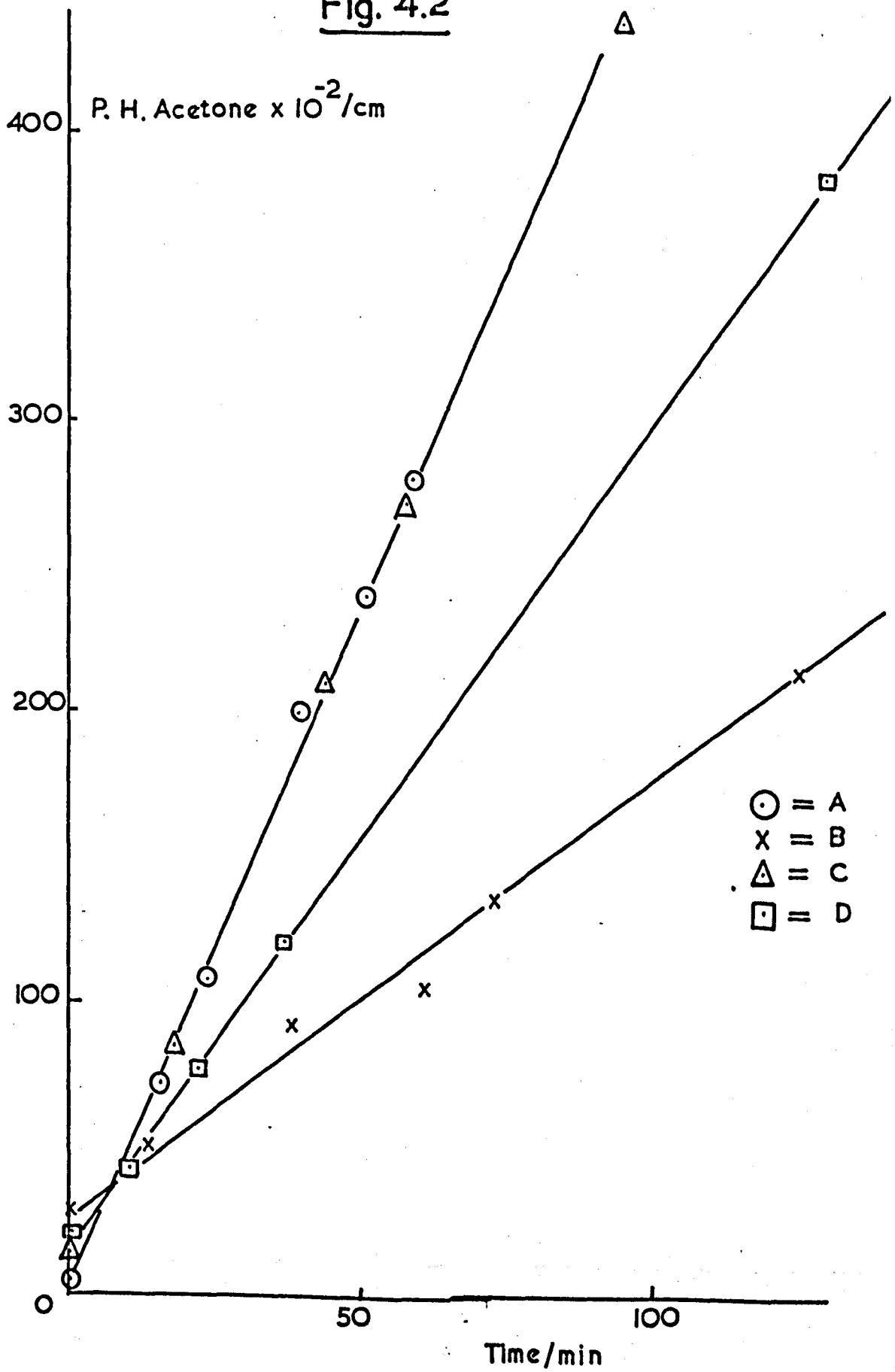

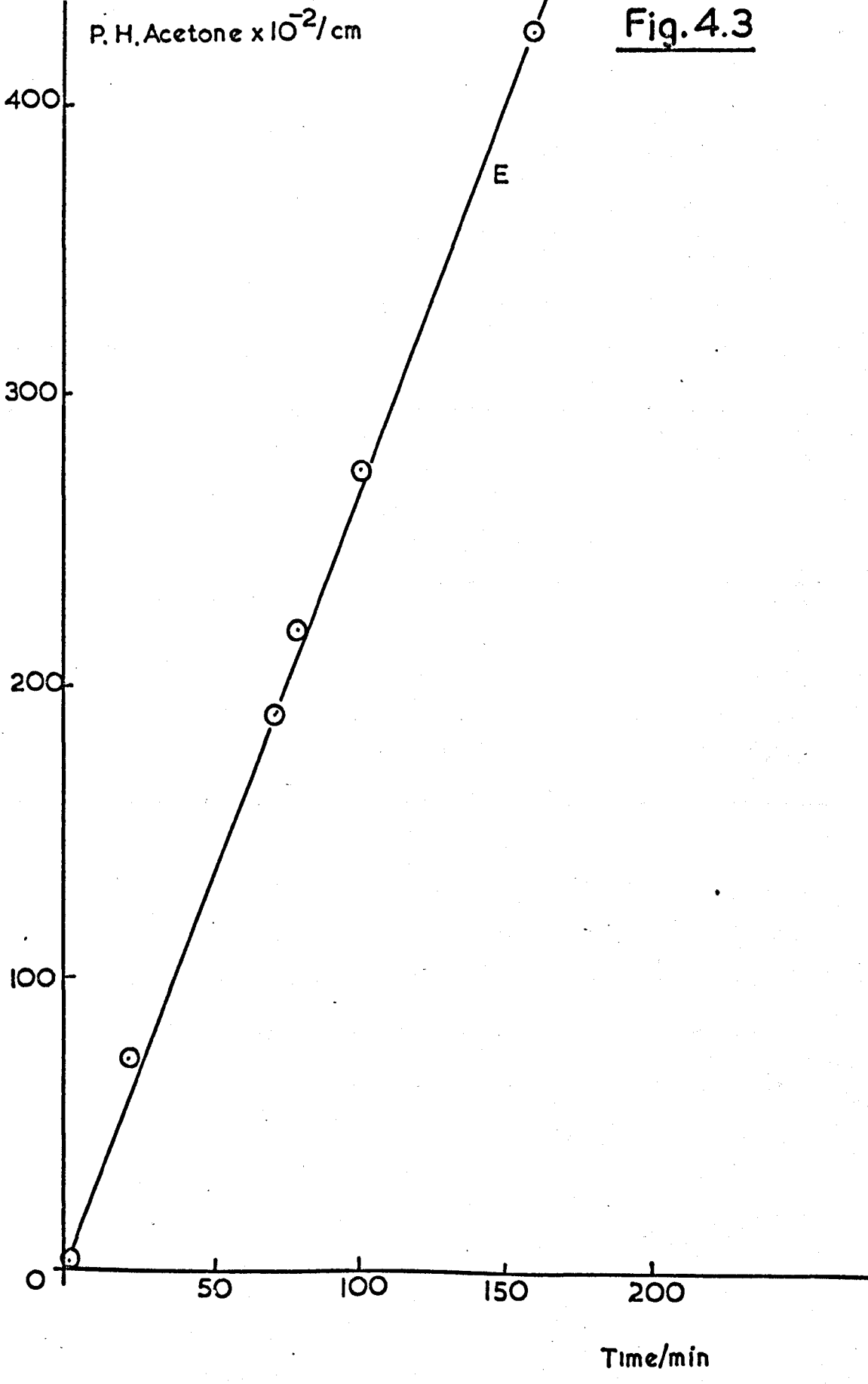

Fig. 4.3

A is 2-pentanone, B is 2-hexanone, C is 4-methyl-2-pentanone, D is 2-heptanone and E is 2-octanone. Analysis of E was on PPG at 100°C. For the others analysis was on APL at 130°C. The results are shown in Figs. 4.2, 4.3 and the slopes are tabulated below.

Compound	Slope, cm min^{-1}	Rate of Acetone, Production, mol $microlitre^{-1}$ min^{-1} x 10^{10}	Intensity q $min^{-1}cm^{-2}$ x 10^{-17}	ø
A	466	2.15	5.17	0.250
B	150	0.692	5.08	0.082
C	444	2.05	5.06	0.244
D	284	1.31	5.05	0.156
E	262	1.57	5.01	0.189

The quantum yields quoted are based on the value for 2-pentanone determined in Section 4.3. The drop in intensity with time is as estimated in Section 4.4. The quantum yield of D was measured again independently with the calibrated medium pressure lamp and gave a value of 0.191. The average of the two values is 0.173.

4.3 Effect of Solvent on Quantum Yield of Photoelimination from 2-Pentanone

As considerable variation exists between different literature values it was decided to measure the quantum yield of acetone formation from 2-pentanone in various solvents. The experiments were carried out using the semi-micro apparatus and the medium pressure mercury lamp in combination with the 313 nm interference filter. The light intensity was measured by ferrioxalate actinometry at three stages during the course of the experiments and was found to fall off linearly. The fairly rapid decay of this usually stable source was attributed to the fact that the arc tube was new, having just been replaced. Intensities for intervening experiments were interpolated from these measured intensities.

As most of the solutions used in these experiments did not absorb all light at 313 nm, the optical density of each experimental solution was measured separately and the percentage light absorption calculated. It was assumed that all light passed by the interference filter was of wavelength 313 nm. In fact some 303 nm light as well as small amounts of 298 and 366 nm light were transmitted by the filter when used with this source, as was found in the experiments outlined in Section 2.3(d). No attempt was made to correct for this effect as it was thought that the shorter wavelengths absorbed strongly would effectively compensate for the longer wavelengths which were not absorbed by the experimental solutions, although all were measured with the ferrioxalate

actinometer.

All solutions were 0.1M in 2-pentanone and were photolysed at 25°C. 1 microlitre aliquots were analysed by gas chromatography. The solution in t-butanol was analysed on a DNP column at 60°C whilst the others were analysed on APL at 130°C. The experimental results are set out below and are shown in Figs. 4.4 and 4.5.

Solvent	Time, min	P.H. Acetone cm
Cyclohexane	0	63
	14.5	267
	32	515
	51	736
	61	828
	68	900
	78	1006
	169.5	1660
Benzene	0	54
	10	86
	42	210
	61	278
	101.5	415
	117	462
	131	520
	167	635
	196	745

Solvent	Time, min	P.H. Acetone cm
t-butanol	0	0
	34	140
	43.5	180
	57	240
	72	300
	86.5	340
	95	380
n-butanol	0	0
	34	408
	51	646
	83.5	1052
	92	1136
iso-Octane	0	10
	9	246
	15	398
	32.5	836
	42	1054
	52.5	1386
	61	1500
2-pentanone	0	130
	21.5	985
	38	1600
	54	2360
	63	2720
	92	4215
	117	5200

Fig. 4.4

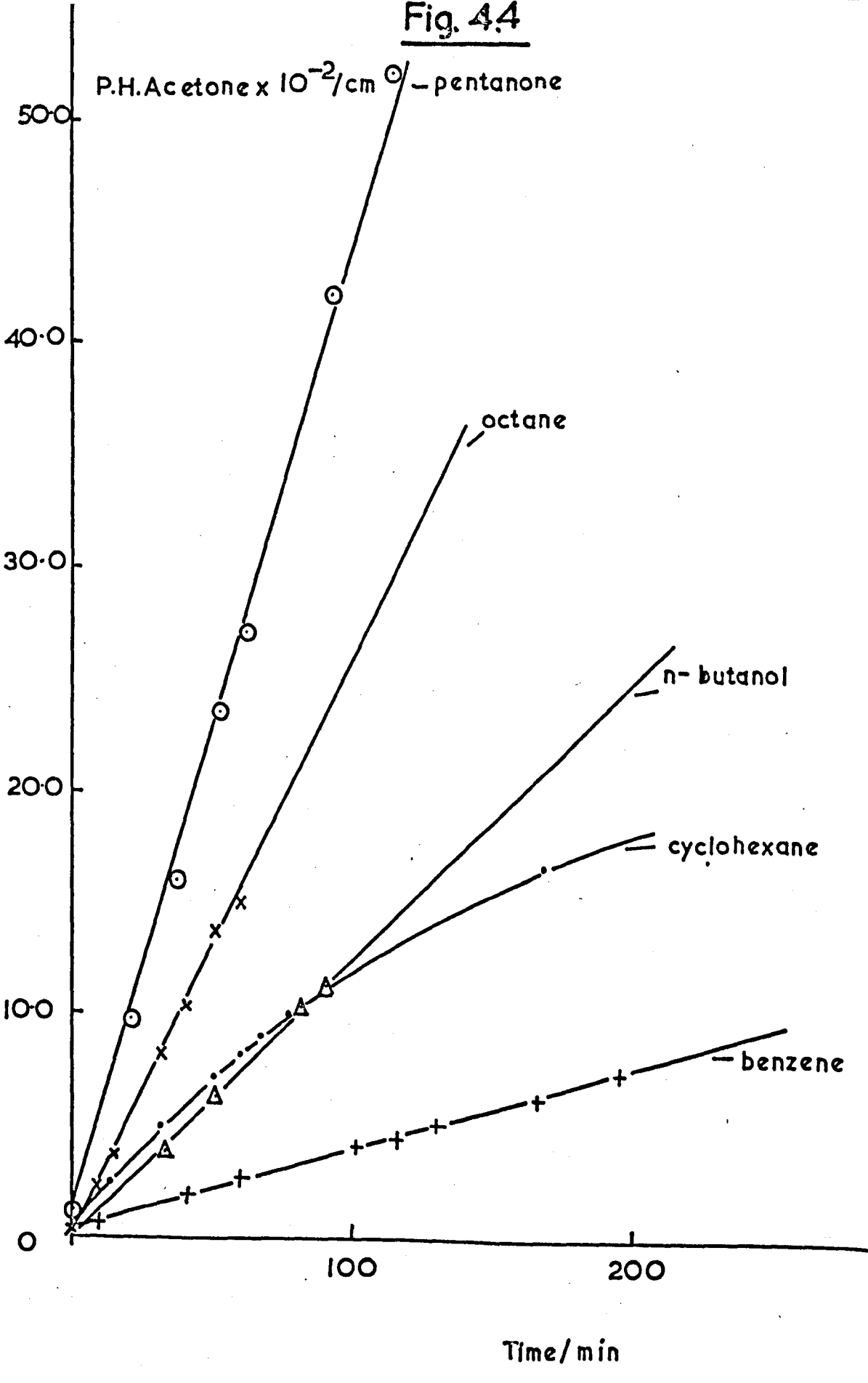
P.H. Acetone x 10^{-2}/cm
50·0
40·0
30·0
20·0
10·0
0
100
200
Time/min
⊙ – pentanone
octane
n- butanol
cyclohexane
benzene

Fig. 4.5

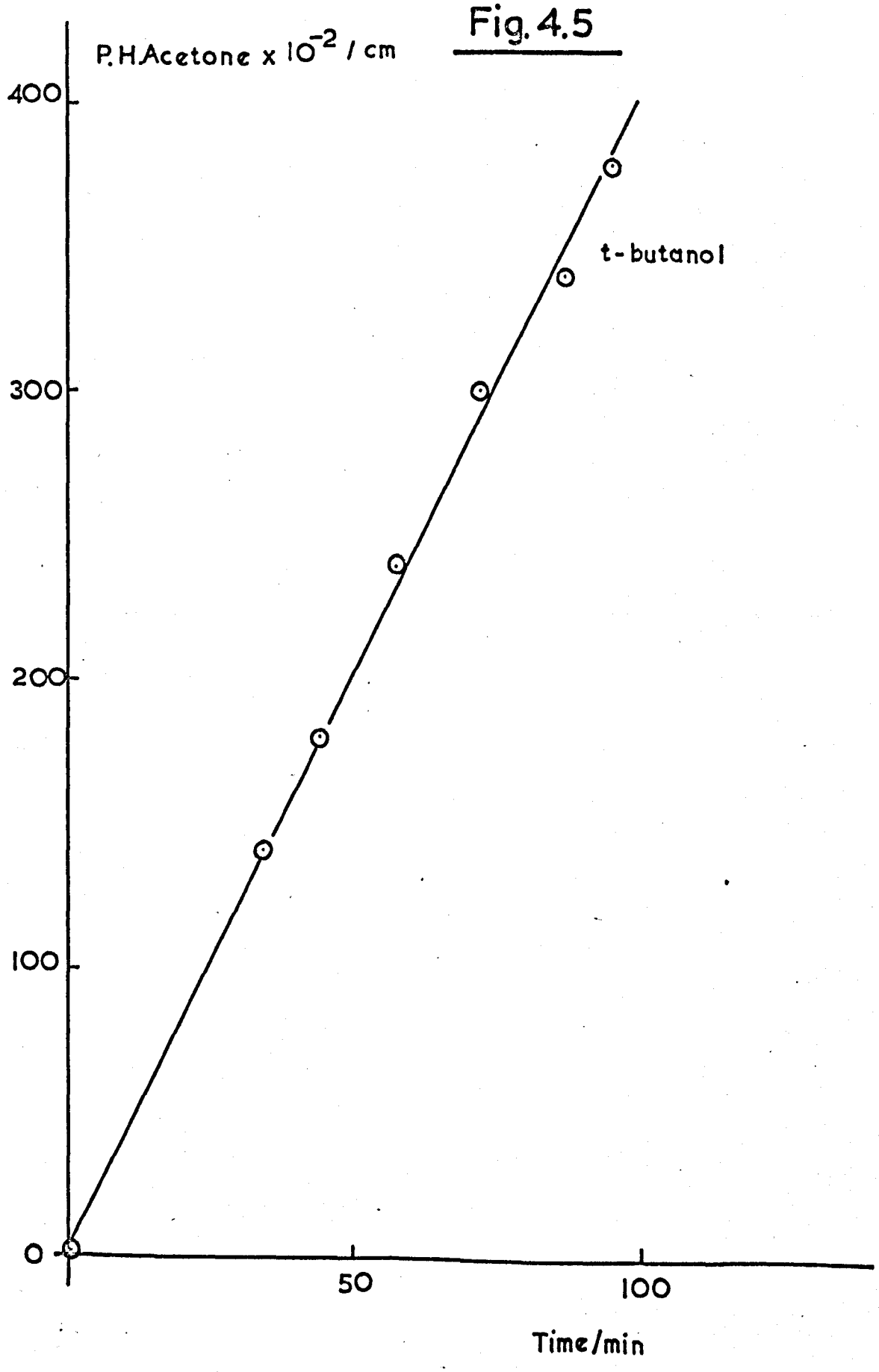

Solvent	Slope, cm min^{-1}	Rate, molecules min^{-1} μl^{-1} x 10^{-13}	% Light absorbed at 313 nm	Incident light intensity q $s^{-1}cm^{-2}$ x 10^{-14}	Light absorbed q $s^{-1}cm^{-2}$ x 10^{-14}
2-pentanone	44.4	1.47	100	9.81	9.81
iso-octane	25.2	0.831	66.9	9.19	6.14
n-butanol	12.4	0.410	46.5	9.48	4.40
cyclohexane	13.35	0.441	71.2	9.95	7.09
benzene	3.55	0.117	66.8	9.74	6.50
t-butanol	4.04	0.753	47.6	9.08	4.32

The percentage light absorption is lower in the case of the butanols due to the 'blue shift' of the n-π^* transition in these more polar solvents. The quantum yields are tabulated below.

Solvent	Ø Acetone
2-pentanone	0.250
iso-octane	0.226
n-butanol	0.155
cyclohexane	0.104
benzene	0.030
t-butanol	0.291

In separate experiments the same quantum yield was measured in ethanol and methanol. The light intensity was estimated by relative measurements. It was not possible to obtain a value in methanol as the points were extremely scattered. In ethanol the value was estimated as 0.12.

The value of $\phi = 0.250$ in 2-pentanone is not consistent with the value of 0.123 found by Sedlar (See Section 3.6) at the same wavelength but is nearer the quoted values in other solvents (See Chapter 5.). This being the case, the experiment was repeated and a value of 0.25 was again found. A repeat of the experiment at 254 nm produced a similar result to that found before in Section 3.6 so that there seems to be a wavelength effect operating in solution. This was not investigated further in the present work.

The value for benzene appears to be low compared to the other solvents. It was suggested that this was due to aromatic impurities acting as triplet quenchers. However, mass spectral and U.V. analysis showed no trace of any impurity. As the benzene was taken as a middle cut from the rectification of 'analar' material impurities were unlikely to be present in any significant amounts.

Experimental note

n-Butanol was Hopkin and Williams Ltd., G.P.R. grade rectified three times collecting at 117°C. No acetone or isopropanol were present in the purified compound and it was transparent down to 250 nm.

t-Butanol came from the same source and was contaminated with benzene and other alcohols. It was rectified twice on the Towers column and the middle fraction boiling at 82°C was collected. This was spectroscopically pure but still contained traces of isomeric alcohols. These were not removed as they were eluted after the tertiary-butanol on the DNP column used and represented about 1% of the pure compound. Although the pure t-butanol freezes at 26°C, the pentanone solution in butanol remained a liquid at the experimental temperature. As both butanols formed viscous solutions they were de-oxygenated with pure nitrogen for longer periods before starting the photolysis.

4.4 Light Intensity of High Pressure Lamp

No direct measurement of the light intensity of the high pressure lamp and chromate filter combination were made due to experimental difficulty. Instead the light intensity were calculated by comparing rates obtained with this arrangement with those obtained for the same systems using the medium pressure lamp and interference filter. In this latter case the intensity was measured by ferrioxalate actinometry. Repeated measurements of the rate of acetone formation from 0.1 Molar 2-pentanone in benzene and in cyclohexane showed that the high pressure lamp was subject to a drop in output with time. This depreciation was estimated as 23.8% over the 160 hours of use during the course of these experiments. The fall off was assumed to be linear so that the intensity used for each experiment could be expressed as a percentage of the intensity at the start of the series (Io). By comparison with the results obtained with the medium pressure lamp this intensity was calculated as 6.57×10^{17} quanta $min^{-1}cm^{-2}$. Using this value the rates obtained with the high pressure lamp could be turned into quantum yields knowing the initial concentration of absorbing species and its extinction coefficient.

4.5 Quenching of Photoelimination in 2-Pentanone at 313 nm.

Experiments were carried out on the quenching of the photoelimination reaction in 2-pentanone both in benzene and cyclohexane using cyclohexene as quencher. The rate of acetone formation was used to monitor the photoelimination whilst the rate of ketone consumption was used to monitor the total photoreaction. The chromatographic conditions used did not allow the following of any cyclobutanol products. All experiments were carried out under a stream of nitrogen in the semi-micro apparatus so that it was not possible to follow ethylene formation. The temperature in all cases was 25°C and the solutions were thoroughly de-oxygenated before each run.

In order to get appreciable depletion of the starting ketone it was found necessary to increase the light intensity as much as possible. This was done by using the 500W high pressure mercury lamp and potassium chromate filter. Even with this arrangement the diminution of starting material was small and many points had to be obtained for each run to average out the errors inherent in sampling. Another source of error was introduced by the slow depletion of solvent caused by the nitrogen flow. Such losses were small except for runs of very long duration and could be corrected for by scaling the ketone peaks to the peak height of constant small impurities observable at the high sensitivities used. Solvent loss placed a limit on the length of the experiment of approx. 5h. The light intensity was calculated as explained in Section 4.4.

It should be noted that small concentrations of acetone were nearly always present in the solutions used for photolysis. The amount varied from run to run as acetone was slowly formed in the samples of purified ketones and not all runs were done at the same time. The concentration of acetone present was small enough to be negligable compared to that produced by photolysis and the ketones were periodically redistilled to remove it. This explains why rate plots for acetone do not always start at the origin.

4.5(a) Oxygen quenching

The effect of oxygen on the photoelimination was ascertained by replacing the nitrogen stream used normally with a fast flow of pure oxygen (10ml min^{-1}). This was done in the middle of a run with pure liquid pentanone. The rate of acetone formation dropped to zero under these conditions.

4.5(b) Quenching by cyclohexene in benzene solution

The experimental results are set out below and in Figs. 4.6 and 4.7. Analysis was on APL at 130^{o} with 1 microlitre aliquots. Measured sensitivities were 0.461×10^{-12} mol cm^{-1} for acetone and 0.386×10^{-12} mol cm^{-1} for 2-pentanone.

Fig.4.6

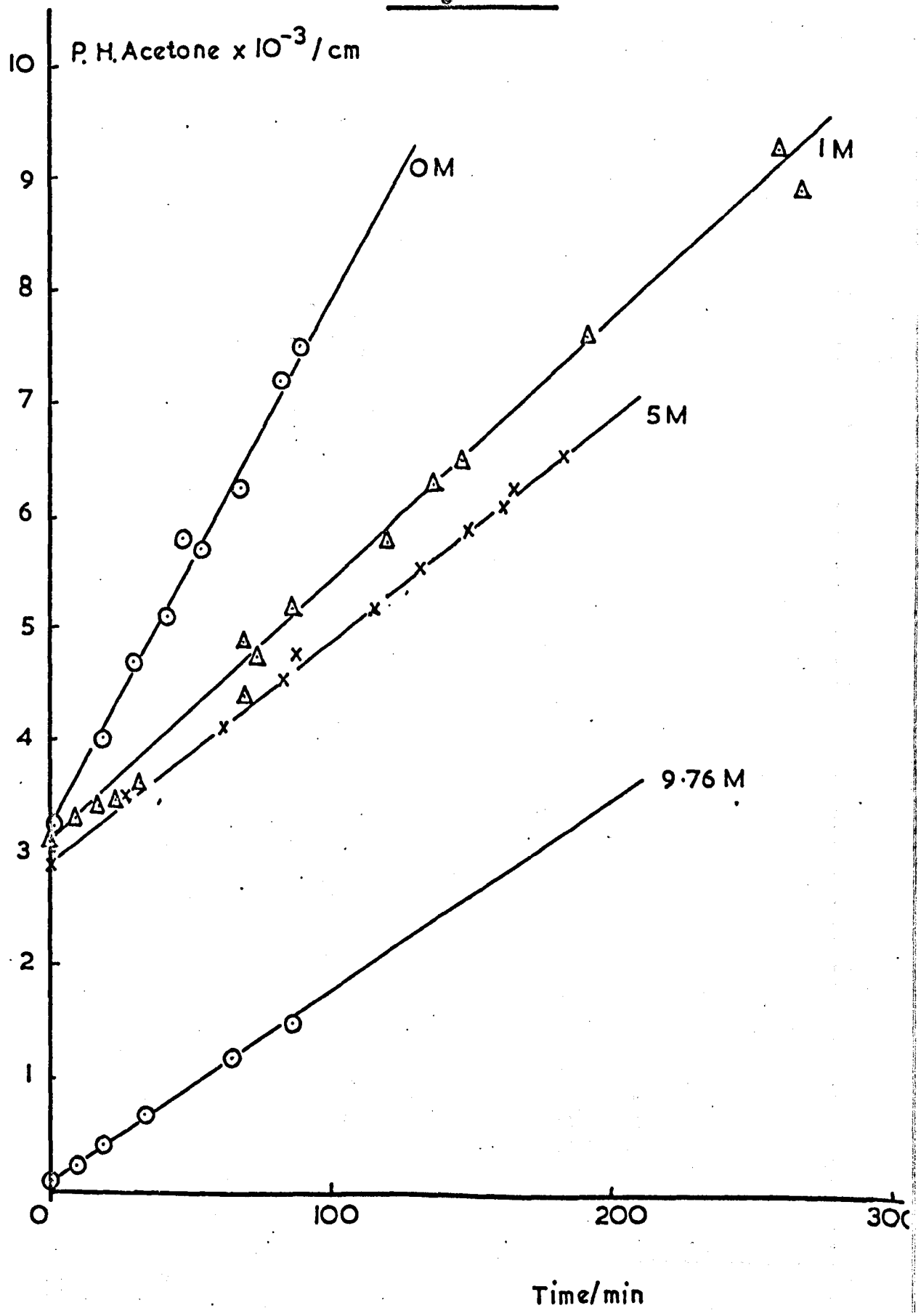
P. H. Acetone x 10^{-3} / cm
10
9
8
7
6
5
4
3
2
1
0
100
200
300
Time/min
0M
1M
5M
9·76 M

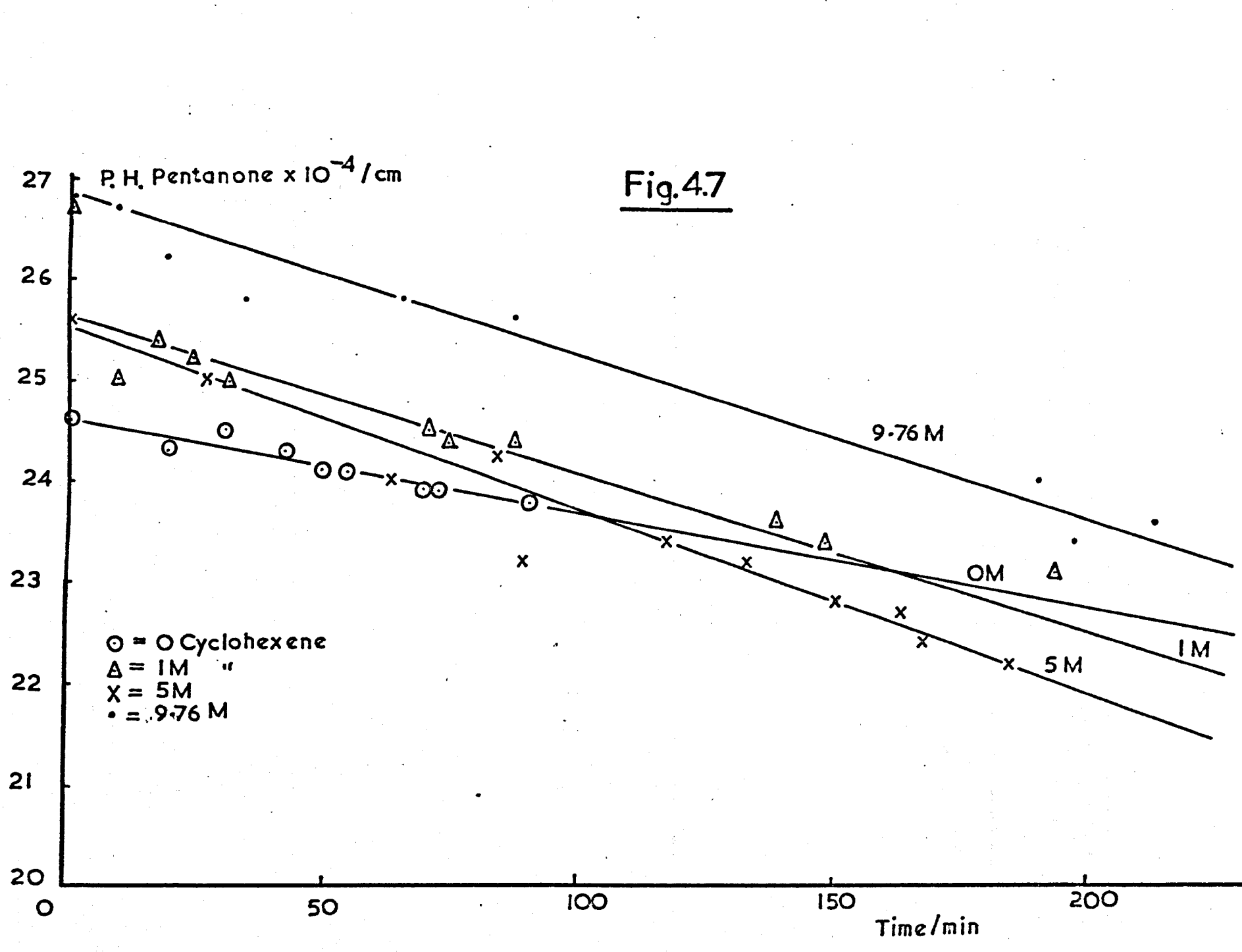
Fig.4.7
P. H. Pentanone x 10⁻⁴ / cm
27
26
25
24
23
22
21
20
0
50
100
150
200
Time/min
9·76 M
OM
1M
5M
⊙ = 0 Cyclohexene
Δ = 1M "
X = 5M
• = 9·76 M

Concentration of Cyclohexene, mol litre^{-1}	Intensity % Io	Time, min	Peak Height of Acetone, cm x 10^{-3}	Peak Height of 2-pentanone cm x 10^{-4}
0	88.3	0	3.25	24.6
		19	4.0	24.3
		30	4.7	24.5
		42	5.1	24.3
		49	5.8	24.1
		54	5.7	24.1
		69	6.25	23.9
		83	7.2	23.9
		90	7.5	23.75
5.0	89.5	0	2.9	25.6
		27	3.5	25.0
		62.5	4.15	24.0
		83.5	4.55	24.25
		89	4.8	23.2
		117	5.2	23.4
		133	5.55	23.2
		150.5	5.9	22.8
		163	6.1	22.7
		167	6.25	22.4
		184.5	6.55	22.2
1.0	91.1	0	3.1	26.7
		9	3.3	25.0
		17	3.4	25.4
		24	3.45	25.2
		31	3.6	25.0
		70	4.9	24.5
		74	4.75	24.4
		87	5.2	24.4

Concentration of Cyclohexene, mol litre^{-1}	Intensity % Io	Time, min	Peak Height of Acetone cm x 10^{-3}	Peak Height of 2-pentanone cm x 10^{-4}
1.0	91.1	121	5.8	-
continued		138.5	6.3	23.6
		148	6.5	23.4
		193	7.6	23.1
		262	9.3	23.8
		265	8.9	21.6
9.76 .	90.0	0	0.10	26.8
		9	0.22	26.7
		19	0.42	26.2
		34.5	0.70	25.8
		65	1.20	25.8
		87	1.50	25.6
		190	2.50	24.0
		197	-	23.4
		213	2.75	23.6

The best values of the slopes are set out below:

Cyclohexene mol litre^{-1}	Slope, Acetone cm min^{-1}	Slope, Pentanone cm min^{-1}	% Io
0	47.0	92.5	88.3
1.0	24.5	156	91.1
5.0	20.0	162	89.5
9.76	17.0	161	90.0

4.5(c) Quenching by cyclohexene in cyclohexane

A similar series of experiments to those in (b) were carried out using cyclohexane as co-solvent to investigate the differences in the reaction in the two solvents. Three different column conditions were tried: APL at 130° as above, PPG at 100° and at 80°. Sensitivities for these last two were measured as 0.60 and 0.951 x 10^{-12} mol cm^{-1} for acetone and 1.10 and 1.862 x 10^{-12} mol cm^{-1} for 2-pentanone respectively. The results for 1 µl aliquots are set out below and in Figs. 4.8 - 4.10.

Fig. 4.8

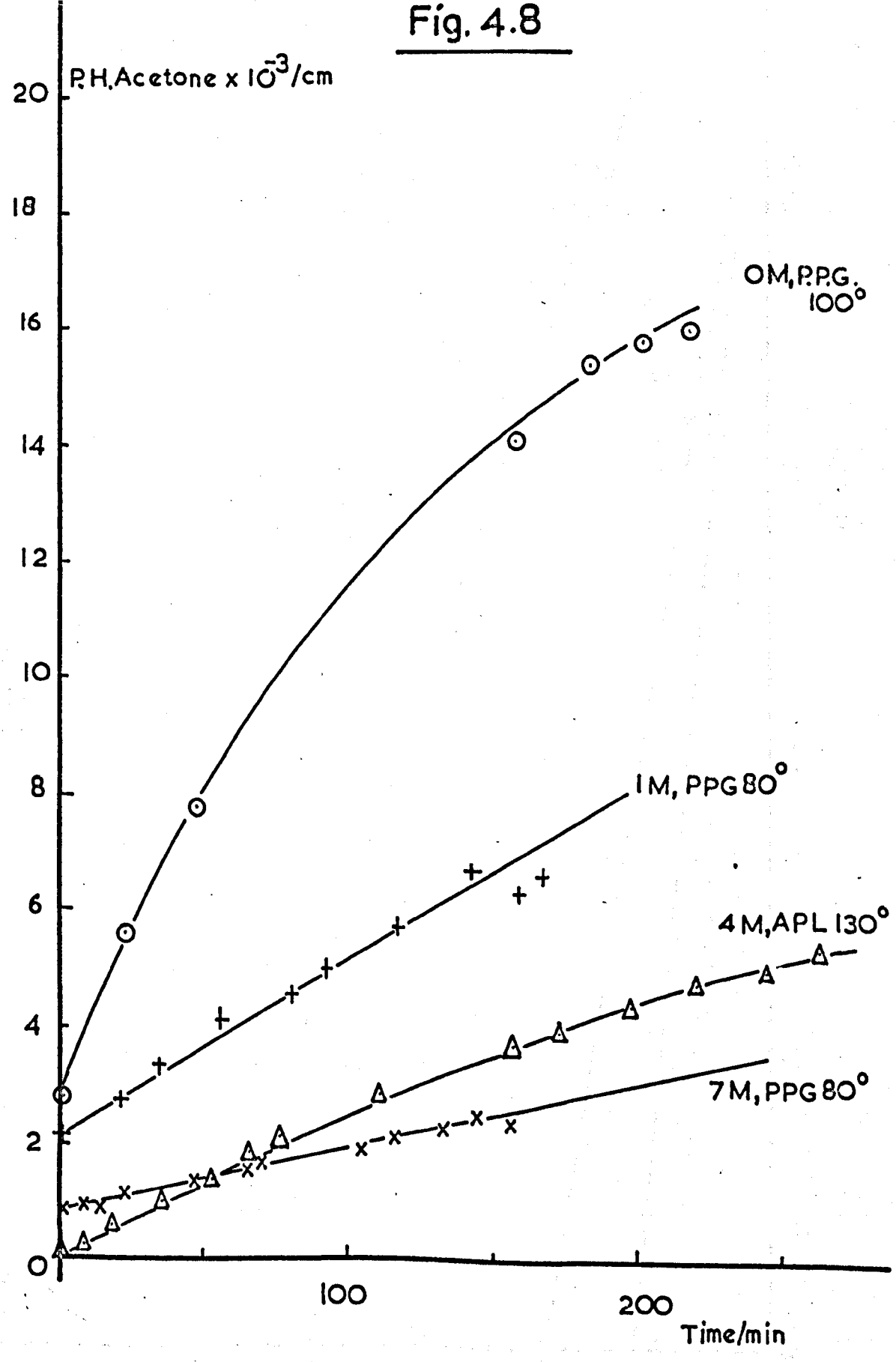
P.H.Acetone x 10^{-3}/cm
20
18
16
14
12
10
8
6
4
2
0
100
200
Time/min
OM, P.P.G. 100°
1M, PPG 80°
4M, APL 130°
7M, PPG 80°

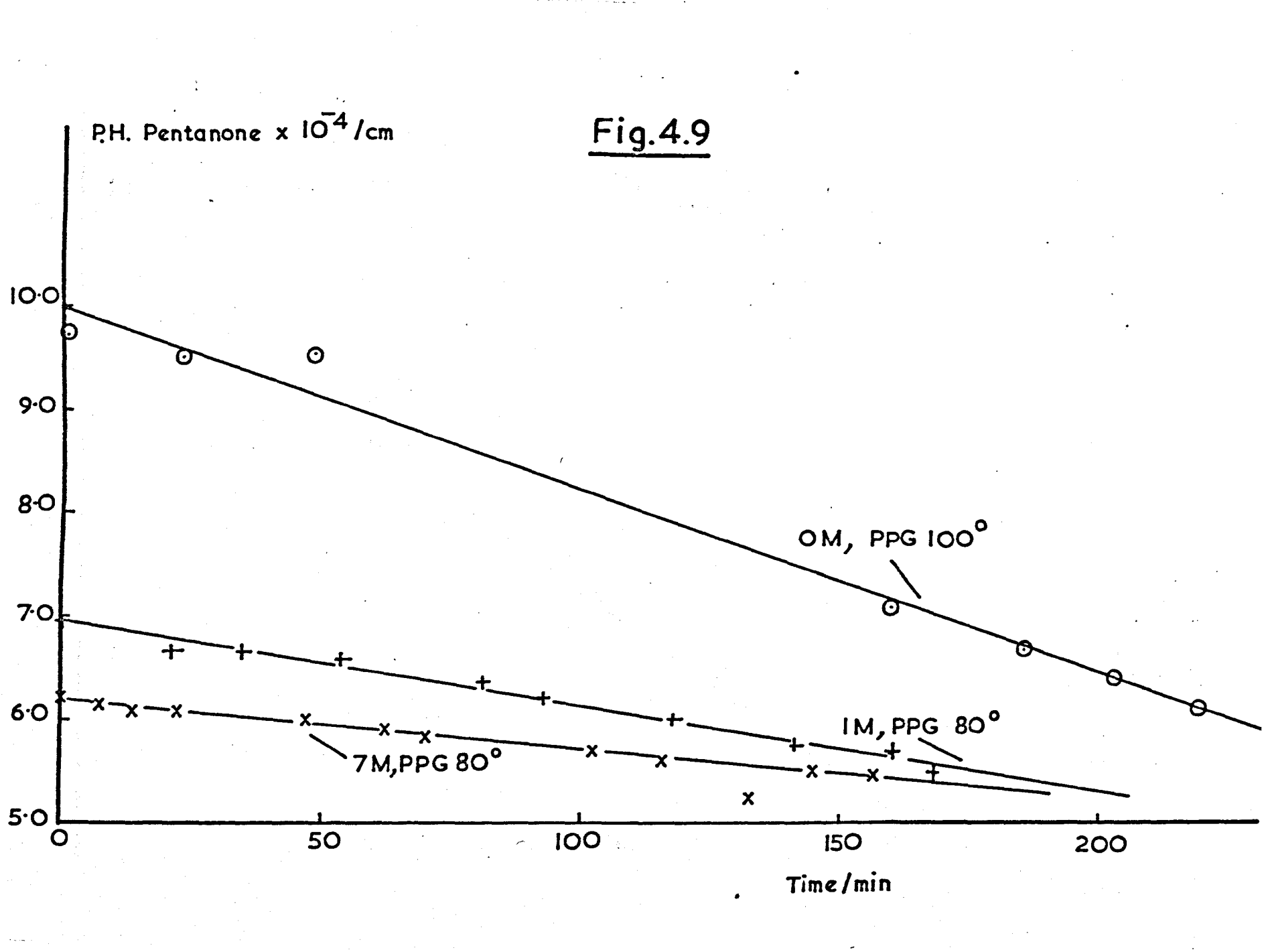
P.H. Pentanone x 10^{-4}/cm
Fig.4.9
10·0
9·0
8·0
7·0
6·0
5·0
0
50
100
150
200
Time/min
0M, PPG 100°
1M, PPG 80°
7M, PPG 80°

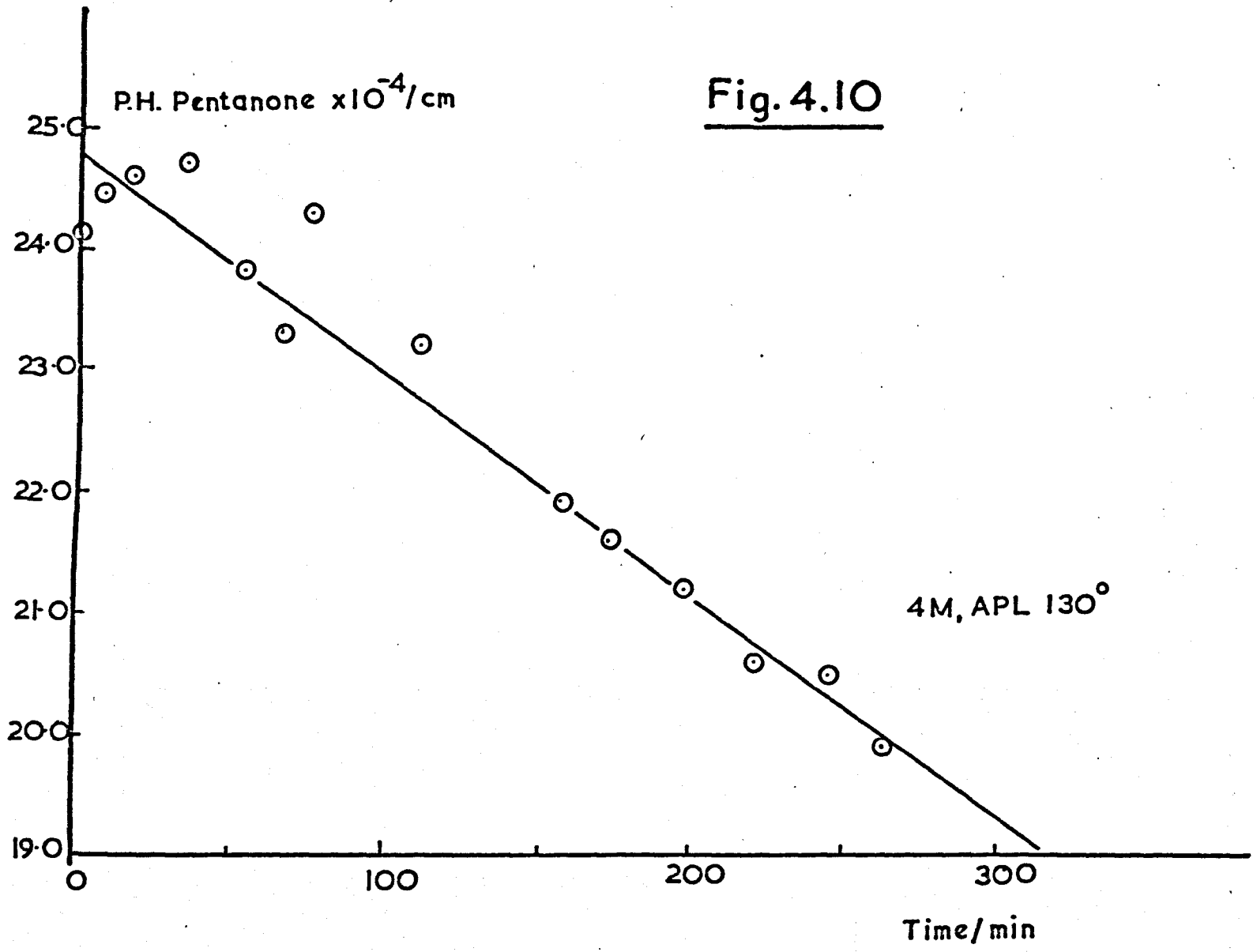
P.H. Pentanone x10^{-4}/cm
25·0
24·0
23·0
22·0
21·0
20·0
19·0
0
100
200
300
Time/min
4M, APL 130°

Fig. 4.10

Concentration of Cyclohexene mol litre^{-1}	Analysis Conditions	Intensity % Io	Time, min	Peak Height of Acetone cm x 10^{-3}	Peak Height of 2-Pentanone cm x 10^{-4}
0	PPG	94.0	0	2.8	9.72
	100°C		22.5	5.6	9.50
			48	7.75	9.55
			159	14.1	7.08
			185	15.4	6.70
			203	15.8	6.43
			219	16.0	6.14
			462	18.0	3.36
7.0	PPG	93.5	0	0.85	6.20
	80°C		8	0.94	6.15
			14	0.90	6.07
			22.5	1.15	6.09
			47	1.35	6.00
			62.5	1.52	5.91
			70	1.65	5.82
			105	1.85	5.70
			116	2.07	5.60
			133	2.25	5.25
			145	2.45	5.50
			156.5	2.35	5.46
1.0	PPG	92.5	0	2.1	6.95
	80°C		21.5	2.7	6.65
			35	3.3	6.65
			58	4.05	6.57
			81	4.5	6.35
			93	5.0	6.20
			118	5.7	5.99

Concentration of Cyclohexene mol litre^{-1}	Analysis Conditions	Intensity % Io	Time min	Peak Height of Acetone cm x 10^{-3}	Peak Height of 2-Pentanone cm x 10^{-4}
1.0 Continued	PPG 80°C	92.5	142	6.65	5.75
			160	6.25	5.70
			168	6.6	5.50
4.0	APL 130°C	89.0	0	0.07	24.1
			8	0.25	24.4
			19	0.60	24.6
			35	1.00	24.7
			53.5	1.40	23.8
			66	1.80	23.3
			76	2.10	24.3
			111	2.80	23.2
			157	3.65	21.9
			173	3.90	21.6
			198	4.30	21.2
			221	4.70	20.6
			245	4.90	20.5
			263	5.30	19.9

The best values of the slopes are set out below:

Cyclohexene mol litre^{-1}	Slope, Acetone cm min^{-1}	Slope, Pentanone cm min^{-1}	% Io
0	112	175	94.0
1.0	31.5	82	92.5
4.0	25.75	182	89.0
7.0	10.75	37	93.5

As can be seen from the figures above, the initial concentration of 2-pentanone varied slightly from run to run (due to the difficulty of making up small volumes of solution accurately). As the solutions were not absorbing all incident light, variation in concentration is important. To allow for this the rates were scaled to the amount of light absorbed by a 0.1M solution using the average value of the extinction coefficients in benzene and cyclohexane, 5.33 $l.mol^{-1}cm^{-1}$. (The extinction coefficient in cyclohexene at 313 nm lies between the values in the other two solvents). The rates were also scaled up to 100% Io to allow for lamp decay.

For example, the slope of the acetone production graph for 5 Molar cyclohexene in benzene is 20.0 cm min^{-1}. The incident intensity is 98.5% of that at the start of this series of experiments. If the lamp intensity had not depreciated this would give a slope of 22.4 cm min^{-1}. The sensitivity measured for acetone on APL at 130°C was 0.461×10^{-12} mol cm^{-1} so that this slope corresponds to 10.3×10^{-12} mol min^{-1} $microlitre^{-1}$. The initial concentration of 2-pentanone was 0.099 mol $litre^{-1}$ corresponding to an optical density of 0.529 meaning that 70.5% of incident light was absorbed in the 1 cm path length cell. A solution 0.1 mol $litre^{-1}$ in pentanone absorbs 70.7% of the incident light so that the scaled rate is 10.35×10^{-12} mol min^{-1} microlitre. In this case the correction due to deviations in concentration is negligable but in other cases it is more appreciable.

Treating the results in this way the following values

are obtained.

Concentration of Cyclohexene mol litre^{-1}	Co-Solvent	Rate of Production of Acetone mol min^{-1}microlitre^{-1} x 10^{12}	Rate of Consumption of Pentanone mol min^{-1} microlitre^{-1} x 10^{12}
0	Benzene	25.2	41.7
1.0	Benzene	12.25	65.0
5.0	Benzene	10.35	65.5
9.76	None	8.65	68.0
0	Cyclohexane	68.9	197
1.0	Cyclohexane	28.8	148
4.0	Cyclohexane	13.8	82.0
7.0	Cyclohexane	10.2	69.0

These results are shown in Fig. 4.11.

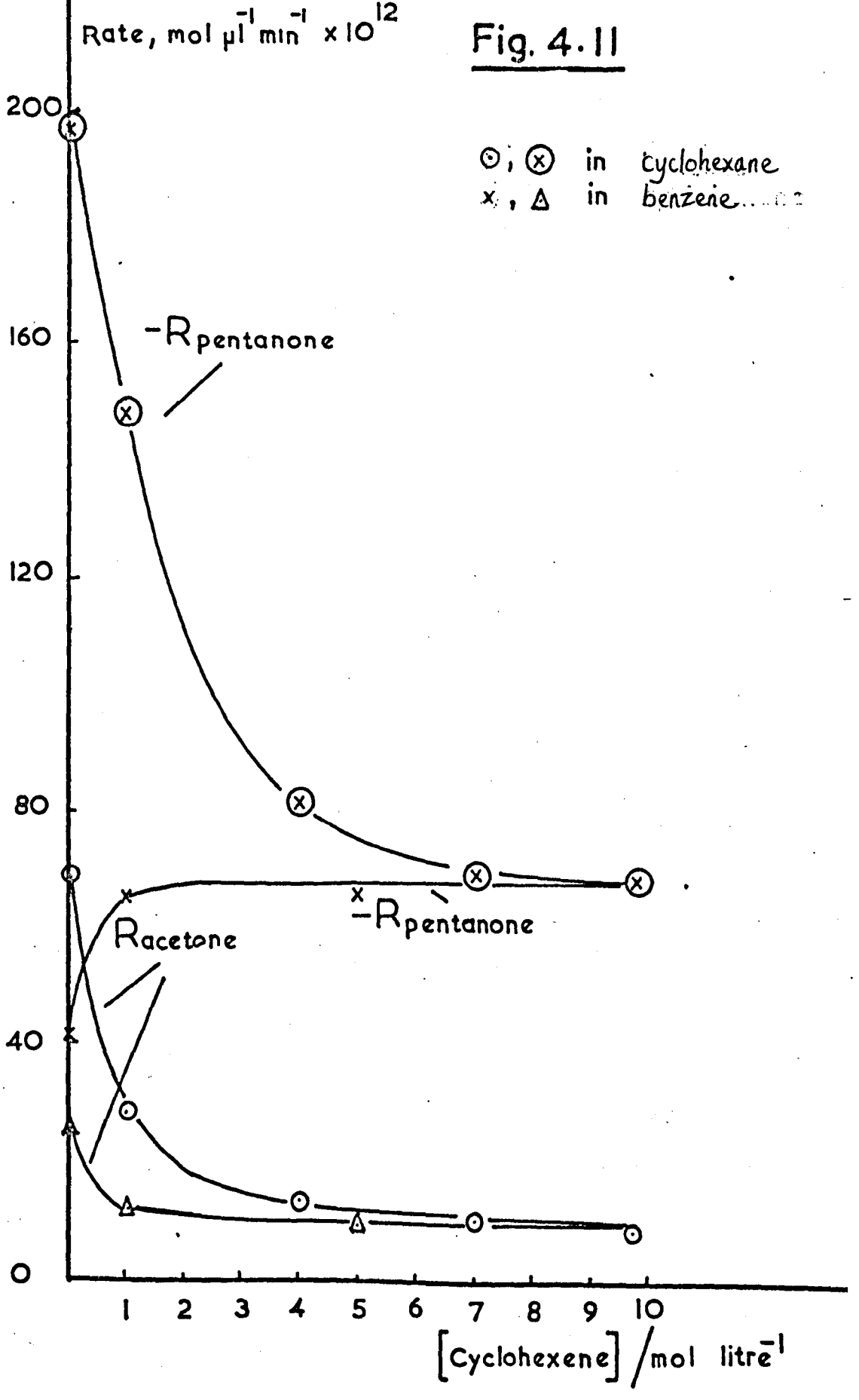
Rate, mol μl^{-1} min^{-1} x 10^{12}
Fig. 4.11
⊙, ⊗ in cyclohexane
x, Δ in benzene
200
160
120
80
40
0
$-R_{pentanone}$
$R_{acetone}$
$-R_{pentanone}$
1 2 3 4 5 6 7 8 9 10
[Cyclohexene] /mol $litre^{-1}$

4.6 Quenching of Photoelimination in 4-Methyl-2-Pentanone (Methyl iso-Butyl Ketone)

4.6(a) Quenching by cyclohexene in benzene solution

The results are tabulated below as for 2-pentanone. Note that the ketone is abbreviated to MIBK. 1 microlitre aliquots. See Figs. 4.12 and 4.13.

Concentration of Cyclohexene mol litre^{-1}	% Io	Analysis Conditions	Time, min	P.H. Acetone cm x 10^{-3}	P.H. MIBK cm x 10^{-4}
0	88.0	PPG 100°C	0	1.5	9.20
			33	4.0	8.95
			70	7.0	8.73
			77	7.1	8.55
			86	7.9	8.80
			102	9.25	8.65
			115	10.2	8.45
			130	11.4	8.35
			160	13.0	8.50
			208	-	8.10
1.0	85.8	PPG 100°C	0	2.1	9.90
			9	2.2	9.82
			16	2.6	9.70
			53	3.9	8.90
			65.5	4.2	9.05
			75	4.2	9.40
			83	4.7	9.10
			98.5	5.0	8.90
			114	5.4	8.70
			122	5.5	8.70

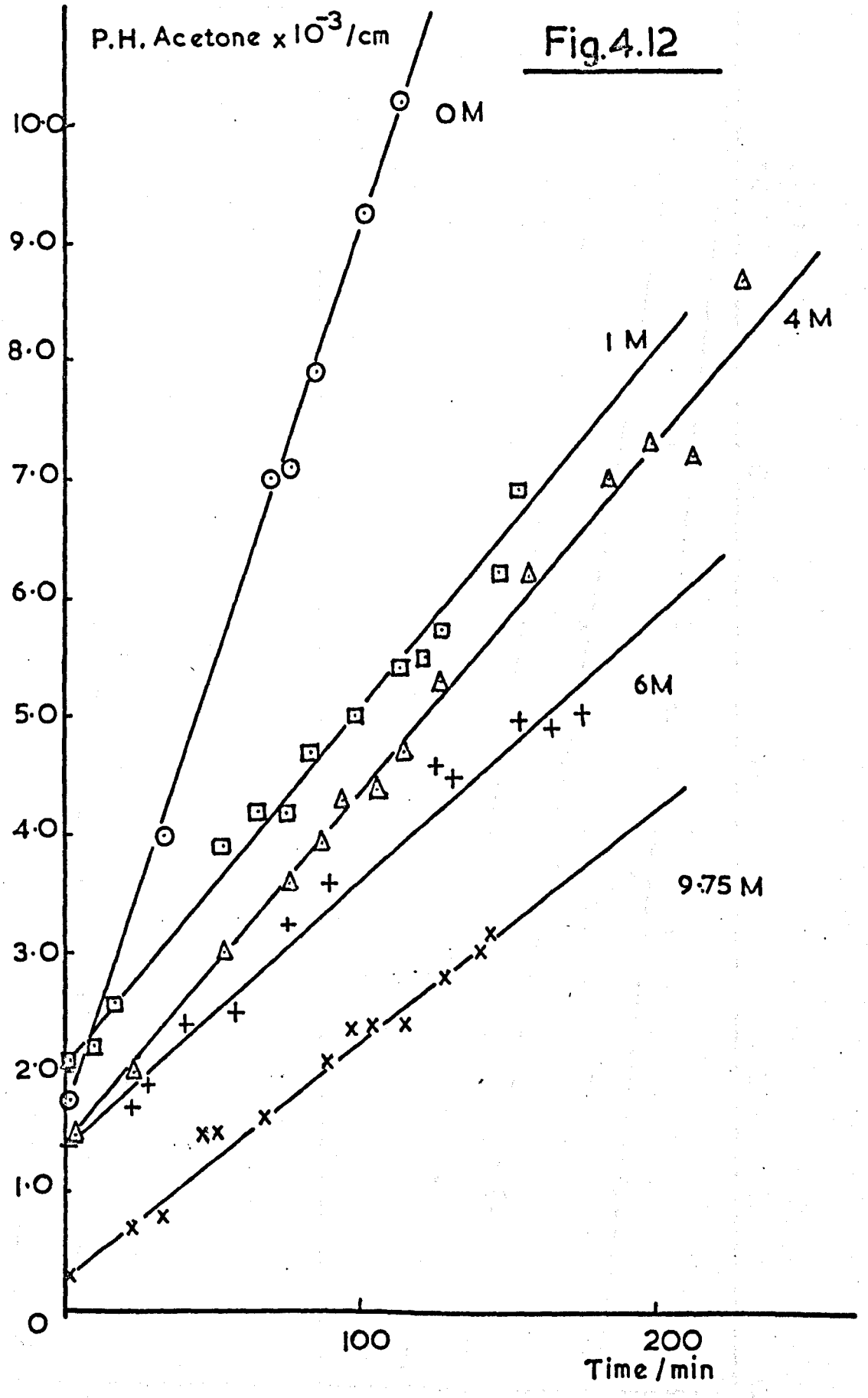
P.H. Acetone x 10^{-3}/cm
Fig.4.12
0M
1 M
4 M
6M
9·75 M
10·0
9·0
8·0
7·0
6·0
5·0
4·0
3·0
2·0
1·0
0
100
200
Time / min

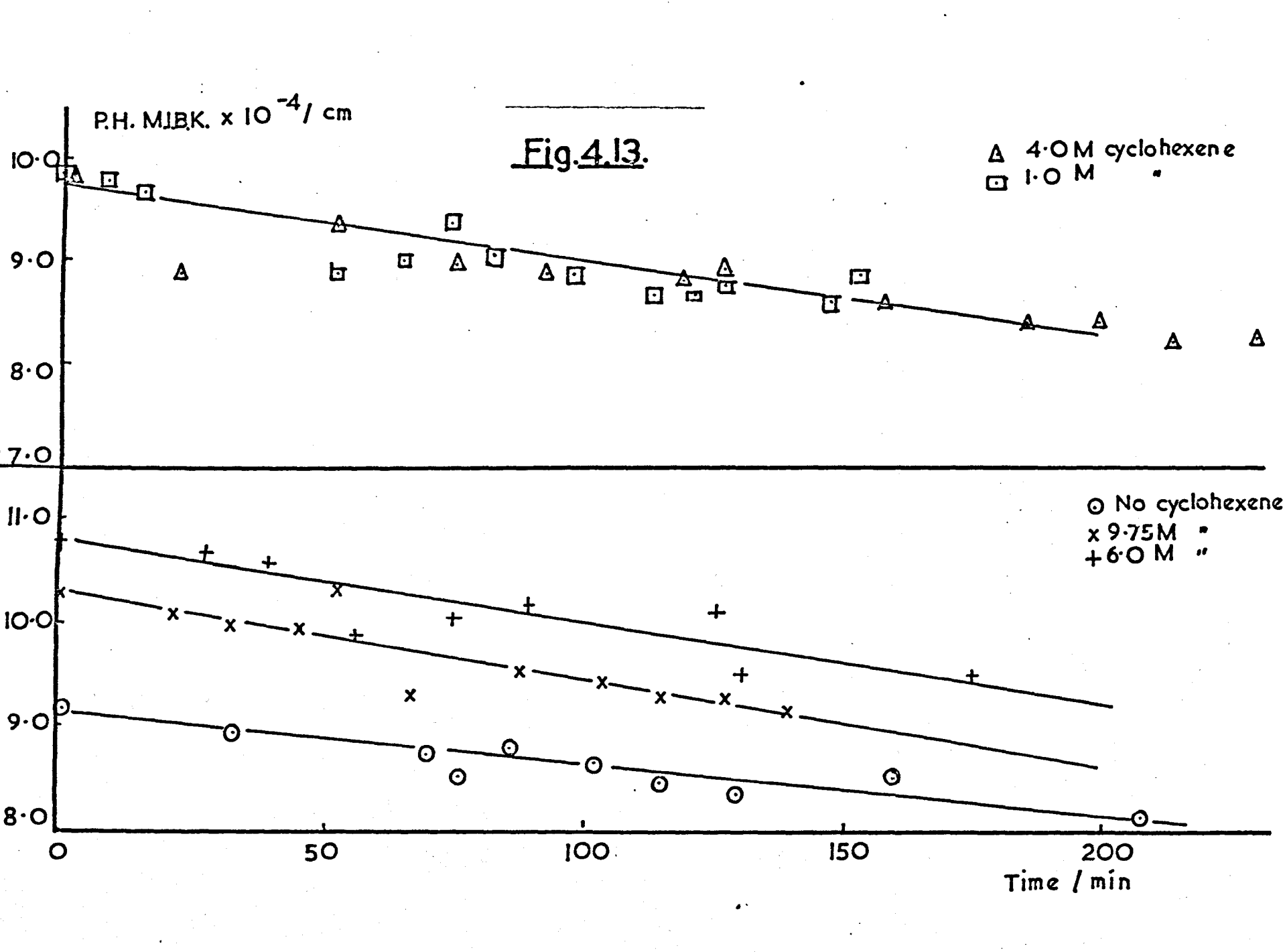
P.H. M.I.B.K. x 10⁻⁴ / cm
Fig.4.13.
Δ 4·0 M cyclohexene
⊡ 1·0 M "
10·0
9·0
8·0
7·0
⊙ No cyclohexene
x 9·75 M "
+ 6·0 M "
11·0
10·0
9·0
8·0
0
50
100
150
200
Time / min

Concentration of Cyclohexene mol litre^{-1}	% Io	Analysis Conditions	Time, min	P.H. Acetone cm x 10^{-3}	P.H. MIBK cm x 10^{-4}
1.0	85.8	PPG	128	5.75	8.80
Continued		100°C	148	6.25	8.65
			154	6.9	8.90
4.0	86.4	PPG	2	1.5	9.80
		100°C	23	2.0	8.90
			53	3.0	9.40
			76	3.6	9.00
			86.5	3.95	-
			93.5	4.3	8.91
			106	4.4	-
			113	4.7	-
			120	-	8.84
			127.5	5.3	8.97
			158	6.2	8.62
			186	7.0	8.45
			200	7.3	8.47
			214	7.2	8.25
			230.5	8.7	8.30
6.0	86.9	PPG	0	1.35	10.80
		100°C	22	1.7	-
			28	1.9	10.70
			40	2.4	10.60
			57	2.5	9.90
			75	3.25	10.10
			90	3.6	10.20
			126	4.6	10.10
			131	4.5	9.52

Concentration of Cyclohexene mol litre^{-1}	% Io	Analysis Conditions	Time, min	P.H. Acetone cm x 10^{-3}	P.H. MIBK cm x 10^{-4}
6.0 Continued	86.9	PPG 100°C	154.5	5.0	-
			165	4.9	-
			175	5.05	9.50
9.75	87.4	PPG 100°C	0	0.3	10.30
			22	0.7	10.10
			32.5	0.8	10.00
			46	1.5	10.00
			53	1.5	10.35
			67	1.65	9.30
			88	2.1	9.55
			98	2.35	-
			104	2.4	9.45
			115.5	2.4	9.30
			128	2.8	9.30
			140	3.0	9.15
			144	3.2	9.45

4.6(b) Quenching by cyclohexene in cyclohexane

As with 2-pentanone a series of experiments was carried out in cyclohexane and the results are tabulated overleaf. All analyses were on PPG at 100°C. The sensitivity for MIBK on this column was measured as 1.01 x 10^{-12} mol cm^{-1}. See Figs. 4.14 - 4.16.

Fig. 4.14

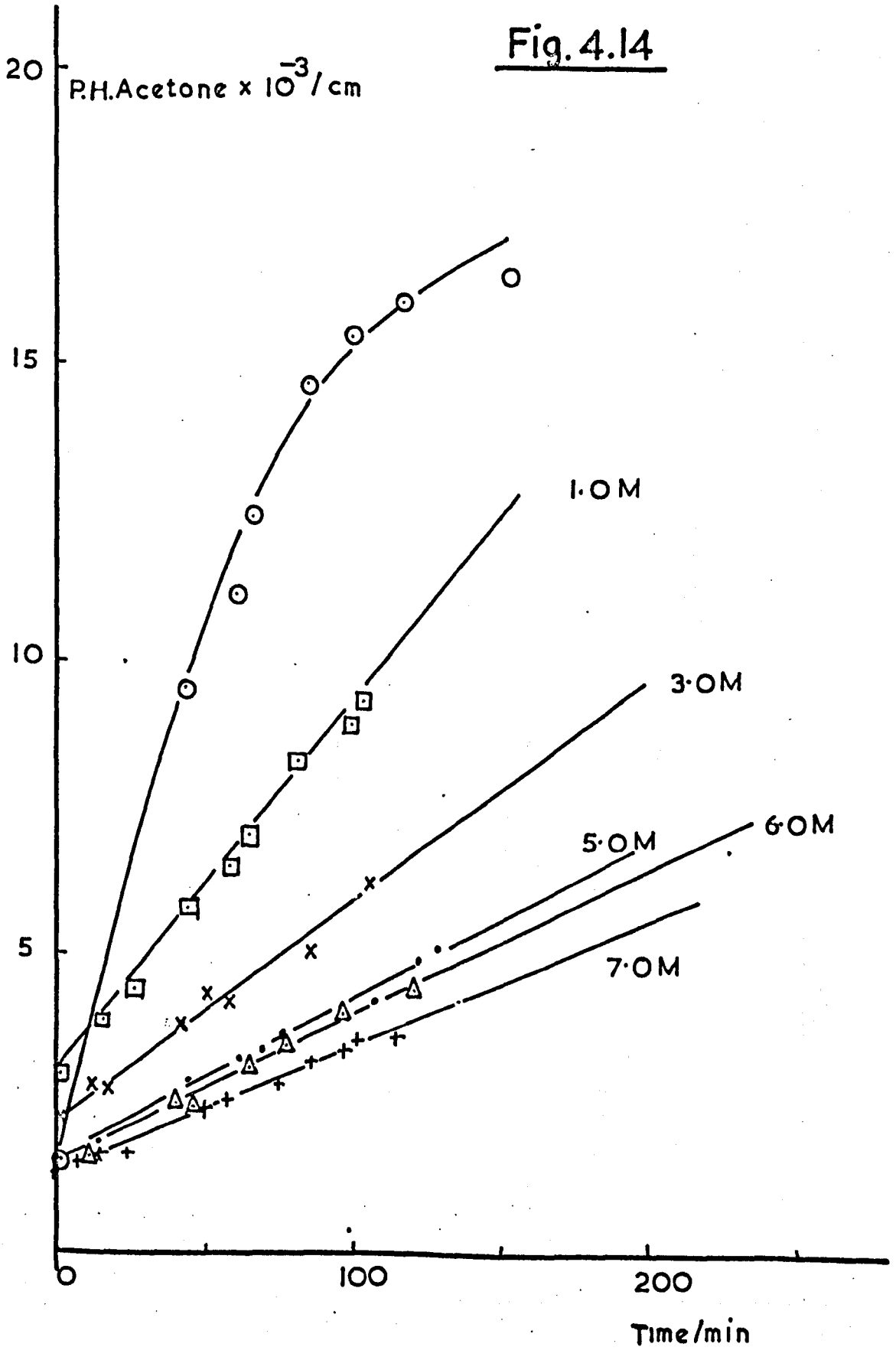
20
15
10
5
P.H.Acetone x 10^{-3}/cm
1·0M
3·0M
5·0M
6·0M
7·0M
0
100
200
Time/min

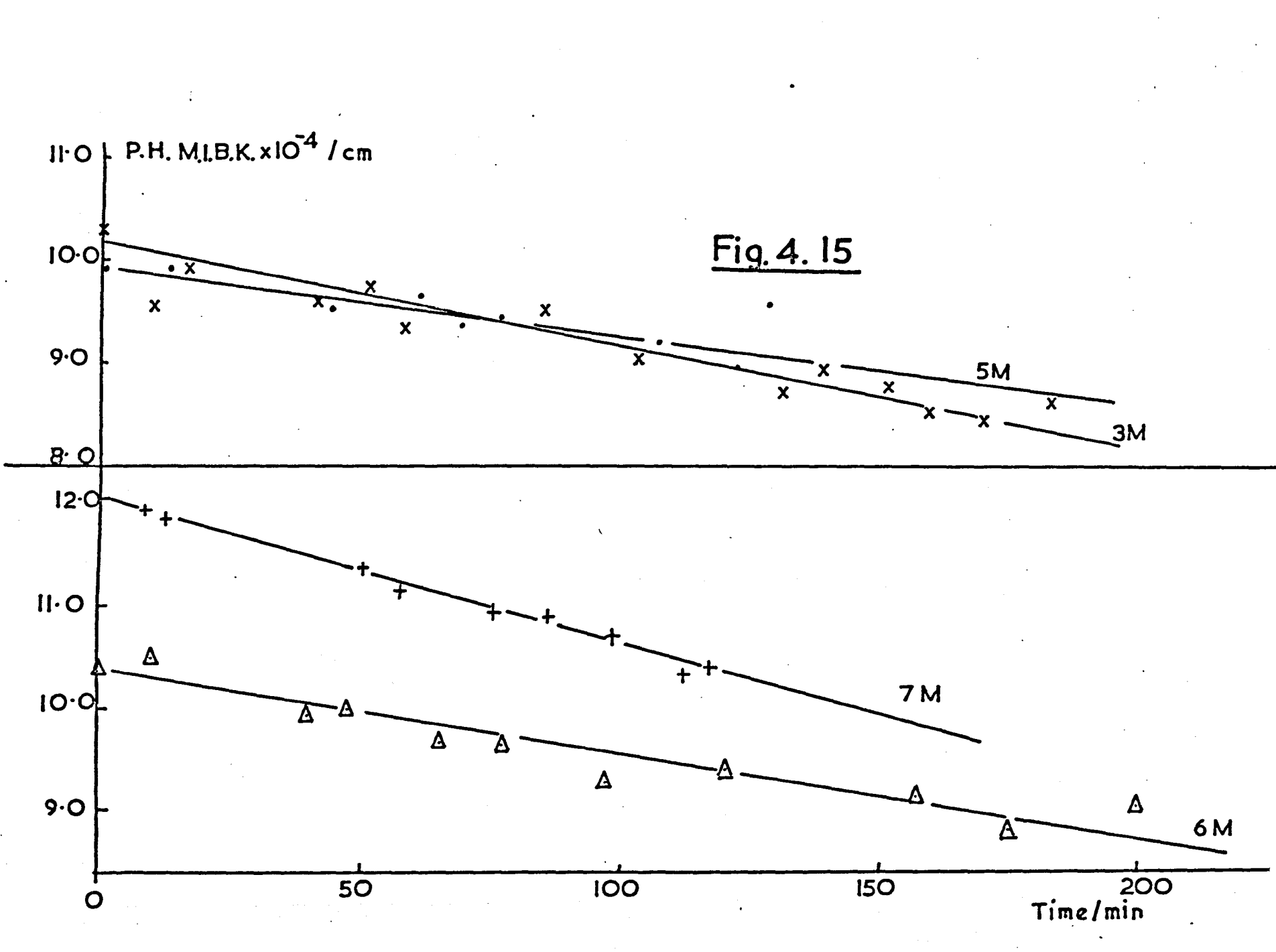
P.H. M.I.B.K. x10⁻⁴ /cm
11·0
10·0
9·0
8·0
5M
3M
12·0
11·0
10·0
9·0
7 M
6 M
0
50
100
150
200
Time/min

Fig. 4. 15

Fig. 4.16

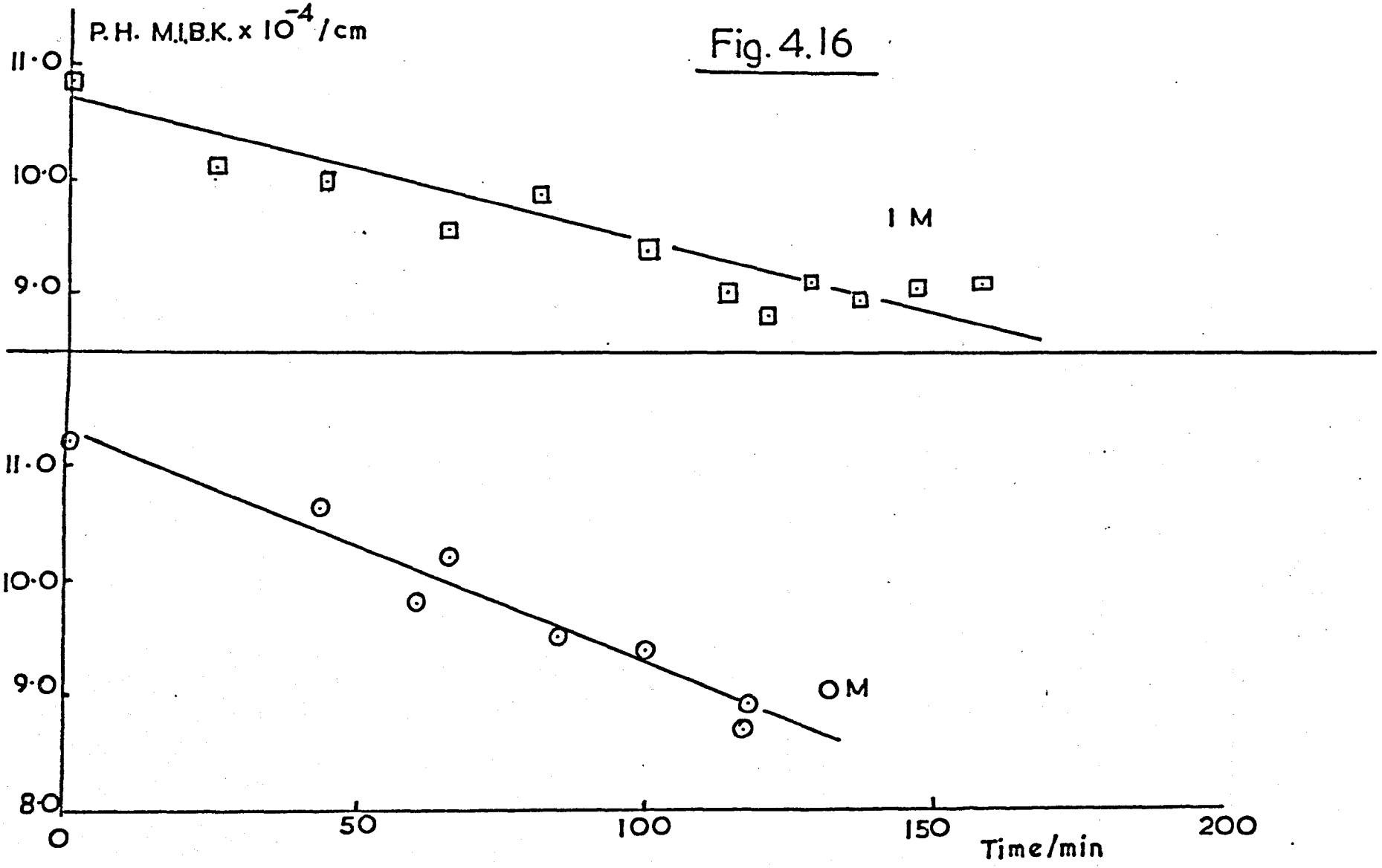
P.H. M.I.B.K. x 10^{-4} /cm
11·0
10·0
9·0
1 M
11·0
10·0
9·0
0 M
8·0
0
50
100
150
200
Time/min

Concentration of Cyclohexene mol litre^{-1}	% Io	Time, min	Peak Height of Acetone cm x 10^{-3}	Peak Height of MIBK cm x 10^{-4}
0	97.5	0	1.51	11.20
		43.5	9.3	10.65
		60	11.1	9.80
		66	12.4	10.20
		84.5	14.6	9.50
		100	15.45	9.40
		117	-	8.70
		118	16.0	8.93
1.0	96.2	0	2.95	10.90
		14.5	3.90	-
		25	4.40	10.10
		44	5.80	10.00
		58	6.50	-
		65	7.00	9.55
		81.5	8.30	9.90
		100	8.90	9.40
		114	9.30	9.00
		121	-	8.82
		128.5	-	9.12
		137	-	8.93
		147	-	9.05
		158.8	-	9.08
3.0	95.7	0	2.2	10.30
		10	2.8	9.55
		17	2.75	9.92
		41	3.80	9.60
		50.5	4.35	9.75
		58	4.20	9.35

Concentration of Cyclohexene mol litre^{-1}	% Io	Time, min	Peak Height of Acetone cm x 10^{-3}	Peak Height of MIBK cm x 10^{-4}
3.0	95.7	85	5.05	9.50
Continued		106	6.23	9.03
		131	-	8.70
		139	-	8.95
		151.5	-	8.77
		159	-	8.50
		170	-	8.42
		183	-	8.60
5.0	96.7	0	1.60	9.9
		13	1.85	9.9
		44	2.90	9.5
		61	3.25	9.6
		69	3.40	9.35
		76	3.60	9.4
		107	4.20	9.2
		122	4.90	8.9
		128.5	5.10	9.6
6.0	95.0	0	1.50	10.40
		10.5	1.60	10.50
		40	2.50	9.95
		47	2.45	10.00
		65.5	3.13	9.70
		77	3.50	9.67
		97	4.00	9.30
		120.5	4.38	9.40
		157	-	9.15
		175	-	8.80
		199.5	-	9.05

Concentration of Cyclohexene mol litre^{-1}	% Io	Time, min	Peak Height of Acetone cm x 10^{-3}	Peak Height of MIBK cm x 10^{-4}
7.0	97.1	0	1.40	-
		8	1.55	11.90
		12	1.60	11.80
		21.5	1.65	-
		50	2.47	11.35
		57	2.60	11.15
		75	2.80	10.95
		85.5	3.20	10.90
		98	3.40	10.70
		112	3.55	10.35
		117	3.60	10.40

The slopes were treated in the same way as those for 2-pentanone in Section 4.5 and the rates obtained are tabulated overleaf. The extinction coefficient was taken as 6.20 l.mol^{-1}cm^{-1}.

Concentration of Cyclohexene mol litre^{-1}	Co-solvent	Rate of production of acetone. mol min^{-1} microlitre^{-1} x 10^{12}	Rate of consumption of MIBK. mol min^{-1} microlitre^{-1} x 10^{12}
0	Cyclohexane	108	201
1.0	Cyclohexane	37.4	125
3.0	Cyclohexane	22.7	104
5.0	Cyclohexane	15.9	73.7
6.0	Cyclohexane	14.9	91.2
7.0	Cyclohexane	12.2	101
9.75	None	13.1	96.0
0	Benzene	40.2	62.0
1.0	Benzene	20.8	82.6
4.0	Benzene	19.7	82.3
6.0	Benzene	14.9	89.7

The results are shown in Fig. 4.17.

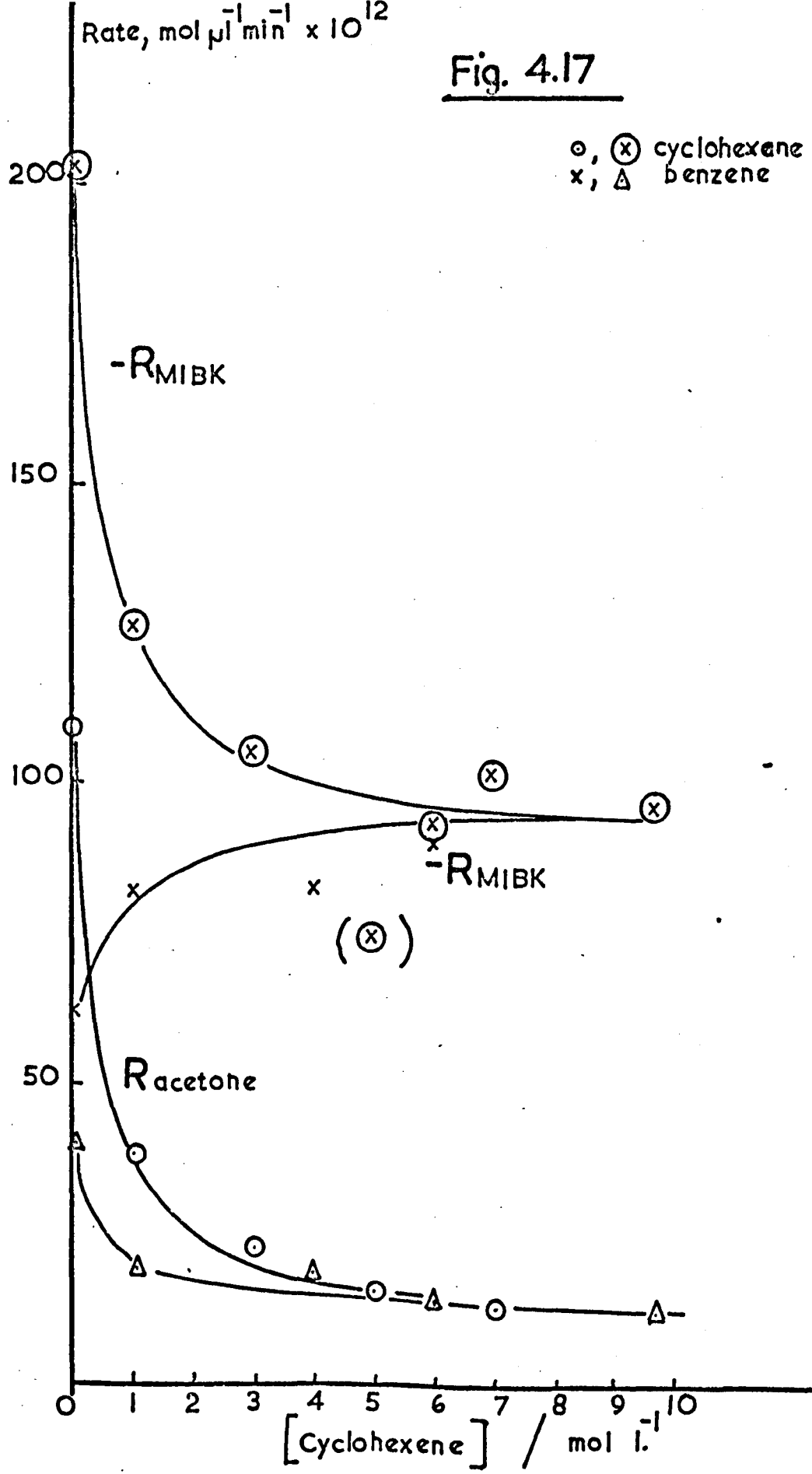
Rate, mol $\mu l^{-1} min^{-1} \times 10^{12}$
Fig. 4.17
⊙, ⊗ cyclohexene
x, Δ benzene
200
150
100
50
$-R_{MIBK}$
$-R_{MIBK}$
(⊗)
$R_{acetone}$
0 1 2 3 4 5 6 7 8 9 10
[Cyclohexene] / mol l^{-1}

4.7 Quenching of Photoelimination in 2-Octanone

4.7(a) Quenching by cyclohexene in benzene

The results are tabulated below. Analysis was on APL at 130°. The sensitivity for 2-octanone under these conditions was 1.48×10^{-12} mol cm^{-1}. See Figs. 4.18, 4.19.

Concentration of Cyclohexene mol $litre^{-1}$	% Io	Time, min	Peak Height of Acetone cm x 10^{-3}	Peak Height of Octanone cm x 10^{-4}
0	84.4	0	3.6	8.80
		29	6.2	8.60
		46	7.15	8.45
		62	8.1	7.95
		121	13.2	7.60
		141	15.6	7.80
		159	17.3	7.70
		170	-	7.80
		189	18.25	7.65
		203	19.5	7.57
1.0	83.8	0	3.0	8.8
		24	5.2	8.7
		45	6.6	8.3
		59	7.4	7.95
		76	9.6	7.95
		91	10.0	8.05
		110	11.5	7.8
		143	14.25	8.1
		180	17.75	7.9

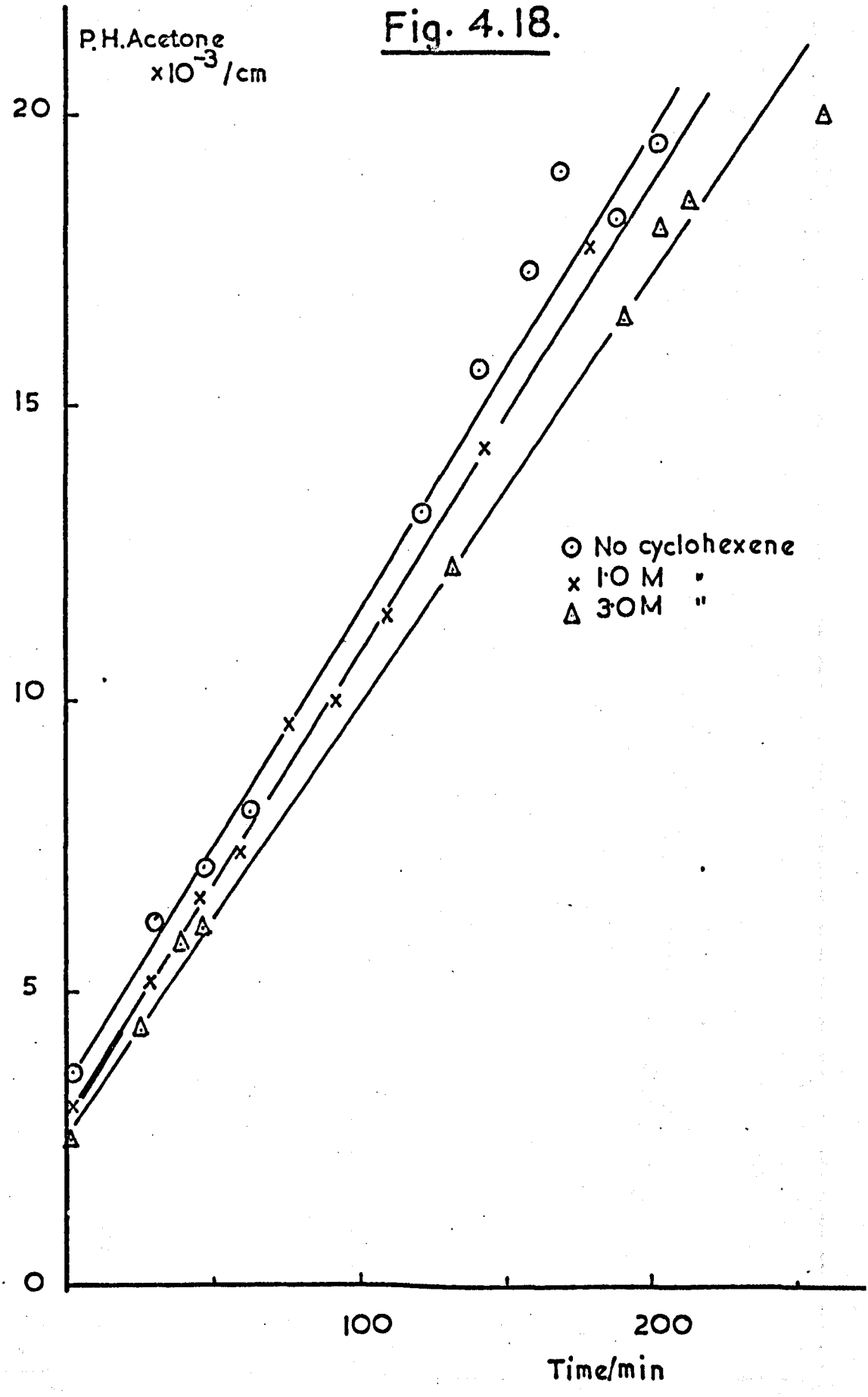
Fig. 4.18.
P.H.Acetone
x10⁻³/cm
20
15
10
5
0
100
200
Time/min
No cyclohexene
1·0 M "
3·0M "

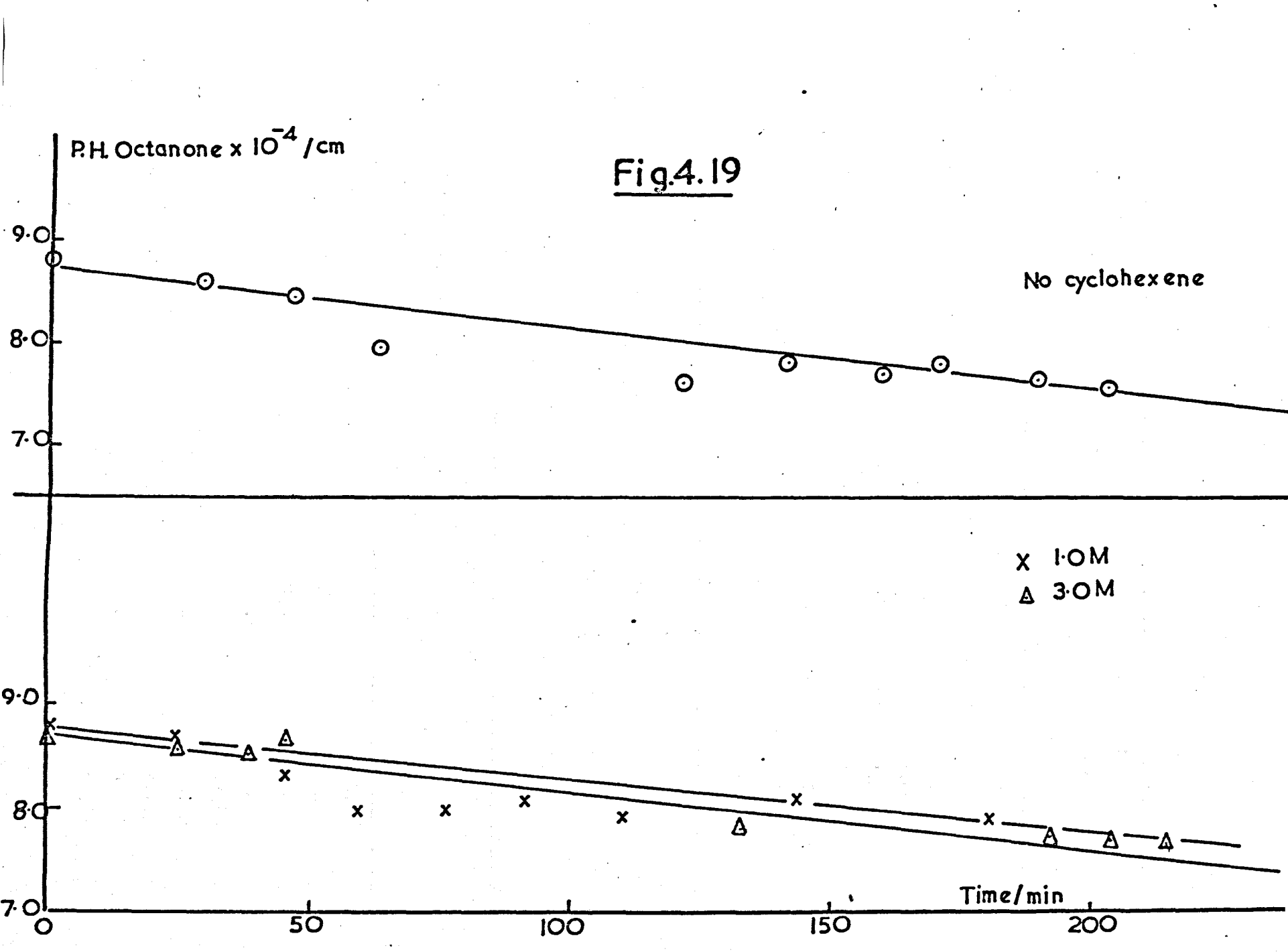
P.H. Octanone x 10^{-4} /cm
Fig.4.19
9·0
8·0
7·0
No cyclohexene
X 1·0M
Δ 3·0M
9·0
8·0
7·0
Time/min
0
50
100
150
200

Concentration of Cyclohexene mol litre^{-1}	% Io	Time, min	Peak Height of Acetone cm x 10^{-3}	Peak Height of Octanone cm x 10^{-4}
3.0	83.3	0	2.5	8.7
		25	4.4	8.6
		38	5.9	8.5
		45.5	6.05	8.65
		132.5	12.3	7.8
		192	16.5	7.7
		204	18.0	7.72
		214.5	18.5	7.65
		240.5	20.7	-

4.7(b) Quenching by cyclohexene in cyclohexane

Analysis for acetone on PPG 100° and for 2-octanone on PEGA at 150°C. 1 microlitre samples. Figs. 4.20 - 4.22.

Concentration of cyclohexene mol litre^{-1}	% Io	Time, min	Peak Height of Acetone cm x 10^{-3}	Peak Height of Octanone cm x 10^{-4}
0	100.0	0	3.15	48.30
		39	6.30	-
		53	7.45	-
		92	11.5	-
		132	-	43.80
		136	-	44.00
		140	-	42.75
		158	-	42.85
		165	-	42.35

Fig. 4.20

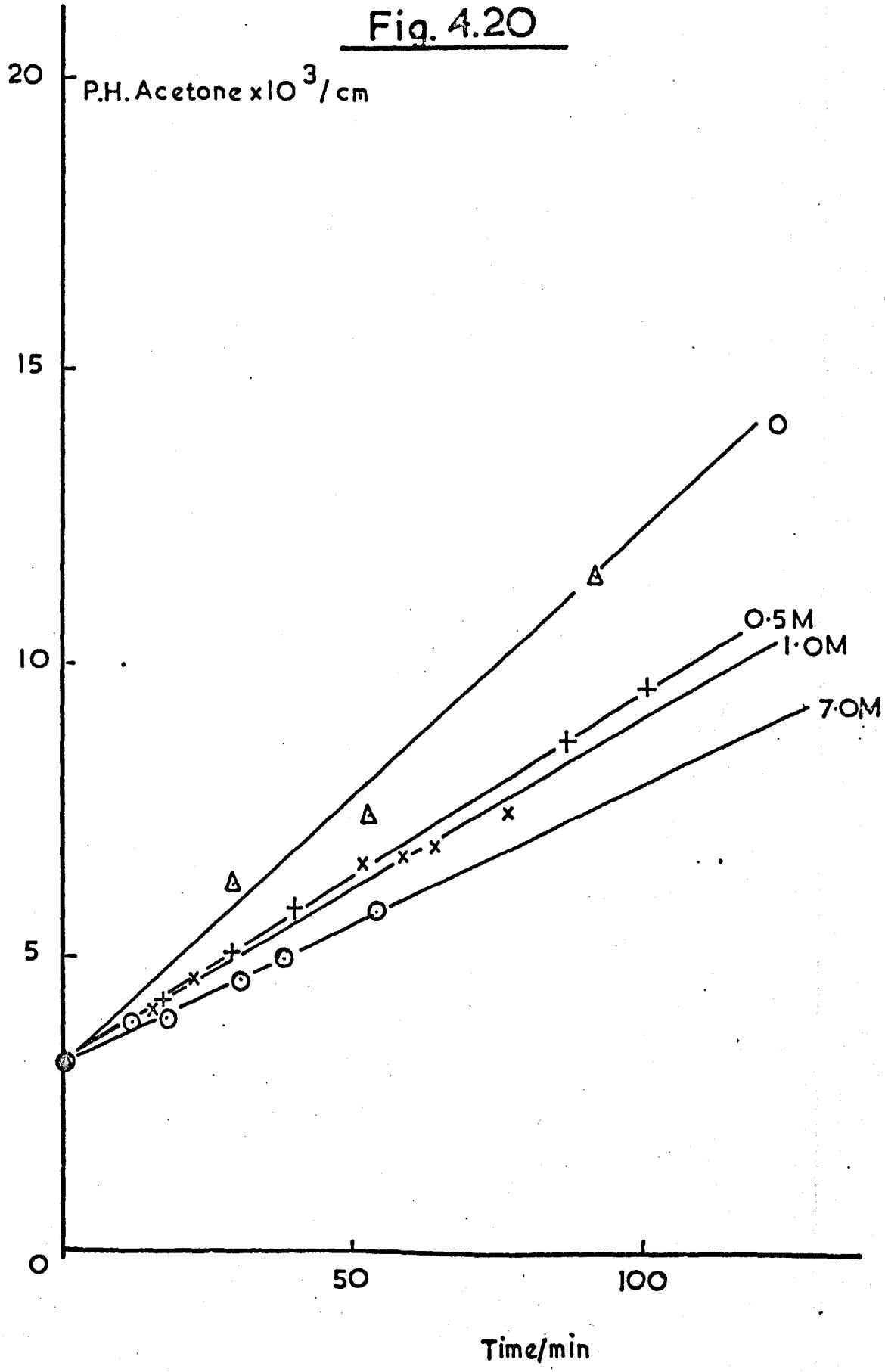

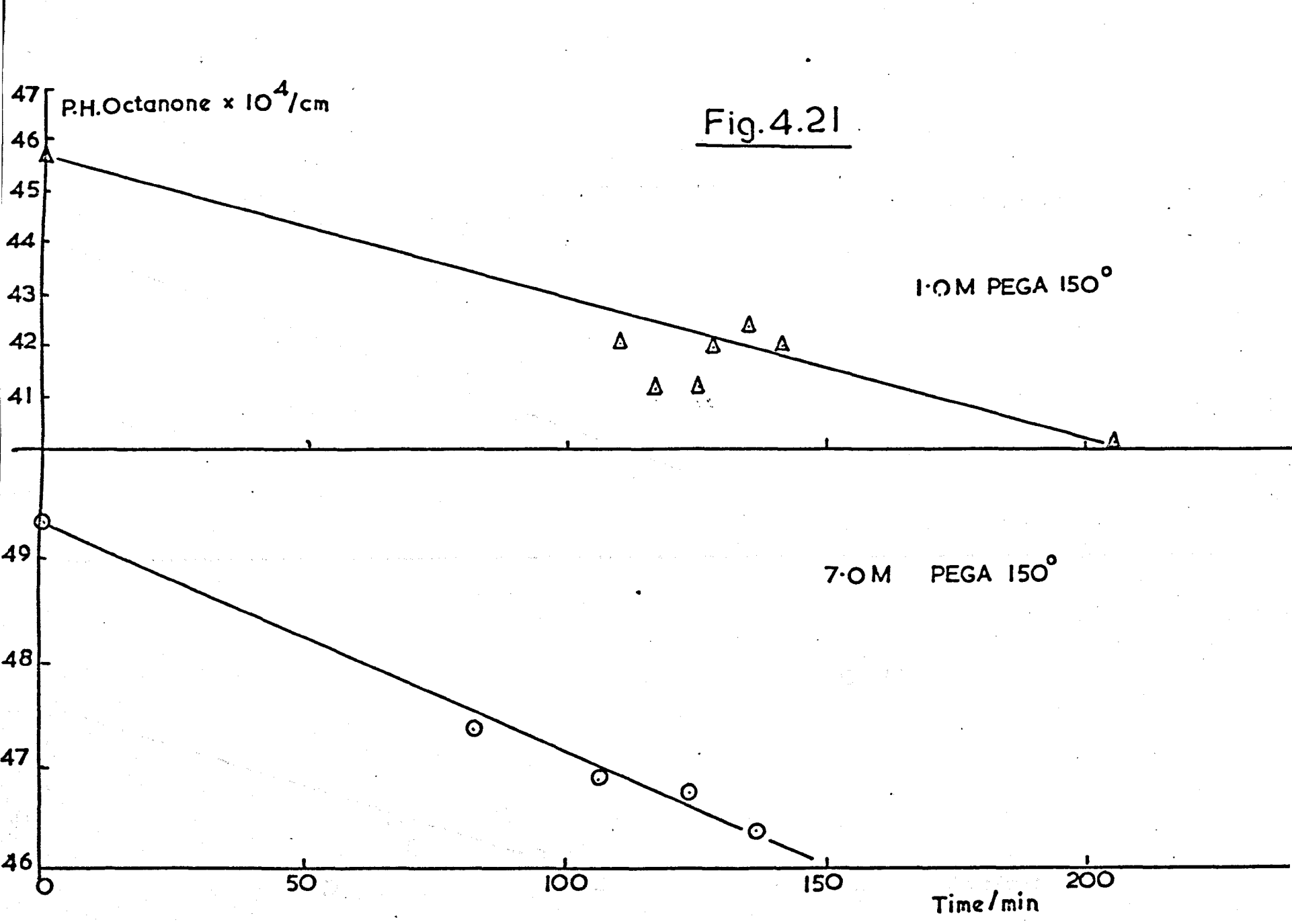
P.H.Octanone × 10⁴/cm
47
46
45
44
43
42
41
1·0M PEGA 150°
49
48
47
46
7·0M PEGA 150°
0
50
100
150
200
Time/min

Fig. 4.21

Fig. 4.22

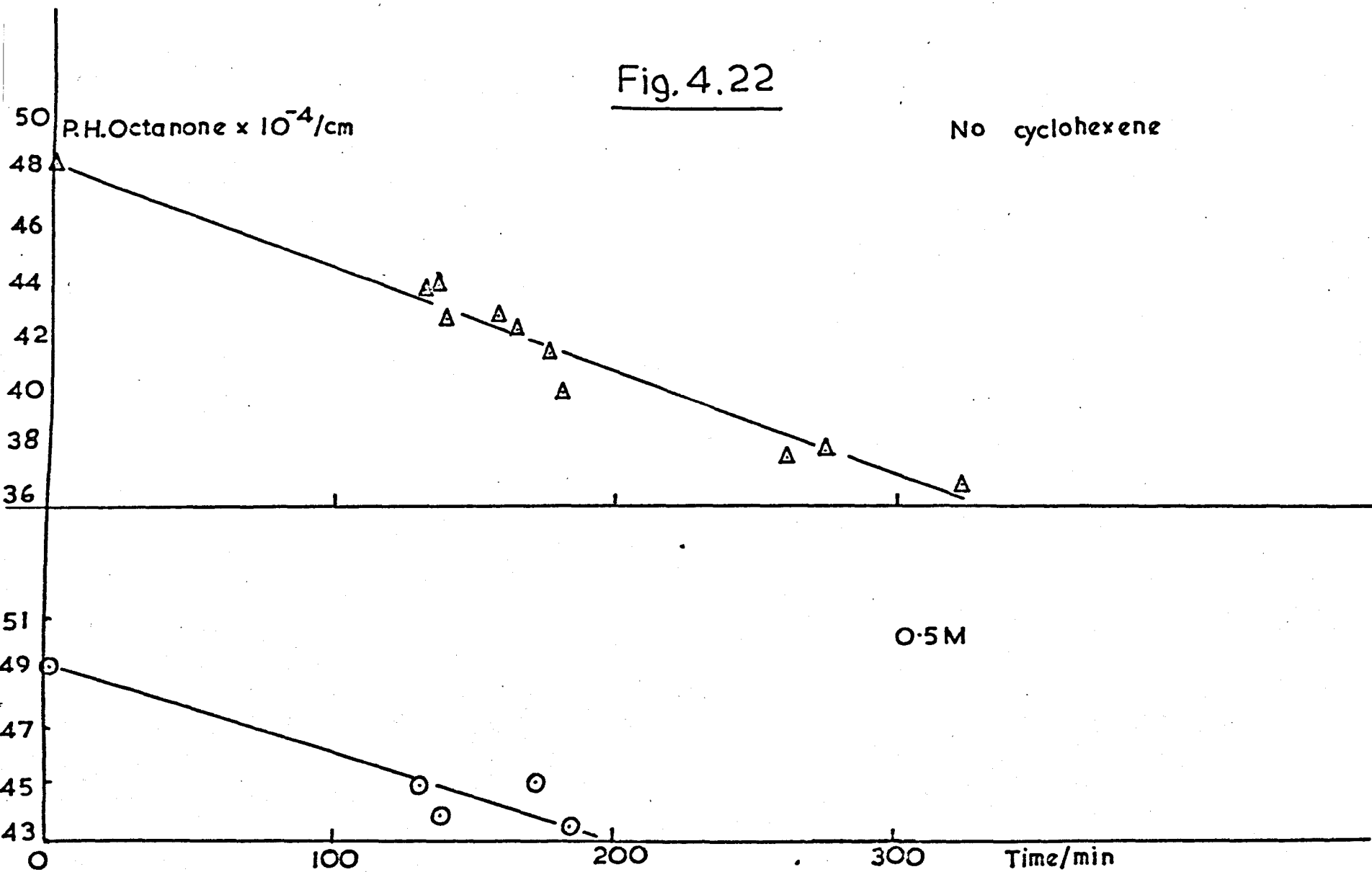
P.H.Octanone x 10^{-4}/cm
No cyclohexene
50
48
46
44
42
40
38
36
0·5 M
51
49
47
45
43
0
100
200
300
Time/min

Concentration of cyclohexene mol litre^{-1}	% Io	Time, min	Peak Height of Acetone cm x 10^{-3}	Peak Height of Octanone cm x 10^{-4}
0	100.0	177	-	41.40
Continued		182	-	40.15
		261.5	-	37.75
		276	-	38.00
		324	-	36.75
0.5	99.0	0	3.05	49.30
		12	3.9	-
		17	4.2	-
		29	5.1	-
		40	5.8	-
		87	8.7	-
		101	9.6	-
		130	-	44.95
		138	-	43.90
		172	-	45.10
		184	-	43.40
1.0	98.5	0	3.25	45.65
		16.5	4.1	-
		23	4.6	-
		52	6.6	-
		59	6.72	-
		64.5	6.9	-
		77	7.5	-
		110	-	42.0
		117	-	41.15
		125	-	41.15
		128	-	41.9

Concentration of cyclohexene mol litre^{-1}	% Io	Time min	Peak Height of Acetone cm x 10^{-3}	Peak Height of Octanone cm x 10^{-4}
1.0	98.5	134.5	-	42.3
Continued		141	-	41.95
		205	-	40.00
7.0	97.8	0	2.98	49.3
		12	3.65	-
		18	3.90	-
		31	4.65	-
		38.5	5.0	-
		54	5.8	-
		82	-	47.35
		106	-	46.85
		123.5	-	46.70
		136	-	46.35

The sensitivity for 2-octanone on PEGA at 150°C was measured as 0.1834 x 10^{-12} mol cm^{-1} whilst that for acetone on PPG at 100°C was 0.689 x 10^{-12} mol cm^{-1} (sensitivity changed from value measured before). Applying the corrections used for the other ketones the rates obtained are tabulated overleaf.

Concentration of cyclohexene mol litre^{-1}	Co-solvent	Rate of production of Acetone, mol min^{-1} microlitre x 10^{12}	Rate of consumption of Octanone, mol min^{-1} microlitre^{-1} x 10^{12}
0	Cyclohexane	59.9	74
0.5	Cyclohexane	46.9	63.5
1.0	Cyclohexane	45.8	55.7
7.0	Cyclohexane	35.9	43.9
0	Benzene	46.1	104
1.0	Benzene	45.8	109
3.0	Benzene	42.7	90.0

The extinction coefficient was taken as 5.44 l. mol^{-1}cm^{-1}. Unlike the lower molecular weight ketones it was possible to follow the production of the olefin formed in the photoelimination. This was done with the cyclohexane solutions and it was found that the 1-pentene rates corresponded closely to those of acetone. (From an exploratory experiment with a different light source the rate of production of acetone in a solution 5.0M in cyclohexene/cyclohexane was 35.7 x 10^{-12} mol min$^{-1}\mu l^{-1}$ when corrected for the different light intensity. This point is included in Fig. 4.23).

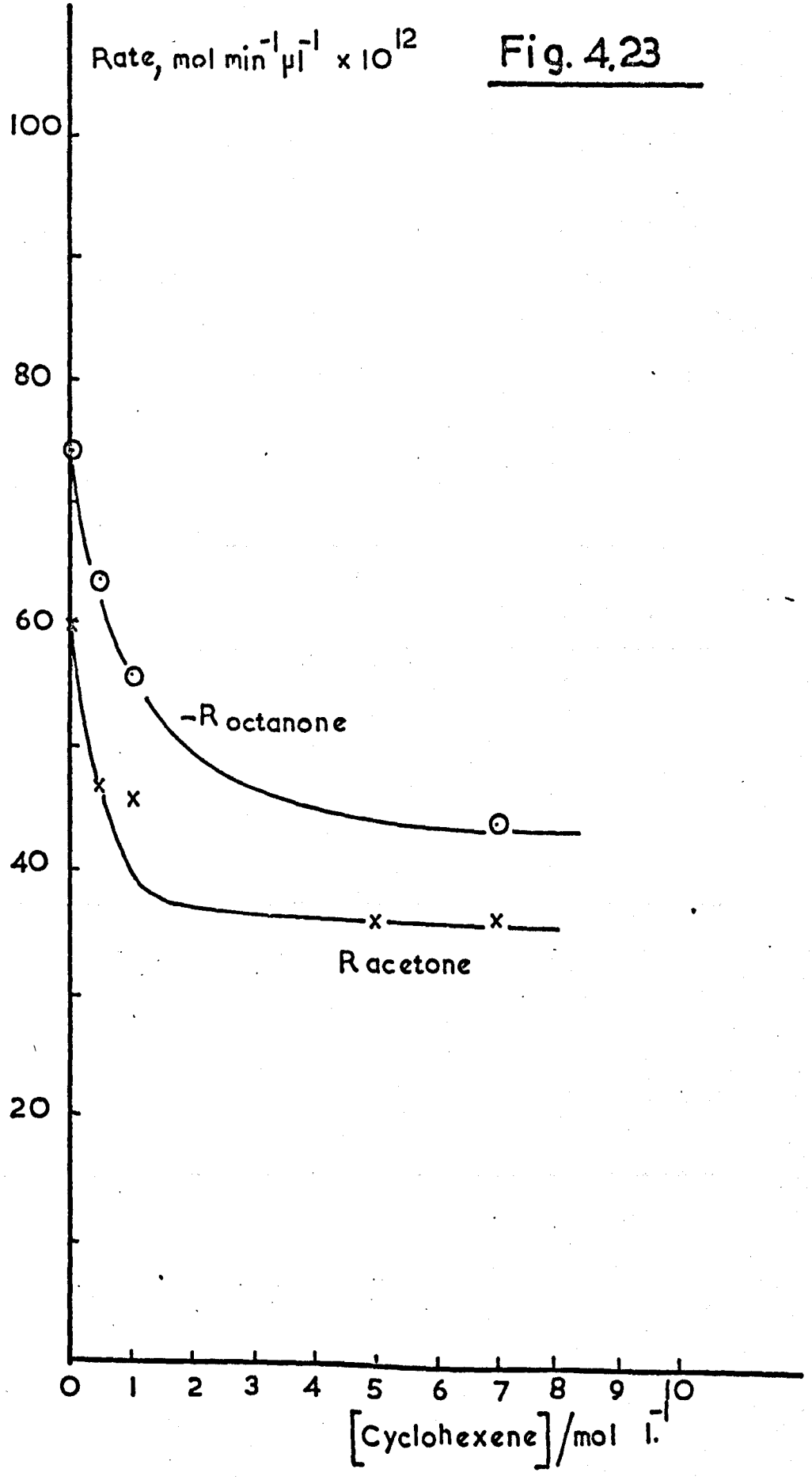
Rate, mol min⁻¹ l⁻¹ x 10¹²
100
80
60
40
20
-R octanone
R acetone
0 1 2 3 4 5 6 7 8 9 10
[Cyclohexene]/mol l⁻¹

Fig. 4.23

4.8 Variation of Quantum Yield of Photoelimination with Concentration in Cyclohexane

A series of experiments was carried out to determine the effect of varying the concentration of 2-pentanone in cyclohexane solution on the rate of acetone production. The results of these experiments are tablulated below and shown in Fig. 4.24. Analysis was on APL at 130° using one microlitre samples. I = 78.0% Io.

% by volume 2-pentanone	Time, min	Peak Height of Acetone, cm x 10^{-2}
100	0	4.5
	15.5	72
	23.5	108
	39.5	200
	51	240
	59	280
50	0	8.0
	9	40
	22	94
	48	200
	72	315
	78	335

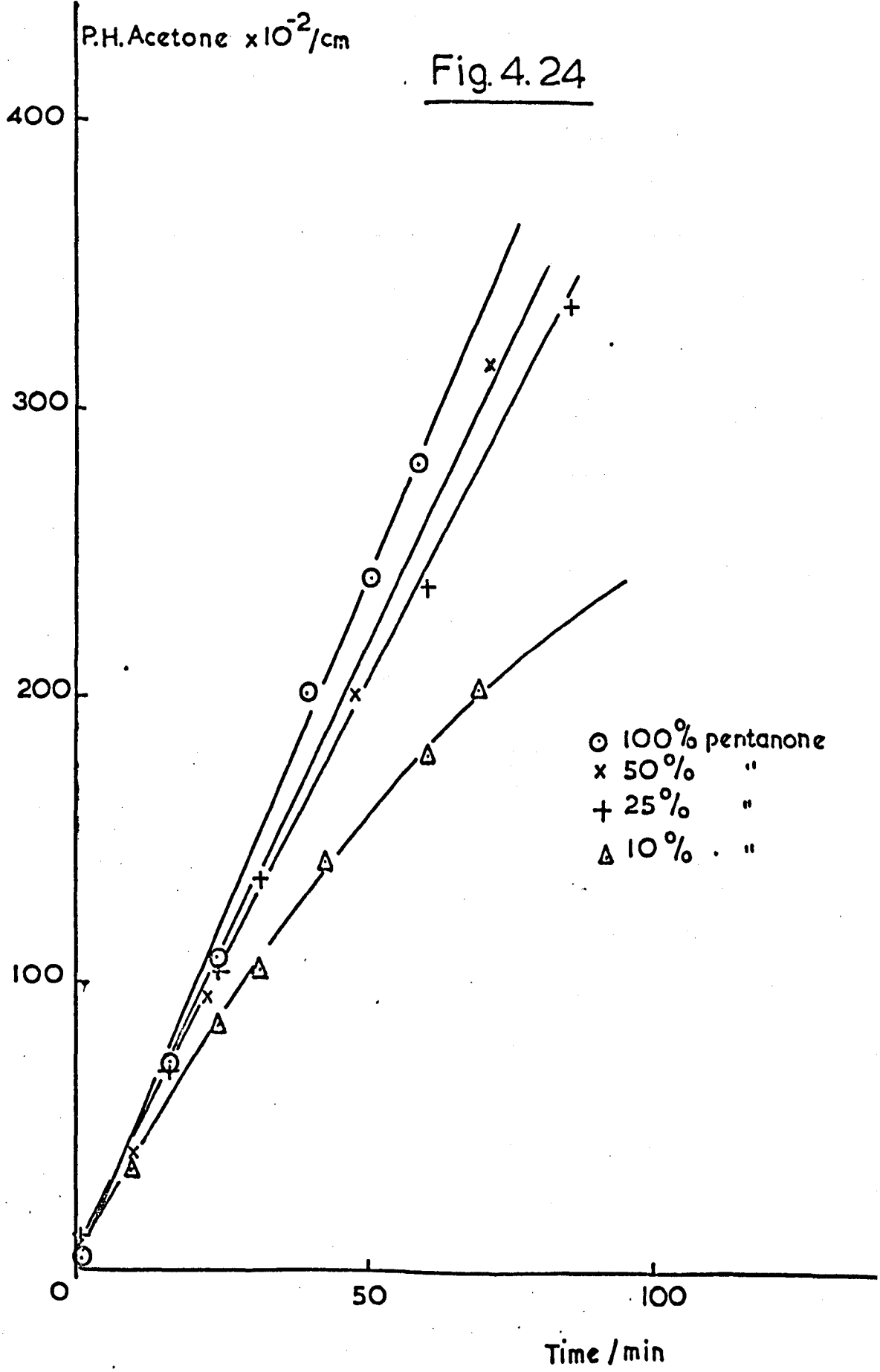
P.H. Acetone x 10^{-2}/cm
Fig. 4.24
400
300
200
100
0
50
100
Time / min
⊙ 100% pentanone
× 50% "
+ 25% "
△ 10% "

/continued

% by volume 2-pentanone	Time, min	Peak Height of Acetone, cm x 10^{-2}
25	0	12.5
	15	69
	24	103
	31.5	136
	61	237.5
	86	335
10	0	9
	9	35.5
	24	84
	31	104
	45	141
	61	178
	69.5	201

All these solutions should absorb effectively all incident light as the extinction coefficient is 5.53 l $mol^{-1}cm^{-1}$ and 100% 2-pentanone is 9.44 mol $litre^{-1}$ at 25°C. The reason for the curvature of the 10% plot was not apparent but the initial slope was used.

% 2-pentanone	Concentration of pentanone mol litre^{-1}	Rate of Acetone Production mol $\mu l^{-1} min^{-1}$ x 10^{12}
100	9.44	216
50	4.72	190
25	2.36	174
10	0.944	142

5. DISCUSSION

As has already been explained, the results are divided into two sections, those on cis-trans isomerisation and those on the quenching of the Norrish type II process. (Chapters 3 and 4 respectively). As these systems are not directly related they will be dealt with separately.

ISOMERISATION OF METHYL TIGLATE

5.1 The De-conjugation Reaction

The formation of the β-γ-unsaturated ester (III) is noticed in all direct photolyses of the cis-trans isomers methyl tiglate and methyl angelate. (See Section 3.3).

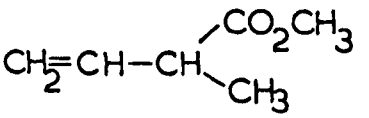

(III)

Rate curves show that the direct precursor of this compound is the angelate and not the tiglate as an induction period is observed with the latter. Formation of compound (III) is not observed in the photosensitised reaction suggesting that the de-conjugation reaction is a singlet process. Photolysis in deuterated methanol leads to the incorporation of deuterium on carbon atom 3.

An acyclic mechanism fails to explain why the precursor is methyl angelate alone and the conclusion is that the double bond migration takes place through a cyclic intermediate by analogy

with the Norrish type II photoelimination reaction.

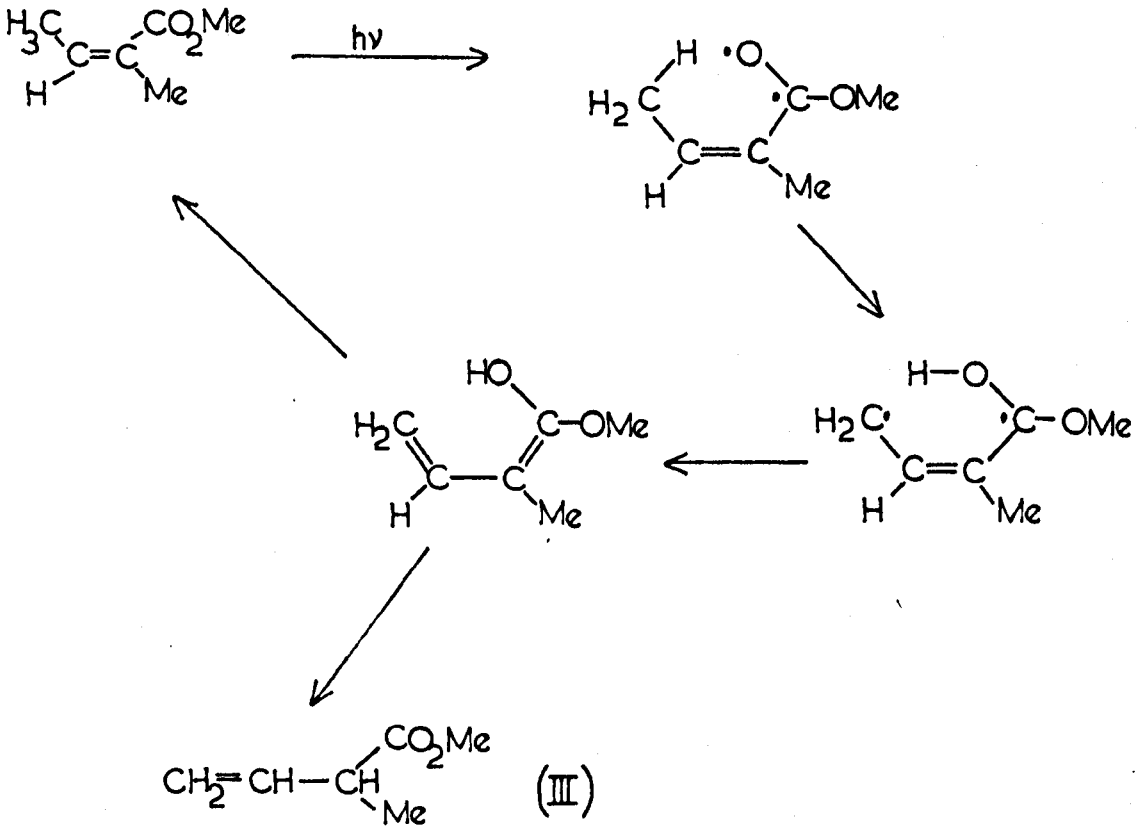

The participation of a six-membered intermediate of the type shown above explains the fact that the ester group must be cis with respect to the γ-carbon atom. The intermediacy of an enol form of the product explains the incorporation of deuterium which becomes attached to carbon atom 3 in the product (III). Similar observations have been made by a number of authors, in particular Barltrop and Wills[1] who studied this reaction in ethyl crotonate.

They also observed that the rate of photoisomerisation to (III) in alcoholic solvents is about twice that in benzene, ether or acetonitrile. This probably reflects a stabilisation of the hydroxy biradical intermediate by hydrogen bonding with the solvent. Jorgenson[2] has also studied the solvent effects of this reaction and found a large deuterium solvent isotope effect on the rate of bond migration in a similar ester. She found a tenfold increase in rate for bond migration in MeOD as compared to MeOH.

The excited state involved in this reaction is probably the n,π^* singlet state of methyl angelate (as the reaction does not occur on photosensitisation) although it is conceivable that a triplet state higher than T_1 could be involved. In the similar type II process it was shown that ketones with lowest π,π^* triplets do not undergo intramolecular hydrogen abstraction reactions whilst those with lowest n,π^* triplets do.[3, 4] If the same difference in reactivity can be assigned to the singlet states, the fact that reaction to form (III) occurs in this system suggests that the lowest excited singlet is n,π^* and not π,π^* in character, although this is not clear from the absorption spectra. The fact that no shoulder or side peak is seen in the U.V. indicates that the energy gap between the two singlets is small. In studies on cyclopropyl acrylic esters Jorgenson[5] came to the conclusion that the photochemical de-conjugation reaction was a reaction of the n,π^* excited singlet and that where the π,π^* singlet was lowest in energy

other reactions predominated.

5.2 Thermal Isomerisation

As has been mentioned in Chapter 1, thermal isomerisations of ethylenic compounds have been found to fall into two classes: those with first order rate constants of the order of $10^{4}\exp.(-25000/RT)$ and those with rate constants around $10^{11}\exp.(-45000/RT)$.[6, 7] Magee, Shand and Eyring showed that two mechanisms can be invoked to explain these rate constants. In the former case, the low activation energy is explained by crossover to the triplet state whilst in the latter case the value is explained in terms of isomerisation in the singlet state involving a higher activation energy but also a higher frequency factor (see Fig. 1.3). Since the triplet energies of simple olefins have energies of 250 - 330 kJ mol^{-1} in excess of the ground state, the triplet mechanism is effectively ruled out in cases where the energy difference between singlet and triplet is small in the perpendicular configuration.[7] Many results in the earlier literature have suggested triplet mechanisms for isomerisations based on low measured activation energies, but in many cases it has been shown that the singlet mechanism pertains when care is taken to avoid heterogeneous catalysis. A recent paper on the thermal isomerisation of the styrylpyridines[8] has shown that, in certain cases, changeover from a triplet to a singlet mechanism takes place as the temperature is raised and the higher activation energy becomes less of a barrier.

Butler and Small[9] have studied the thermal isomerisation of

methyl crotonate - a compound closely related to methyl tiglate. They found that it undergoes a homogeneous unimolecular cis-trans isomerisation in the gas phase at temperatures from 400 - 560°C. The rate constant was found to be independent of pressure in the range 13.3 to 1333 Nm^{-2} and the equilibrium trans/cis ratio was approximately 4.5 and independent of temperature in the range studied. They found $k = 10^{13.2}\exp.(-242 \pm 6.3\ kJ/RT)$. It was also found that simultaneous free radical reactions also occur of which the most important was de-conjugation to methyl vinyl acetate, which is analogous to the photochemical production of compound (III) discussed in Section 5.1. Lin and Laidler[10] quote values for the Arrhenius parameters of several ethylenic compounds whose thermal isomerisation has been investigated and found to proceed through a singlet pathway. Activation energies measured vary from 272 kJ mol^{-1} for cis-butene to 174 kJ mol^{-1} for cis-methyl cinnamate. A value of 215 ± 15.5 kJ mol^{-1} is quoted for crotonitrile[11] which is another molecule similar to methyl tiglate. The value quoted for cis-stilbene is 179 kJ mol^{-1}.

It seems likely that the parameters for methyl tiglate isomerisation will be similar to those of methyl crotonate found by Butler and Small, i.e. an activation energy of 240 kJ mol^{-1} and a normal frequency factor of around $10^{13}s^{-1}$. Although the observations in Section 3.4 are limited, it can be said that the observed rate is consistent with these parameters. (The observed 7% conversion after 92h at 300°C corresponds to a first order rate

constant of approx. $10^{-8}s^{-1}$ whilst the predicted value is approx, $10^{-8.5}s^{-1}$).

5.3 The Potential Energy Diagram of Methyl Tiglate/Angelate

The α,β-unsaturated ester system is basically a modified butadiene structure. An approximate energy level diagram determined from simple Hückel M.O. calculations (neglecting overlap) is presented in Fig. 5.1.[12] The energy levels of an enone are shown for comparison. The two transitions which should be seen in the accessible ultra-violet, the n-π* and the π-π* are indicated by arrows. As has already been discussed, it seems likely that these transitions are very close in energy in methyl tiglate and that the lowest excited singlet state is n,π* in character. As an estimate of the energy of this transition, the onset of absorption in the U.V. can be taken as 260 nm. This corresponds to an energy of 456 kJ mol^{-1}.

Estimates of the lowest triplet energy of methyl tiglate can be made from two sets of observations. Spectroscopic estimates of the 'vertical' triplet energy in ethyl iodide solution (See Section 3.14) put the triplet energy at approx. 300 kJ mol^{-1}. Photosensitisation also indicates the energy of the lowest triplet state of methyl tiglate, although these estimates do not take into account 'non-vertical' energy transfer if operative. It was found that the isomerisation of methyl tiglate is sensitised by acetone, benzophenone and acetophenone. In the case of acetone and acetophenone the photostationary state ratio of trans/cis was unity

Fig. 5.1.

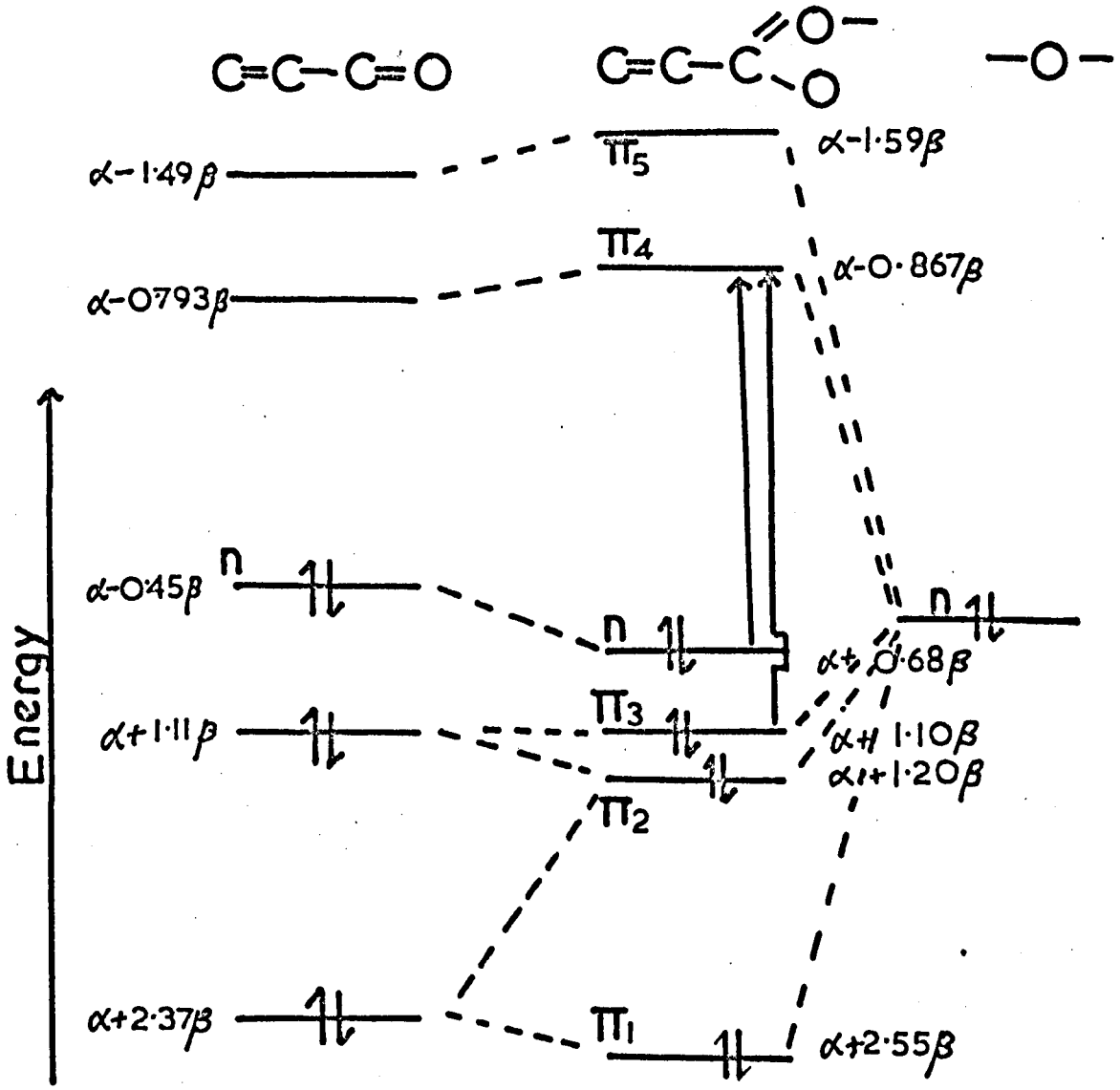

Taken from reference 11.

suggesting that the triplet energy of the sensitiser is greater than that in the two isomers. (See introduction). With benzophenone the trans/cis stationary state ratio increases to 1.13. This suggests a triplet energy for methyl angelate of between 310 and 288 kJ mol^{-1}, the triplet energies of acetophenone and benzophenone respectively.[13]

Barltrop and Wills[1] found that acetone, benzophenone and acetophenone sensitised the isomerisation of ethyl crotonate but did not try sensitisers of lower energy. Jorgenson and Gundel[14] found that the same three sensitisers photosensitised the isomerisation of a tertiary butyl crotonic ester but that acetonaphthone (E_T = 247 kJ mol^{-1}) and phenanthrene (E_T = 260 kJ mol^{-1}) did not act as sensitisers. This is consistent with the triplet energy estimated above and also with that of simple enones. Brand and Williamson found this to be around 290 kJ mol^{-1} for acrolein.[15]

The nature of the lowest triplet state is open to question. Some controversy has surrounded the assignment of this state in α,β-unsaturated ketones. Yang et al.[16] have suggested that the differences in reactivity towards de-conjugation reactions in α,β-unsaturated ketones can be rationalised by saying that the unreactive ketones are those that possess π,π^* lowest triplets. This has been discussed by Wagner and Hammond[17] in their review of the reactions of the triplet states of organic molecules. They point out that in many cases any n,π^* states formed decay rapidly to a relatively unreactive π,π^* triplet. They also show that much of the lack of reactivity in enones can be ascribed to rapid relaxation to a twisted

triplet state in which the hydrogens on the γ-carbon atom of the enone are bent too far away from the carbonyl oxygen for reaction to occur. Finally, they suggest that some of the reactivity of such compounds could be explained by reaction in the n,π* singlet state occurring fast enough to compete with inter-system crossing to the triplet state.

Some confirmation of this idea that there is relaxation to a twisted unreactive state in unsaturated ketones is given by the calculations of potential energy diagrams mentioned in Chapter 1. Combining the results of Becker et al.[18] and McCullough et al.[19] discussed in Section 1.6(f), the potential energy diagram for acrolein for the lowest excited states and the ground state should be shown by Fig. 5.2. Since acrolein is a symmetrical molecule, in the isomerisation sense, the shape of these curves is symmetrical about 90° of twist. This will not be the case in molecules possessing distinct cis and trans isomers, when generally the energy of the cis planar isomer will be higher than that of the trans planar isomer. The relative displacement of these curves is subject to considerable uncertainty but it seems that in acrolein there is a crossover between n,π* and π,π* triplet states at around 30° of twist about the double bond. The shape of the n,π* singlet excited state curve was not calculated by either of the above sets of authors although McCullough did show that the n,π* triplet state increases in energy on twisting. It seems reasonable to suppose that the equivalent singlet state behaves in a similar fashion. A simple picture of the bonding would

Fig.5.2

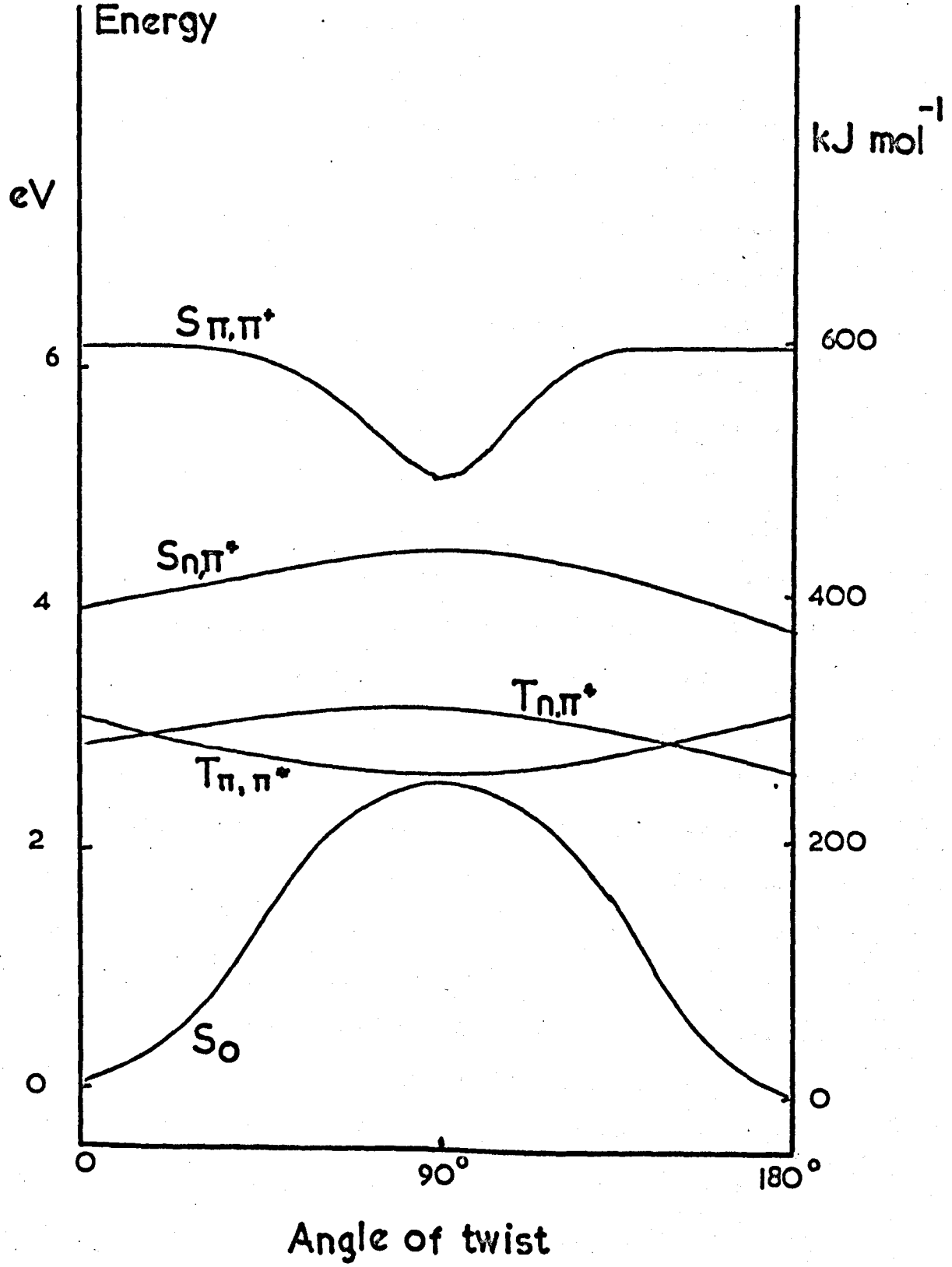
Energy
eV
kJ mol⁻¹
Sπ,π*
Snπ*
Tnπ*
Tπ,π*
So
6
4
2
0
600
400
200
0
0
90°
180°
Angle of twist

suggest that in an n,π* excited state there is still a certain amount of resistance to rotation remaining in an ethylenic bond whilst in a π,π* excited state there is effectively only a single bond with no resistance to rotation. Since the n,π* and π,π* triplets are so close together in acrolein it is quite possible that in homologous carbonyl compounds the relative energies of the two states may change with substitution and solvent effects explaining the different reactivities of similar compounds.[16, 17]

The effect of introducing another oxygen into the π-system as in methyl tiglate will clearly have a considerable effect on the potential energy curves for excited states. Inspection of Fig. 5.1 shows that the n-π* transition is increased in energy to a greater extent than the π-π*, though both are increased relative to acrolein. This is reflected in the U.V. spectrum of methyl tiglate as compared to an α,β-unsaturated ketone. The large high intensity π,π* peak is not shifted as much as the smaller 'forbidden' n,π* peak which undergoes a hypsochromic shift to the extent that it is hidden under the main peak. These shifts correspond to approx. 20 kJ mol^{-1} for the π,π* singlet and approx. 138 kJ mol^{-1} for the n,π* singlet.

The resulting diagram should be represented by Fig. 5.3, though this is of necessity highly speculative. In this diagram it is assumed that the equilibrium geometry of methyl angelate is not planar but twisted by some 30° in order to reduce the steric hindrance between the methyl and ester groups. This was observed for stilbene[20] (though in this case the repulsion was electronic as

Fig. 5.3

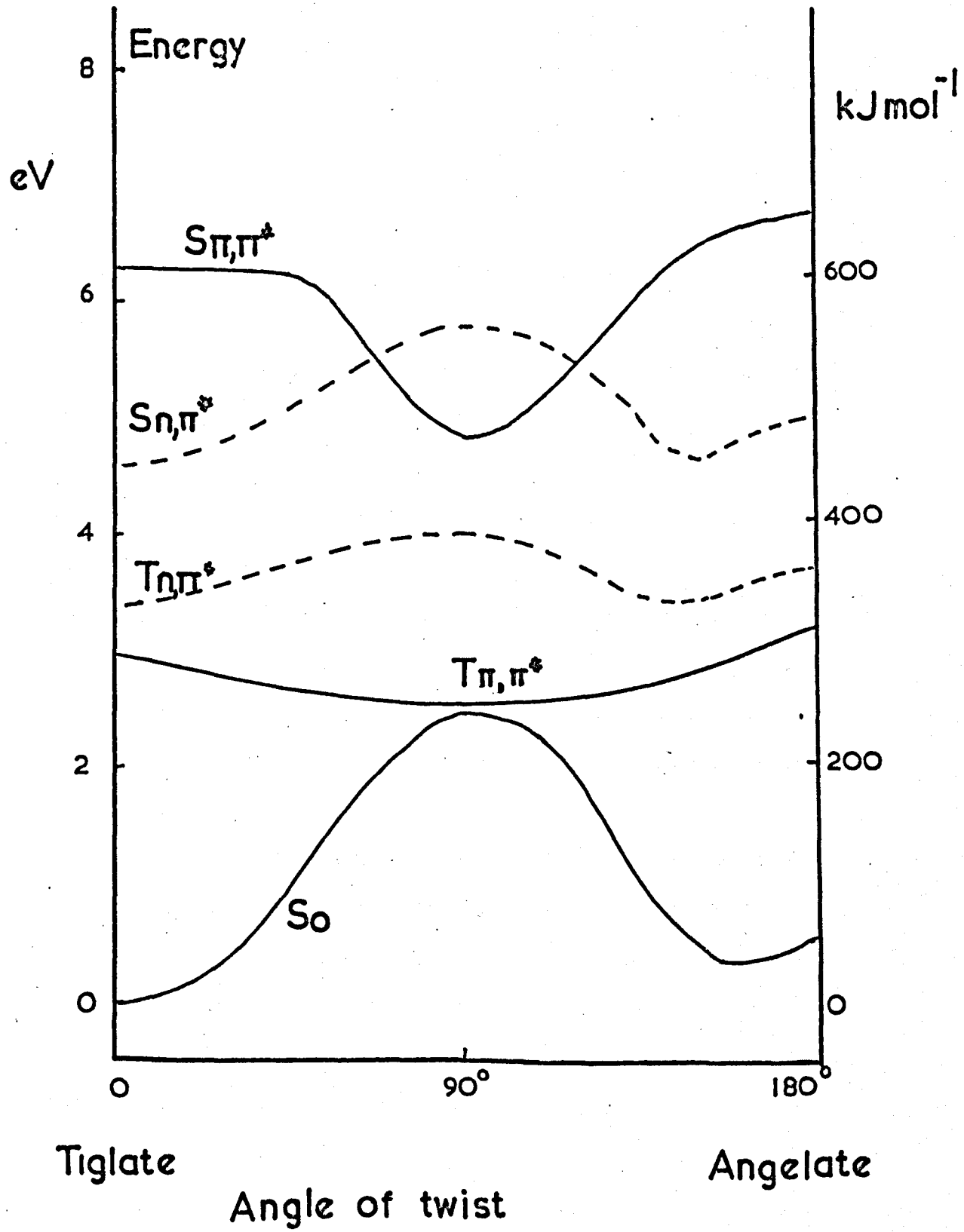
Energy
eV
kJmol⁻¹
8
6
4
2
0
600
400
200
0
Sπ,π*
Sn,π*
Tn,π*
Tπ,π*
So
0
90°
180°
Tiglate
Angelate
Angle of twist

steric factors were not allowed for in the calculations). The curve for the triplet n,π^* state has been moved up in energy compared to acrolein on the basis that the separation between n,π^* singlet and triplet states is smaller than with π,π^* states. The energy barrier in the ground state can be directly equated with the activation energy for the thermal isomerisation estimated above to be about 240 kJ mol^{-1}. This figure is in good agreement with the value estimated for acrolein by Becker[18] of around 250 kJ mol^{-1}. An important assumption in this diagram is that the n,π^* and π,π^* singlet states cross in the twisted configuration.

5.4 Mechanism for Direct Isomerisation

The observations that have to be explained by an isomerisation mechanism are

1. Low quantum yields for isomerisation in both directions. ϕ trans → cis = 0.090 and ϕ cis → trans = 0.032 at 25°C. These appear to be independent of concentration and are possibly subject to a small temperature effect. (The more reliable semi-micro results are taken).

2. Quenching of direct isomerisation of tiglate to angelate by oxygen and paramagnetic salts to the same extent i.e. by 28%.

Clearly it is not easy to explain these observations on the basis of the predicted energy diagram in Fig. 5.3. However, diagrams which would explain the results more easily do not fit in with the predictions of other work in the field. Starting with methyl tiglate, excitation at 254 nm causes molecules to be raised

to first excited n,π* singlet, in which state a considerable barrier to rotation is predicted. From this state the quantum yield shows that 9% of the excited molecules isomerise and 91% return to the original configuration. Possible sites for isomerisation are either the singlet or triplet π,π* states both of which are predicted to have energy minima at around 90° of twist.

It is proposed that most of the isomerisation takes place in the singlet π,π* state but that some of the molecules cross into the triplet π,π* state and isomerise there. Any molecule which gets into a state represented by the bottom of a potential well in the perpendicular form will isomerise with a quantum efficiency of 0.5. It is suggested that there is a fairly low probability associated with the crossover in the excited singlet states as this involves a change in electronic symmetry; in the same way that there is a low probability associated with excitation to an n,π* state in the first instance. This combination of an energy barrier and a low probability could explain the low quantum yield in the singlet state. It is a necessary postulate that there is a highly efficient means of returning to the ground state with retention of configuration by internal conversion, fluorescence or inter-system crossing.

It would be interesting to have information on the fluorescence and phosphorescence yields of these compounds but equipment was not available for such measurements. The natural fluorescence lifetime of an excited state can be calculated

approximately from the formula,

$$\tau_o = \frac{3.47 \times 10^8}{\omega^2} \Big/ \int \varepsilon d\omega \qquad 21$$

where ω is the frequency of the absorption band in the U.V. and ε is the extinction coefficient. If the n,π^* absorption peak were a triangle centered at 250 nm with a half-width of 5×10^3 cm^{-1} and $\varepsilon max = 150$ $l.mol^{-1}cm^{-1}$ then τ_o would be approximately 3×10^{-7}s, although the n,π^*peak is not observed. Other processes should be faster than this so that fluorescence is probably not an important decay process.

Inspection of Fig. 5.3 shows that inter-system crossing to the triplet state should result in efficient isomerisation. The fact that this is not the case suggests that the dominant mode of deactivation from the excited singlet state is radiationless internal conversion. The mechanism for this decay is not clear since the excited molecule must lose over 420 kJ mol^{-1} of electronic energy, though in solution loss of such energy by collision is more favourable than in the gas phase. The mechanism of radiationless internal conversion is not yet fully understood. (See for example reference 22). Low quantum yields for direct isomerisation are not confined to this system. Direct excitation of the 1,3-pentadienes gives $\phi c \rightarrow t = 0.09$ and $\phi t \rightarrow c = 0.11$.[23] Saltiel explains this by assuming the intermediacy of cyclopropyl methylene biradicals which cannot undergo cis-trans isomerisation (See Section 1.6(b)), but this

explanation is only speculative. Whitten and McCall[24] found that the quantum yields for direct isomerisation of the stilbazoles and 1,2-bis-pyridyl-ethylenes (nitrogen containing analogues of stilbene) were much lower than those observed in stilbene and also lower than those observed with photosensitisers. For instance, ϕ trans→cis in 4,4'-bis-pyridyl-ethylene is 0.003 whilst in stilbene it is 0.48. They point out that there is evidence for azaaromatics with lowest lying n,π^* singlet states having rapid rates of internal conversion. It is known that pyridine neither fluoresces nor phosphoresces and photosensitisation studies with 2-butene indicate very low quantum efficiencies for formation of the pyridine triplet.[25] In spite of this no permanent or transient products have been detected.[26] Hochstrasser and Marzzacco[27] concluded that compounds which have either n,π^* lowest excited states or π,π^* states where n,π^* -π^*,π^* mixing occurs show enhanced rates of radiationless decay. They have suggested recently[28] that, "overlap or mixing of orbitally different states causes a severe breakdown of the Born-Oppenheimer approximation with consequential broadening of electronic spectra and acceleration of radiationless transitions".[24] They say that this spectral broadening should be apparent at low temperatures and in regions of n,π^* - π,π^* overlap. It seems possible that these remarks can be taken to apply to the esters studied here, which have lowest n,π^* singlet states (or singlet states with mixed n,π^* - π,π^* character) However, although a high yield of internal conversion is implicated spectral broadening is not apparent at normal temperatures.

Quenching by paramagnetic species could be explained by saying that those molecules isomerising in the triplet state are progressively quenched but that those molecules isomerising in the singlet state are unaffected. Once in the middle of the potential well quenching to the ground state will not affect the degree of isomerisation in a molecule. The lower yield of cis→trans isomerisation can be explained by saying that the barrier to crossover in the excited singlet states is greater than in the reverse process so that internal conversion becomes even more favourable. (De-conjugation to compound (III), $\phi = 0.005$ does not have much effect on the isomerisation).

If the assumption is made that only the triplet reaction is quenched by paramagnetic ions and that isomerisation proceeds via singlet and triplet mechanisms then a modified Stern-Volmer mechanism can be applied (see later).

$$(R_A - R_A^{\infty})^{-1} = A/I + B[Q]/I$$

where R_A is the rate of angelate production and I is the intensity. [Q] is the quencher concentration and A and B are constants compounded of the various rate constants. R_A^{∞} is the rate of angelate production when the reaction is fully quenched (i.e. singlet reaction). A plot of $(R_A - R_A^{\infty})^{-1}$ against [Q] gives a straight line of slope/intercept $= B/A = k_q\tau$, where kq = rate constant for quenching τ = triplet lifetime. The values of these variables for quenching by Mn^{2+} ions are tabulated

below. (See Section 3.21)

$R_A^{\infty} = 1.15 \times 10^{11}$

Concentration of Mn^{2+}, Molar, [Q]	Rate of Angelate Production mol $min^{-1}\mu l^{-1}$ x 10^{11}	$R_A - R_A^{\infty}$ mol $min^{-1}\mu l^{-1}$ x 10^{-11}	$(R_A - R_A^{\infty})^{-1}$ $mol^{-1} min\ \mu l$ x 10^{-11}
0	1.60	0.47	2.13
0.0164	1.33	0.20	5.0
0.103	1.19	0.06	16.7
0.205	1.16	0.03	33.3

The modified Stern-Volmer plot is shown in Fig. 5.4. Slope/Intercept = 70.4 l mol^{-1}. If kq is taken as being diffus ion controlled then it should have a value of approximately 5×10^9 l $mol^{-1}s^{-1}$. [29] A value of $\tau = 1.41 \times 10^{-8}$S is thus indicated. This is a very reasonable value for a triplet lifetime in solution. (See for example reference 30). The value of R_A^{∞} also indicates that 28% of the isomerisation proceeds via the triplet mechanism.

5.5 Photosensitisation

If Fig. 5.3 is a fair representation of the potential energy curves for the triplet states of methyl tiglate then simple excitation of the lowest triplet state (π,π^*) should result in ideal yields for isomerisation ($\phi c \rightarrow t = \phi t \rightarrow c = 0.5$) assuming that the quantum yield of inter-system crossing in the sensitiser is unity as has been shown in

Fig. 5.4

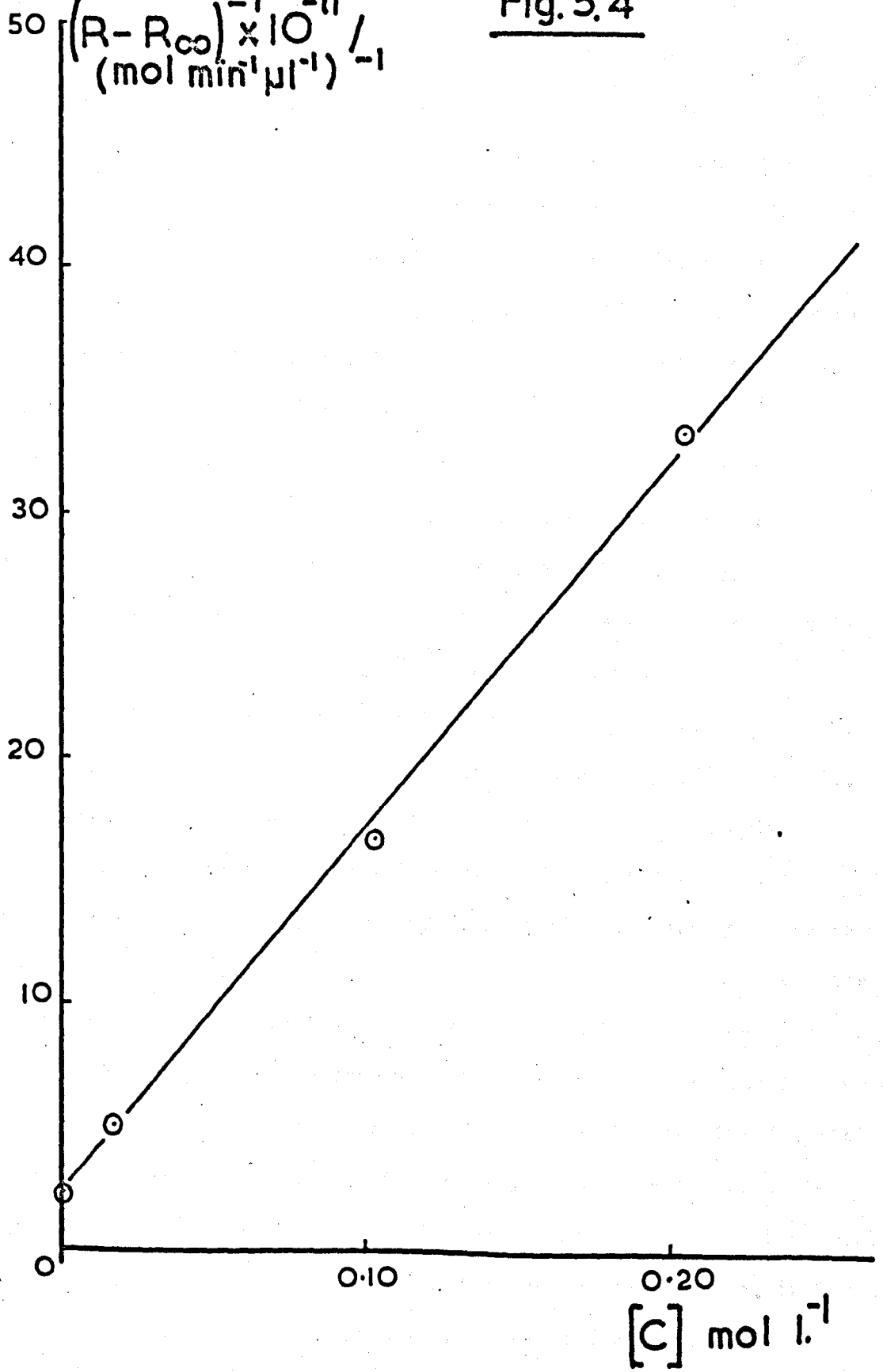
$(R-R_{co})^{-1} \times 10^{-11}$ / l^{-1}
(mol min^{-1} μl^{-1})
50
40
30
20
10
0
0·10
0·20
[C] mol $l.^{-1}$

the phenyl ketones.[31, 32] These yields are not observed with any of the sensitisers tried. Photosensitisation seems to be accompanied by addition to form oxetanes, at least in the case of benzophenone and anthraquinone. Another interesting point is that biphenyl does not act as a sensitiser for the reaction whilst anthraquinone is an energy donor, albeit an inefficient one. This is despite the fact that the triplet energy of biphenyl is considerably higher than that of anthraquinone (275 kJ mol^{-1} as against 263 kJ mol^{-1}). At the same time the triplet energy of anthraquinone is below that of methyl tiglate as predicted by ethyl iodide spectra and theoretical considerations. (Fig. 5.3).

Similar observations have been made by other workers using different cis-trans isomers.[33 - 35] Yang et al. studied the photosensitised isomerisation of 3-methyl-2-pentene using benzaldehyde (E_T = 299 kJ mol^{-1}), benzophenone (E_T = 278 kJ mol^{-1}), and triphenylene (E_T = 278 kJ mol^{-1}). Their results clearly indicated that, in the systems investigated, the Paterno-Büchi reaction to form oxetanes competed with bimolecular energy transfer to the olefin, with resulting isomerisation. Benzophenone transferred energy more effectively than benzaldehyde, and triphenylene, despite a triplet energy only marginally below benzophenone, was completely ineffective as a photosensitiser. They found that the triplet state of the carbonyl compound was the common intermediate for both the oxetane formation and the olefin isomerisation and that the bimolecular rate constants for olefin isomerisation, or energy transfer, in these systems were substantially less than for collisional transfer or

diffusion-controlled rate processes.

To explain their results they suggested that the mechanism of energy transfer was via a biradical Schenck intermediate.[36]

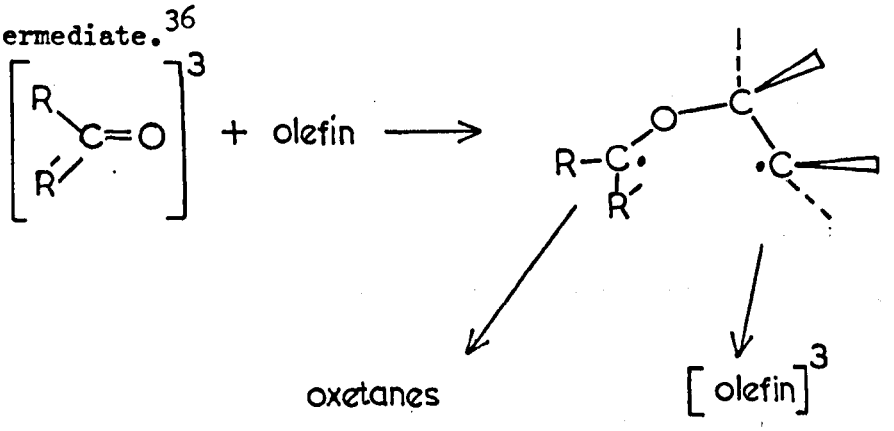

Schematically, the biradical intermediate may cyclise to give the oxetanes or dissociate to give back the carbonyl compound and the triplet state of the olefin in a non-planar configuration (or isomerisation may take place by rotation around the single bond in the biradical intermediate). The low quantum yields of isomerisation are explained by the competing oxetane formation. In this way energy transfer involves two steps and consequently there is no violation of the Franck-Condon principle involved in the concept of 'non'vertical' energy transfer to olefins as suggested by Hammond et al. (See reference 37 and Chapter 1). An alternative way of looking at this process is to say that the vacant n orbital of the n,π^* triplet state of the donor may polarise the π system of the olefin

during the energy transfer process so that the olefin moiety in the transition state is no longer planar. It is well known that the Paterno-Büchi reaction involves the n,π^* state of the carbonyl compound[38] and this explains why compounds with lowest lying π,π^* triplets such as triphenylene do not take part in this endothermic energy transfer.

Saltiel et al.[35] have extended these ideas by suggesting that different processes are involved with different sensitisers. They suggest that with high energy sensitisers the triplet energy transfer process, in which olefin triplets are formed by excitation transfer from the sensitiser, is dominant but as the sensitiser triplet energy is lowered the Schenck intermediate becomes increasingly involved. The simplest general scheme for sensitised cis-trans photoisomerisation is given below where X* represents an unspecified common intermediate and other symbols have their usual meanings.

$S^o \rightarrow S^1 \rightarrow S^3$	$h\nu$
$S^3 \rightarrow S^o$	k_4
$S^3 + t^o \rightarrow X^*$	k_5
$S^3 + c^o \rightarrow X^*$	k_6
$X^* \rightarrow \alpha t^o + (1-\alpha)\, c^o$	k_7

(c = cis, t = trans and S is sensitiser).

Applying the steady state approximation to S^3 and X* the

following relationships can be shown :

$$([t]/[c])_{s.s.} = (k_6/k_5)\alpha/(1-\alpha)]$$

$$1/\phi_{t\rightarrow c} = 1/(1-\alpha)\ (1 + k_4/k_5[t])$$

$$1/\phi_{c\rightarrow t} = 1/\alpha(1 + k_4/k_6[c])$$

The top equation represents the photostationary trans/cis ratio. The efficiency of inter-system crossing is taken as unity and oxetane formation is neglected. This is valid so long as oxetane formation does not depend on the isomer used and oxetane formation is a minor reaction. Reaction 4 includes any reaction with the solvent.

If these assumptions are applied to the system benzophenone + methyl tiglate/angelate (Section 3.19) then the values of ϕ^{-1} against (ester concentration)$^{-1}$ are tabulated below.

Initial Tiglate concentration mol litre^{-1}	(Tiglate)$^{-1}$ concentration	$\phi_{t\rightarrow ang.}$	$(\phi_{t\rightarrow a})^{-1}$
0.0100	100	0.087	11.5
0.0133	75.2	0.115	8.70
0.0200	50	0.141	7.10
0.0400	25	0.187	5.35
0.0600	16.7	0.266	3.76

Initial Angelate concentration mol litre^{-1}	(Angelate)$^{-1}$ concentration	$\phi_{ang.\rightarrow t}$	$(\phi_{a\rightarrow t})^{-1}$
0.00826	121	0.103	9.67
0.0100	100	0.128	7.81
0.0133	75.2	0.147	6.80
0.0200	50	0.196	5.10
0.0400	25	0.278	3.60

These quantum yields are calculated on the basis of an intensity of 5.61×10^{14} quanta $s^{-1}cm^{-2}$. With a benzophenone concentration of 5×10^{-3} mol litre^{-1} the light absorbed is 49.9% of incident intensity in 1 cm path length.

Plots of [ester]$^{-1}$ vs. ϕ^{-1} are shown in Fig. 5.5. The plots are good straight lines suggesting that the proposed simple mechanism is valid. They are also very similar to those obtained by Saltiel et al. in reference 35. The decay ratio, $\alpha/(1-\alpha)$, is obtained from the ratio of the intercepts in Fig. 5.5 = 1.20. The ratio of the slopes = 1.46 and should represent $(k_6/k_5)(\alpha/(1-\alpha))$, the photostationary ratio. This was determined at 1.13 experimentally and probably reflects the fact that the true photostationary state had not been reached in the experiment. Alternatively oxetane formation may occur preferentially from one geometric isomer. Other information obtained from these plots is that the excitation ratio, k_6/k_5 = 1.21 and the limiting quantum yields at high ester concentration are 0.416 and 0.50 for tiglate to angelate and angelate to tiglate

Fig. 5.5

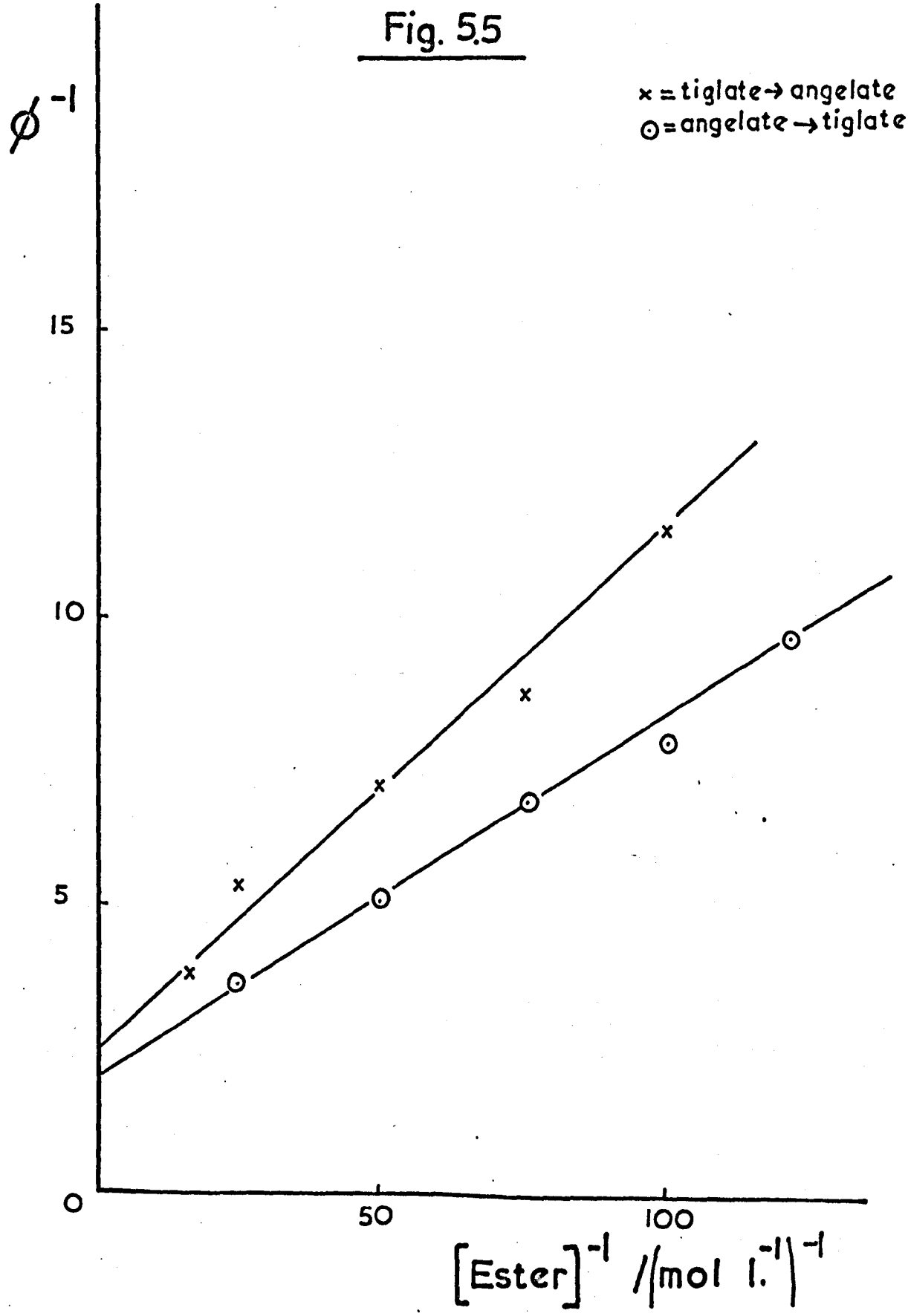
× = tiglate → angelate
⊙ = angelate → tiglate
ϕ^{-1}
15
10
5
0
50
100
$[\text{Ester}]^{-1}$ /(mol $l.^{-1}$)$^{-1}$

respectively.

The results obtained are similar to those obtained from the acetone photosensitised isomerisation of 2-pentene.[35] These were that the excitation ratio = 1.30, the decay ratio = 1.17 and the observed and predicted photostationary ratios = 1.52. Saltiel explained these results on the basis that the deviation of the decay ratio from unity is a measure of the involvement of the Schenck intermediate in the photoisomerisation. Thus the decay ratio of 1.20 obtained above indicates that the photosensitisation proceeds largely by triplet excitation transfer and that the Schenck intermediate is involved to a minor extent. This fits in with the suggestion made in Section 5.3 that energy transfer from benzophenone is very slightly exothermic. It is expected that with acetone the mechanism will be exclusively triplet excitation transfer but that with anthraquinone the Schenck mechanism should predominate with a high photostationary ratio. (Saltiel found that with energy transfer from acetophenone to 2-pentene the decay ratio was 1.90 and the photostationary state ratio was predicted as 5.4. They found that with low energy sensitisers the photostationary ratio was close to the thermodynamic ratio). The fact that biphenyl does not act as a sensitiser reflects the fact that its triplet is π,π^* in nature and does not form a Schenck intermediate.

It would be of interest to carry out further studies along these lines which lack of time did not permit in the present study.

QUENCHING OF THE NORRISH TYPE II REACTION

The remainder of this discussion deals with the second part of the work. The results for this study of the photoelimination reaction in ketones are described in Chapter 4. The work is introduced in Section 1.5 of the Introduction.

5.6 Background to Present Work

The study outlined in Chapter 4 was initiated by the results of Borrell and Sedlar,[39] obtained in this laboratory. During the course of a wider study of the reactions of ketones and olefins, they came upon an interesting observation concerning the quenching of the photoelimination reaction in 2-pentanone by cyclohexene. Cyclohexene was found to be an inefficient quencher of this reaction and the rate of acetone formation was found to drop, as expected, to a limiting value at high cyclohexene concentration. Less expected, was the fact that the rate of consumption of pentanone increased with increasing cyclohexene concentration. The two curves for rate against olefin concentration were found to be symmetrical and the assumption was made that the quenching took place by compound formation to form an addition product, presumably an oxetane, though this was not investigated.

In order to discuss the results of Chapter 4 in this light it is necessary to outline the kinetics behind their approach. The following mechanism was postulated :

$P + h\nu \rightarrow P^1$	I
$P^1 \rightarrow P$	k_1
$P^1 \rightarrow P^3$	k_2
$P^1 \rightarrow$ Type II products	k_{3a}
$P^1 \rightarrow$ Cyclobutanol products	k_{3b}
$P^3 \rightarrow P$	k_4
$P^3 \rightarrow$ Type II products	k_{5a}
$P^3 \rightarrow$ Cyclobutanol products	k_{5b}
$P^3 + C \rightarrow$ Addition products	k_6

In the above, P represents 2-pentanone and P^1 and P^3 its excited singlet and triplet states. C represents cyclohexene. It has been shown by Wagner and Hammond[40] that both types of product are produced by both singlet and triplet states (See Section 1.5). In this case the type II products are acetone and ethylene. Only acetone was followed and the difference between the rate of production of acetone and the rate of consumption of pentanone was taken to represent the rate of production of cyclobutanol, at zero olefin concentration. The addition products in reaction 6 were taken to be similar to those found in a separate study of the reactions of acetone and cyclohexene.[41] This seems reasonable as cyclohexene is known to form oxetanes with a variety of carbonyl compounds.[42] The increase in ketone consumption is due to the fraction of excited molecules which normally revert to the ground state by reaction 4 which are consumed by reaction 6 in the presence of olefin.

Steady state approximations can be made for P^1 and P^3. Expressions can then be derived for the rate of production of acetone, R_A, and the rate of consumption of ketones, $-R_p$, where I is the light absorbed.

$$R_A = A\left(k_{3a} + \frac{k_2 k_{5a}}{k_4+k_5+k_6[C]} \right)$$

$$-R_p = A\left(k_3 + \frac{k_2(k_5+k_6[C])}{k_4+k_5+k_6[C]} \right)$$

If the superscripts o and ∞ refer to zero and limiting olefin concentration then the limiting rates can be expressed as

$$R_A^{\,o} = A\left(k_{3a} + \frac{k_2 k_{5a}}{k_4+k_5} \right)$$

$$R_A^{\,\infty} = \frac{k_{3a} I}{k_1+k_2+k_3}$$

$$-R_p^{\,o} = A\left(k_3 + \frac{k_2 k_5}{k_4+k_5} \right)$$

$$-R_p^{\,\infty} = A\left(k_2+k_3\right)$$

In the above $k_3 = k_{3a} + k_{3b}$, $k_5 = k_{5a} + k_{5b}$ and $A = (I/k_1+k_2+k_3)$.

Modified Stern-Volmer relationships can be used by plotting $(R_A - R_A^{\infty})^{-1}$ versus [C] with slope/intercept equal to K_6/k_4+k_5) and $(-R_p+R_p^{\,o})^{-1}$ versus $[C]^{-1}$ with slope/intercept equal to $(k_4+k_5)/k_6$. Borrell and Sedlar obtained reasonable straight line plots for these relationships giving values of 20 and 18.2 $l.mol^{-1}$ for $k_6/(k_4+k_5)$. They therefore concluded that the mechanism is valid. Having established the mechanism, they then went on to show that by taking ratios of limiting rates and the quantum yield for zero quencher, the proportions of the various internal processes in the ketone can be established. If it is assumed that singlet and triplet states break down in the same proportion to type II and cyclobutanol products, then

$$\frac{R_A^{\,o}}{-R_p^{\,o}} = \frac{k_{3a}}{k_3} = \frac{k_{5a}}{k_5} = 0.70$$

From equations above, $\dfrac{R_A^{\infty}}{-R_p^{\infty}} = \dfrac{k_{3a}}{k_2+k_3} = \dfrac{0.7k_3}{k_2+k_3}$

From the rate vs. olefin concentration graph,

$$\frac{k_3}{k_2+k_3} = \frac{\text{singlet reaction}}{\text{total reaction}} = 0.15$$

$$\therefore \underline{k_3 = 0.175k_2}$$

$$\frac{-R_p^{\,o}}{-R_p^{\infty}} = \frac{k_3k_4 + k_3k_5 + k_2k_5}{(k_4+k_5)(k_2+k_3)}$$

Using $k_3 = 0.175k_2$, $\dfrac{0.85k_5}{k_4+k_5} + 0.149 = \dfrac{-R_p^{\,o}}{-R_p^{\infty}} = 0.65$

$$\therefore \underline{k_5 = 1.44k_4}$$

$$\phi^{\circ}_{-p} = \phi^{\circ}\text{singlet} + \phi^{\circ}\text{ triplet}$$

Borrell and Sedlar took a figure of 0.20 for the quantum yield of ketone consumption although this figure was not measured directly in their experiments but taken as an estimate from the results of Sedlar[43] in neat ketone and Hammond[44] in hexane solution (0.18 and 0.42 respectively). Using this figure and the ratios derived, together with the steady state conditions, a series of simultaneous equations can be set up and solved for the quantum yields of each process.

$$\phi_3 = 0.175\phi_2$$

$$\phi_5 = 1.44\phi_4$$

$$\phi_3 + \phi_5 = \phi^{\circ}_{-p} = 0.20$$

$$\phi_1 + \phi_4 = 0.80$$

$$\phi_1 + \phi_2 + \phi_3 = 1.00$$

Thus, $\phi_1 = 0.693$, $\phi_2 = 0.262$, $\phi_3 = 0.046$, $\phi_4 = 0.107$ and $\phi_5 = 0.154$.

The final picture emerging from this work can be represented diagrammatically below :

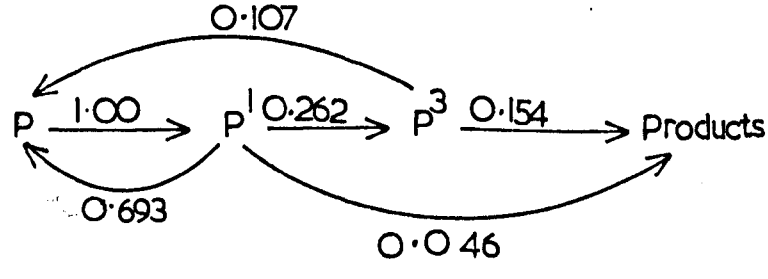

(Note that the figures in the original paper differ slightly as the authors used slightly different ratios from the graphs. The difference, however is small).

Wagner and Hammond[44] obtained a value for the quenching of the pentanone triplet by a piperylene, a ratio equivalent to $k_6/(k_4+k_5)$. They obtained the value $kq\tau = 50$ l.mol^{-1} or 2.5 times the equivalent rate for chemical reaction with cyclohexene. If the triplet lifetime is assumed to be the same in both cases then $k_6 = kq/2.5$. If Wagner's value of the diffusion controlled rate constant is taken as 5×10^9 l. mol^{-1}s^{-1} then $k_6 = 2\times10^9$ l.mol^{-1}s^{-1} and $k_4+k_5 = 10^8$s^{-1}. Using the ratios derived above, $k_4 = 4.1 \times 10^7$s^{-1} and $k_5 = 5.1 \times 10^{-7}$s^{-1}.

To obtain their results Borrell and Sedlar used the vacuum capillary technique described in Chapter 2. They used benzene as solvent at 313 nm. It was decided to repeat their experiments using the semi-micro technique and to try to apply the same method to different ketones. Different solvent media were tried to see if the reactions above were general.

5.7 Quenching Experiments in Benzene

The results above were repeated in benzene using the semi-micro method. The reaction in 4-methyl-2-pentanone with twice the number of γ-hydrogens and in 2-octanone with secondary γ-hydrogens was also followed. The plots of rate against concentration of cyclohexene are shown in Figs. 4.11 and 4.17 for 2-pentanone and 4-methyl-2-pentanone. The results for 2-octanone (q.v) show virtually no quenching in benzene.

The quality of the original data is rather poor and this is reflected in these results. This must be put down to the technique used. It seems that the semi-micro method, although the best method for studying the isomerisation results is not the best way of following the type II reaction. It is possible that the acetone production data is subject to a certain degree of error due to the purging effect of the nitrogen stream. Larger errors come in trying to follow the depletion of starting material. Due to evaporation of the solvent photolyses could not be carried out for longer than about 5h. Beyond this time errors due to changing concentration become significant. On the other hand, conversions obtained in this length of time are not large enough to fully overcome the inherent error of sampling with a microlitre syringe (±3%). Many points have to be taken in order to obtain a fair estimate of the rate of ketone depletion and these rates are subject to a large standard error. An alternative would be to use a cell of smaller volume with a larger incident light intensity, but such equipment was not available for this work. It should be pointed out, however, that the capillary technique would probably not be much better due to the difficulty of filling tubes uniformally with samples of relatively involatile solutes in a volatile solvent, such as 2-octanone in benzene. (See Chapter 2).

Having said this, it is still possible to obtain some useful figures from the results.

5.7(a) 2-Pentanone in Benzene

Inspection of Fig. 4.11 shows that the results obtained for this compound are qualitatively similar to those of Borrell and Sedlar.[39] The curves are not so symmetrical as the quenching of the acetone rate appears less than the increase in pentanone consumption on adding olefin. The rate of acetone production is 60.5% of the rate of ketone consumption at zero cyclohexane concentration. This compares with 70% found by Borrell and Sedlar[39] and 68% found by Wagner and Hammond.[40] Modified Stern-Volmer plots of $(R_A - R_A^{\infty})^{-1}$ vs.[C] and $(-R_p + R_p^{o})^{-1}$ vs. $[C]^{-1}$ can be drawn for these curves. The data for acetone production is tabulated below together with the equivalent data for 4-methyl-2-pentanone.

[C] mol $l.^{-1}$	R_A, mol $\mu l^{-1} \times 10^{12} min^{-1}$		$R_A - R_A^{\infty}$		$(R_A - R_A^{\infty})^{-1}$	
	Pentanone	4 - M - 2-Pentanone	Pentanone	4 - M - 2-Pentanone	Pentanone	4 - M - 2-Pentanone
0	25.2	40.0	16.0	26.5	0.0625	0.038
1	12.2	20.0	3.0	6.5	0.33	0.154
2	11.0	17.0	1.8	3.5	0.55	0.286
3	10.5	16.0	1.3	2.5	0.77	0.400
4	10.2	15.5	1.0	2.0	1.00	0.500
5	10.0	15.0	0.8	1.5	1.25	0.667
Limiting	9.2	13.5	0	0	∞	∞

The plots are shown in Fig. 5.6. The points fall on fair straight lines with slope/intercept ratios of 4.0 $l.mol^{-1}$ for 2-pentanone and 2.72 $l.mol^{-1}$ for 4-methyl-2-pentanone. For 2-pentanone

Fig. 5.6

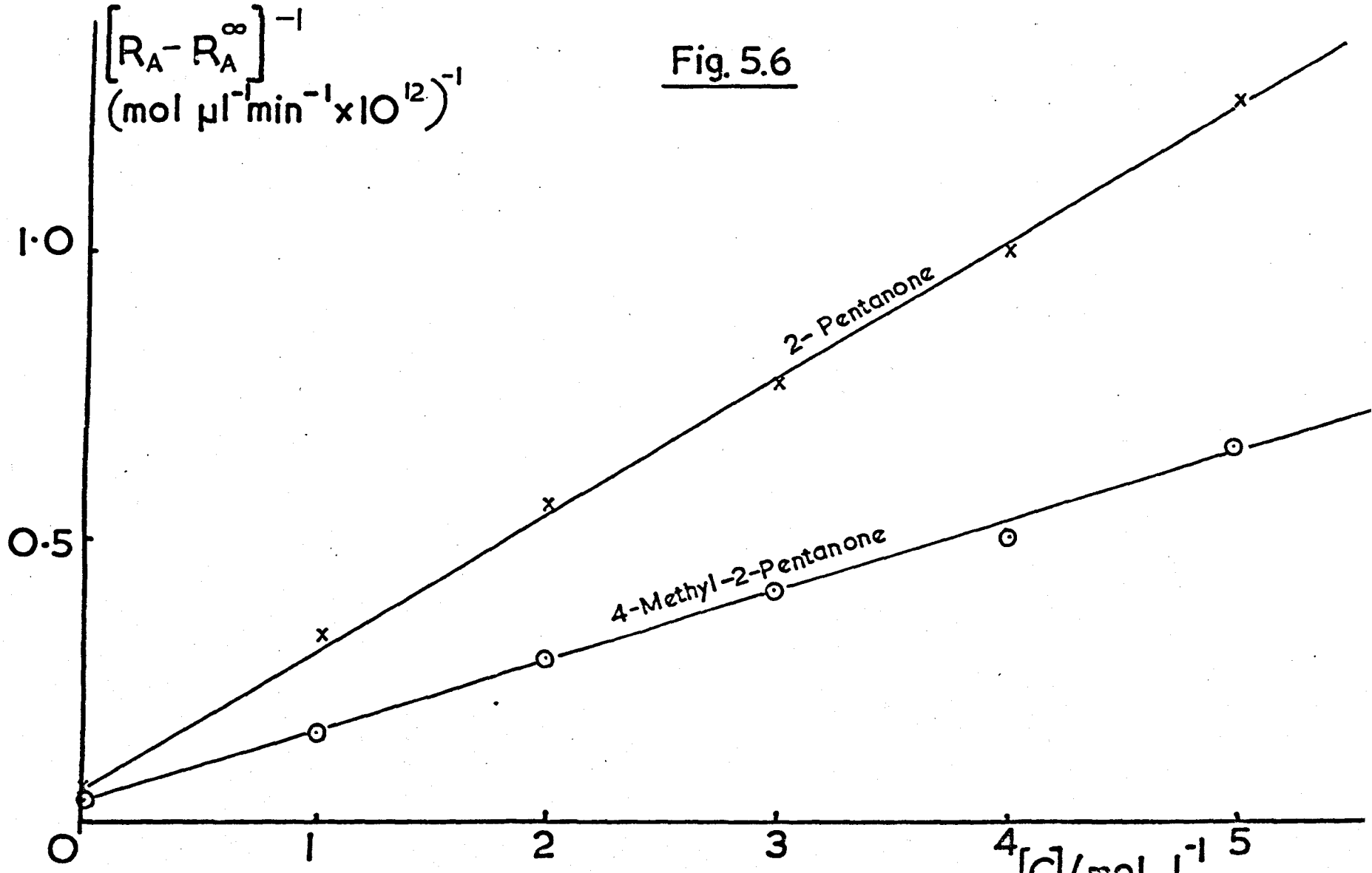
$[R_A - R_A^\infty]^{-1}$
(mol $\mu l^{-1} min^{-1} \times 10^{12})^{-1}$
1·0
0·5
0
1
2
3
4
5
[C]/mol l^{-1}
2-Pentanone
4-Methyl-2-Pentanone

the equivalent plot for ketone consumption gives a similar plot of intercept/slope ratio = 14.8 $l.mol^{-1}$, nearer the value quoted by Borrell. The difference in these values reflects the different shape of the two curves and also the inaccuracy involved in drawing reciprocal plots which depend heavily on a limiting value subject to an error of as much as ±5%.

If the assumption is made that the mechanism described in Section 5.6 is valid then treatment of the results in the same way, using the ratios $R_A/-R_p^{\infty} = 0.135$, $R_A^{o}/-R_p^{o} = 0.605$ and $-R_p^{o}/-R_p^{\infty} = 0.614$ and $\phi_{-p}^{o} = 0.0495$ (See result in Section 4.3, $\phi_A = 0.030$) gives the following quantum yields.

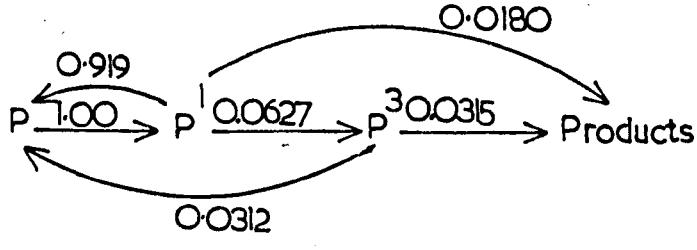

5.7(b) 4-Methyl-2-Pentanone in Benzene

As with 2-pentanone the results are qualitatively similar to those obtained before. Employing the same assumptions and the ratios $R_A^{o}/-R_k^{o} = 0.645$, $-R_k^{o}/-R_k^{\infty} = 0.674$ and $R_A^{\infty}/-R_k^{\infty} = 0.163$ together with $\phi_{-k}^{o} = 0.074$ the quantum yields are found to be:

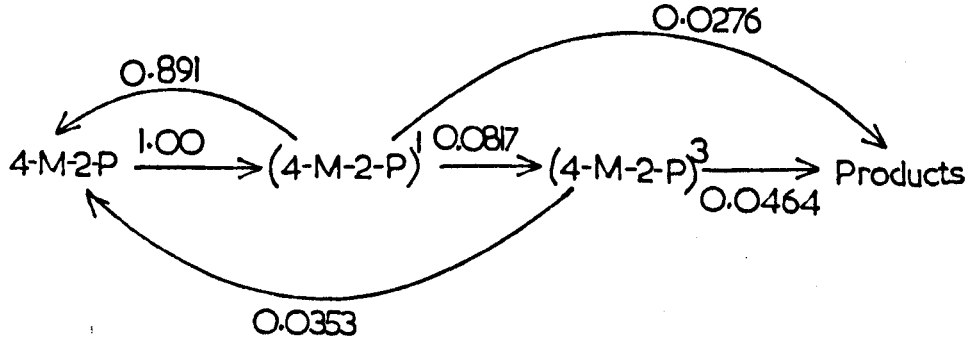

5.7(c) Comparisons

The quantum yields for the two ketones are presented below together with the results of Borrell and those of Yang et al,[45]

	2-Pentanone (Present Work)	2-Pentanone (Borrell and Sedlar)	2-Pentanone (Yang et al.)	4-Methyl-2-Pentanone (Present Work)
Solvent	Benzene	Benzene	Hexane	Benzene
Overall ϕ - K	0.0495	0.20	0.38	0.074
ϕ_1	0.9193	0.693	0.35	0.8907
ϕ_2	0.0627	0.262	0.63	0.0817
ϕ_3	0.0180	0.046	0.025	0.0276
ϕ_4	0.0312	0.107	0.27	0.0353
ϕ_5	0.0315	0.154	0.36	0.0464

The agreement between the published values for the overall quantum yields for 2-pentanone is not good. Barltrop and Coyle[46] quote ϕ_{-K} in benzene = 0.43 whilst Wagner and Hammond quote 0.42 in hexane.[40] On the other hand, Yang and Feit[47] quote a value of 0.27 in hexane. It should be pointed out that the agreement between the present work and that of Borrell and Sedlar is improved considerably if the same quantum yield is used (the ratios derived from the quenching experiments are similar). Since they estimated a quantum yield by reference to published values in different solvent systems it seems

reasonable to take the present value of 0.05 measured directly under the same conditions as quenching and in the same solvent.

The values derived by Yang[45] rely upon the quenching of the reaction by piperylene, which has since been shown to be an effective quencher of the singlet reaction[48] (see introduction) at high concentrations of the diene. Wettack[48] et al. have corrected the data of Wagner and Hammond for the piperylene quenching of 2-pentanone and estimate that the proportion of triplet reaction to type II products is about 70%. Borrell's figure is 77% whilst that estimated from the present work is 63.6% (Yang's uncorrected figure is 93.5%). These figures compare to the gas phase value of 65% calculated by Wettack and Noyes.[49] Another difference between Yang's results and the present work is that Yang used hexane as solvent. The effects of solvent on the reaction will be discussed in Section 5.8.

The most noticeable feature of the results presented above is the very high yield of internal conversion from the excited singlet state. With 2-pentanone it is estimated that 92% take this path whilst the figure is 89% in 4-methyl-2-pentanone. This high yield of internal conversion has been rationalised by Yang[45] by postulating the formation of a singlet biradical intermediate which can either react to give products or return to the ground state without spin inversion. (See Section 1.5). Although this explains why the type II reaction is generally inefficient it does not, in itself, explain why the overall quantum yield is so much lower in benzene than in other solvents. This will be discussed below. The proportion of triplet reaction to

give products in 4-methyl-2-pentanone is very similar to that in 2-pentanone itself (62.6%) and reflects the fact that both molecules have similar primary γ-hydrogens the only difference being that the substituted pentanone has more of them, giving a higher overall quantum yield.

5.8 Effect of Solvent

The quantum yield of acetone production from 2-pentanone was measured in various solvents as tabulated in Section 4.3. Except in the case of benzene and cyclohexane the quantum yield of pentanone disappearance was not measured. These results were obtained using the medium pressure lamp for stable light output and this light did not give sufficient conversion for Ø-K to be measured. Clearly there are considerable solvent effects operating and these may be compounded of a number of separate effects.

The first of these is the well known effect of solvent polarity. It has been shown by Wagner[50] and by Barltrop[51] that the effect of increasing solvent polarity is to increase the overall quantum yield such that it approaches unity in the case of certain aryl alkyl ketones, though this is not so marked in aliphatic ketones. They have suggested that this is due to the solvation of the proposed triplet biradical intermediate tending to drive the reaction to completion. Such a solvent effect is not noticed in the fully quenched singlet reaction,[46] presumably due to the shorter lifetime of the singlet state intermediate.

Another effect of solvent on the photoelimination is the degree to which hydrogen abstraction from the solvent may take place.

It is well known that aromatic ketones such as benzophenone do abstract from solvents such as isopropanol. It has also been reported that aliphatic ketones abstract hydrogen from hydrocarbon solvents, the triplet n,π* excited state being thought to be the abstracting species. (See Section 1.4(i) and references therein). Rapid hydrogen abstraction from the solvent will have the effect of increasing the overall quantum yield of disappearance of ketone at the expense of acetone production. It has been suggested that the triplet n,π* ketone molecules can be compared in reactivity to t-butoxy radicals[52] (In which case abstraction from cyclohexane is 570 times easier than abstraction from benzene.[53]) However, Wagner[54] has reported that hydrogen abstraction is not observed with 2-hexanone in hexane or t-butanol although hydrogen abstraction products (2-hexanol) are observed using tri-butyl stannane as solvent.

A third variable with solvent is the energy level of the ketone. It has been established that the position of the n-π* transition in carbonyl compounds is influenced by solvent, suffering a hypsochromic shift in polar solvents. This must reflect an increase in singlet energy and is probably accompanied by a corresponding increase in triplet energy. If the triplet energies of the donor ketone and quenching olefin are very close, as must be the case with cyclohexene then it is possible that small changes in solvent nature such as those on going from benzene to cyclohexane are sufficient to change the relative energies of the two. An example of changing the relative energies of donor and acceptor is shown by the competition between photocycloaddition and energy transfer with the carbonyl n,π*

triplet and norbornene,[55] When the ratio of oxetane/triplet energy transfer products goes from 0/70 to 46/4 in changing from a donor energy of 308 kJ to 300 kJ mol^{-1}. In another case[56] a change of only 2.5 kJ mol^{-1} in donor energy was sufficient to change a similar ratio from 0/100 to 43/57.

Another factor determined by solvent is chemical reaction with the solvent. In a very recent paper Schuster and Brizzolara[57] proposed that some observed results of ketone photochemistry in benzene (e.g. reference 58) can be explained by a mechanism of reversible addition to benzene to form a biradical :-

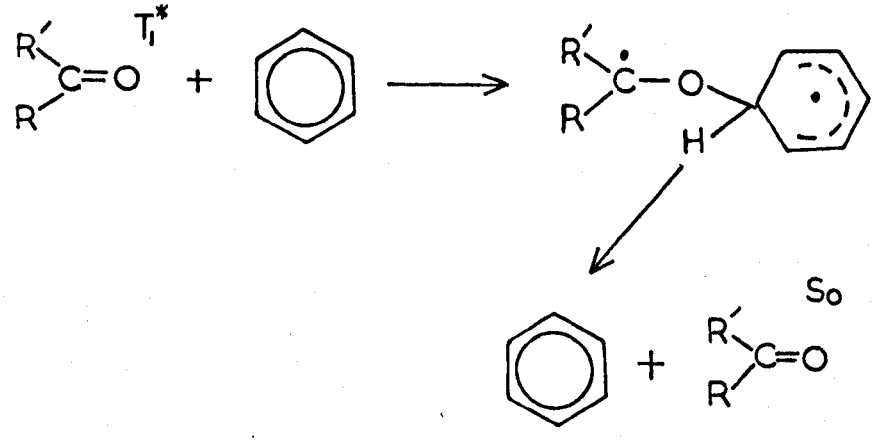

This provides a mechanism for efficient deactivation of ketone triplets which could explain the low quantum yield of reaction in benzene observed. This does not, however, explain the fact that Barltrop[46] reported the overall quantum yield from 2-pentanone in benzene as being 0.43, almost 10 times the value found in the present work.

Finally, solvent could affect the proportion of reaction to give acetone and olefin, on the one hand, and cyclobutanol on the other; though both products have been shown to come from the same biradical intermediate.[51] It is difficult to speculate as to what this effect will be as only acetone was followed. However, it is clear from Wagner's work[50] that the ratio of overall quantum yield to the yield of acetone production varies with solvent.

In trying to explain the difference in the observed reaction in benzene and cyclohexane several of these solvent effects may be invoked. The involvement of the adduct shown above seems the only way to explain the low quantum yield in benzene. The difference in the observed behaviour of the rate of ketone consumption is probably best explained by postulating a slight difference in the relative energies of ketone and cyclohexene triplets in the two cases. It is known that the triplet energies of the two are very close (of the order of 310 kJ mol^{-1}). In the case of benzene the triplet energy of the cyclohexene must be just above that of the ketone, resulting in oxetane formation, whilst changing to cyclohexane may increase the triplet energy of the ketone just sufficiently to make energy transfer the dominant process. It is reassuring to note that as the co-solvent is progressively replaced by cyclohexene the values of the two rates tend to the same value. Another possibility would be attack of cyclohexene on the biradical adduct with benzene, though this may amount to the same thing. This explanation could explain why the type II reaction of 2-octanone in benzene is barely affected by cyclohexene. The increased chain length is expected to

lower the triplet energy marginally and this may be sufficient to make reaction rather inefficient.

Inspection of the figures in Section 4.3 for the type II reaction of 2-pentanone in different solvents suggests that the increase in polarity does increase the quantum yield of acetone formation. However, without data on the quantum yield of ketone consumption it is not possible to conclude what other effects are operative. The yield of acetone is greatest, as expected, in t-butanol. Barltrop[46] quotes a value of 0.85 for the quantum yield of disappearance of the ketone so that the yield of other reactions is 0.56, or 66%, much higher than the corresponding figure of 39.5% observed in benzene. Similar figures are tabulated below :

Solvent	Ø Acetone (Present Work)	Ø-K	% Reactions other than Type II
Benzene	0.030	0.0495 (a)	39.5
Cyclohexane	0.104	0.30 (a)	65.4
t-Butanol	0.291	0.85 (b)	66.0
Ethanol	0.12	1.0 (c)	88.0
iso-Octane	0.226	0.42 (d)	46.2

In the above table, (a) = present work, (b) = Barltrop and Coyle[46], (c) = estimated value from reference 46 and (d) = value for n-hexane from reference 44. If, as Wagner found, hydrogen abstraction from the solvent is unimportant, then the variations in % Type II reaction

must be explained by variation in the ratio of acetone to cyclobutanol formed. If, however, Yang's report[45] of abstraction products being formed in hexane is the case then the variations from solvent to solvent could also be attributed to hydrogen abstraction. A combination of the two seems the most likely. 2-pentanol was not observed as a product of photolysis in the present experiments but under the usual conditions its retention time would be very long, making the chromatograph peak flat and not readily noticed. The value for the rate of acetone formation in pure 2-pentanone seems to fit with other solvents on the basis of polarity but is higher than found by Sedlar[43] (0.12). Repeat experiments, however, confirmed the higher value, though the value seems to be near that found by Sedlar at 254 nm.

Finally, the results in Section 4.8 show that as pure ketone is replaced by cyclohexane as solvent the quantum yield falls from 0.25 towards the cyclohexane value of 0.10, though there is no simple relationship between $\emptyset$ and concentration of cyclohexane.

5.9 Quantum Yield of Acetone Production in Different Ketones

Section 4.2 lists the quantum yields found for acetone production in various pure ketones. The values are similar for the two ketones with primary γ-hydrogens but are lower for the three with secondary γ-hydrogens. As has already been said, the value in 2-pentanone is higher than that found by Sedlar. The value in 2-heptanone (0.156) is lower than the value quoted by Calvert and Pitts of 0.23.[59] The quantum yield is 2-hexanone measured as 0.082 is also slightly lower than that measured by Sedlar[60] of 0.100. No

values for the rates of ketone consumption were measured, or have been published, but it is possible that the ratio of type II reaction to cyclobutanol formation may vary in the different ketones as suggested in Section 5.8 making interpretation of these results difficult.

5.10 Quenching in Cyclohexane

The quantum yields of acetone production and ketone consumption for zero olefin concentration and limiting concentration of olefin are tabulated below for the three ketones. These were evaluated from the data shown in Figs. 4.11, 4.17 and 4.23.

Ketone	ϕ_A^0	ϕ_A^∞	ϕ_{-K}^0	ϕ_{-K}^∞	ϕ_A^0 / ϕ_{-K}^0	$\phi_A^\infty / \phi_{-K}^\infty$
2-Pentanone	0.10	0.014	0.30	0.10	0.35	0.14
4-Methyl-2-Pentanone	0.13	0.15	0.24	0.11	0.54	0.13
2-octanone	0.074	0.043	0.091	0.054	0.81	0.79

The ratios in the last two columns express the fact that the rate of consumption of ketone does not fall with quencher to the same extent as the acetone is quenched. This suggests that energy transfer, although the dominant process, is accompanied by some compound formation. This seems likely if the energy levels are only slightly shifted

compared to benzene as would be expected in two such similar solvents. It seems probable that a Schenck type adduct is involved which may either result in energy transfer or may cyclise to form an oxetane. With 2-octanone the degree of quenching is less than in the other two ketones. This suggests that the proportion of reaction through the singlet state is greater in this case (58.4%). Compound formation also seems less marked than in the other cases and this may be due to steric hindrance in the proposed intermediate.

Modified Stern-Volmer plots can be drawn for the acetone quenching as before (using data taken from the curves drawn through the original points). Plots of $(R_A - R_A^{\infty})$ vs.[C] are shown in Fig. 5.7. The slope/intercept ratios of these plots give values of $k_q\tau_t$, where k_q is the sum of the rate constants for quenching by energy transfer and by compound formation and τ_t is the triplet lifetime.

Ketone	$k_q\tau_t$, $l.mol^{-1}$
2-Pentanone	3.6
4-Methyl-2-Pentanone	10.6
2-Octanone	4.0

The maximum value of k_q will be the diffusion controlled rate of around $5 \times 10^9 l.mol^{-1}s^{-1}$ which gives a minimum value of τ_t of around 10^{-9}s. The variations between the ketones could be explained either

Fig. 5.7

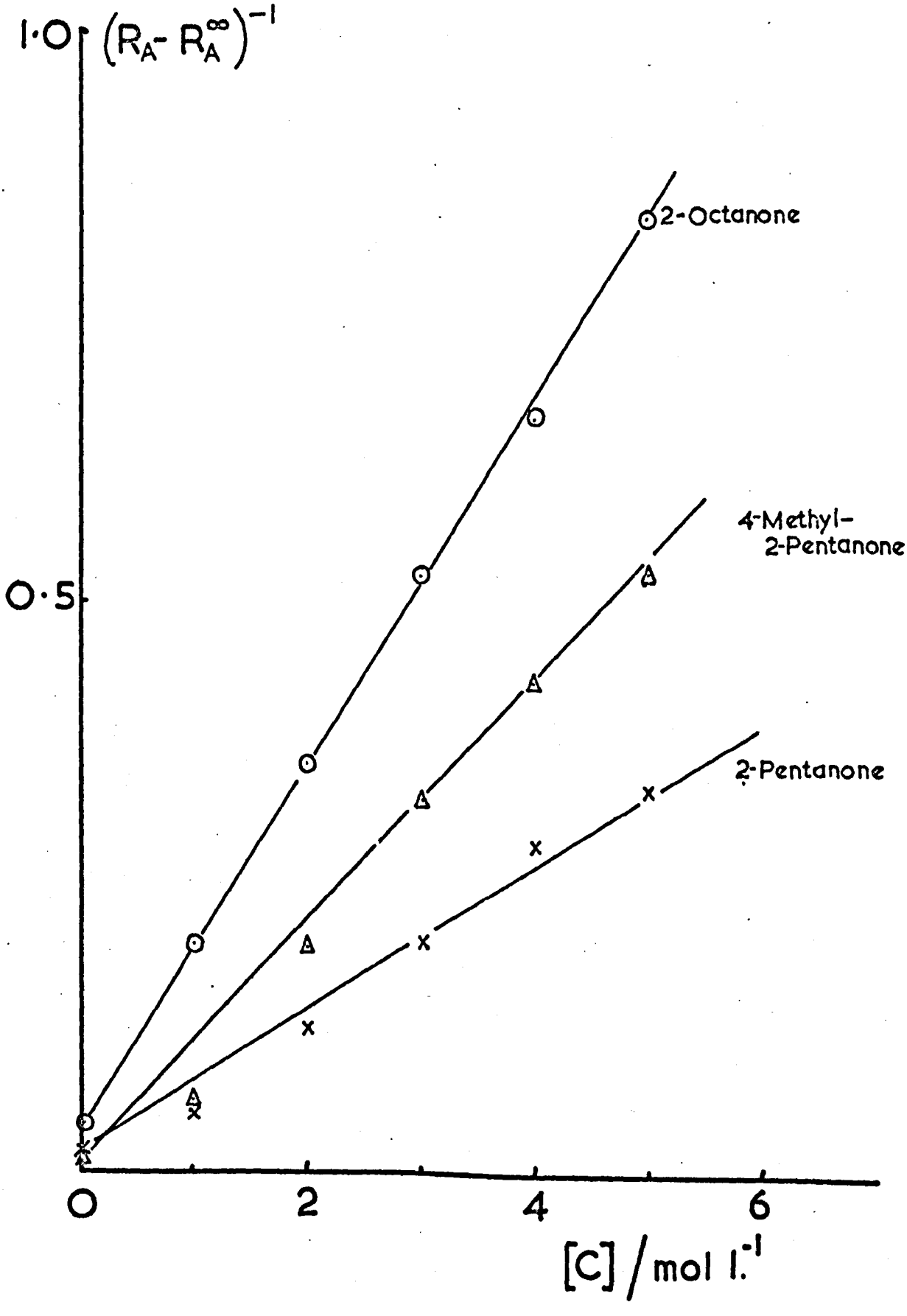
1·0
$(R_A - R_A^{\infty})^{-1}$
0·5
2-Octanone
4-Methyl-
2-Pentanone
2-Pentanone
0
2
4
6
[C] / mol l.$^{-1}$

by changes in k_q or τ_t and without further data it is not possible to say which.

5.11 Summary and Suggestions for Further Work

The results for the photoisomerisation of methyl tiglate provide sufficient information when combined with previous work to enable a speculative potential energy diagram to be drawn. The validity of such diagrams in explaining photoisomerisation is open to question when chemical reactions involving radicals are invoked to explain observed results. The results suggest an efficient process for internal conversion as the major route for deactivation of the excited molecules as has been observed for certain other n,π^* systems. Photosensitisation of the isomerisation seems to involve a certain amount of adduct formation and competing reaction to form addition products.

It would be of interest to have further information on photosensitisation using sensitisers of different energy and following oxetane production as well as isomerisation on the lines indicated in Section 5.5. It would also be useful to have a computer-drawn energy diagram based on molecular orbital theory as produced for stilbene.

The later results on the quenching of photoelimination indicate the usefulness of following quenching in ketone-olefin pairs of similar triplet energy as a means of obtaining detailed information about the internal processes taking place on excitation of such molecules. Clearly such reactions are highly sensitive

to the relative triplet energies of donor and acceptor and also to the solvent system. These various effects need much further investigation using different ketones and quenchers under conditions where all the rate parameters of the reaction can be followed.

REFERENCES TO CHAPTER 5.

1. J.A. Barltrop and J. Wills, Tetrahedron Letters, 4987, (1968).
2. M.J. Jorgenson, J.Amer.Chem.Soc., 91, 198, (1969).
3. P.J. Wagner and G.S. Hammond, J.Amer.Chem.Soc., 88, 1245, (1966).
4. J.N. Pitts, H.W. Johnson and T. Kuwana, J.Phys.Chem., 66, 2456, (1962).
5. M.J. Jorgenson, J.Amer.Chem.Soc., 91, 6432, (1968).
6. J.L. Magee, W. Shand and H. Eyring, J.Amer.Chem.Soc., 63, 677, (1941).
7. R.B. Cundall in Prog.Reaction Kinetics, Vol.2 (Ed.G. Porter) Pergamon, Oxford, (1964), pp. 167 - 215.
8. P. Bortolus and G. Cauzzo, Trans.Faraday Soc., 66, 1161, (1970).
9. J.N. Butler and G.J. Small, Can.J.Chem., 41, 2492, (1963).
10. M.C. Lin and K.J. Laidler, Can.J.Chem., 46, 973, (1968).
11. J.N. Butler and R.D. McAlpine, Can.J.Chem., 41, 2487, (1963).
12. W.D. Closson, S.F. Brady and P.J. Orenski, J.Org.Chem., 30, 4026, (1965).
13. N.J. Turro in 'Energy Transfer and Organic Photochemistry', Vol. XIV in series 'Technique of Organic Chemistry' (Ed. P.A. Leermakers and A. Weissberger), Interscience, New York, (1969) pp. 135 - 295.
14. M.J. Jorgenson and L. Gundel, Tetrahedron Letters, 4991, (1968).

15. J.C.D. Brand and D.G. Williamson, Disc.Faraday Soc., 35, 18, (1963).

16. N.C. Yang and M.J. Jorgenson, Tetrahedron Letters, 1203, (1964).

17. P.J. Wagner and G.S. Hammond in 'Advances in Photochemistry', Vol. 5, (1968) p. 120.

18. R.S. Becker, K. Inuzuka and J. King, J.Chem.Phys., 52, 5164, (1970).

19. J.J. McCullough, H. Ohorodnyk and D.P. Santry, Chem. Commun., 571, (1969).

20. P. Borrell and H.H. Greenwood, Proc.Roy.Soc., A298, 453, (1967).

21. J.G. Calvert and J.N. Pitts, 'Photochemistry', Wiley, New York, (1966).

22. D. Phillips, J. Lemaire, C.S. Burton and W.A. Noyes, 'Advances in Photochemistry' Vol.5, 329 (1968).

23. J. Saltiel, L. Metts and M. Wrighton, J.Amer.Chem.Soc., 92, 3227, (1970).

24. D.G. Whitten and M.T. McCall, J.Amer.Chem.Soc., 91, 5097, (1969).

25. J. Lemaire, J.Phys.Chem., 71, 612, (1967).

26. B. Roquitte, unpublished results quoted in reference 22, above.

27. R.M. Hochstrasser and C. Marzzacco, J.Chem.Phys., 46, 4155 (1967).

28. R.M. Hochstrasser and C. Marzzacco, J.Chem. Phys., 49, 971, (1968).

29. W.G. Herkstroeter and G.S. Hammond, J.Amer.Chem.Soc., 88, 4769. (1966).

30. P.J. Wagner, J.Amer.Chem.Soc., 89, 5898, (1967).

31. E.H. Gilmore, G.E. Gibson and D.S. McClure, J.Chem.Phys., 23, 1772 (1955).

32. J.A. Bell and H. Lipschitz, J.Amer.Chem.Soc., 85, 528 (1963).

33. N.C. Yang, J.L. Cohen and A. Shani, J.Amer.Chem.Soc., 90, 3264 (1968).

34. R.A. Caldwell and G.W. Sovocool, J.Amer.Chem.Soc., 90, 7138 (1968).

35. J. Saltiel, K.R. Neuberger and M. Wrighton, J.Amer.Chem.Soc., 91, 3658 (1969).

36. G.O. Schenck and R. Steinmetz, Bull.Soc.Chim.Belges, 71, 781, (1962).

37. G.S. Hammond and J. Saltiel, J.Amer.Chem.Soc., 85, 2515 (1963), et seq.

38. D.R. Arnold Advances in Photochem.6, 301 (1968).

39. P. Borrell and J. Sedlar, J.Chem.Soc., accepted for publication (1970).

40. P.J. Wagner and G.S. Hammond, J.Amer.Chem.Soc., 87, 4009 (1965), et seq.

41. P. Borrell and J. Sedlar, Trans.Faraday Soc., 66, 1670 (1970).

42. D.R. Arnold, 'Advances in Photochemistry' Vol. 6, pp.301 - 418 (1968).

43. P. Borrell and J. Sedlar, J.Sci.Instrum., 2, 439 (1969).

44. P.J. Wagner and G.S. Hammond, J.Amer.Chem.Soc., 88, 1245 (1966).

45. N.C. Yang, S.P. Elliott and B. Kim, J.Amer.Chem.Soc., 91, 7551 (1969).

46. J.A. Barltrop and J.D. Coyle, Tetrahedron Letters, 3235, (1968).

47. N.C. Yang and E.D. Feit, J.Amer.Chem.Soc., 90, 505, (1968).

48. F.S. Wettack et al. J.Amer.Chem.Soc., 99, 1793 (1970).

49. F.S. Wettack and W.A. Noyes, J.Amer.Chem.Soc., 90, 3901 (1968).

50. P.J. Wagner, J.Amer.Chem.Soc., 89, 5898, (1967).

51. J.A. Barltrop and J.D. Coyle , J.Amer.Chem.Soc., 90, 6584 (1968).

52. C. Walling and M.J. Gibson, J.Amer.Chem.Soc., 87, 3361 (1965).

53. A.L. Williams, E.A. Oberright and J.W. Brooks, J.Amer.Chem.Soc., 78, 1190 (1956).

54. P.J. Wagner, Tetrahedron Letters, 5385 (1968).

55. D.R. Arnold, R.N. Hinman and A.H. Glick, unpublished, quoted in 'Advances in Photochemistry', Vol. 6. p.332.

56. L.A. Singer and P.D. Bartlett, Tetrahedron Letters, 1887 (1964).

57. D.I. Schuster and D.F. Brizzolara, J.Amer.Chem.Soc., 92, 4357 (1970).

58. C.A. Parker and T.A. Joyce, Chem.Commun., 749, (1968).

59. J.G. Calvert and J.N. Pitts, 'Photochemistry' John Wiley, New York (1966).

60. J. Sedlar, Postdoctoral report, unpublished (1968).